Institut für Technische Mechanik
Abteilung Dynamik

Dissertation

Identification of general time-varying systems

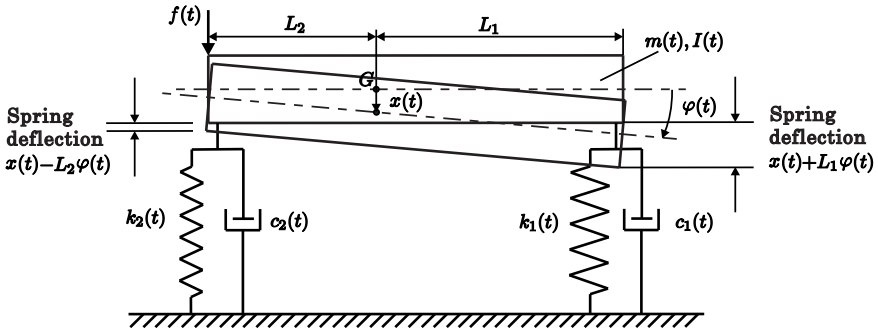

M. Eng. Han Hu

Karlsruhe Institute of Technology

Figure on the front page: A 2-DOF linear time-varying non-chainlike system

Identification of general time-varying systems

Zur Erlangung des akademischen Grades

Doktor der Ingenieurwissenschaften

der
Fakultät für Maschinenbau
Karlsruher Institut für Technologie (KIT)

genehmigte
Dissertation

von

M. Eng. Han Hu
aus Hunan

Tag der mündlichen Prüfung:	08. Februar 2017
Hauptreferent:	Prof. Dr.-Ing. Carsten Proppe
Korreferent:	Prof. Dr.-Ing. Michael Beer

Acknowledgements

First and foremost, I would like to express my sincere gratitude to my principal supervisor, Prof. Dr.-Ing. Carsten Proppe, for his inspirational guidance with patience, unfailing help and considerate support both in academic field and in life. He has been a respectable and extraordinary mentor. His academic enthusiasm and rigorous academic attitude influences me and has provided me with the right attitude and impetus to complete my work. It is my great honor and privilege to be his PhD student.

I would like to express my sincere appreciation to my second supervisor, Prof. Dr.-Ing. Michael Beer of Institute for Risk and Reliability at Leibniz University Hannover, for his professional guidance, valuable suggestions and selfless help on my work.

I would like to express my sincere appreciation to Prof. Dr.-Ing. Dr. h.c. Jörg Wauer for his kindness and support. Because of his recommendation, I have the chance and honor to be the PhD student of Professor Proppe.

Special thanks to Professor Jianye Ching from Department of Civil Engineering at National Taiwan University for proposing an effective and powerful algorithm - the transitional Markov chain Monte Carlo method for Bayesian model updating and model class selection.

Special thanks to my colleagues Dr.-Ing. Nicole Gaus and Dr.-Ing. Daniel Schwarzer for their valuable suggestions and help in Matlab programming during the first year of my PhD work.

I would like to thank M.-Eng. Thanh Chung Pham for his help with LATEX problems and similar software issues.

Special thanks to my dear parents and my friends Jiahui Li, Zhihua Dai, Dr.-Ing. Jing Gao, Xingyu Yao, Dr.-Ing. Xiaoyu Zhang, Dr.-Ing. Fabian Bauer, Dipl.-Ing. Christoph Baum, Dr.-Ing. Toni Liong, Dr.-Ing. Dipl.-Math. Alexander Karmazin and M.Sc. Kai Becker for their considerate support and endless encouragement.

Karlsruhe, den 25.10.2016
M. Eng. Han Hu

Abstract

Since most systems in the real world exhibit non-stationary and non-linear dynamical performance, parameter identification for general time-variant systems is of utmost importance. This dissertation investigates the identification of general time-variant systems using the Hilbert-Huang transform (HHT) and Bayesian model updating and model class selection method. An identification technique based on the HHT for parametric identification of linear time-varying chainlike systems is extended for identification of general linear time-varying systems including non-chainlike and chainlike systems. The proposed method decomposes the system responses into intrinsic mode functions (IMFs) and residues by the empirical mode decomposition, and then analyzes the IMFs and residues by Hilbert transform to obtain the analytical IMFs and analytical residues. After that, it synthesizes these analytical signals to form new analytical response signals and uses the new synthesized analytical responses together with the original system responses to identify system stiffness and damping parameters. The method is later extended for identification of weakly nonlinear time-varying systems including Duffing and Van der Pol systems with the help of the approximations generated according to Hahn's formula and the theory of Feldman. In application of the HHT-based identification technique, uncertainties due to model structure errors, model parameter errors or model order errors may exist. To update the uncertainties which might occur, a Bayesian model updating and model class selection method implemented by the transitional Markov chain Monte Carlo method is combined with the proposed HHT-based identification method. It updates initial knowledge about the system responses and the white noise in these system responses based on measured system responses. Then, it defines a set of model classes by assigning different values to the ratio between the prediction error variance (PEV) of displacement and that of the corresponding acceleration as well as the ratio between the PEV of velocity and that of the corresponding acceleration, chooses the most probable model class by performing Bayesian model class selection, and generates sample system responses by using the posterior distributions of the noise parameters obtained for the most probable model class and the reference values of the system responses, which are later processed by the HHT-based identification method, yielding the statistical distributions of system stiffness and damping parameters. To address the identification of system structural parameters, a new Bayesian inference based parameter identification method has been developed. It updates initial knowledge about the system structural parameters and the PEVs of the IMFs of the acceleration responses based on measured system responses with the likelihood function formulated as the product of three probability density functions, one relating to the IMFs of the acceleration responses, the other two relating to the IMFs of the corresponding velocity responses and the IMFs of the corresponding displacement responses. Then, it defines a set of candidate model classes by assigning different values to the ratio between the PEV of each IMF of each velocity response and that of the corresponding acceler-

ation response as well as the ratio between the PEV of each IMF of each displacement response and that of the corresponding acceleration response, and determines the most probable model class by performing Bayesian model class selection, resulting in the posterior distribution of the system structural parameters for the most probable model class. Numerical simulations are carried out on 1-DOF and 2-DOF general linear time-varying systems and weakly nonlinear time-varying systems with smooth, abrupt and periodical stiffness variations and white noise perturbations in the system responses to demonstrate the effectiveness, accuracy and robustness of the proposed methods.

Contents

List of symbols

$(\varepsilon_{i,q}^{a})^2$ Prediction error variance (PEV) of the acceleration corresponding to the ith degrees of freedom and the qth experiment 77

$(\varepsilon_{i\chi}^{a})^2$ PEV of the χth IMFs of the ith acceleration response 93

$(\varepsilon_{i\chi}^{d})^2$ PEV of the χth IMFs of the ith displacement response 93

$(\varepsilon_{i\chi}^{v})^2$ PEV of the χth IMFs of the ith velocity response 93

α The ratio between the PEV of the IMF of the velocity response and that of the corresponding acceleration response of the same DOF in the same experiment . 93

$\boldsymbol{\Theta}$ Parameter space 14

$\boldsymbol{\theta}$ Parameter vector 14

$\boldsymbol{\theta}_{j,l}^{C}$ The candidate sample in the lth Markov chain at the jth iteration stage of the transitional Markov chain Monte Carlo method 18

$\boldsymbol{\theta}_{j,l}^{now}$ The current sample in the lth Markov chain at the jth iteration stage of the transitional Markov chain Monte Carlo method 18

$\boldsymbol{M}$ The set of models classes 18

$\ddot{\mathbf{y}}$ The acceleration vector 10

$\ddot{Y}$ The analytical signal of $\ddot{\mathbf{y}}$ 11

$\ddot{y}_i$ The ith element of $\ddot{\mathbf{y}}$ corresponding to the ith DOF 22

$\ddot{y}_{i,q}$ The system acceleration response corresponding to the ith degrees of freedom and the qth experiment 27

δ The cubic stiffness factor of Duffing system 51

$\dot{\mathbf{y}}$ The velocity vector 10

$\dot{Y}$ The analytical signal of $\dot{\mathbf{y}}$ 11

$\dot{y}_i$ The ith element of $\dot{\mathbf{y}}$ corresponding to the ith DOF 22

$\dot{y}_{i,q}$ The system velocity response corresponding to the ith degrees of freedom and the qth experiment 27

η The ratio between the PEV of displacement and that of the corresponding acceleration 77

γ The ratio between the PEV of the IMF of the displacement response and that of the corresponding acceleration response of the same DOF in the same experiment 93

$\mathbb{R}$ Space of real numbers 14

$\mathbf{C}$ System damping matrix 10

$\mathbf{F}$ The analytical signal of $\mathbf{f}$ 11

$\mathbf{f}$ The excitation vector 10

$\mathbf{K}$ System stiffness matrix 10

$\mathbf{M}$ System mass matrix 10

$\mathbf{Y}$ The analytical signal of $\mathbf{y}$ 11

Σ Covariance matrix 15

$H[\cdot]$ Hilbert transform 10

$IMF_{i\chi k}^{E\cdot}$ The observed value of the χth IMF of the ith system response in the kth measurement 92

$IMF_{i\chi}^{M\cdot}$ The model value of the χth IMF of the ith system response 92

NE The number of trials 27

$Nstd$ The ratio of the standard corresponding to the ith degrees of freedom 27

μ The damping factor of Van der Pol system 60

μ_l The structural parameter of a 2-DOF weakly nonlinear periodically varying chain-like Van der Pol system 69

ω Instantaneous frequency 10

ψ Instantaneous phase angle 10

ρ The ratio between the PEV of velocity and that of the corresponding acceleration 77

σ The evaluation function 9

$\mathrm{Im}[\cdot]$ Imaginary part 10

$\mathrm{Re}[\cdot]$ Real part 10

$\tilde{\cdot}$	Hilbert transform of any signal 10
A	Instantaneous amplitude 10
a	The mode amplitude 9
c_i	The damping coefficient corresponding to ith degrees of freedom 22
c_{ji}	The element in the jth row and ith column of system damping matrix 22
D	Experimental data set from measurements 14
e	The prediction error 15
e_{max}	The maximal envelope of a signal 9
e_{min}	The minimal envelope of a signal 9
h, T	The structural parameters of a 2-DOF linear periodically varying non-chainlike system 129
I	The mass moment of inertia 22
k_i	The stiffness coefficient corresponding to the ith degrees of freedom 22
k_{ji}	The element in the jth row and ith column of system stiffness matrix 22
k_{linear}	The linear stiffness coefficient 51
m	The mass coefficient 22
M^*	The most probable model class 78
m_i	The mass coefficient corresponding to ith degrees of freedom 22
m_{ji}	The element in the jth row and ith column of system mass matrix 22
M_{mi}	The mith model class 14
$mean$	The mean envelope of a signal 9
mo	The model output 15
mo^a	The model acceleration 77
mo^d	The model displacement 77
mo^v	The model velocity 77
n	The number of degrees of freedom 8
N_E	The number of samples of each distribution 77

N_L The number of DOFs of the system responses obtained in n experiments 92

N_p The number of uncertain parameters 14

N_{class} The number of model classes 18

P Cauchy principal value 10

r Residue of a signal obtained by empirical mode decomposition 9

s_f Prescribed scaling factor in Metropolis-Hastings algorithm 18

so The system output 15

$std(\cdot)$ The function of MATLAB for calculating the standard deviation of any signal. 79

t Time 8

t_L The structural parameter of a 2-DOF linear smoothly varying non-chainlike system 41

t_l The structural parameter of a 1-DOF linear smoothly varying system 96

t_{duff} The structural parameter of a 2-DOF weakly nonlinear smoothly varying chainlike Duffing system 67

$w(\cdot)$ The plausibility weight of samples 17

y_i The ith element of $\mathbf{y}$ corresponding to the ith DOF 11

y_{ij} The jth intrinsic mode function extracted from y_i by empirical mode decomposition 11

Y_i The ith element of $\mathbf{Y}$ corresponding to the ith DOF 11

$\mathbf{y}$ The displacement vector 10

ap_t The Metropolis-Hastings acceptance probability 16

N_o The number of observed degrees of freedom 15

N_s The number of sets of experimental data 15

Y_{ij} The analytical signal of y_{ij} 11

$y_{i,q}$ The system displacement response corresponding to the ith degrees of freedom and the qth experiment 27

List of abbreviations

AM/FM Amplitude and frequency modulated . . . 7
AMH Adaptive Metropolis-Hastings . . . 16
COV Coefficient of variation . . . 18
EMD Empirical mode decomposition . . . 3
FT Fourier transform . . . 1
HHT Hilbert-Huang transform . . . 3
HT Hilbert transform . . . 3
IF Instantaneous frequency . . . 7
IFT Inverse Fourier transform . . . 1
IMF Intrinsic mode function . . . 7
MCMC Markov chain Monte Carlo . . . 15
MDOF Multi-degrees of freedom . . . 3
MH Metropolis-Hastings . . . 15
MTF Multiplicative transfer function . . . 2
PDF Probability density function . . . 14
PEV Prediction error variance . . . 77
STFT Short time Fourier transform . . . 2
SVD Singular value decomposition . . . 3
TMCMC Transitional Markov chain Monte Carlo . . . 5
TV-STFT Time-varying short time Fourier transform . . . 2
WT Wavelet transform . . . 2

List of tables

List of figures

1 Introduction

Prediction, modeling, and identification are omnipresent in natural science. Accurate descriptions of the dynamic properties of the interested systems are often required in many engineering applications. Accurate models characterizing these dynamic properties which are based on first principles of physics, mechanics, biology and so on are difficult to derive because of the lack of detailed specialist knowledge. Another way of constructing models is system identification, which deals with the problem of constructing mathematical models to provide a better understanding and characterization of the interested dynamic systems based on experiments and observations. System identification has evolved considerably during the past 30 years [1, 2]. The techniques of system identification can be usually divided into time domain techniques and frequency domain techniques. In the time domain, linear time-invariant systems, which are often used to model systems with stationary properties, form indisputably the most common class of models for dynamic systems considered in practice and in literature. However, as linear time-invariant systems are not able to capture the instantaneous dynamic properties of the systems, they can not be applied to systems with non-stationary properties. Linear time-varying systems are often used to model systems with non-stationary properties and might often oscillate with small magnitude vibrations. Since most systems in the real world exhibit non-stationary dynamical performance, the identification of linear time-varying systems has received increasing attention in a wide variety of scientific fields, e.g. in electrical and control engineering [3], civil engineering [4], biology [5], aero engineering [6] and mechanical engineering. In mechanical engineering, applications range from robotics to dynamics of machines and rotors.

1.1 Identification methods for linear time-varying systems

Spectral analysis based on Fourier transform (FT) is the most commonly used method when the global power-frequency distribution of a given signal is of interest, and forms a relation between time domain and frequency domain. By application of Inverse Fourier transform (IFT), a signal is expressed as the superposition of complex exponentials of various frequencies with complex amplitudes defined by FT. Due to its simplicity and versatility, it has become the predominant method for data analysis since it was discovered [7]. However, due to the critical limitations such as: the system to be analyzed must be linear and the data to be analyzed must be strictly periodic or stationary, the application of Fourier spectral analysis is limited. In spite of these limitations, Fourier spectral analysis is still widely used to process data with finite duration and nonstationarity for lack of alternatives. The uncritical use of Fourier spectral analysis and the casual adoption of the stationary and linear assumptions may give misleading results [8].
As Fourier basis functions are localized in frequency but not in time, an alternative method

naming the Short time Fourier transform (STFT) was proposed by Denis Gabor for application of speech communication [9]. Gabor multiplied a signal by a pre-fixed window function which is nonzero for only a short period of time, then took the Fourier transform of the modified signal when the window was sliding along the time axis, resulting in the sinusoidal frequency and phase content of sections of the signal. Portnoff [10] developed a representation for discrete-time signals and linear time-varying systems based on STFT and the time-varying frequency response. Based on Portnoff's work, Kozek and Hlawatsch [11] proposed a time-frequency representation for linear time-varying systems using the Weyl Symbol. Later, Benisty et al [12] introduce a Time-varying short time Fourier transform (TV-STFT) defined by a time-varying window length. Based on Multiplicative transfer function (MTF) approximation [13], by controlling the length of the analysis window, an adaptive scheme is presented to achieve a relatively low steady state error without degrading its convergence rate.
However, due to the limit given by the Heisenberg uncertainty principle, the frequency resolution of STFT is inversely proportional to its time resolution (window length), and variations of window length compromise the frequency resolution. Even if optimized joint time-frequency localization is assumed, the trade-off between time and frequency resolution is unavoidable. This limitation of STFT prompts the need for an alternative method for time-frequency analysis. For this reason, a multi-resolution analysis method with its basis functions compactly supported in both time and frequency domain, namely Wavelet transform (WT) has been proposed [14, 15].
The original wavelet representations were developed mainly during the 1980s, and Ingrid Daubechies [16] developed the most famous wavelet representations, namely the orthonormal compactly supported wavelets. Similar to STFT, WT results in a time-frequency representation, but other than representing signals by sinusoidal functions, WT represents a signal by the superposition of its projections on a set of daughter wavelets generated by scaling and translating a pre-assumed wavelet basis function known as the mother wavelet in both time domain and frequency domain, offering very good time and frequency localization of the signal. By using a mother wavelet which is both shifted and dilated, WT mitigates the limitations of FT and STFT. Furthermore, WT is able to use time window shorter than that of the STFT to generate accurate signal spectrum, and thus is able to detect model variations more quickly. Nonetheless, wavelet theory is still limited by the Heisenberg uncertainty principle.
Many authors have proposed WT-based methods for identification of linear time-varying systems. Ghanem and Romeo [17] estimated the system parameters with a differential equation model relating input and output measurements which has been discretized by a Wavelet-Galerkin method. Park et al [18] derived an algebraic equation of linear time-varying systems by expanding the input-output data and the time-varying impulse response with normalized Haar wavelets. By solving the algebraic equation, unknown wavelet coefficients for the system impulse response can be estimated and the system impulse response can be synthesized. Shan and Burl [19] estimated the system parameters from the system's "local" transfer function based on its time-frequency representation using the continuous wavelet transform. A non-linear least square algorithm coupled with a scale selection algorithm was used to carry out the parameter estimation.

According to the definitions, both STFT and WT are methods with a priori fixed choice of a basis, their application to the identification of system parameters has been difficult [17] and yields very often instantaneous modal parameters only. And as mentioned before, due to the limit of Heisenberg uncertainty principle, their time and frequency resolutions cannot have the same precision simultaneously. To conquer the limitations of these methods, further research and methods are anticipated.
In the late 20th century, some efforts have been made in extending the discrete-time state-space methods to linear time-varying systems [20–22]. Shokoohi and Silverman [20] proposed a Hankel matrix decomposition method based on impulse response data to identify the state-space model of a linear time-varying system. Based on their work, Verhaegen and Yu [21] extracted successive discrete transition matrices of a linear time-varying system by a subspace-based algorithm from an ensemble of input and output data. Later on, Liu developed another Singular value decomposition (SVD)-based state-space method to identify linear time-varying systems [22]. With respect to the previous work of Verhaegen and Yu, Liu's method guarantees the invariability of the eigenvalues of the estimated transition matrix and extends the modal concepts of linear time-varying systems by proposing the concept of pseudomodal parameters which are determined from the eigenvalues of the varying transition matrix to characterize the dynamical properties of systems. Nevertheless, this SVD-based method cannot obtain characteristic time and frequency scales, and due to the fact that the eigenfunctions are difficult to interpret, the applicability of this method to the parametric identification of linear time-varying systems seems to be limited.
At the end of the 1990s, Huang et al [8] proposed the Empirical mode decomposition (EMD) method for non-stationary data analysis. The main idea is to decompose a general signal into a finite number of mono-component signals called intrinsic mode functions by a sifting process. As it is based on the local characteristics of the signal, EMD method can be applied to nonlinear and non-stationary processes. EMD method combined with Hilbert transform (HT) was denoted as Hilbert-Huang transform (HHT) [8]. It can describe the instantaneous dynamic properties of the signal both in time and frequency domain. HHT has been applied to identify modal parameters of Multi-degrees of freedom (MDOF) linear systems including the natural frequencies and damping ratios as well as the mass, damping and stiffness matrices of the systems [23, 24]. However, these HHT-based applications often relate to time-invariant systems. Recently, HHT method has been successfully applied to linear time-varying chain-like systems by Shi and Law, in which only one set of IMFs is required to identify the system parameters [25, 26].
In the application of the aforementioned identification methods, uncertainties may exist. These uncertainties may be due to model structure errors which would be caused by some uncertainties concerning the governing physical equations of the system, usually related to the chosen mathematical model, which might occur typically in the modeling of processes and strongly nonlinear behavior in certain engineering systems, and due to model parameter errors which would be caused by the application of inappropriate boundary conditions and inaccurate assumptions used in order to simplify the model of the system, the environmental influence, manufacturing tolerances and the artificial introduction of system damping, etc, and also due to model order errors which might be caused by the discretization of complex systems, since real structures are continuous and have infinite

DOFs, but the DOFs of the discretized model is limited [27]. In order to update the uncertainties which might occur in the identification of linear time-varying systems and weakly nonlinear systems, we adopt Bayesian inference in this thesis.

1.2 Bayesian inference

In statistical analysis, probability can be interpreted in different ways: frequency probability (physical probability) and Bayesian inference (evidential probability). The former treats probability as the limit of an event's relative frequency in a large number of trials and thus its application is limited since probability can only be assigned to an event in which a random experiment is possible; whereas the latter can assign probabilities to any event, even when a random experiment is not possible. Bayesian inference is based on Bayes' theorem [28, 29] developed by Thomas Bayes in 1760s, which states that the conditional probability (posterior probability) of an event A conditioned on the available data of another event B is given by the product of the prior probability of A and the conditional probability (likelihood function) of B (conditioned on A) divided by the prior probability of B. Bayes' theorem is one of the most frequently occurring eponyms in the literature of statistics.
Based on Bayes' work, Harold Jeffreys [30], Richard T. Cox [31] and Edwin T. Jaynes [32–34] significantly developed the Bayesian theory, since then Bayesian inference has been widely used in different areas of natural sciences and engineering, such as statistical physics [33, 35], medical sciences [36, 37], computer science [38], engineering geology [39], system reliability [40, 41], mechanical engineering [42], aerospace engineering [43], etc.

1.3 Motivations and aims

As there exist still limitations in identification of time-varying systems, the aim of this thesis is to propose an HHT-based identification method for the parametric identification of general linear time-varying systems (including chainlike and non-chainlike systems) as well as weakly nonlinear time-varying systems (such as Duffing and Van der Pol oscillators). The broad-based aims of this thesis are summarized as follows:

1. Extend the parametric identification method of linear time-varying chainlike systems proposed by Shi and Law to general linear time-varying systems (including chainlike and non-chainlike systems).
2. Extend the parametric identification method of general linear time-varying systems (including chainlike and non-chainlike systems) to weakly nonlinear time-varying systems (such as Duffing and Van der Pol oscillators).
3. Apply Bayesian inference for both general linear time-varying systems and weakly nonlinear systems to get the statistical distributions of the system parameters.

1.4 Outline of the thesis

This thesis contains 6 chapters. Chapter 2 introduces the theoretical bases of the HHT-based identification method. First, the detailed concepts and procedures of HHT as well as its application in linear time-varying MDOF systems are introduced. Then, the theoretical knowledge about Bayesian inference methods is also presented.
Chapter 3 first proposes the main ideas and procedures of the HHT-based identification method for general linear time-varying MDOF systems (including chainlike and non-chainlike systems). Then, three types of time variation of stiffness: smooth, abrupt and periodical variations are studied on 1-DOF and 2-DOF mass-spring-damper dynamical systems to demonstrate the effectiveness and accuracy of the HHT-based identification method for general linear time-varying systems.
Chapter 4 first introduces some basic knowledge about Duffing oscillators and Van der Pol oscillators, then extends the HHT-based identification method for general linear time-varying MDOF systems to the identification of weakly nonlinear time-varying MDOF Duffing systems and Van der Pol systems, respectively. As in Chapter 3, three types of time variation of stiffness: smooth, abrupt and periodical variations are also studied on 1-DOF and 2-DOF Duffing as well as Van der Pol systems to demonstrate the effectiveness and accuracy of the proposed method for weakly nonlinear time-varying systems.
Chapter 5 proposes the main ideas and procedures of Bayesian inference based methods which use the Transitional Markov chain Monte Carlo (TMCMC) method for sampling for both general linear time-varying systems and weakly nonlinear time-varying systems. As in the above two chapters, 1-DOF and 2-DOF general linear time-varying systems as well as weakly nonlinear time-varying systems are studied with smooth, abrupt and periodical stiffness variations and white noise disturbance. The resulting statistical distributions of the system parameters demonstrate the effectiveness, accuracy and robustness of the Bayesian inference based methods for both general linear time-varying systems and weakly nonlinear time-varying systems.
Finally, Chapter 6 summarizes the conclusions of the thesis and presents recommendations for future research that could be possible extensions to this work.

2 Theoretical bases

2.1 Hilbert-Huang Transform

HHT is the combination of EMD method and HT. It is an adaptive method and has been proposed by Huang et al in 1998 for nonlinear and non-stationary data analysis. It was proved to be effective for the characterization of a wide range of nonlinear and non-stationary signals in terms of Intrinsic mode function (IMF) obtained by the application of EMD to the signals [8, 44, 45]. Due to its huge potential, HHT has been widely used in many applications, such as financial applications, medical applications, plasma diagnostics, study of ozone records, damage detection, aeroelastic flight data analysis, gearbox and roller bearing fault diagnosis, and nonlinear vibration characterization [46–54].

2.1.1 Empirical Mode Decomposition

A very successful approach to study time-varying dynamic properties of a system is the HT [55, 56], which is able to decompose signals in the time-frequency domain to catch the time and frequency localization information of the signals. At any given time instance, most signals in real world such as human speech, radar signals, wireless signals and mechanical signals may involve more than one harmonic component [57–59]. For the purpose of obtaining meaningful Instantaneous frequency (IF), general signals have to be processed into mono-component signals, each of which admits an unambiguous definition of instantaneous frequency and amplitude through HT. This kind of mono-component signals are termed as IMFs, which are defined as functions satisfying two conditions: (1) in the whole data set, the number of extrema and the number of zero crossings must either be equal or differ at most by one; and (2) at any point, the mean value of the envelope defined by the local maxima and the envelope defined by the local minima is zero. The first condition makes sure that the IMFs are narrow band signals. Since there is no precise definition for mono-component signals, narrow band requirement was adopted as a limitation on signals so that the signals are quasi mono-component signals with meaningful IFs. The second condition modifies the classical global requirement to a local one and is essential to make sure that the IF will not have unwanted fluctuations induced by asymmetric waveforms [8]. Based on these two conditions, the resulting IMFs are Amplitude and frequency modulated (AM/FM) zero mean signals suitable for Hilbert transform.
Huang et al. [8] proposed empirical mode decomposition to decompose a general signal into a finite number of IMFs. Compared with conventional decomposition methods, which accomplish the analysis by projecting the considered signal into numbers of pre-assumed basis vectors, EMD represents the signal as an expansion of signal-dependent IMFs generated via an iterative sifting process. Therefore, it can be applied to nonstationary and nonlinear signals. As the results are not biased by the predetermined basis, the IMFs

are able to retain the physical meaning of the intrinsic processes underlying the signal. After applying HT to the IMFs, meaningful IFs can be obtained, offering a time-frequency representation of the signal.
Suppose the signal under consideration is a signal of an n-DOF system $x(t)$, the sifting process is presented in detail as follows:

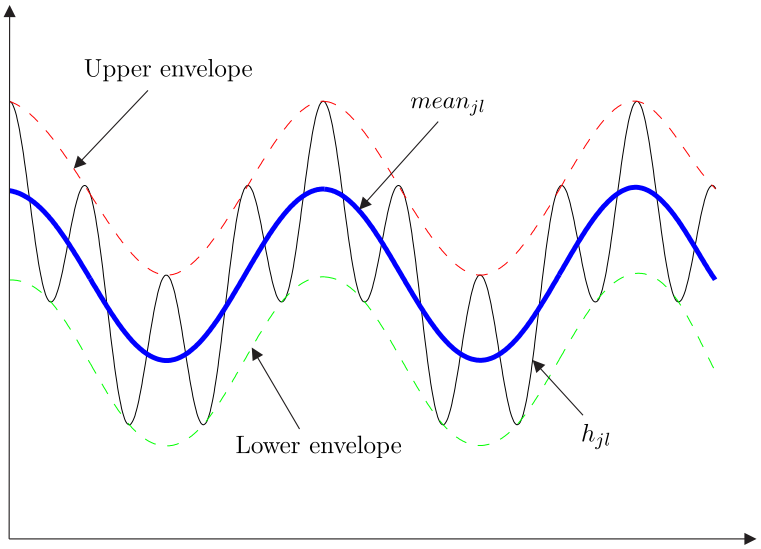

Figure 2.1: Quantities related to the lth iteration for generating the jth IMF.

First, all local maxima and minima of the signal $x(t)$ have to be identified and connected by cubic splines as the upper envelope, and lower envelope respectively (see Figure 2.1);
Second, the mean of the upper and lower envelopes (designated as $mean_1$) is computed and subtracted from the original signal to form a new signal:

$$h_1 = x(t) - mean_1 \tag{2.1}$$

Third, h_1 is treated as the signal to be sifted, and the previous two steps are repeated, then we have:

$$h_{11} = h_1 - mean_{11} \tag{2.2}$$

The above sifting steps are repeated l times, until the resulting new signal h_{1l} satisfies the two conditions for an IMF:

$$h_{1l} = h_{1(l-1)} - mean_{1l} \tag{2.3}$$

$$x_1 = h_{1l} \tag{2.4}$$

where x_1 is the first IMF component of the signal $x(t)$. A stop criterion for the sifting process has to be determined to make sure that the IMF components maintain enough

physical sense of both amplitude and frequency modulations, which is achieved by limiting the size of the standard deviation as follows

$$SD = \sum_{t=0}^{T} \left[\frac{\left| h_{1(l-1)}(t) - h_{1l}(t) \right|^2}{h_{1(l-1)}^2(t)} \right] \tag{2.5}$$

Then, the first IMF x_1 should be subtracted from the original signal to form another new signal:

$$r_1 = x(t) - x_1 \tag{2.6}$$

As the new signal r_1 still contains information of longer period components, the previous three steps have to be repeated on r_1:

$$r_2 = r_1 - x_2$$

The previous four steps should be repeated on all the subsequent r_js($j \geq 2$), until the residual signal r_n becomes a monotonic function from which no more IMFs can be extracted or becomes smaller than a predetermined value.

$$r_j = r_{j-1} - x_j \ , \quad \dots \ , \quad r_n = r_{n-1} - x_n \tag{2.7}$$

Finally, the original signal $x(t)$ can be expressed as

$$x(t) = \sum_{j=1}^{n} x_j(t) + r_n(t) \tag{2.8}$$

in which x_j, $j = 1, 2, \dots, n$ are the IMFs of the original signal $x(t)$, $r_n(t)$ is the residue. Following the above EMD algorithm, MATLAB scripts were later developed by P. Flandrin [60] with a new stop criterion as an improvement to the aforementioned criterion (see Equation (2.5)). This new criterion tests if the evaluation function $\sigma(t) = |mean(t)/a(t)|$ ($mean(t)$ is the mean envelope of the signal, $a(t) = (e_{max}(t) - e_{min}(t))/2$ is the mode amplitude, $e_{max}(t)$ is maximal envelope and $e_{min}(t)$ is minimal envelope) is smaller than γ_1 for some prescribed fraction $(1 - \alpha_p)$ of the total duration, and is smaller than γ_2 for the remaining fraction [61]. If the new criterion test is positive and if the number of zero crossings and the number of extrema differ by no more than 1, the iterations for extracting a single IMF are stopped.

2.1.2 Hilbert Transform

HT was first proposed by David Hilbert in 1905. Later, Gabor introduced HT to signal theory and defined the amplitude and other instantaneous characteristics of an arbitrary signal with the help of the HT [9]. In order to obtain meaningful IF, a general signal has to be decomposed into IMFs suitable for HT.

For an IMF $x_j(t)$, the HT of $x_j(t)$ is denoted by $\tilde{x}_j(t)$ as

$$\tilde{x}_j(t) = H[x_j(t)] = \frac{1}{\pi} P \int_{-\infty}^{+\infty} \frac{x_j(\tau)}{t-\tau} \mathrm{d}\tau, \tag{2.9}$$

where P denotes the Cauchy principal value. $x_j(t)$ and $\tilde{x}_j(t)$ form a complex conjugate pair. The analytical signal $X_j(t)$ of $x_j(t)$ is expressed as

$$X_j(t) = x_j(t) + j\tilde{x}_j(t) = A_j(t) \exp[j\psi_j(t)] \tag{2.10}$$

in which

$$\begin{aligned} x_j(t) &= A_j(t) \cos\left[\psi_j(t)\right] \\ A_j(t) &= \sqrt{x_j^2(t) + \tilde{x}_j^2(t)} \\ \psi_j(t) &= \arctan\left[\tilde{x}_j(t)/x_j(t)\right] \end{aligned} \tag{2.11}$$

where $A_j(t)$ is the instantaneous amplitude and $\psi_j(t)$ is the instantaneous phase angle, and non-subscript $j = (-1)^{1/2}$. The IF $\omega_j(t)$ is the time-derivative of the instantaneous phase angle given as

$$\omega_j(t) = \dot{\psi}_j(t) = \frac{x_j(t)\dot{\tilde{x}}_j(t) - \dot{x}_j(t)\tilde{x}_j(t)}{A_j^2(t)} = \mathrm{Im}\left[\frac{\dot{X}_j(t)}{X_j(t)}\right] \tag{2.12}$$

The time-derivative of the instantaneous amplitude can be expressed as

$$\dot{A}_j(t) = \frac{x_j(t)\dot{x}_j(t) + \tilde{x}_j(t)\dot{\tilde{x}}_j(t)}{A_j(t)} = A_j(t)\mathrm{Re}\left[\frac{\dot{X}_j(t)}{X_j(t)}\right] \tag{2.13}$$

Equations (2.10) - (2.13) describe the instantaneous behavior of an IMF at any time t through HT.

2.2 Linear time-varying MDOF systems

The equation of a linear time-varying MDOF system can be expressed as

$$\mathbf{M}(t)\ddot{\mathbf{y}}(t) + \mathbf{C}(t)\dot{\mathbf{y}}(t) + \mathbf{K}(t)\mathbf{y}(t) = \mathbf{f}(t) \tag{2.14}$$

Suppose the system is an n-DOF system, then $\mathbf{y}(t) = [y_1(t), y_2(t), \ldots, y_n(t)]^T$ is the displacement vector, $\mathbf{f}(t)$ is the excitation vector ($\mathbf{f}(t) = 0$ for free vibration), $\mathbf{M}(t)$ the mass matrix, $\mathbf{C}(t)$ the damping matrix, $\mathbf{K}(t)$ the stiffness matrix. They are all $n \times n$ matrices. The displacement vector $\mathbf{y}(t)$ is decomposed using EMD method. The ith element of the displacement vector can be expressed as

$$y_i(t) = \sum_{j=1}^{n} y_{ij}(t) + r_i(t) = \sum_{j=1}^{n} A_{ij}(t) \cos[\psi_{ij}(t)] + r_i(t) \tag{2.15}$$

in which $y_{ij}(t)$ is the jth IMF extracted from the ith element of the displacement vector which corresponds to the ith DOF.
From Bedrosian's theorem on the HT of the product of two signals [62], suppose $lp(t)$ is the low-pass portion of a signal, $hp(t)$ is the high-pass portion of the same signal, their spectra are non-overlapping, then $H[lp(t)hp(t)] = lp(t)H[hp(t)]$. If the coefficient matrices $\mathbf{M}(t)$, $\mathbf{C}(t)$ and $\mathbf{K}(t)$ don't vary quickly over time, we have:

$$\begin{aligned} H[\mathbf{M}(t)\ddot{\mathbf{y}}(t)] &= \mathbf{M}(t)H[\ddot{\mathbf{y}}(t)] = \mathbf{M}(t)\ddot{\tilde{\mathbf{y}}}(t) \\ H[\mathbf{C}(t)\dot{\mathbf{y}}(t)] &= \mathbf{C}(t)H[\dot{\mathbf{y}}(t)] = \mathbf{C}(t)\dot{\tilde{\mathbf{y}}}(t) \\ H[\mathbf{K}(t)\mathbf{y}(t)] &= \mathbf{K}(t)H[\mathbf{y}(t)] = \mathbf{K}(t)\tilde{\mathbf{y}}(t) \end{aligned} \tag{2.16}$$

This assumption is violated for abruptly varying systems. We will further discuss this in the simulations of abruptly varying systems in next chapter.
If we apply the HT to both sides of Equation (2.14), and consider Equation (2.16), we get:

$$\mathbf{M}(t)\ddot{\tilde{\mathbf{y}}}(t) + \mathbf{C}(t)\dot{\tilde{\mathbf{y}}}(t) + \mathbf{K}(t)\tilde{\mathbf{y}}(t) = \tilde{\mathbf{f}}(t) \tag{2.17}$$

Multiplying each term of Equation (2.17) by the imaginary number j and adding it to the corresponding term of Equation (2.14), the differential equation of the linear time-varying n-DOF system can be expressed with analytic signals as follows:

$$\mathbf{M}(t)\ddot{\mathbf{Y}}(t) + \mathbf{C}(t)\dot{\mathbf{Y}}(t) + \mathbf{K}(t)\mathbf{Y}(t) = \mathbf{F}(t) \tag{2.18}$$

in which $\mathbf{F}(t) = [F_1(t), F_2(t), \ldots, F_n(t)]^T$ is the analytic signal of the excitation vector, $\mathbf{Y}(t) = [Y_1(t), Y_2(t), \ldots, Y_n(t)]^T$ is the analytic signal of the displacement vector. From Equations (2.10) - (2.11), the ith element of the analytic signal which corresponds to the ith DOF can be expressed by the superposition of n analytical IMFs and an analytical residue:

$$Y_i(t) = \sum_{j=1}^{n} Y_{ij}(t) + R_i(t) = \sum_{j=1}^{n} A_{ij}(t)\exp[j\psi_{ij}(t)] + R_i(t) \tag{2.19}$$

where the instantaneous amplitude $A_{ij}(t)$, the instantaneous phase angle $\psi_{ij}(t)$, the IF $\omega_{ij}(t)$ and the time-derivative of $A_{ij}(t)$ are expressed according to Equations (2.11) - (2.13), except that their subscripts are changed from j to ij.
According to Equations (2.11) - (2.13) and (2.19), we obtain

$$\dot{Y}_{ij}(t) = Y_{ij}(t)[\dot{A}_{ij}(t)/A_{ij}(t) + j\omega_{ij}(t)] \tag{2.20}$$

$$\ddot{Y}_{ij}(t) = Y_{ij}(t)[\ddot{A}_{ij}(t)/A_{ij}(t) - \omega_{ij}^2(t) + j(2\dot{A}_{ij}(t)\omega_{ij}(t)/A_{ij}(t) + \dot{\omega}_{ij}(t))] \tag{2.21}$$

where

$$\dot{\omega}_{ij}(t) = \mathrm{Im}\left[\frac{\ddot{Y}_{ij}(t)}{Y_{ij}(t)}\right] - 2\frac{\dot{A}_{ij}(t)\omega_{ij}(t)}{A_{ij}(t)} \tag{2.22}$$

$$\ddot{A}_{ij}(t) = A_{ij}(t)\left(\mathrm{Re}\left[\frac{\ddot{Y}_{ij}(t)}{Y_{ij}(t)}\right] + \omega_{ij}^2(t)\right) \tag{2.23}$$

2.3 An HHT-based identification method for linear time-varying MDOF chainlike systems based on forced vibration data

Since most systems in the real world exhibit time-varying dynamical performance, identification for linear time-varying systems is utmost required. To this end, Shi et al developed an identification algorithm for linear time-varying MDOF chainlike systems based on HHT with forced vibration response data [26]. Since the system model introduced in Section 2.2 was adopted for linear time-varying MDOF systems, all the equations in Section 2.2 can be also used in this section. The identification algorithm is given as follows:
For Equation (2.18), the jth analytical signal of the analytical displacement vector $\mathbf{Y}(t) = \sum_{j=1}^{n} \mathbf{Y}_j(t)$ can be written as

$$\mathbf{Y}_j(t) = [Y_{1j}, Y_{2j}, \ldots, Y_{nj}]^T \tag{2.24}$$

Then, substitute Equations (2.20) and (2.21) for $\dot{\mathbf{Y}}(t)$ and $\ddot{\mathbf{Y}}(t)$ in Equation (2.18), we obtain

$$\mathbf{M}(t)[\gamma^m]\mathbf{Y}(t) + \mathbf{C}(t)[\gamma^c]\mathbf{Y}(t) + \mathbf{K}(t)\mathbf{Y}(t) = \mathbf{F}(t) \tag{2.25}$$

in which $[\gamma^m]$ and $[\gamma^c]$ are coefficient matrices, the elements of which are given by

$$\gamma_{ij}^m = [\ddot{A}_{ij}(t)/A_{ij}(t) - \omega_{ij}^2(t)] + j[2\dot{A}_{ij}(t)\omega_{ij}(t)/A_{ij}(t) + \dot{\omega}_{ij}(t)] \tag{2.26}$$

$$\gamma_{ij}^c = \dot{A}_{ij}(t)/A_{ij}(t) + j\omega_{ij}(t) \tag{2.27}$$

Assume any two IMFs $y_f(t)$ and $y_g(t)$ satisfy the orthogonal relationship $y_f(t) \cdot y_g(t) = 0$. Based on Bedrosian's theorem, it is easy to obtain

$$\mathbf{Y}_f(t) \cdot \mathbf{Y}_g(t) = 0 \tag{2.28}$$

Multiply the two sides of Equation (2.25) with $\mathbf{Y}_j^T(t)$, we have

$$\mathbf{Y}_j^T(t)\mathbf{M}(t)[\gamma^m]\mathbf{Y}_j(t) + \mathbf{Y}_j^T(t)\mathbf{C}(t)[\gamma^c]\mathbf{Y}_j(t) + \mathbf{Y}_j^T(t)\mathbf{K}(t)\mathbf{Y}_j(t) = \mathbf{Y}_j^T(t)\mathbf{F}(t) \tag{2.29}$$

Assume the mass matrix is known, with the help of Equations (2.12), (2.13), (2.22) and (2.23), Equation (2.29) can be simplified and written in compact matrix notation as

$$\boldsymbol{Q}^c\boldsymbol{\beta}^c + \boldsymbol{Q}^k\boldsymbol{\beta}^k = \boldsymbol{Q}^m \tag{2.30}$$

where $\boldsymbol{\beta}^c = [c_1, c_2, \ldots, c_i, \ldots, c_n]^T$, $\boldsymbol{\beta}^k = [k_1, k_2, \ldots, k_i, \ldots, k_n]^T$, $\boldsymbol{Q}^c$ $\boldsymbol{Q}^k$ and $\boldsymbol{Q}^m$ are the coefficient matrices and vector, whose elements in the jth row are expressed as

$$\boldsymbol{Q}_j^c = \begin{bmatrix} Y_{1j}\gamma_{1j}^c Y_{1j} \\ Y_{1j}(\gamma_{1j}^c Y_{1j} - \gamma_{2j}^c Y_{2j}) + Y_{2j}(\gamma_{2j}^c Y_{2j} - \gamma_{1j}^c Y_{1j}) \\ \vdots \\ Y_{i-1j}(\gamma_{i-1j}^c Y_{i-1j} - \gamma_{ij}^c Y_{ij}) + Y_{ij}(\gamma_{ij}^c Y_{ij} - \gamma_{i-1j}^c Y_{i-1j}) \\ \vdots \\ Y_{n-1j}(\gamma_{n-1j}^c Y_{n-1j} - \gamma_{nj}^c Y_{nj}) + Y_{nj}(\gamma_{nj}^c Y_{nj} - \gamma_{n-1j}^c Y_{n-1j}) \end{bmatrix}^T$$

$$\boldsymbol{Q}_j^k = \begin{bmatrix} Y_{1j}^2 \\ Y_{1j}(Y_{1j}-Y_{2j})+Y_{2j}(Y_{2j}-Y_{1j}) \\ \vdots \\ Y_{i-1j}(Y_{i-1j}-Y_{ij})+Y_{ij}(Y_{ij}-Y_{i-1j}) \\ \vdots \\ Y_{n-1j}(Y_{n-1j}-Y_{nj})+Y_{nj}(Y_{nj}-Y_{n-1j}) \end{bmatrix}^T \tag{2.31}$$

$$\boldsymbol{Q}_j^m = \mathbf{Y}_j^T\mathbf{F} - (Y_{1j}m_1\gamma_{1j}^m Y_{1j} + Y_{2j}m_2\gamma_{2j}^m Y_{2j} + \cdots + Y_{ij}m_i\gamma_{ij}^m Y_{ij} + \cdots + Y_{nj}m_n\gamma_{nj}^m Y_{nj})$$

According to its real and imaginary parts, the complex Equation (2.30) can be assembled as follows

$$\begin{bmatrix} \mathrm{Re}(\boldsymbol{Q}^c) & \mathrm{Re}(\boldsymbol{Q}^k)) \\ \mathrm{Im}(\boldsymbol{Q}^c) & \mathrm{Im}(\boldsymbol{Q}^k) \end{bmatrix} \begin{bmatrix} \boldsymbol{\beta}^c \\ \boldsymbol{\beta}^k \end{bmatrix} = \begin{Bmatrix} \mathrm{Re}(\boldsymbol{Q}^m) \\ \mathrm{Im}(\boldsymbol{Q}^m) \end{Bmatrix} \tag{2.32}$$

For an n-DOF linear time-varying chainlike system, Equation (2.32) contains $2n$ time-varying equations. By solving Equation (2.32), time-varying unknown system parameters can be obtained at any time instant t.
For a 1-DOF linear time-varying system, the stiffness and damping coefficients can be expressed as

$$k(t) = m\omega_0^2(t), c(t) = 2mh_0(t) \tag{2.33}$$

where $\omega_0(t)$ and $h_0(t)$ are the instantaneous undamped natural frequency and the instantaneous damping coefficient of the system respectively, which are given by

$$\begin{aligned} \omega_0^2(t) &= \frac{k(t)}{m} \\ &= \omega^2(t) + \frac{\mathrm{Re}(\boldsymbol{F}(t)/Y(t))}{m} - \frac{\mathrm{Im}(\boldsymbol{F}(t)/Y(t))\dot{A}(t)}{m\omega(t)A(t)} - \frac{\ddot{A}(t)}{A(t)} + \frac{2\dot{A}^2(t)}{A^2(t)} + \frac{\dot{\omega}(t)\dot{A}(t)}{\omega(t)A(t)} \end{aligned} \tag{2.34}$$

$$h_0(t) = \frac{\mathrm{Im}(\boldsymbol{F}(t)/Y(t))}{2m\omega(t)} - \frac{\dot{A}(t)}{A(t)} - \frac{\dot{\omega}(t)}{2\omega(t)} \tag{2.35}$$

in which $\omega(t)$, $\dot{A}(t)$, $\dot{\omega}(t)$ and $\ddot{A}(t)$ are the instantaneous coefficients.

2.4 Bayesian model updating

Model updating focuses on improving the mathematical model based on the experimental data such that the updated model describes the dynamic properties of the subject structure more correctly. Since there always exist uncertainties (the origin of the uncertainties can be found in Section 1.1) in the modeling process, model updating is required. Model updating can be divided into general model updating and Bayesian model updating, the former

assumes that the updated model parameter is a single value, whereas the latter assumes that the updated model parameter is a random variable with probability distribution. As the updated model parameter obtained by general model updating is a single value, the updated model obtained by this method is the model which has the minimal error between the experimental data and the model itself, general model updating method is not able to show uncertainty of the model parameter. However, Bayesian model updating can solve this problem: the Probability density function (PDF) of the updated model parameter obtained by Bayesian model updating is capable of expressing uncertainty of the model parameter. It is a powerful tool to update the uncertainties in a model response by using experimental data [63].

2.4.1 Bayesian model updating for a given model class

For a given model class M_{mi}, suppose D is a set of experimental data from measurements of a dynamic system which might be the modal shapes and frequencies of the system, the measured system structural response in terms of acceleration, or the spectral density of the response. The goal of Bayesian model updating is to use D to update the relative plausibility of each model in the chosen model set which is defined by the parameter vector $\boldsymbol{\theta} \in \boldsymbol{\Theta} \in \mathbb{R}^{N_p}$. According to the well known Bayes' theorem, a posterior (updated) probability distribution of model parameter conditioned on the available data is proportional to the product between the prior probability distribution and the likelihood function which are defined in some ways, so the relative plausibility of each model in the chosen model class is given by

$$p(\boldsymbol{\theta}|D, M_{mi}) = \frac{p(D|\boldsymbol{\theta}, M_{mi})p(\boldsymbol{\theta}|M_{mi})}{p(D|M_{mi})} \tag{2.36}$$

where $p(\boldsymbol{\theta}|D, M_{mi})$ is the posterior PDF of $\boldsymbol{\theta}$ which represents the probability of obtaining model parameter vector $\boldsymbol{\theta}$ given the experimental data D and the model class M_{mi}; $p(\boldsymbol{\theta}|M_{mi})$ is the prior PDF given the model class M_{mi}, which represents the initial knowledge about the dynamic system when D are not obtained and quantifies the prior plausibility of each model in the model class M_{mi}. Generally the real value of $\boldsymbol{\theta}$ is unknown, so a reasonable PDF will be set as the prior PDF of $\boldsymbol{\theta}$; $p(D|\boldsymbol{\theta}, M_{mi})$ is the likelihood function which represents the probability of obtaining D given $\boldsymbol{\theta}$ and the model class M_{mi}. The closer the distribution of $\boldsymbol{\theta}$ is to the real value of the parameter vector, and the closer M_{mi} is to the real dynamic system, the closer the predicted system responses will be to the experimental data D, and the larger the obtained likelihood will be; $p(D|M_{mi})$ is the evidence for the model class M_{mi} provided by the experimental data D which is a normalizing constant to make the area of $p(D|\boldsymbol{\theta}, M_{mi})p(\boldsymbol{\theta}|M_{mi})$ equal to 1, so it does not have an effect on the shape of the posterior distribution. All the above probabilities are conditional on the chosen Bayesian model class M_{mi}.

2.4.2 Formulation of the likelihood function

The likelihood function $p(D|\boldsymbol{\theta}, M_{mi})$ is a measure of the data fit between the system output (experimental data) and the corresponding structural model output, whose value for each

parameter vector $\boldsymbol{\theta}$ is given by a probability model for the prediction error, which is the difference between the system output that will be measured (experimental data) and that predicted by the structural model for a specified value of the parameter vector $\boldsymbol{\theta}$. As the Gaussian PDF gives the largest amount of uncertainty among all probability distributions for a real variable whose first two moments are specified, a Gaussian distribution with zero mean and covariance matrix Σ justified by the principle of maximum entropy is chosen as the PDF model for the prediction error e.
Assume the system output (experimental data) is denoted as so, the corresponding structural model output is denoted as $mo(\boldsymbol{\theta})$, the connection between these two outputs is given as

$$so = mo(\boldsymbol{\theta}) + e \ , \quad e \sim N(0, \Sigma) \tag{2.37}$$

Then, the PDF model for the system output is given by a Gaussian PDF with the mean equal to the model value $mo(\boldsymbol{\theta}) \in R^{N_o}$ and with a covariance matrix $\Sigma(\boldsymbol{\theta}) \in R^{N_o \times N_o}$:

$$p(so|\boldsymbol{\theta}) = \frac{1}{(2\pi)^{N_o/2}|\Sigma(\boldsymbol{\theta})|^{1/2}} \exp\left[-\frac{1}{2}(so - mo(\boldsymbol{\theta}))^T(\Sigma(\boldsymbol{\theta}))^{-1}(so - mo(\boldsymbol{\theta}))\right] \tag{2.38}$$

where N_o is the number of observed degrees of freedom.
Assume the experimental data $D = \{so : ki = 1, \ldots, N_s\}$ from measurements consist of N_s sets of data, and the prediction errors are modeled as statistically independent of each other, then the likelihood function can be given as

$$\begin{aligned} p(D|\boldsymbol{\theta}, M_{mi}) &= \prod_{ki=1}^{N_s} p(so|\boldsymbol{\theta}) \\ &= \frac{1}{(2\pi)^{N_o N_s/2} \prod_{ki=1}^{N_s} |\Sigma(\boldsymbol{\theta})|^{1/2}} \exp\left[-\frac{1}{2}\sum_{ki=1}^{N_s}(so - mo(\boldsymbol{\theta}))^T(\Sigma(\boldsymbol{\theta}))^{-1}(so - mo(\boldsymbol{\theta}))\right] \end{aligned} \tag{2.39}$$

2.4.3 Markov chain Monte Carlo simulations – Metropolis-Hastings algorithm

In order to take samples from the posterior PDF $p(\boldsymbol{\theta}|D, M_{mi})$, stochastic simulation methods [64–66] which can estimate any value of interest $E[\vartheta|D, M_{mi}]$ with the help of Law of Large Numbers $E[\vartheta|D, M_{mi}] \approx \sum_{l=1}^{N} \vartheta(\boldsymbol{\theta}_l)/N$ ($\{\boldsymbol{\theta}_l : l = 1, \ldots, N\}$ are the samples taken from $p(\boldsymbol{\theta}|D, M_{mi})$) are often used in Bayesian inference. Among the stochastic simulation methods, Markov chain Monte Carlo (MCMC) methods are very famous methods proposed to gain a sample distributed as a PDF $p(\boldsymbol{\theta})$ without sampling or simulating directly from $p(\boldsymbol{\theta})$ in the recent two decades [67]. It is constituted by Markov Chain process and Monte Carlo integration. The principle of MCMC is: for any random starting value $\boldsymbol{\theta}_{(0)}$, an ergodic Markov chain $\boldsymbol{\theta}_{(t)}$ is generated using a transition kernel with stationary distribution $p(\boldsymbol{\theta})$, the distribution of $\boldsymbol{\theta}_{(t)}$ will converge to $p(\boldsymbol{\theta})$ and has nothing to do with the choice of $\boldsymbol{\theta}_{(0)}$.
Among the MCMC methods, the Metropolis-Hastings (MH) algorithm which was first

proposed by Metropolis et al. [68] then generalized and applied for Bayesian analysis by Hastings [69] is the most famous MCMC method. There are two important distributions in MH algorithm, one is the target PDF $p(\boldsymbol{\theta})$, the other is the proposal distribution $q(\cdot|\cdot)$, also called transition function. Consider Bayesian model updating and set the posterior PDF $p(\boldsymbol{\theta}|D, M)$ as the target PDF $p(\boldsymbol{\theta})$, the MH algorithm is as follows:

1. Choose $\boldsymbol{\theta}_{(0)}$ as any variable sample and set $t = 0$;
2. Generate a candidate point Y from $q(\cdot|\boldsymbol{\theta}_{(t)})$;
3. Generate a random number u from a standard uniform distribution, $u \sim U(0, 1)$;
4. If $u \leq ap_t$, then set $\boldsymbol{\theta}_{(t+1)} = Y$, otherwise set $\boldsymbol{\theta}_{(t+1)} = \boldsymbol{\theta}_{(t)}$, where $ap_t = min\left(1, \frac{p(Y)q(\boldsymbol{\theta}_{(t)}|Y)}{p(\boldsymbol{\theta}_{(t)})q(Y|\boldsymbol{\theta}_{(t)})}\right)$ is the Metropolis-Hastings acceptance probability;
5. Set $t = t + 1$;

Repeating step 2 to 5 N times, a Markov chain sample $\{\boldsymbol{\theta}_{t+1} : t = 0, \ldots, N\}$ can be obtained. The period before the sample becomes stationary is called burn-in period, the sample obtained within this period is not obtained from the posterior PDF, so it should be discarded. If the Markov chain has simulated through the whole sample space (ergodic), after discarding the sample within the burn-in period, the sample left will be distributed as the posterior PDF.
The choice of the proposal distribution $q(\cdot|\cdot)$ should follow two rules: (1) The proposal distribution should approach the target PDF $p(\boldsymbol{\theta})$ as close as possible; (2) It should be easy to sample from the proposal distribution. The MH algorithm depends only on the ratio $p(Y)/p(\boldsymbol{\theta}_{(t)})$ and $q(\boldsymbol{\theta}_{(t)}|Y)/q(Y|\boldsymbol{\theta}_{(t)})$, therefore it is independent of normalizing constants and can be used to solve Bayesian statistical problems where the posterior target distribution is usually a normalizing constant.

2.4.4 The transitional Markov chain Monte Carlo method

MCMC are often inefficient when the uncertain variables are highly correlated conditioning on the data; and when it is difficult to choose a suitable proposal distribution, it is inapplicable. To overcome these defects, a sophisticated MCMC-based algorithm called Adaptive Metropolis-Hastings (AMH) method has been developed by Beck and Au [70], the core of which is to avoid directly sampling from the target PDF but to sample from a series of simpler intermediate PDFs that converges to the target PDF. However, this method is inefficient for high-dimensional problems as kernel density estimation which is inefficient for high-dimensional problems is required. A simulation-based method called the TMCMC method, which is motivated by the intermediate PDF idea from AMH and based on MCMC, is proposed by Ching and Chen for Bayesian model updating, model class selection and model averaging problems [71]. The TMCMC method inherits the advantages of AMH but avoids inefficient kernel density estimation, so it is applicable to very peaked, flat and multimodal posterior PDFs and is efficient for high-dimensional problems. Moreover, the TMCMC method is capable of automatically selecting intermediate PDFs,

and can evaluate the evidence for the chosen model class as a by-product, which is the key component for Bayesian model class selection and Bayesian model averaging.
According to Equation (2.36), the following relation is considered

$$p(\boldsymbol{\theta}|D, M_{mi}) \propto p(D|\boldsymbol{\theta}, M_{mi})p(\boldsymbol{\theta}|M_{mi}) \tag{2.40}$$

Since the geometry of the likelihood function $p(D|\boldsymbol{\theta}, M_{mi})$ cannot be fully known in advance, directly sampling from posterior PDF $p(\boldsymbol{\theta}|D, M_{mi})$ can be difficult. Following the intermediate PDF idea of AMH, the TMCMC method avoids directly sampling from difficult posterior PDF, but samples from a sequence of intermediate PDFs which are defined by

$$p_j(\boldsymbol{\theta}) \propto p(\boldsymbol{\theta}|M_{mi}) \cdot p(D|\boldsymbol{\theta}, M_{mi})^{\beta_j} \tag{2.41}$$

where the stage number $j = 0, \ldots, sn$ and $0 = \beta_0 < \beta_1 < \cdots < \beta_{sn} = 1$.
According to this definition, the intermediate PDFs $p_j(\boldsymbol{\theta})$ will converge from the prior PDF $p_0(\boldsymbol{\theta}) = p(\boldsymbol{\theta}|M_{mi})$ to the posterior PDF $p_{sn}(\boldsymbol{\theta}) = p(\boldsymbol{\theta}|D, M_{mi})$. It is noted that, although the change between $p(\boldsymbol{\theta}|M_{mi})$ and $p(\boldsymbol{\theta}|D, M_{mi})$ can be prominent, the change between two adjacent intermediate PDFs can be small, which makes it possible to generate samples from $p_{j+1}(\boldsymbol{\theta})$ based on $p_j(\boldsymbol{\theta})$. By applying the MH algorithm in each intermediate stage to generate samples according to $p_j(\boldsymbol{\theta})$, the TMCMC method can gradually contract the parameter space to the region which has significant probability mass.
For each resampling stage, the following procedure is processed:
Given N_j samples $\{\boldsymbol{\theta}_{j,l} : l = 1, \ldots, N_j\}$ from $p_j(\boldsymbol{\theta})$, compute the plausibility weight of these samples with respect to $p_{j+1}(\boldsymbol{\theta})$

$$w(\boldsymbol{\theta}_{j,l}) = \frac{p(\boldsymbol{\theta}_{j,l}|M_{mi})p(D|\boldsymbol{\theta}_{j,l}, M_{mi})^{\beta_{j+1}}}{p(\boldsymbol{\theta}_{j,l}|M_{mi})p(D|\boldsymbol{\theta}_{j,l}, M_{mi})^{\beta_j}} = p(D|\boldsymbol{\theta}_{j,l}, M_{mi})^{\beta_{j+1}-\beta_j} \tag{2.42}$$

where the l denotes the sample index in the jth iteration stage.
Then generate each sample from $p_{j+1}(\boldsymbol{\theta})$ using the MH algorithm: the starting point of a Markov chain is a previous sample that is selected according to the probability equal to its normalized weight

$$\boldsymbol{\theta}_{j+1,l} = \boldsymbol{\theta}_{j,i} \quad \text{with probability} \quad \frac{w(\boldsymbol{\theta}_{j,i})}{\sum_{i=1}^{N_j} w(\boldsymbol{\theta}_{j,i})} \quad l = 1, \ldots, N_{j+1} \tag{2.43}$$

If N_j and N_{j+1} are large, then samples $\{\boldsymbol{\theta}_{j+1,l} : l = 1, \ldots, N_{j+1}\}$ will be distributed as $p_{j+1}(\boldsymbol{\theta})$, and we can obtain

$$\frac{\sum_{l=1}^{N_j} w(\boldsymbol{\theta}_{j,l})}{N_j} \approx \frac{\int p(\boldsymbol{\theta}|M_{mi})p(D|\boldsymbol{\theta}, M_{mi})^{\beta_{j+1}} \mathrm{d}\boldsymbol{\theta}}{\int p(\boldsymbol{\theta}|M_{mi})p(D|\boldsymbol{\theta}, M_{mi})^{\beta_j} \mathrm{d}\boldsymbol{\theta}} \tag{2.44}$$

The proposal distribution for the MH algorithm is a Gaussian distribution centered at the previous sample with a covariance matrix Σ_j equal to the scaled version of the estimated covariance matrix of $p_{j+1}(\boldsymbol{\theta})$

$$\Sigma_j = s_f^2 \sum_{l=1}^{N_j} \frac{w(\boldsymbol{\theta}_{j,l})}{\sum_{l=1}^{N_j} w(\boldsymbol{\theta}_{j,l})} (\boldsymbol{\theta}_{j,l} - \bar{\boldsymbol{\theta}}_j)(\boldsymbol{\theta}_{j,l} - \bar{\boldsymbol{\theta}}_j)^T \tag{2.45}$$

where

$$\bar{\boldsymbol{\theta}}_j = \frac{\sum_{i=1}^{N_j} w(\boldsymbol{\theta}_{j,i})\boldsymbol{\theta}_{j,i}}{\sum_{i=1}^{N_j} w(\boldsymbol{\theta}_{j,i})} \tag{2.46}$$

The parameter s_f is the prescribed scaling factor used to suppress the rejection rate and make large MCMC jumps at each stage.
The above steps are repeated until the samples are generated from the posterior PDF $p(\boldsymbol{\theta}|D, M_{mi})$ ($\beta_j = 1$).

The complete procedure of the TMCMC method is presented as follows:

1. Generate samples $\{\boldsymbol{\theta}_{0,l} : l = 1, \ldots, N_0\}$ from the prior PDF $p_0(\boldsymbol{\theta}) = p(\boldsymbol{\theta}|M_{mi})$. Repeat step 2-3 for $j = 0, \ldots, sn - 1$.

2. Choose β_{j+1} so that the Coefficient of variation (COV) of the set of plausibility weights $\{w(\boldsymbol{\theta}_{j,l}) = p(D|\boldsymbol{\theta}_{j,l}, M_{mi})^{\beta_{j+1}-\beta_j}, l = 1, \ldots, N_j\}$ is equal to a prescribed threshold, then compute the plausibility weight $w(\boldsymbol{\theta}_{j,l}) = p(D|\boldsymbol{\theta}_{j,l}, M_{mi})^{\beta_{j+1}-\beta_j}$ for $l = 1, \ldots, N_j$ and compute $S_j = \sum_{l=1}^{N_j} w(\boldsymbol{\theta}_{j,l})/N_j$.

3. Create N_j Markov chains: generate the starting point of the lth Markov chain at $\boldsymbol{\theta}_{j,l}^{now} = \boldsymbol{\theta}_{j,l}$, where $\boldsymbol{\theta}_{j,l}^{now}$ represents the current sample in the lth Markov chain. With probability $w(\boldsymbol{\theta}_{j,i})/\sum_{i=1}^{N_j} w(\boldsymbol{\theta}_{j,i})$, extract the candidate sample $\boldsymbol{\theta}_{j,l}^{C}$ from a Gaussian distribution $N(\boldsymbol{\theta}_{j,l}^{now}, \Sigma_j)$ where Σ_j is defined by Equation (2.45). Set $\boldsymbol{\theta}_{j+1,l} = \boldsymbol{\theta}_{j,l}^{C}$ and $\boldsymbol{\theta}_{j,l}^{now} = \boldsymbol{\theta}_{j,l}^{C}$ with probability $p_{j+1}(\boldsymbol{\theta}_{j,l}^{C})/p_{j+1}(\boldsymbol{\theta}_{j,l}^{now})$; otherwise, set $\boldsymbol{\theta}_{j+1,l} = \boldsymbol{\theta}_{j,l}^{now}$. Repeat this step for $l = 1, \ldots, N_{j+1}$ to obtain samples $\{\boldsymbol{\theta}_{j+1,l} : l = 1, \ldots, N_{j+1}\}$.

After sn stages, samples $\{\boldsymbol{\theta}_{sn,l} : l = 1, \ldots, N_{sn}\}$ are asymptotically distributed as the posterior PDF $p(\boldsymbol{\theta}|D, M_{mi})$, and the evidence is given by the product of the intermediate ratios

$$p(D|M_{mi}) \approx S^{(mi)} = \prod_{j=0}^{sn-1} S_j = \prod_{j=0}^{sn-1} \frac{\sum_{l=1}^{N_j} w(\boldsymbol{\theta}_{j,l})}{N_j} \tag{2.47}$$

According to the Law of Large Numbers, the expectation of $p(\boldsymbol{\theta}|D, M_{mi})$ can be estimated as

$$E[p(\boldsymbol{\theta}|D, M_{mi})] \approx \frac{1}{N_{sn}} \sum_{l=1}^{N_{sn}} p(\boldsymbol{\theta}_{sn,l}|D, M_{mi}) \equiv p(\boldsymbol{\theta}|D, \boldsymbol{M})_{TMCMC}^{(mi)} \tag{2.48}$$

If the above procedure is repeated for a set of model classes $\boldsymbol{M} = \{M_{mi} : mi = 1, \ldots, N_{class}\}$, where N_{class} is the number of model classes, then Bayesian model class selection, and model averaging can be done as follows:

$$\begin{aligned} p(M_{mi}|D, \boldsymbol{M}) &= \frac{p(D|M_{mi})p(M_{mi}|\boldsymbol{M})}{p(D|\boldsymbol{M})} \\ &\approx S^{(mi)} \cdot p(M_{mi}|\boldsymbol{M}) / \left[\sum_{mk=1}^{N_{class}} S^{(mk)} p(M_{mk}|\boldsymbol{M}) \right] = p_{TMCMC}^{(mi)} \end{aligned} \tag{2.49}$$

$$E[p(\boldsymbol{\theta}|D,\boldsymbol{M})] \approx \sum_{mi=1}^{N_{class}} p(\boldsymbol{\theta}|D,\boldsymbol{M})_{TMCMC}^{(mi)} \cdot p_{TMCMC}^{(mi)} \equiv p(\boldsymbol{\theta}|D,\boldsymbol{M})_{TMCMC}^{average} \tag{2.50}$$

where the prior PDF $p(M_{mi}|\boldsymbol{M}) = 1/N_{class}$, since all model classes are considered as equally likely apriori.

3 HHT-based Identification of general linear time-varying systems

3.1 HHT-based identification method for general linear time-varying systems

Compared with the HHT-based identification method proposed by Shi and Law which can solve only linear time-varying chainlike systems, the HHT-based identification method proposed here extends the identification of linear time-varying chainlike systems to general linear time-varying systems including not only chainlike systems, but also non-chainlike systems.

The governing differential equation of a general linear time-varying n-DOF system which is given by Equation (2.14) can be embodied by

$$\begin{bmatrix} m_{11}(t) & \dots & m_{1i}(t) & \dots & m_{1n}(t) \\ \vdots & \vdots & \vdots & \vdots & \vdots \\ m_{j1}(t) & \dots & m_{ji}(t) & \dots & m_{jn}(t) \\ \vdots & \vdots & \vdots & \vdots & \vdots \\ m_{n1}(t) & \dots & m_{ni}(t) & \dots & m_{nn}(t) \end{bmatrix} \begin{bmatrix} \ddot{y}_1(t) \\ \vdots \\ \ddot{y}_i(t) \\ \vdots \\ \ddot{y}_n(t) \end{bmatrix} + \begin{bmatrix} c_{11}(t) & \dots & c_{1i}(t) & \dots & c_{1n}(t) \\ \vdots & \vdots & \vdots & \vdots & \vdots \\ c_{j1}(t) & \dots & c_{ji}(t) & \dots & c_{jn}(t) \\ \vdots & \vdots & \vdots & \vdots & \vdots \\ c_{n1}(t) & \dots & c_{ni}(t) & \dots & c_{nn}(t) \end{bmatrix} \begin{bmatrix} \dot{y}_1(t) \\ \vdots \\ \dot{y}_i(t) \\ \vdots \\ \dot{y}_n(t) \end{bmatrix}$$

$$+ \begin{bmatrix} k_{11}(t) & \dots & k_{1i}(t) & \dots & k_{1n}(t) \\ \vdots & \vdots & \vdots & \vdots & \vdots \\ k_{j1}(t) & \dots & k_{ji}(t) & \dots & k_{jn}(t) \\ \vdots & \vdots & \vdots & \vdots & \vdots \\ k_{n1}(t) & \dots & k_{ni}(t) & \dots & k_{nn}(t) \end{bmatrix} \begin{bmatrix} y_1(t) \\ \vdots \\ y_i(t) \\ \vdots \\ y_n(t) \end{bmatrix} = \begin{bmatrix} f_1(t) \\ \vdots \\ f_i(t) \\ \vdots \\ f_n(t) \end{bmatrix} \quad (3.1)$$

Therefore, the coefficient matrices in Equation (2.14) can be embodied by

$$\mathbf{M}(t) = \begin{bmatrix} m_{11}(t) & \dots & m_{1i}(t) & \dots & m_{1n}(t) \\ \vdots & \vdots & \vdots & \vdots & \vdots \\ m_{j1}(t) & \dots & m_{ji}(t) & \dots & m_{jn}(t) \\ \vdots & \vdots & \vdots & \vdots & \vdots \\ m_{n1}(t) & \dots & m_{ni}(t) & \dots & m_{nn}(t) \end{bmatrix}$$

$$\mathbf{C}(t) = \begin{bmatrix} c_{11}(t) & \dots & c_{1i}(t) & \dots & c_{1n}(t) \\ \vdots & \vdots & \vdots & \vdots & \vdots \\ c_{j1}(t) & \dots & c_{ji}(t) & \dots & c_{jn}(t) \\ \vdots & \vdots & \vdots & \vdots & \vdots \\ c_{n1}(t) & \dots & c_{ni}(t) & \dots & c_{nn}(t) \end{bmatrix} \quad (3.2)$$

$$\mathbf{K}(t) = \begin{bmatrix} k_{11}(t) & \dots & k_{1i}(t) & \dots & k_{1n}(t) \\ \vdots & \vdots & \vdots & \vdots & \vdots \\ k_{j1}(t) & \dots & k_{ji}(t) & \dots & k_{jn}(t) \\ \vdots & \vdots & \vdots & \vdots & \vdots \\ k_{n1}(t) & \dots & k_{ni}(t) & \dots & k_{nn}(t) \end{bmatrix}$$

where $\ddot{y}_i(t), \dot{y}_i(t), y_i(t), i = 1, \dots, n$ are the accelerations, velocities and displacements of the system, respectively; $f_j(t), j = 1, \dots, n$ are the excitation signals of the system; $m_{ji}(t), c_{ji}(t), k_{ji}(t), j, i = 1, \dots, n$ are the elements of the system mass, stiffness and damping matrices, respectively.

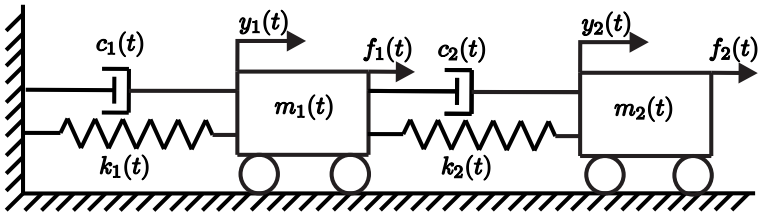

Figure 3.1: A 2-DOF linear time-varying chainlike system.

The following 2-DOF systems illustrate the difference between chainlike and non-chainlike systems:
If the system is a 2-DOF linear time-varying chainlike system shown in Figure 3.1, $m_j(t), c_j(t), k_j(t), j = 1, 2$ are the mass, damping and stiffness coefficients respectively, then the governing differential equations of the system are given by

$$\begin{bmatrix} m_1(t) & 0 \\ 0 & m_2(t) \end{bmatrix} \begin{bmatrix} \ddot{y}_1(t) \\ \ddot{y}_2(t) \end{bmatrix} + \begin{bmatrix} c_1(t) + c_2(t) & -c_2(t) \\ c_2(t) & c_2(t) \end{bmatrix} \begin{bmatrix} \dot{y}_1(t) \\ \dot{y}_2(t) \end{bmatrix} + \begin{bmatrix} k_1(t) + k_2(t) & -k_2(t) \\ -k_2(t) & k_2(t) \end{bmatrix} \begin{bmatrix} y_1(t) \\ y_2(t) \end{bmatrix} = \begin{bmatrix} f_1(t) \\ f_2(t) \end{bmatrix} \tag{3.3}$$

If the system is a 2-DOF linear time-varying non-chainlike system shown in Figure 3.2, $m(t), I(t), k_j(t), c_j(t), j = 1, 2$ are the mass, mass moment of inertia, stiffness and damping coefficients respectively, then the governing differential equations of the system are given by

$$\begin{bmatrix} m(t) & 0 \\ 0 & I(t) \end{bmatrix} \begin{bmatrix} \ddot{x}(t) \\ \ddot{\varphi}(t) \end{bmatrix} + \begin{bmatrix} c_1(t) + c_2(t) & c_1(t)L_1 - c_2(t)L_2 \\ c_1(t)L_1 - c_2(t)L_2 & c_1(t)L_1^2 + c_2(t)L_2^2 \end{bmatrix} \begin{bmatrix} \dot{x}(t) \\ \dot{\varphi}(t) \end{bmatrix} + \begin{bmatrix} k_1(t) + k_2(t) & k_1(t)L_1 - k_2(t)L_2 \\ k_1(t)L_1 - k_2(t)L_2 & k_1(t)L_1^2 + k_2(t)L_2^2 + k_R(t) \end{bmatrix} \begin{bmatrix} x(t) \\ \varphi(t) \end{bmatrix} = \begin{bmatrix} f(t) \\ -f(t)L_2 \end{bmatrix} \tag{3.4}$$

With the help of Equations (3.3) - (3.4), it is noted that: For n-DOF linear time-varying chainlike systems, the type of motion of each DOF is the same (it might be a translation in the same/parallel direction or a rotation around the same axis). The system stiffness and damping coefficient matrices are tridiagonal matrices, and the elements of the system

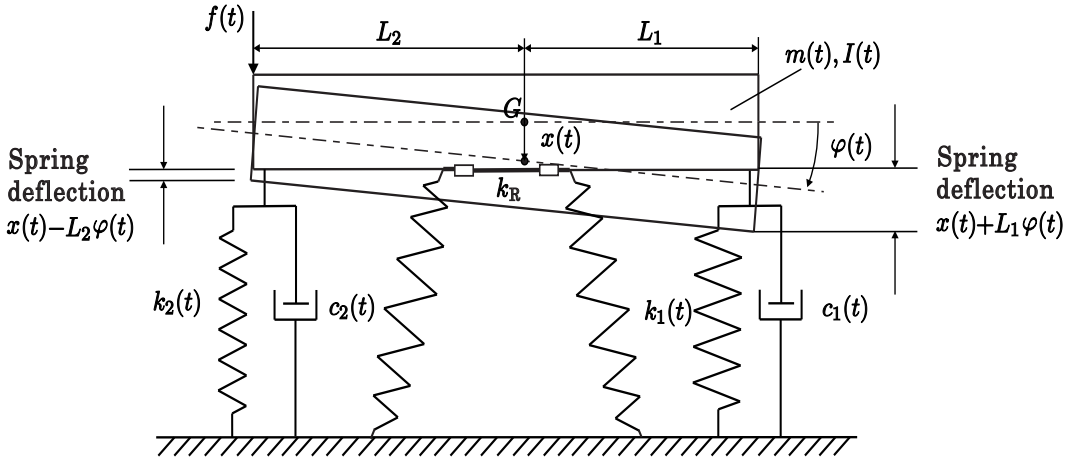

Figure 3.2: A 2-DOF linear time-varying non-chainlike system.

stiffness and damping coefficient matrices are simply related to the system stiffness and damping coefficients as in following expressions:
$c_{jj}(t) = c_j(t) + c_{j+1}(t), k_{jj}(t) = k_j(t) + k_{j+1}(t)$ when $j = 1, \ldots, n-1, n \geq 2$;
$c_{jj-1}(t) = c_{j-1j}(t) = -c_j(t), k_{jj-1}(t) = k_{j-1j}(t) = -k_j(t)$ when $j = 2, \ldots, n, n \geq 2$;
$c_{jj-2}(t) = c_{j-2j}(t) = 0, k_{jj-2}(t) = k_{j-2j}(t) = 0$ when $j = 3, \ldots, n, n \geq 3$;
$c_{jj}(t) = c_j(t), k_{jj}(t) = k_j(t)$ when $j = n$.
Thus, the identified results of n-DOF linear time-varying chainlike systems can be obtained from 2n time-varying equations.
For n-DOF linear time-varying non-chainlike systems, the type of motion of each DOF can be different (it might be a translation, a rotation, a translation in a direction perpendicular to the aforementioned translation or a rotation around an axis perpendicular to the aforementioned rotational axis). The relations between the elements of the system stiffness and damping coefficient matrices and the corresponding system stiffness and damping coefficients are dependent on the motions of individual DOFs and thus have no uniform expressions as those of chainlike systems. Thus, $n \times 2n$ time-varying equations are required to obtain the identified result of each element of the system stiffness and damping coefficient matrices first, and then the identified results of individual system stiffness and damping coefficients are obtained from the motion-dependent relations (These two procedures are also available for n-DOF linear time-varying chainlike systems).

The main procedures of the HHT-based identification method for general linear time-varying systems are presented as follows:

1. Use EMD and HT to process the system response signals (displacements $y_i(t)$, velocities $\dot{y}_i(t)$ and accelerations $\ddot{y}_i(t)$) of Equation (3.1), n IMFs and a residue as well as n analytical IMFs and an analytical residue are obtained corresponding to each original response signal.

2. Sum the n analytical IMFs and the analytical residue of each original response signal to form new analytical signals $Y_i(t)$, $\dot{Y}_i(t)$ and $\ddot{Y}_i(t)$. Here, the subscript i denotes the

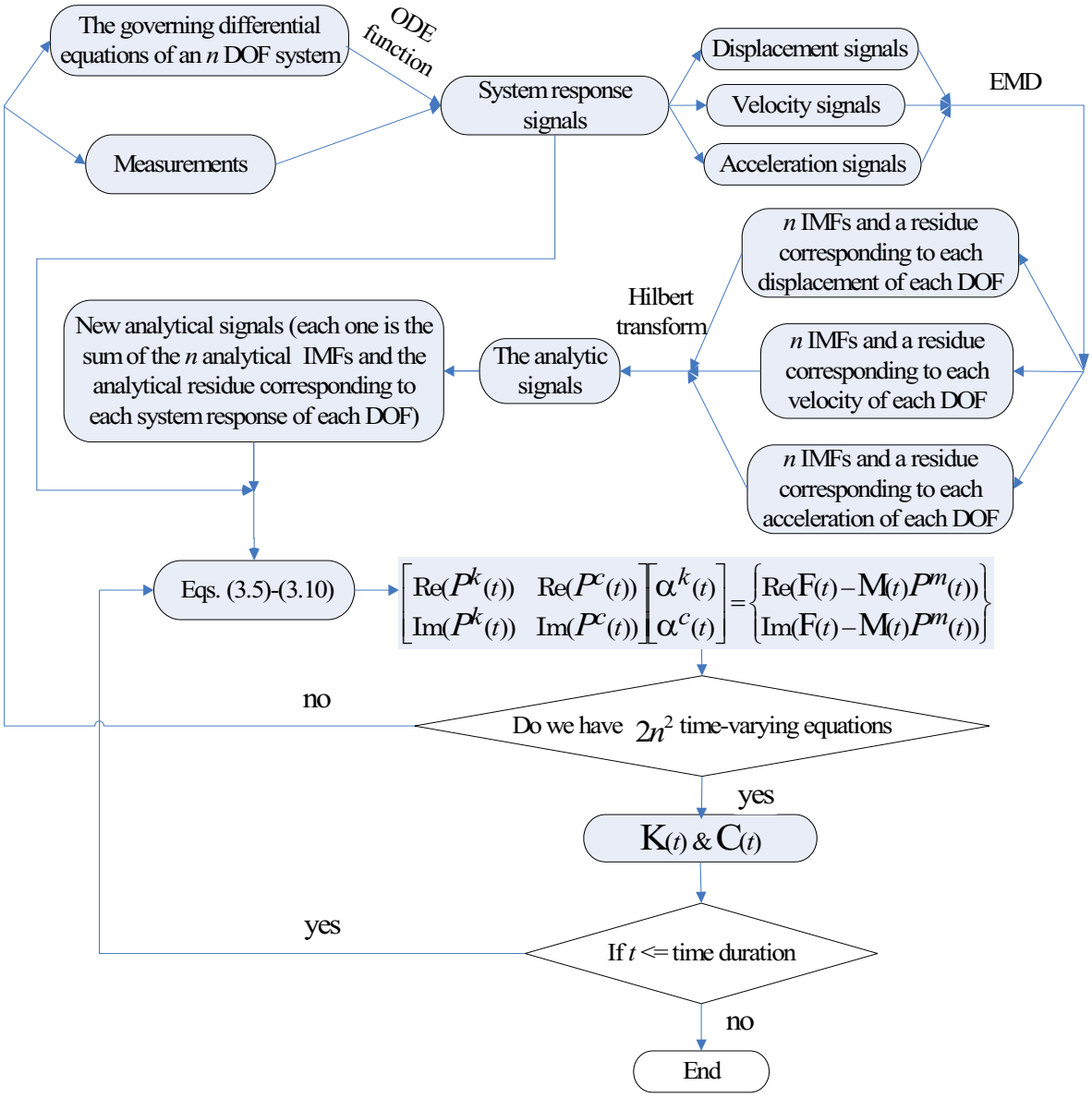

Figure 3.3: Main procedures of the HHT-based identification method for general linear time-varying systems.

ith element of the signal which corresponds to the ith DOF. A differential equation expressed by the analytical signals $Y_i(t)$, $\dot{Y}_i(t)$ and $\ddot{Y}_i(t)$ can be obtained for a general linear time-varying system.

3. With the help of the system response signals $y_i(t)$, $\dot{y}_i(t)$ and $\ddot{y}_i(t)$ as well as the new synthesized analytical signals $Y_i(t)$, $\dot{Y}_i(t)$ and $\ddot{Y}_i(t)$, the differential equation on the analytical signals at one time step can be simplified and written in compact matrix notation as

$$\boldsymbol{P}^k(t)\boldsymbol{\alpha}^k(t) + \boldsymbol{P}^c(t)\boldsymbol{\alpha}^c(t) = \boldsymbol{F}(t) - \mathbf{M}(t)\boldsymbol{P}^m(t) \tag{3.5}$$

in which

$$\boldsymbol{\alpha}^k(t) = [k_{11}(t), \ldots, k_{1n}(t), \ldots, k_{i1}(t), \ldots, k_{in}(t), \ldots, k_{n1}(t), \ldots, k_{nn}(t)]^T \tag{3.6}$$

$$(n^2 \times 1)$$

$$\boldsymbol{\alpha}^c(t) = [c_{11}(t), \ldots, c_{1n}(t), \ldots, c_{i1}(t), \ldots, c_{in}(t), \ldots, c_{n1}(t), \ldots, c_{nn}(t)]^T \tag{3.7}$$

$$(n^2 \times 1)$$

$$\boldsymbol{P}^k(t) = \begin{bmatrix} Y_1(t) & \cdots & Y_n(t) & & & & & & \\ & & & \ddots & & & & \mathbf{0} & \\ & & & & Y_1(t) & \cdots & Y_n(t) & & \\ & \mathbf{0} & & & & & & \ddots & \\ & & & & & & & Y_1(t) & \cdots & Y_n(t) \end{bmatrix} \tag{3.8}$$

$$(n \times n^2)$$

$$\boldsymbol{P}^c(t) = \begin{bmatrix} \dot{Y}_1(t) & \cdots & \dot{Y}_n(t) & & & & & & \\ & & & \ddots & & & & \mathbf{0} & \\ & & & & \dot{Y}_1(t) & \cdots & \dot{Y}_n(t) & & \\ & \mathbf{0} & & & & & & \ddots & \\ & & & & & & & \dot{Y}_1(t) & \cdots & \dot{Y}_n(t) \end{bmatrix} \tag{3.9}$$

$$(n \times n^2)$$

$$\boldsymbol{P}^m(t) = [\ \ddot{Y}_1(t) \quad \cdots \quad \ddot{Y}_i(t) \quad \cdots \quad \ddot{Y}_n(t)]^T\ ] \tag{3.10}$$

$$(n \times 1)$$

As the coefficients above are complex numbers, Equation (3.5) can be assembled as

$$\begin{bmatrix} \mathrm{Re}(\boldsymbol{P}^k(t)) \\ \mathrm{Im}(\boldsymbol{P}^k(t)) \end{bmatrix} \boldsymbol{\alpha}^k(t) + \begin{bmatrix} \mathrm{Re}(\boldsymbol{P}^c(t)) \\ \mathrm{Im}(\boldsymbol{P}^c(t)) \end{bmatrix} \boldsymbol{\alpha}^c(t) = \begin{Bmatrix} \mathrm{Re}(\boldsymbol{F}(t) - \mathbf{M}(t)\boldsymbol{P}^m(t)) \\ \mathrm{Im}(\boldsymbol{F}(t) - \mathbf{M}(t)\boldsymbol{P}^m(t)) \end{Bmatrix} \tag{3.11}$$

$$(2n \times n^2) \qquad (2n \times n^2) \qquad (2n \times 1)$$

or

$$\begin{bmatrix} \mathrm{Re}(\boldsymbol{P}^k(t)) & \mathrm{Re}(\boldsymbol{P}^c(t)) \\ \mathrm{Im}(\boldsymbol{P}^k(t)) & \mathrm{Im}(\boldsymbol{P}^c(t)) \end{bmatrix} \begin{bmatrix} \boldsymbol{\alpha}^k(t) \\ \boldsymbol{\alpha}^c(t) \end{bmatrix} = \begin{Bmatrix} \mathrm{Re}(\boldsymbol{F}(t) - \mathbf{M}(t)\boldsymbol{P}^m(t)) \\ \mathrm{Im}(\boldsymbol{F}(t) - \mathbf{M}(t)\boldsymbol{P}^m(t)) \end{Bmatrix} \tag{3.12}$$

$$(2n \times 2n^2) \qquad (2n^2 \times 1) \qquad (2n \times 1)$$

4. Repeat step 3 until the results in the required time history are obtained.

Equation (3.11) or Equation (3.12) contains $2n$ time-varying equations, so we can only estimate 2n unknows at any time instant t by solving Equation (3.11) or Equation (3.12) if we know only one set of system responses $y_i(t)$, $\dot{y}_i(t)$ and $\ddot{y}_i(t)$. However, we have $2n^2$ unknown elements of the system stiffness and damping coefficient matrices in Equation (3.11) or Equation (3.12). In order to get the values of all the $2n^2$ unknown elements, we should run n experiments to get n sets of system responses $y_i(t)$, $\dot{y}_i(t)$ and $\ddot{y}_i(t)$ (for each experiment, the same initial conditions are given at a different DOF of the system), thus we have $n \times 2n$ time-varying equations.
For the 1-DOF case, the above Equation (3.11) or Equation (3.12) has only 2 time-varying equations and 2 unknown elements, so we can solve Equation (3.11) or Equation (3.12) when we have only one set of system responses $y_i(t)$, $\dot{y}_i(t)$ and $\ddot{y}_i(t)$ for the 2 unknown elements, which can be simplified as

$$\boldsymbol{\alpha}^c(t) = c(t) = \frac{\mathrm{Im}(\boldsymbol{F}(t)/Y(t))}{\omega(t)} - m(t)\left(\frac{2\dot{A}(t)}{A(t)} + \frac{\dot{\omega}(t)}{\omega(t)}\right) \tag{3.13}$$

$$\boldsymbol{\alpha}^k(t) = k(t) = m(t)\omega_0^2(t) \tag{3.14}$$

in which

$$\begin{aligned}\omega_0^2(t) &= \frac{k(t)}{m(t)} \\ &= \omega^2(t) + \frac{\mathrm{Re}(\boldsymbol{F}(t)/Y(t))}{m(t)} - \frac{\mathrm{Im}(\boldsymbol{F}(t)/Y(t))\dot{A}(t)}{m(t)\omega(t)A(t)} - \frac{\ddot{A}(t)}{A(t)} + \frac{2\dot{A}^2(t)}{A^2(t)} + \frac{\dot{A}(t)\dot{\omega}(t)}{A(t)\omega(t)}\end{aligned} \tag{3.15a}$$

$$\omega(t) = \dot{\psi}(t) = \frac{y(t)\dot{\tilde{y}}(t) - \dot{y}(t)\tilde{y}(t)}{A^2(t)} = \mathrm{Im}\left[\frac{\dot{Y}(t)}{Y(t)}\right] \tag{3.15b}$$

$$\dot{A}(t) = \frac{y(t)\dot{y}(t) + \tilde{y}(t)\dot{\tilde{y}}(t)}{A(t)} = A(t)\mathrm{Re}\left[\frac{\dot{Y}(t)}{Y(t)}\right] \tag{3.15c}$$

$$\dot{\omega}(t) = \mathrm{Im}\left[\frac{\ddot{Y}(t)}{Y(t)}\right] - 2\frac{\dot{A}(t)\omega(t)}{A(t)} \tag{3.15d}$$

$$\ddot{A}(t) = A(t)\left(\mathrm{Re}\left[\frac{\ddot{Y}(t)}{Y(t)}\right] + \omega^2(t)\right) \tag{3.15e}$$

Equations (3.14) - (3.15) of the proposed method are equivalent to the corresponding equations of HHT-based method proposed by Shi and Law for 1-DOF case (see Section 2.3). In order to demonstrate the effectiveness, accuracy and robustness of the proposed HHT-based identification method for general linear time-varying systems, we will process simulations on 1-DOF and 2-DOF linear time-varying systems in the next section.

3.2 HHT-based Identification of general linear time-varying systems from simulated time histories

Simulation is the imitation of the operation of a real-world process or system over time which involves the generation of an artificial history of the system and the observation of the artificial history to draw inferences concerning the operating characteristics of the real system that is represented [72]. It is widely used in many fields, such as performance optimization [73], safety engineering [74], testing and training [75, 76], education, business, social science and engineering [77]. Usually, simulation can be divided into physical simulation and computer simulation. The former is defined as an imitation of the operation of a real system in which physical objects are substituted for the system, whereas the latter is defined as an imitation of the operation of a real system on a computer. Computer simulation has many advantages, for example, it allows experimentation without disruptions to existing systems, allows concepts to be tested prior to the installation of new systems, detects unforeseen problems or bugs that may exist in systems' design, gains in knowledge on systems, speeds up the analysis of systems, forces analysts to fully define all parameters pertinent to the operations of systems, and enhances creativity in the design of systems [78].
Since it has so many benefits, we will carry out computer simulation on general linear time-varying systems with the aid of MATLAB in this section. For an n-DOF general linear time-varying system, the procedures of the identification simulation are as follows:

1. Run n experiments to get n sets of noiseless system responses in the required time history (for each experiment, solve ODE of the system with the same initial conditions given at a different DOF of the system, obtaining each set of system responses: displacement $y_{i,q}(t)$, velocity $\dot{y}_{i,q}(t)$ and acceleration $\ddot{y}_{i,q}(t)$ at each time instant where the subscripts $i = 1, \ldots, n$ denotes the index of DOF and $q = 1, \ldots, n$ denotes the index of experiment). Apply EMD method to decompose these noiseless system responses to obtain their corresponding IMFs. Use these IMFs in the proposed HHT-based identification method to obtain the identified results of the elements of system stiffness and damping coefficient matrices, and then the identified results of individual system stiffness and damping coefficients can be obtained from the motion-dependent relations (see Section 3.1).

2. For each noiseless system response obtained in step (1), given the ratio *Nstd* of the standard deviation of the added noise and that of the corresponding noiseless system response as well as the number *NE* of trials, a different white noise signal is generated with the same ratio *Nstd* by standard normally distributed pseudorandom numbers and added to the corresponding noiseless system response in each trial to obtain *NE* noise-added system responses as the measured system responses in *NE* trials. Since there exists white noise in the measured system responses, directly decomposing the system responses by EMD will leave noise remain in IMFs. In order to remove the high-frequency noise from the noise-added system responses

before they are decomposed by EMD, a fourth-order zero-lag Butterworth low-pass digital filter [79] is used with the proper cutoff frequency of the filter determined by a residual analysis proposed by Winter[80]. For a raw signal with N sample points, the residual at any cutoff frequency is calculated as follows:

$$R(f_c) = \sqrt{\frac{1}{N}\sum_{i=1}^{N}(X_i - \hat{X}_i)^2} \tag{3.16}$$

in which f_c is the cutoff frequency of the fourth-order zero-lag low-pass filter, X_i is the ith sample of the raw signal and $\hat{X}_i$ is the ith sample of the filtered signal obtained at f_c. By application of Equation (3.16), the raw signal is filtered at a wide range of cutoff frequencies, and a residual amplitude versus cutoff frequeny curve is plotted, in which a linear regression line is determined where the residual becomes a linear function of the cutoff frequeny and represents estimate of the noise residual. With the help of the linear regression line, the proper cutoff frequency is selected with the compromise that the amount of signal distortion and the amount of noise passed through the filter are equal. Then, the proper cutoff frequency is verified by the power spectral density estimation and Hilbert spectral analysis. After filtered by the fourth-order zero-lag Butterworth low-pass filter with the selected proper cutoff frequencies, the *NE* system responses are decomposed by EMD to obtain their corresponding IMFs (the number of IMFs should be $n \times NE$). Then, these IMFs are averaged to obtain n ensemble means of IMFs for the *NE* noise-added system responses.

3. Use the ensemble means of IMFs of n sets of system responses (the number of the IMFs should be $3n^3$) in the proposed HHT-based identification method to obtain the identified results of the elements of system stiffness and damping coefficient matrices, and then the identified results of individual system stiffness and damping coefficients can be obtained from the motion-dependent relations (see Section 3.1). Compare these identified results with their counterparts obtained in step (1).

The aforementioned identification simulation is carried out on 1-DOF and 2-DOF linear time-varying mass-spring-damper dynamical systems in forced vibrations with three types of time variation of stiffness coefficients: smooth, abrupt and periodical variations to demonstrate the effectiveness, accuracy and robustness of the HHT-based identification method for general linear time-varying systems. The identification simulation is processed by MATLAB programs. The time interval between two adjacent data points in the simulations is 0.01 seconds, and the whole time history is 10 seconds. The noiseless system responses are obtained by solving the system differential equations, and the noise-added system responses are generated with the ratio of the standard deviation of the added white noise and that of the corresponding noiseless system response *Nstd* set as 0.05 and the number of trials *NE* set as 15.
For 1-DOF linear time-varying systems, the following common information is given ([26]):

the mass of the system is assumed to be known as $m = 1$kg, the initial conditions are given as $y(0) = 1$m and $\dot{y}(0) = 0$m/s. An impact excitation is given at the mass by $f(t) = 1$N when $t = 0$s, $f(t) = 0$N otherwise. For 2-DOF linear time-varying non-chainlike systems which adopt the model shown in Figure 3.2, the following common information is given ([81]): the system damping coefficients are given by: $c_1 = 0$Ns/m, $c_2 = 0$Ns/m, the mass and the mass moment of inertia as well as the length parameters of the system are assumed to be known as $m = 840/2$kg, $I = 820$ kgm^2, $L_1 = 0.7$m, $L_2 = 0.75$m. The initial conditions for the two experiments are given as $x(0) = 0$m, $\varphi(0) = 1$rad, $\dot{x}(0) = 0$m/s, $\dot{\varphi}(0) = 0$rad/s as well as $x(0) = 1$m, $\varphi(0) = 0$rad, $\dot{x}(0) = 0$m/s, $\dot{\varphi}(0) = 0$rad/s. An impact excitation is given at mass 1 by $f_1(t) = 200$N when $t = 0$s, $f_1(t) = 0$N otherwise. For 2-DOF linear time-varying chainlike systems which adopt the model shown in Figure 3.1, the following common information is given ([26]): the system damping coefficients are given by: $c_1 = 30$Ns/m, $c_2 = 0$Ns/m, the system mass coefficients are assumed to be known as $m_1 = m_2 = 50$kg. The initial conditions for the two experiments are given as $y_1(0) = 0$m, $y_2(0) = 1$m, $\dot{y}_1(0) = 0$m/s, $\dot{y}_2(0) = 0$m/s as well as $y_1(0) = 1$ m, $y_2(0) = 0$m, $\dot{y}_1(0) = 0$m/s, $\dot{y}_2(0) = 0$m/s. An impact excitation is given at mass 1 by $f_1(t) = 200$N when $t = 0$s, $f_1(t) = 0$N otherwise. By application of the proposed HHT-based identification method, the identified values of the elements of the system stiffness and damping coefficient matrices can be obtained, and according to their relations with the system coefficients $k_j(t), c_j(t), j = 1$ or $j = 1, 2$ (see Section 3.1), the identified results of the system coefficients $k_j(t), c_j(t), j = 1$ or $j = 1, 2$ can be obtained. The identified stiffness coefficients of the smoothly and abruptly varying systems are presented in the following sections, whereas the identified damping coefficients of the former systems and all the identified results of the periodically varying systems are presented in Appendices A.1.1 - A.1.4.

3.2.1 HHT-based Identification of 1-DOF linear time-varying systems

For 1-DOF linear time-varying forced vibration systems to be simulated, the system stiffness coefficients with three types of time variation and system damping coefficients are given as follows ([26]):

Table 3.1: System coefficients of 1-DOF linear time-varying systems

System coefficients / Type of systems	System stiffness coefficient and damping coefficient
1-DOF linear smoothly varying system	$k(t) = 100\pi^2\text{N/m}, c(t) = 0.7\text{Ns/m}$ when $t < 2\text{s}$, $k(t) = 100\pi^2 - 10\pi^2 t\text{N/m}, c(t) = 0.7 + 0.15t\text{Ns/m}$ when $2\text{s} \leq t \leq 4\text{s}$, $k(t) = 80\pi^2\text{N/m}, c(t) = 1.0\text{Ns/m}$ when $t > 4\text{s}$.
1-DOF linear abruptly varying system	$k(t) = 100\pi^2\text{N/m}$ when $t < 1.5\text{s}$, $k(t) = 60\pi^2\text{N/m}$ when $1.5\text{s} \leq t \leq 3.5\text{s}$, $k(t) = 80\pi^2\text{N/m}$ when $t \geq 3.5\text{s}$, $c(t) = 0.7\text{Ns/m}$ for any t.
1-DOF linear periodically varying system	$k(t) = 100\pi^2 - 10\pi^2 \sin(2\pi t)\text{N/m}$ for any t, $c(t) = 1.26\text{Ns/m}$ for any t.

The identified results of the stiffness coefficients of the 1-DOF linear smoothly and abruptly varying systems, their relative errors as well as the time-frequency distribution of the response signal of the 1-DOF linear abruptly varying system are shown in Figures 3.4 - 3.6. It can be seen from the figures that: For the 1-DOF linear smoothly varying system, when noiseless system responses are used as input of the HHT-based identification method, the identified stiffness coefficient matches the true value of the corresponding system stiffness coefficient quite well; even when noise-added system responses are used as input, although the identified stiffness coefficient is contaminated by noise, it is still close to its true value (with maximal relative error less than 2.1%); For the 1-DOF linear abruptly varying system, two abrupt jumps of the IF are noticed around $t = 1.5\text{s}$ and $t = 3.5\text{s}$ in Figure 3.5, which means that there are abrupt changes in the physical parameter of the system at these two time points. And the identified results of the stiffness coefficient (shown in Figure 3.6) obtained by using noiseless and noise-added system responses as input of the HHT-based identification method have large identification errors around $t = 1.5\text{s}$ and $t = 3.5\text{s}$, which accord with the observed changes of IF in Figure 3.5, and are due to the abrupt changes of the true system stiffness at these time instants. This implies that the proposed method has bad ability to capture the abrupt change of the system parameters due to the limitations of Equation (2.16). At other time instants, the identified results of the stiffness coefficient are close to its true value and have small relative errors (always less than 2.7%). For both systems, the identified stiffness coefficients gained by the proposed HHT-based identification method are equivalent to their respective counterparts which are obtained by the HHT-based method proposed by Shi and Law, since the two methods share the same equations for 1-DOF systems.

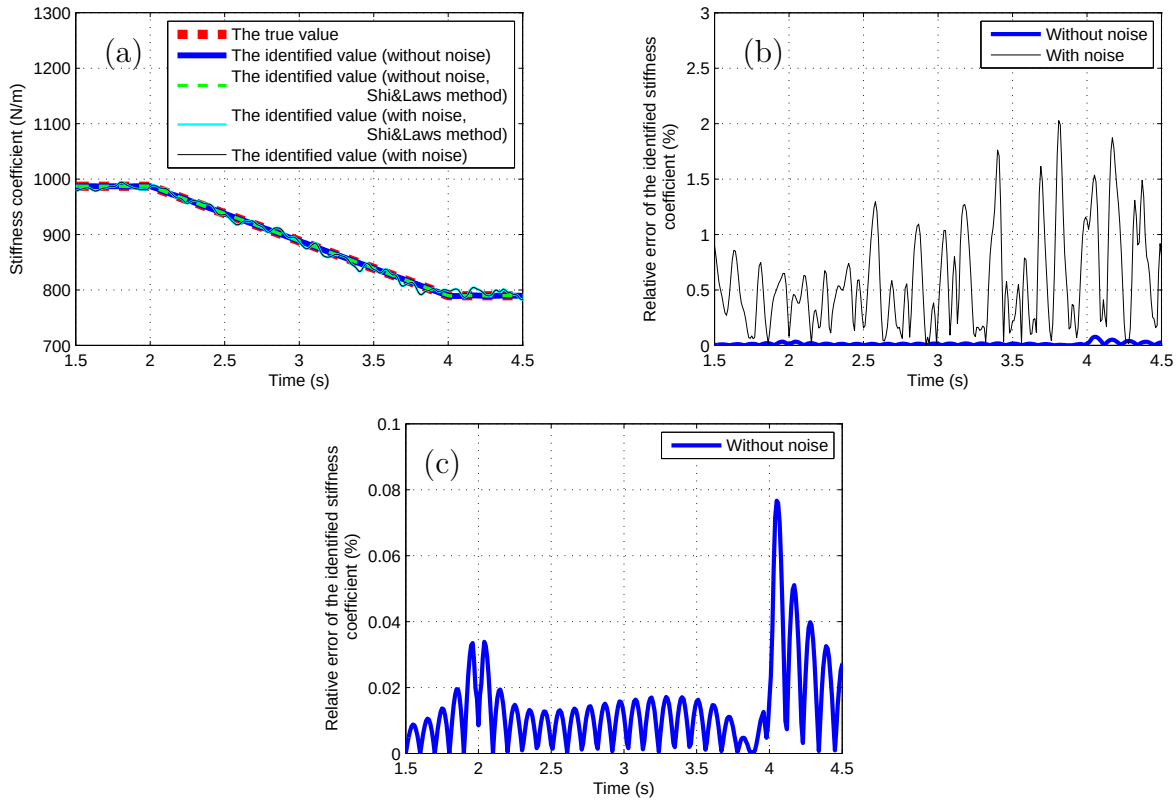

Figure 3.4: Stiffness coefficient of a 1-DOF linear smoothly varying forced vibration system: (a) The true value and the identified values of the stiffness coefficient, (b) Relative errors of the identified values of the stiffness coefficient, (c) Relative errors of the identified values of the stiffness coefficient (without noise in system responses).

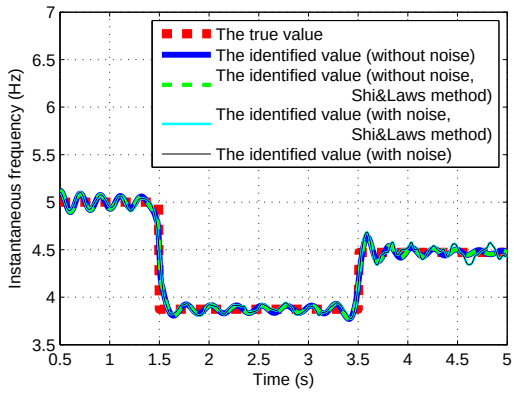

Figure 3.5: Instantaneous frequency of a 1-DOF linear abruptly varying forced vibration system.

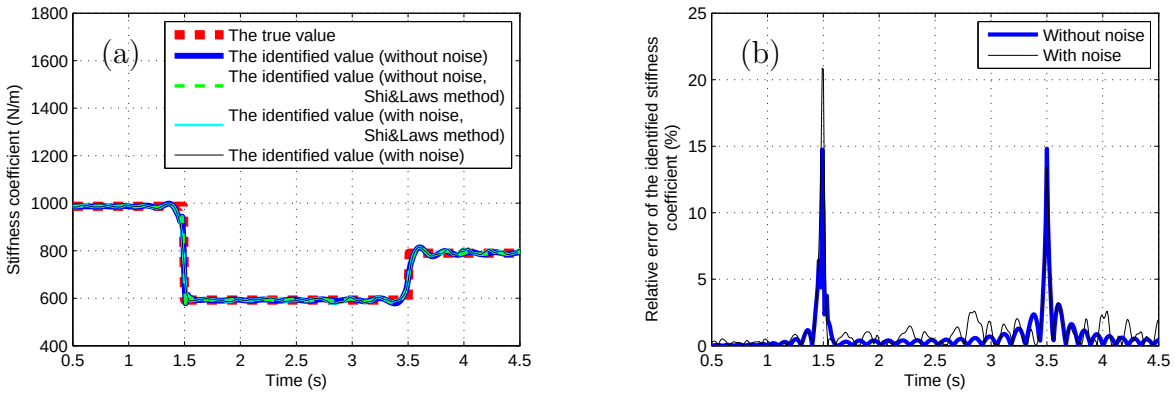

Figure 3.6: Stiffness coefficient of a 1-DOF linear abruptly varying forced vibration system: (a) The true value and the identified values of the stiffness coefficient, (b) Relative errors of the identified values of the stiffness coefficient.

3.2.2 HHT-based Identification of 2-DOF linear time-varying non-chainlike systems

For the 2-DOF linear time-varying non-chainlike forced vibration systems which adopt the model shown in Figure 3.2, the system stiffness coefficients are given as follows:

Table 3.2: System stiffness coefficients of 2-DOF linear time-varying non-chainlike systems

System coefficients / Type of systems	System stiffness coefficient (N/m)
2-DOF linear smoothly varying system	$k_2(t) = 10000$ when $t < 1$s, $k_2(t) = 10000 - 100(t-1)$ when $1\text{s} \le t \le 3$s, $k_2(t) = 9800$ when $t > 3$s, $k_1(t) = 10000$, $k_R(t) = 25000$ for any t.
2-DOF linear abruptly varying system	$k_1(t) = 10000$ when $t \le 3$s, $k_1(t) = 9000$ when $t > 3$s, $k_2(t) = 10000$, $k_R(t) = 25000$ for any t.
2-DOF linear periodically varying system	$k_1(t) = 10000$ when $t < 2$s, $k_1(t) = 10000 - 100\sin[\pi(t-2)]$ when $t \ge 2$s, $k_2(t) = 10000$, $k_R(t) = 25000$ for any t.

Figures 3.7 - 3.10 present the identified results of the system stiffness coefficients and their relative errors of the 2-DOF linear smoothly and abruptly varying non-chainlike forced vibration systems.
It is found from the figures that: For the 2-DOF linear smoothly varying non-chainlike forced vibration system, when noiseless system responses are used as input of the HHT-based identification method, the identified stiffness coefficients match their respective true values quite well, except around $t = 1$s and $t = 3$s abrupt changes are found, due to the abrupt changes of the true system stiffness at these time instants. When noise-added system responses are used as input, the identified results are contaminated by noise, though the identified stiffness coefficients are still found very close to their corresponding true values, and have small relative errors (whose maxima are less than 0.69% and 0.60% respectively); For the 2-DOF linear abruptly varying non-chainlike forced vibration system, no matter using noiseless or noise-added system responses as input of the HHT-based identification method, the identified stiffness coefficients have relatively large identification errors around time instant $t = 3$s (with maximal relative error of k_1 less than 5.3% and that of k_2 less than 1.6%), which implies that the adopted method has bad ability to capture the abrupt change of the system parameters due to the limitations of Equation (2.16). Nevertheless, these relatively quite large identification errors can be used to detect the abrupt stiffness variations of the system. At other time instants, the identified stiffness

coefficients are close to their respective true values with small relative errors (the maximal relative error of k_1 is less than 1.1% and the maximal relative error of k_2 is less than 0.89%).

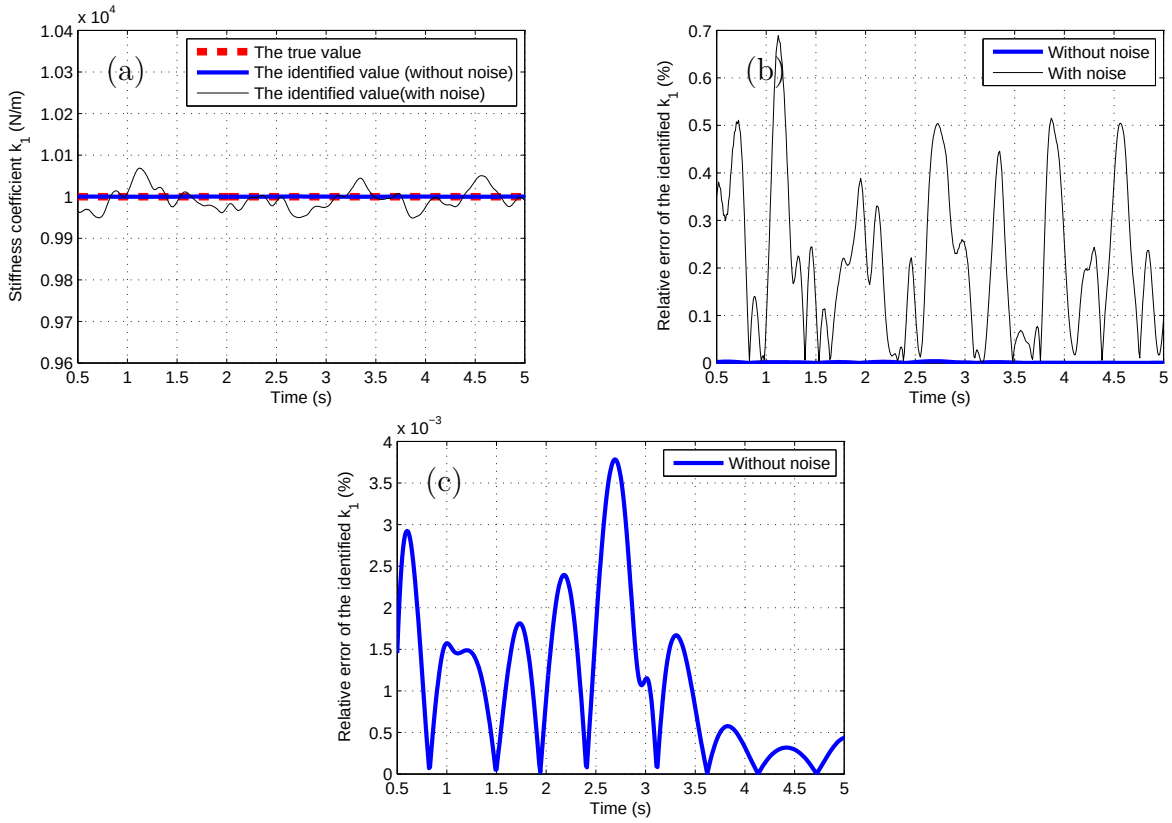

Figure 3.7: Stiffness coefficient k_1 of a 2-DOF linear smoothly varying non-chainlike forced vibration system: (a) The true value and the identified values of k_1, (b) Relative errors of the identified values of k_1, (c) Relative error of the identified value of k_1(without noise in system responses).

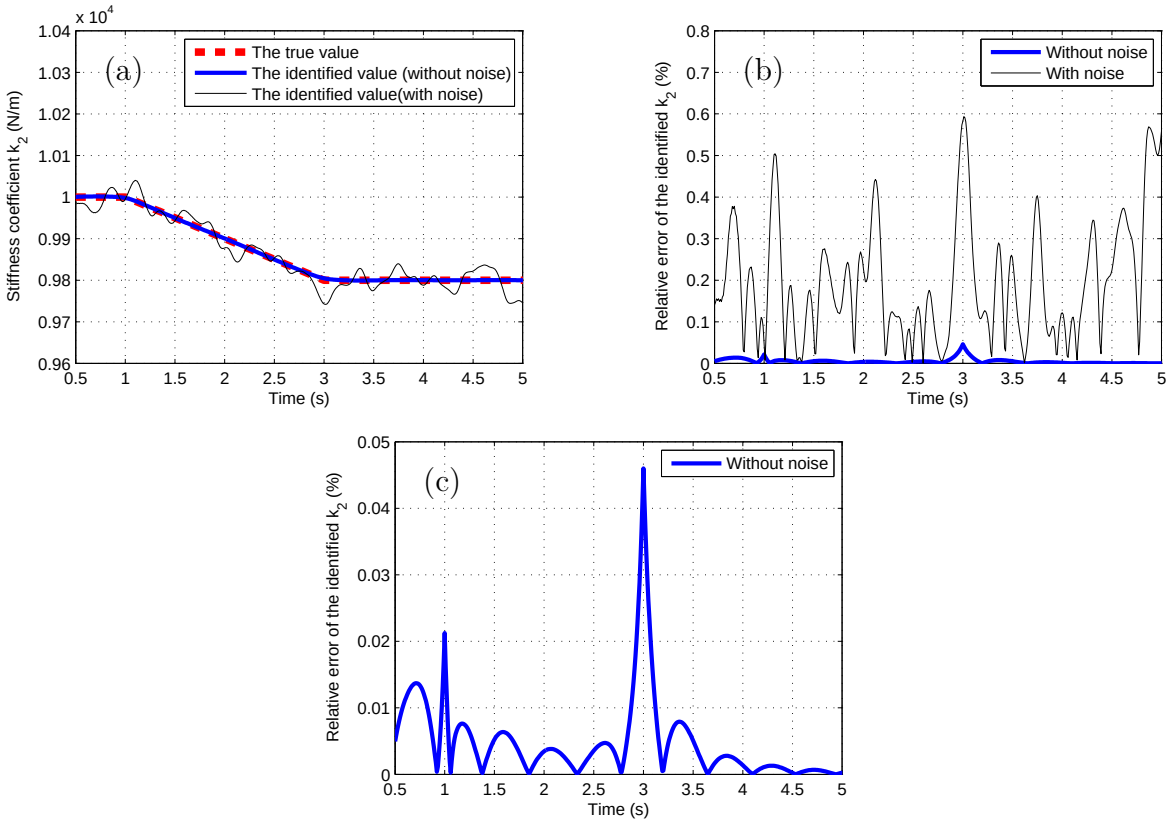

Figure 3.8: Stiffness coefficient k_2 of a 2-DOF linear smoothly varying non-chainlike forced vibration system: (a) The true value and the identified values of k_2, (b) Relative errors of the identified values of k_2, (c) Relative error of the identified value of k_2 (without noise in system responses).

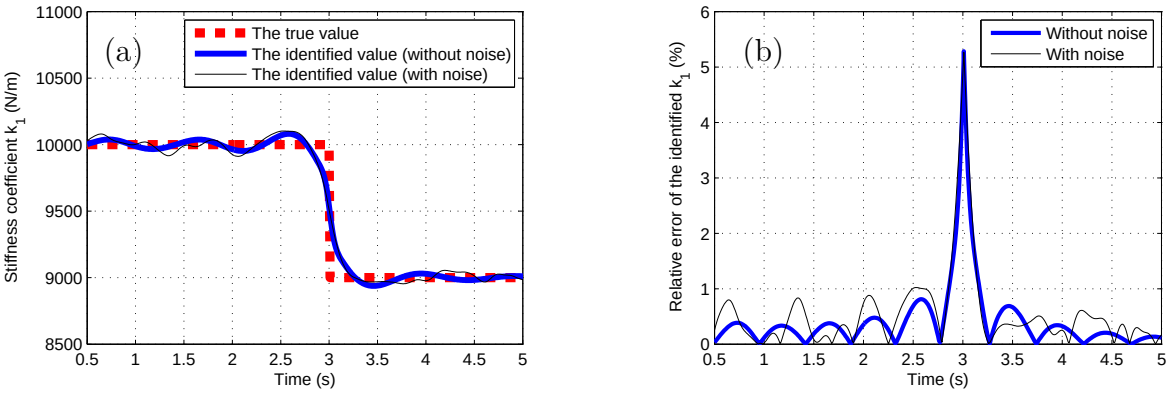

Figure 3.9: Stiffness coefficient k_1 of a 2-DOF linear abruptly varying non-chainlike forced vibration system: (a) The true value and the identified values of k_1, (b) Relative errors of the identified values of k_1.

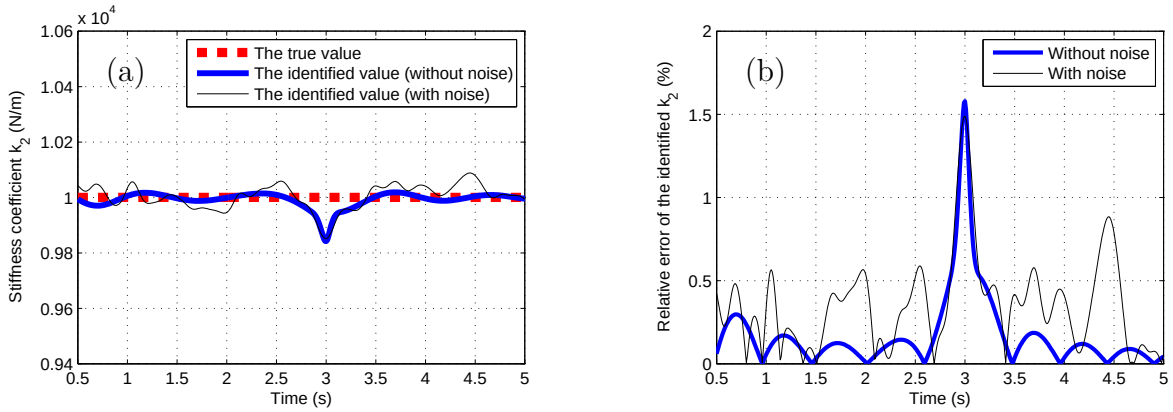

Figure 3.10: Stiffness coefficient k_2 of a 2-DOF linear abruptly varying non-chainlike forced vibration system: (a) The true value and the identified values of k_2, (b) Relative errors of the identified values of k_2.

3.2.3 HHT-based Identification of 2-DOF linear time-varying chainlike systems

For the 2-DOF linear time-varying chainlike forced vibration systems which adopt the model shown in Figure 3.1, the system stiffness coefficients are given as follows ([26]):

Table 3.3: System stiffness coefficients of 2-DOF linear time-varying chainlike systems

System coefficients / Type of systems	System stiffness coefficient (N/m)
2-DOF linear smoothly varying system	$k_2(t) = 87552$ when $t < 1$s, $k_2(t) = 87552 - 8755.2(t-1)$ when $1\text{s} \leq t \leq 3.5$s, $k_2(t) = 70042$ when $t > 3$s, $k_1(t) = 40053$ for any t.
2-DOF linear abruptly varying system	$k_1(t) = 40053$, $k_2(t) = 87552$ when $t \leq 3$s, $k_1(t) = 36048$, $k_2(t) = 70042$ when $t > 3$s.
2-DOF linear periodically varying system	$k_1(t) = 40053$ when $t < 2$s, $k_1(t) = 40053 - 4005.3\sin[\pi(t-2)]$ when $t \geq 2$s, $k_2(t) = 87552$ for any t.

The identified results of the system stiffness coefficients and their relative errors of the 2-DOF linear smoothly and abruptly varying chainlike forced vibration systems are presented in Figures 3.11 - 3.14.
From these figures, it is noted that: For the 2-DOF linear smoothly varying chainlike forced vibration system, like those in the non-chainlike case, when noiseless system responses are used as input of the HHT-based identification method, the identified stiffness coefficients obtained in chainlike case are quite close to their true values, their relative errors have decreasing trend as time increases, except around $t = 1$s and $t = 3$s where abrupt changes are found, due to the abrupt changes of the system stiffness coefficient at these time instants. However, when noise-added system responses are used as input, the identified results of the stiffness coefficients are contaminated by noise. Nevertheless, they are still close to their respective true values with sufficiently small relative errors (the maximal relative error of k_1 is less than 5.6% and that of k_2 is less than 1.6%); For the 2-DOF linear abruptly varying chainlike forced vibration system, when noiseless system responses are used as input of the HHT-based identification method, the identified stiffness coefficients are quite close to their true values, except around the time instant $t = 3$s, they have relatively quite large identification errors. This implies that the proposed method has bad ability to capture the abrupt change of the system parameters due to the limitations of Equation (2.16). When noise-added system responses are used as input, although they are contaminated by noise, the identified stiffness coefficients still match their respective true values well with small relative errors (the maximal relative error of k_1 is less than 5.0%

and that of k_2 is less than 1.4%) at time instants which are not around $t = 3$s. For both systems, it can be found that the identified results of stiffness coefficients and damping coefficients (see Appendix A.1.3) denoted by black solid lines and blue solid lines which are obtained by the HHT-based identification method are better than their counterparts denoted by orange solid lines and green solid lines which are obtained by the HHT-based identification method proposed by Shi and Law [26], possibly because the latter method uses single IMFs as input while discarding the signal residues obtained by EMD method which might still contain some information about the system responses, and adopts the assumption of orthogonality between any two IMFs.
Similar identified results can be also obtained for numerical simulations of 1-DOF and 2-DOF linear time-varying non-chainlike/chainlike systems in free vibrations with the system coefficients and initial conditions given the same as those in the above simulations of the corresponding systems in forced vibrations.

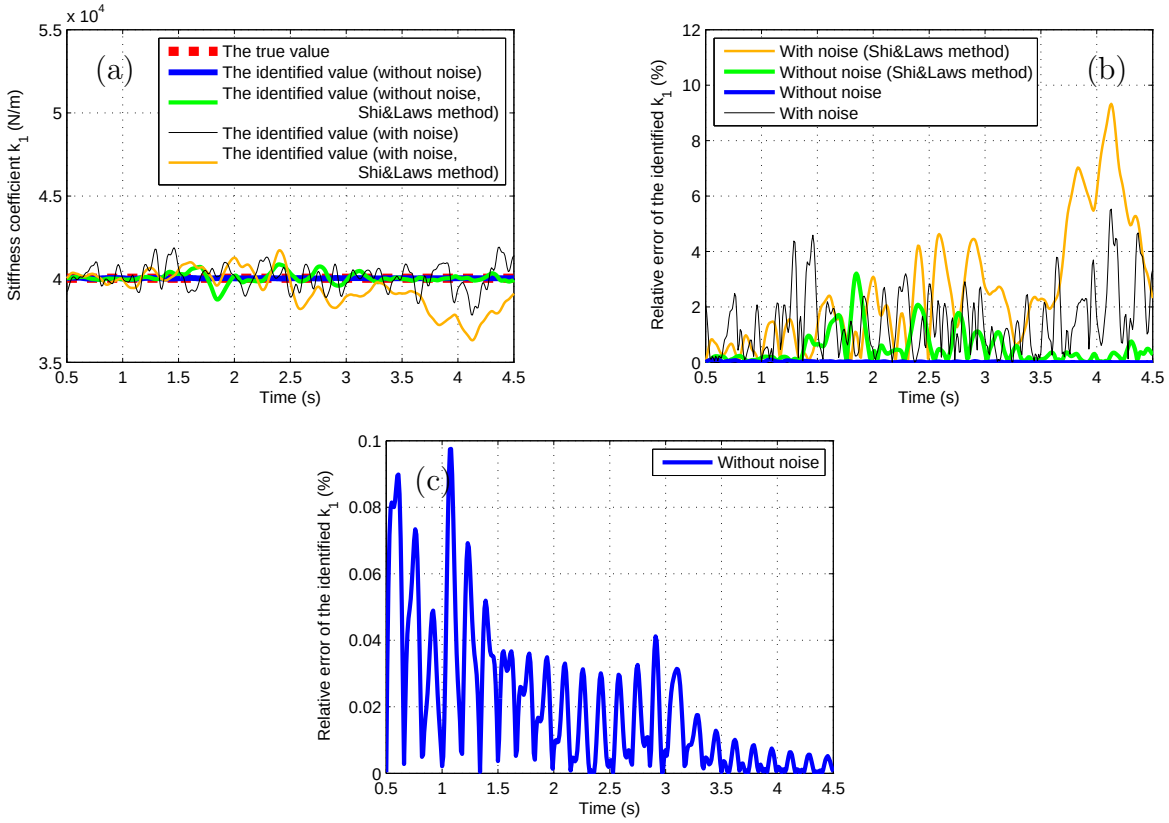

Figure 3.11: Stiffness coefficient k_1 of a 2-DOF linear smoothly varying chainlike forced vibration system: (a) The true value and the identified values of k_1, (b) Relative errors of the identified values of k_1, (c) Relative error of the identified value of k_1 (without noise in system responses).

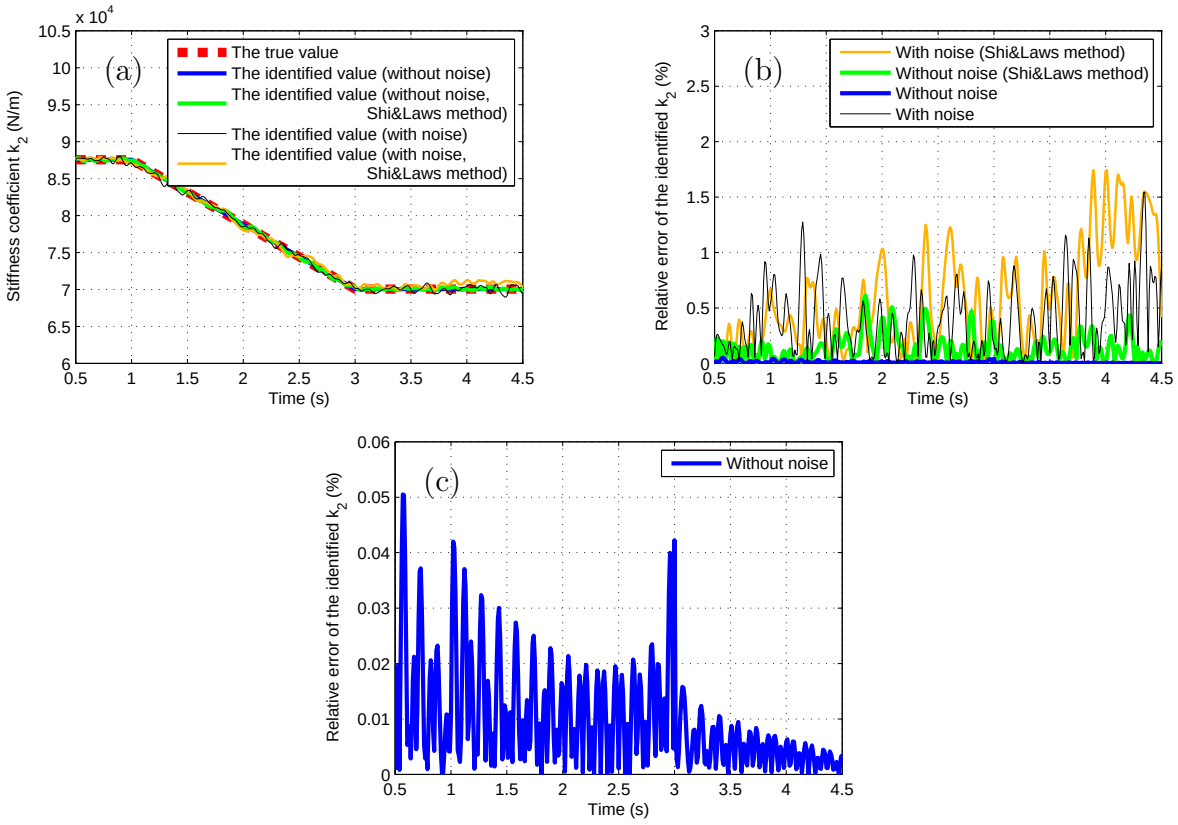

Figure 3.12: Stiffness coefficient k_2 of a 2-DOF linear smoothly varying chainlike forced vibration system: (a) The true value and the identified values of k_2, (b) Relative errors of the identified values of k_1, (c) Relative error of the identified value of k_2 (without noise in system responses).

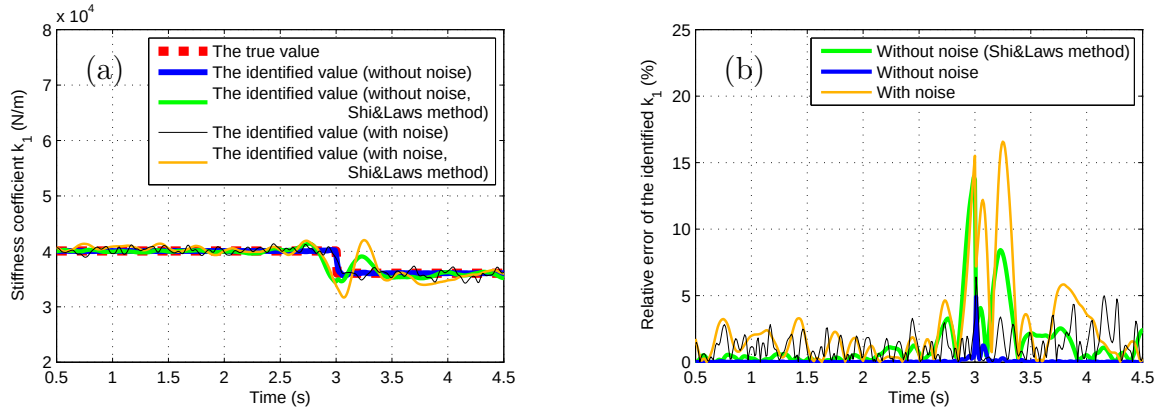

Figure 3.13: Stiffness coefficient k_1 of a 2-DOF linear abruptly varying chainlike forced vibration system: (a) The true value and the identified values of k_1, (b) Relative errors of the identified values of k_1.

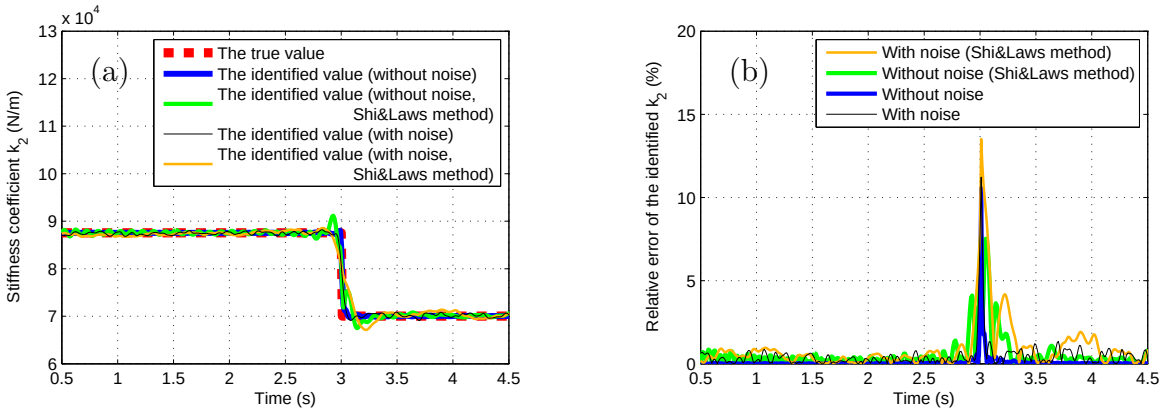

Figure 3.14: Stiffness coefficient k_2 of a 2-DOF linear abruptly varying chainlike forced vibration system: (a) The true value and the identified values of k_2, (b) Relative errors of the identified values of k_2.

3.3 Parameter studies on general linear time-varying systems

In the first part of this section, parameter studies are processed on forced vibration simulations of 2-DOF linear time-varying non-chainlike systems to find the proper value ranges of the structural parameters which are variable factors in the system coefficients, for which good identified results can be obtained by the proposed method. Like in the above simulations, noise-added system responses ($Nstd = 0.05$, $NE = 15$) are considered in the parameter studies.
In the second part of this section, different values of the control parameters of EMD program are applied in the forced vibration simulations of 2-DOF linear time-varying chainlike systems with three types of stiffness variations. The identified results obtained by using the identification method proposed by Shi and Law and the proposed HHT-based identification method when applying different value sets of control parameters are compared, gaining appropriate values of the control parameters of the EMD program which can result in good identified results.

3.3.1 Parameter studies on 2-DOF linear time-varying non-chainlike systems

Parameter studies are processed on the forced vibration simulations of 2-DOF linear smoothly varying and periodically varying non-chainlike systems. As the proposed method has bad ability to capture the abrupt change of the system parameters of 2-DOF linear abruptly varying systems due to the limitations of Equation (2.16), the resulting relative and absolute errors of the system parameters can be extremely large at the time instants when the system parameters have abrupt changes, which would shadow the changes of relative and absolute errors caused by the change of structural parameters and make the parameter study senseless. As a result, parameter study will not processed on 2-DOF linear abruptly varying systems. Results of the parameter study on the forced vibration simulation of a 2-DOF linear smoothly varying non-chainlike system are presented in the following, whereas those of the parameter study on the forced vibration simulation of a 2-DOF linear periodically varying non-chainlike system can be found in Appendix A.1.5.

Parameter study on the forced vibration simulation of a 2-DOF linear smoothly varying non-chainlike system:
The system coefficients, initial conditions as well as the external force are given the same as those of the 2-DOF linear smoothly varying non-chainlike forced vibration system in Section 3.2.2, except that the system stiffness k_2 adopts the model shown in Figure 3.15:
$k_2 = k_{up}$ when $t < 1$s,
$k_2 = k_{up} - (k_{up} - k_{down})/t_L(t-1)$ when $1\text{s} \le t \le t_L + 1\text{s}$,
$k_2 = k_{down}$ when $t > t_L + 1$s,
$k_{up} = 10000$N/m, $k_{down} = 9800$N/m for any t,
where t_L is a variable structural parameter in the interval (0, 10]s with the time interval

between two adjacent t_L values equal to 0.01s (The special case $t_L = 0$s stands for an abruptly varying system).

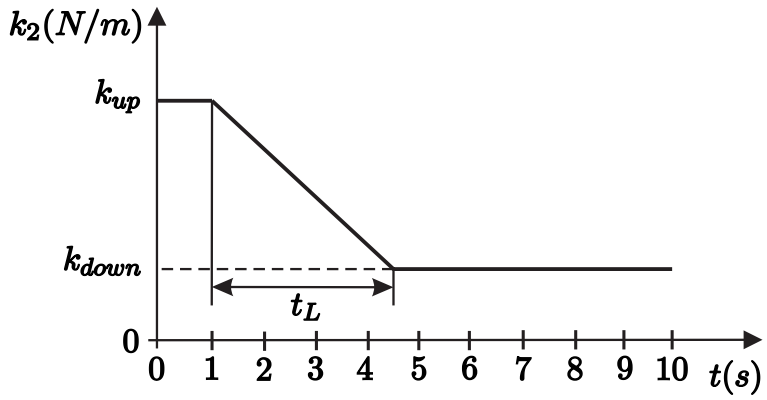

Figure 3.15: Stiffness coefficient k_2 of a 2-DOF linear smoothly varying non-chainlike forced vibration system with variable t_L.

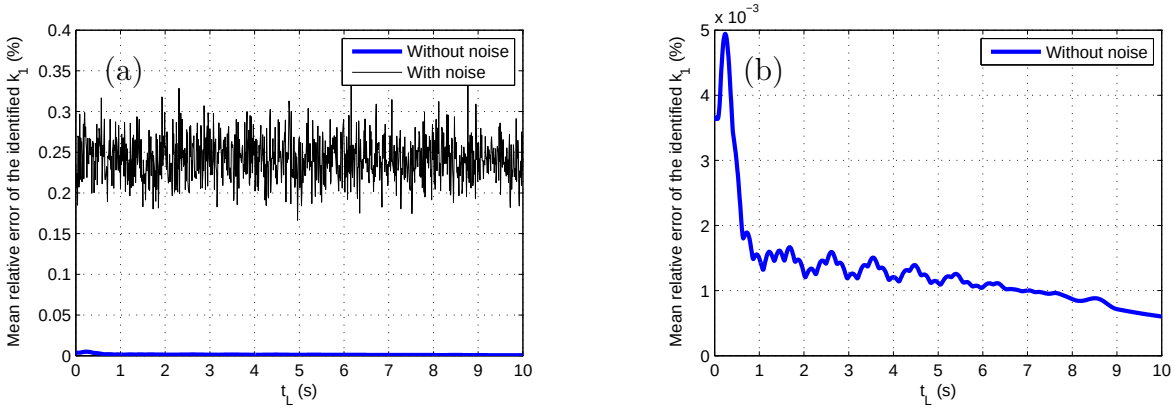

Figure 3.16: Mean relative error of stiffness coefficient k_1 of a 2-DOF linear smoothly varying non-chainlike forced vibration system with respect to t_L: (a) Mean relative error of the identified values of k_1, (b) Mean relative error of the identified values of k_1 (without noise in system responses).

The mean relative errors of the stiffness coefficients k_1 and k_2, as well as the mean absolute errors of damping coefficients c_1 and c_2 are obtained and shown in Figures 3.16 - 3.19. We can note that: when noiseless system responses are used as input, the mean relative and absolute errors (denoted with blue lines) of the system coefficients have an increase and reach their respective maximum values as t_L takes values in the interval $(0, 0.24]$s, then they have large and rapid decrease as t_L increases to 1s. After that, they have slight decreasing trend as t_L increases in the interval $[1, 10]$s. And good identified results of the system coefficients with small mean relative or absolute errors (less than 0.0062% for stiffness coefficients and less than 0.084Ns/m for damping coefficients) are obtained as t_L takes large values in the interval $[1, 10]$s; whereas when noise-added system responses

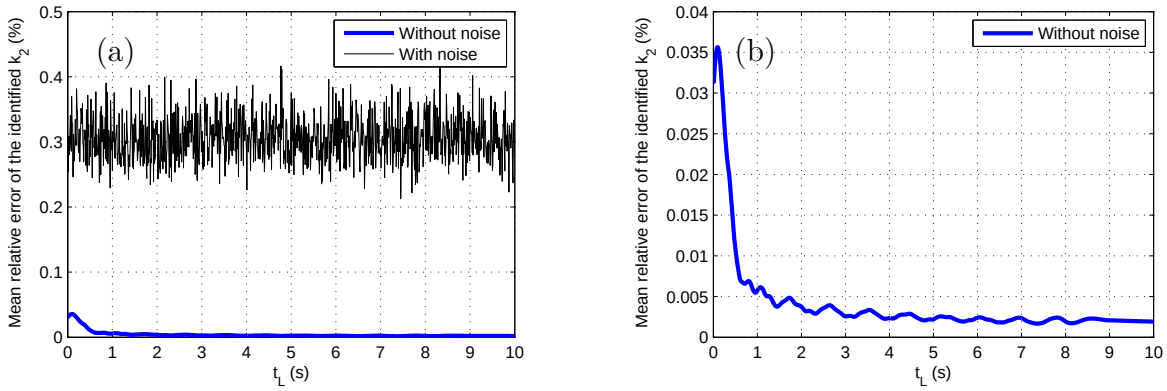

Figure 3.17: Mean relative error of stiffness coefficient k_2 of a 2-DOF linear smoothly varying non-chainlike forced vibration system with respect to t_L: (a) Mean relative error of the identified values of k_2, (b) Mean relative error of the identified values of k_2 (without noise in system responses).

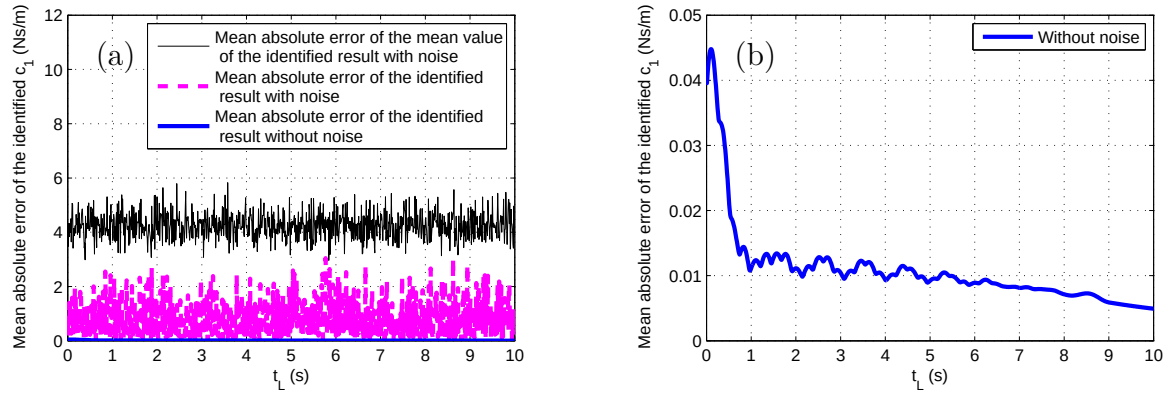

Figure 3.18: Mean absolute error of damping coefficient c_1 of a 2-DOF linear smoothly varying non-chainlike forced vibration system with respect to t_L: (a) Mean absolute error of the identified values of c_1, (b) Mean absolute error of the identified values of c_1 (without noise in system responses).

are used as input, all errors keep fluctuating around some constant values, and although their magnitudes are larger than their counterparts (denoted with blue lines) obtained by using noiseless system responses, the magnitudes of the mean relative errors of the identified stiffness coefficients k_1 and k_2 are still sufficiently small (whose maxima are less than 0.34% and 0.43% respectively). The mean absolute errors of identified c_1 and c_2 denoted with black lines are quite large, but the mean absolute errors of identified c_1 and c_2 denoted with pink dashed lines (whose maxima are less than 3.1Ns/m and 4.1Ns/m respectively) are relatively smaller than the former (For calculation of the mean relative error or the mean absolute error denoted with black line, first we calculate the relative or absolute error between each identified damping coefficient and its true value at each time instant for different t_L, then we take the mean value of the relative or absolute error of

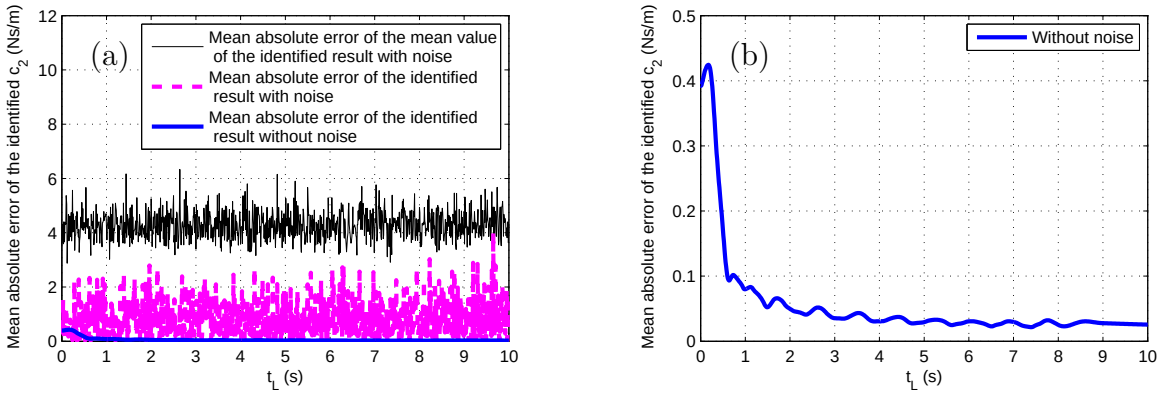

Figure 3.19: Mean absolute error of damping coefficient c_2 of a 2-DOF linear smoothly varying non-chainlike forced vibration system with respect to t_L: (a) Mean absolute error of the identified values of c_2, (b) Mean absolute error of the identified values of c_2 (without noise in system responses).

each identified damping coefficient over the time duration $0.5 \sim 5$s for different t_L; For calculation of the mean relative error or the mean absolute error denoted with pink dashed line, first we take the mean value of each identified damping coefficient over the time duration $0.5 \sim 5$s for different t_L, then we calculate the relative or absolute error between the mean value of each identified damping coefficient and its true value for different t_L). At $t_L = 2$s (case of the 2-DOF linear smoothly varying non-chainlike forced vibration system in Section 3.2.2), the mean absolute errors of identified c_1 and c_2 denoted with pink dashed lines are sufficiently small (less than 1.4Ns/m and 0.92Ns/m respectively).
In conclusion, by using noiseless system responses as input of the proposed method, good identified results of the system coefficients with small mean relative or absolute errors are obtained as the variable parameter t_L takes large values in the interval $[1, 10]$s (which represents that the system stiffness varies slowly); whereas by using noise-added system responses as input, the variation of t_L has almost no influence on the identified results of the system coefficients, yet good identified results of the stiffness coefficients with small mean relative errors are still obtained for any t_L. As a result, it is proper to choose large values in the interval $[1, 10]$s for t_L.

3.3.2 Study of the control parameters of EMD program on 2-DOF linear time-varying chainlike systems

In this section, an EMD program proposed by P. Flandrin [60] is applied to the decomposition of noiseless forced vibration system responses in the identification method proposed by Shi and Law (see Section 2.3) and the proposed HHT-based identification method (see Section 3.1). The EMD program controls the sifting process to extract each IMF (of each DOF) by testing: (1) if the number of zero crossings and the number of extrema differ by no more than 1; (2) if the evaluation function $\sigma(t)$ (see Section 2.1.1) is smaller than γ_1

for some prescribed fraction $(1 - \alpha_p)$ of the total duration, and is smaller than γ_2 for the remaining fraction (the default values of γ_1, γ_2 and α_p are set as $\gamma_1 \approx 0.05$, $\gamma_2 \approx 10 * \gamma_1$ and $\alpha_p \approx 0.05$)[61]. The sifting process is iterated until both tests are positive.
In order to get appropriate values of control parameters of the EMD program which can result in good identified results when applied in the proposed HHT-based identification method and the identification method proposed by Shi and Law, forced vibration simulations are processed on 2-DOF linear smoothly, abruptly and periodically varying chainlike systems with the respective system coefficients, the initial conditions as well as the external excitation given the same as in Section 3.2 and Appendix A.1.4. The noiseless system responses of these 2-DOF systems are used as input of the two aforementioned identification methods. Six cases with different value sets of the control parameters are applied in the EMD program in the simulations, of which the values are presented in Table 3.4.

Table 3.4: Different value sets of the control parameters of the EMD program

Control parameters / Case index	γ_1	γ_2	α_p
Case 0 (default)	0.05	0.5	0.05
Case 1	0.005	0.05	0.05
Case 2	5e-04	0.005	0.05
Case 3	5e-05	5e-04	0.05
Case 4	5e-06	5e-05	0.05
Case 5	5e-07	5e-06	0.05

Maximal relative/absolute error of the identified system coefficients of 2-DOF linear time-varying chainlike systems obtained by using the identification method proposed by Shi and Law and the proposed HHT-based identification method which apply the value sets of the six cases are collected in Tables 3.5-3.6.

Table 3.5: Maximal relative error of the identified system coefficients of 2-DOF linear time-varying chainlike systems

Value of maximal relative error / Case index / System coefficient	Case 0	Case 1	Case 2	Case 3	Case 4	Case 5	Applied method
k_2 of the 2-DOF linear smoothly varying system	3.1%	1.5%	0.75%	0.57%	0.92%	0.78%	Shi&Law's method
	0.20%						The proposed method
c_1 of the 2-DOF linear smoothly varying system	220%	67%	50%	52%	56%	58%	Shi&Law's method
	5.6%						The proposed method
k_1 of the 2-DOF linear abruptly varying system	10%	2.3%	1.9%	2.1%	2.2%	2.5%	Shi&Law's method
	0.20%						The proposed method
k_1 of the 2-DOF linear periodically varying system	6.7%	1.3%	1.7%	1.6%	2.5%	2.3%	Shi&Law's method
	0.079%						The proposed method

By comparing the obtained identified results, it is found out that:
For linear time-varying chainlike forced vibration systems identified by the identification method proposed by Shi and Law, since the input of the method are single IMFs of the system responses, the accuracy of extracting a single IMF or rather the values of the control parameters $(\gamma_1, \gamma_2, \alpha_p)$ of the EMD program has direct influence on the accuracies of the identified results. The identified results of Case 0 (obtained by applying the default values of the control parameters $\gamma_1 = 0.05, \gamma_2 = 10 * \gamma_1, \alpha_p = 0.05$) are worse than their counterparts of other cases (obtained by applying smaller values of γ_1 and γ_2 with α_p kept constant). When the values of γ_1 and γ_2 decrease, the magnitudes of the relative/absolute errors of the resulting identified results have decreasing trend. And the identified results

Table 3.6: Maximal absolute error of the identified system coefficients of 2-DOF linear time-varying chainlike systems

Value of maximal absolute error / Case index / System coefficient	Case 0	Case 1	Case 2	Case 3	Case 4	Case 5	Applied method
c_2 of the 2-DOF linear abruptly varying system	37Ns/m	20Ns/m	10Ns/m	10Ns/m	11Ns/m	11Ns/m	Shi&Law's method
	3.4Ns/m						The proposed method
c_2 of the 2-DOF linear periodically varying system	37Ns/m	20Ns/m	10Ns/m	8.2Ns/m	6.8Ns/m	8.2Ns/m	Shi&Law's method
	0Ns/m						The proposed method

of Case 2, Case 3, Case 4 and Case 5 have similar magnitudes of relative/absolute errors. Thus, in consideration of the expense of computational time, the value set of Case 2 ($\gamma_1 = 5\text{e-}04$, $\gamma_2 = 5\text{e-}03$ and $\alpha_p = 0.05$) are preferable in order to get good identified results when applying the identification method proposed by Shi and Law.

For linear time-varying chainlike forced vibration systems identified by the proposed HHT-based identification method, since the proposed HHT-based identification method uses synthesized analytical system responses (which are obtained by first processing the original system responses with HHT, and then summing the obtained analytical IMFs and analytical residues to gain the corresponding synthesized analytical signals) as input, the changes of the control parameters $(\gamma_1, \gamma_2, \alpha_p)$ have no influence on the accuracy of the identified results. It is clear that the corresponding identified results of different cases have same maximal relative/absolute errors (see Tables 3.5-3.6). Therefore, in consideration of the large expense of computational time when applying small values of γ_1 and γ_2, the default values of the control parameters $(\gamma_1 = 0.05, \gamma_2 = 10 * \gamma_1, \alpha_p = 0.05)$ are preferably taken in order to get good identified results when applying the proposed HHT-based identification method.

3.4 Conclusion

From the numerical simulations of linear smoothly varying, abruptly varying as well as periodically varying non-chainlike and chainlike systems in forced vibration, it is noted that: for 1-DOF and 2-DOF systems, the identified results of smoothly varying and periodically varying systems gained by the proposed method are quite good, whereas the identified results of abruptly varying systems have extremely large identification errors at some time instants, which implies that the adopted method is not suitable for abruptly varying systems due to the limitations of Equation (2.16). And the identified results of chainlike systems are found much better than those obtained by the identification method proposed by Shi and Law. When there exists white noise in system responses, good identified results with small relative as well as absolute errors are obtained by the proposed method, demonstrating the robustness of the method to noise.
Parameter studies are processed on 2-DOF linear smoothly varying and periodically varying non-chainlike forced vibration systems, gaining the relation between the relative as well as absolute errors of identified system coefficients and the variable parameters (t_L, h and T) in the system stiffness coefficients. When the values of these variable parameters are in the appropriate ranges (t_L takes large values in the interval of $[1, 10]$s, h takes small values in the interval of $[0, 5000]$N/m, and T takes large values in the interval of $[1, 10]$s), good identified results of the system stiffness coefficients with small magnitudes of mean relative errors can be obtained by the proposed method no matter noiseless system responses or noise-added system responses are used as input of the proposed HHT-based identification method. However, due to the sensitivity of damping coefficients to noise, the identified results of the system damping coefficients are found having large maximal mean relative error and maximal mean absolute error. When the variable parameters take specific values ($t_L = 2$s for case of the 2-DOF linear smoothly varying non-chainlike forced vibration system in Section 3.2.2, $h = 100$N/m and $T = 2$s for case of the 2-DOF linear periodically varying non-chainlike forced vibration system in Appendix A.1.4), the mean relative and mean absolute errors of the system damping coefficients denoted by pink dashed lines are sufficiently small.
Study of the control parameters of an EMD program is processed on 2-DOF linear time-varying chainlike forced vibration systems by applying 6 cases in the EMD program. Each case applies a different value set of the control parameters $(\gamma_1, \gamma_2, \alpha_p)$. For the identification method proposed by Shi and Law, small values of the control parameters γ_1 and γ_2 can result in identified parameters with smaller relative and absolute errors. In consideration of the expense of computational time, the value set of Case 2 ($\gamma_1 = 5$e-04, $\gamma_2 = 5$e-03 and $\alpha_p = 0.05$) is preferable for application of the identification method proposed by Shi and Law. For the proposed HHT-based identification method, the changes of the control parameters $(\gamma_1, \gamma_2, \alpha_p)$ have no influence on the accuracy of identified results. In consideration of the large expense of computational time when applying small values of γ_1 and γ_2, the default values of the control parameters ($\gamma_1 = 0.05, \gamma_2 = 10 * \gamma_1, \alpha_p = 0.05$) should be taken for the proposed HHT-based identification method.
In conclusion, no matter white noise exists in the system responses or not, the proposed HHT-based identification method can solve the system coefficients of MDOF linear time-

varying non-chainlike and chainlike systems having three types of stiffness variations in both forced vibrations and free vibrations with good accuracy, effectiveness and robustness.

4 HHT-based Identification of weakly nonlinear time-varying systems

In this chapter, the HHT-based identification method for general linear time-varying system proposed in the previous chapter is extended to weakly nonlinear time-varying MDOF Duffing systems and Van der Pol systems. Since the systems contain nonlinear parameters, Bedrosian's theorem is not valid for the application of HT, we make some approximations with the help of the formula of Hahn and the theory of Feldman to modify the HHT-based identification method for weakly nonlinear time-varying MDOF Duffing systems and Van der Pol systems respectively. By application of the modified HHT-based identification method, numerical simulations are processed on 1-DOF and 2-DOF weakly nonlinear time-varying Duffing as well as Van der Pol systems with smooth, abrupt and periodical stiffness variations as well as white noise perturbations in system responses to demonstrate the effectiveness, accuracy and robustness of the proposed method for weakly nonlinear time-varying MDOF systems.

4.1 HHT-based Identification of weakly nonlinear time-varying Duffing systems

Duffing oscillator was proposed by G. Duffing [82] in 1918, who introduced a nonlinear oscillator with a cubic stiffness term to describe the hardening spring effect. Since then, Duffing equation has become famous describing nonlinear dynamic characteristics for many nonlinear oscillatory systems in mechanics [83], engineering [84], physics [85] and mathematics [86]. The differential equation of a damped Duffing oscillator is given by

$$m(t)\ddot{y}_1(t) + c(t)\dot{y}_1(t) + k_{linear}(t)y_1(t) + \delta(t)y_1^3(t) = f_1(t) \tag{4.1}$$

where $k_{linear}(t)$ is the linear stiffness coefficient which controls the size of the restoring force, $\delta(t)$ is the cubic stiffness factor which controls the amount of non-linearity in the restoring force. The Duffing equation is further classified according to the signs and values of the parameters k_{linear} and δ [87]:
$k_{linear} > 0$, $\delta > 0$ Hard spring Duffing equation;
$k_{linear} > 0$, $\delta < 0$ Soft spring Duffing equation;
$k_{linear} < 0$, $\delta > 0$ Inverted Duffing equation;
$k_{linear} = 0$, $\delta > 0$ Nonharmonic Duffing equation.
Suppose we have an n-DOF chainlike system with a weakly nonlinear time-varying hard/-soft spring Duffing oscillator. Its governing differential equations can be still expressed by Equation (3.1), but with a stiffness element given by $k_{11}(t) = k_{11linear}(t) + \delta(t)y_1^2(t)$. For simplicity, we assume that $\delta(t) = r_d k_{11linear}$.

Since $k_{11}(t)$ contains the square of system response $y_1^2(t)$, when applying HT to process the governing differential equation of the system, Bedrosian's theorem is not valid for $H\{k_{11}(t)y_1(t)\}$. According to the formula of Hahn, suppose $n(t)$ and $x(t)$ are two fast varying functions whose frequency bands do overlap, if one of the functions can be represented in the form of a sum of two parts $n(t) = \bar{n}_{slow} + \overset{\leftrightarrow}{n}_{fast}$, then the HT of the product of these functions with overlapping spectra can be written in the form of a sum of two parts too [88]:

$$H[n(t)x(t)] = H[\bar{n}_{slow} + \overset{\leftrightarrow}{n}_{fast}]x(t) = \bar{n}_{slow}\tilde{x} + \tilde{n}_{fast}x(t) \tag{4.2}$$

where $\bar{n}_{slow}$ is the slow (low-pass) part of the real function, $\overset{\leftrightarrow}{n}_{fast}$ is the fast (high-pass) one and $\tilde{n}_{fast}$ is the HT pair component of the fast component $\overset{\leftrightarrow}{n}_{fast}$. Note that $x(t)$, $\bar{n}_{slow}$ and $\overset{\leftrightarrow}{n}_{fast}$ have non-overlapping spectra, $x(t)$ is high-pass signal with respect to $\bar{n}_{slow}$, but low-pass signal with respect to $\overset{\leftrightarrow}{n}_{fast}$, thus Bedrosian's theorem can be applied to $\bar{n}_{slow}x(t)$ and $\overset{\leftrightarrow}{n}_{fast}x(t)$ separately. Following this equation, Feldman [89] gave the example of the HT of the square of the harmonic signal $x^2 = (\cos\varphi)^2$:

$$H[x^2] = H[xx] = H[(0+x)x] = 0 + \tilde{x}x = \sin\varphi\cos\varphi = 0.5\sin 2\varphi \tag{4.3}$$

which coincides with $H[x^2] = H[\cos\varphi^2] = H[0.5 + 0.5\cos 2\varphi] = 0.5\sin 2\varphi$. This equation can be also approximately applied to the square of the response $y_1(t)$ of the n-DOF chainlike weakly nonlinear Duffing system since $y_1(t)$ is a harmonic signal similar to $\cos\varphi$.
Since the spectra of $y_1^2(t)$ and $y_1(t)$ of the 1-DOF and 2-DOF weakly nonlinear Duffing systems to be simulated can be approximately seen as non-overlapping and $y_1^2(t)$ can be treated as high-pass signal with respect to $y_1(t)$, we obtain $H[y_1^2(t)y_1(t)] \approx H[y_1^2(t)]y_1(t)$. Then, with the help of the assumption that $\delta(t)$ doesn't vary quickly over time, we obtain the following expression for the n-DOF chainlike system with a weakly nonlinear time-varying hard/soft spring Duffing oscillator:

$$\begin{aligned} H\{k_{11}(t)y_1(t)\} &= H\left\{\left[\delta(t)/r_d + \delta(t)y_1^2(t)\right]y_1(t)\right\} \\ &\approx \delta(t)/r_d H[y_1(t)] + \delta(t)H[y_1^2(t)]y_1(t) \\ &= \delta(t)/r_d H[y_1(t)] + \delta(t)H\left\{[0 + y_1(t)]y_1(t)\right\}y_1(t) \\ &\approx \delta(t)/r_d H[y_1(t)] + \delta(t)H[y_1(t)]y_1(t)y_1(t) \\ &= \delta(t)\left\{\tilde{y}_1(t)/r_d + \tilde{y}_1(t)y_1^2(t)\right\} \end{aligned} \tag{4.4}$$

The HHT-based identification procedures for general linear time-varying systems can be used for identification of the n-DOF chainlike weakly nonlinear time-varying system which contains a weakly nonlinear time-varying hard/soft spring Duffing oscillator, except that Equations (3.6) and (3.8) are modified as follows:

$$\boldsymbol{\alpha}^k(t) = [\delta(t), k_{12}(t), \ldots, k_{1n}(t), \ldots, k_{i1}(t), \ldots, k_{in}(t), \ldots, k_{n1}(t), \ldots, k_{nn}(t),]^T \tag{4.5}$$

$$\boldsymbol{P}^k(t) = \begin{bmatrix} Y_1(t)/r_d + Y_1(t)y_1^2(t) & Y_2(t) & \cdots & Y_n(t) & & & & & \\ & & & & \ddots & & & \mathbf{0} & \\ & & & & & Y_1(t) & \cdots & Y_n(t) & \\ & & \mathbf{0} & & & & & \ddots & \\ & & & & & & & Y_1(t) & \cdots & Y_n(t) \end{bmatrix} \tag{4.6}$$

$$(n \times n^2)$$

In the following sections, by application of the modified HHT-based identification method, we process the simulations on 1-DOF and 2-DOF weakly nonlinear time-varying systems, each of which contains a weakly nonlinear time-varying hard spring Duffing oscillator with smooth, abrupt or periodical stiffness variations. The identification simulations are processed by MATLAB programs, the time interval between two adjacent data points is set as 0.01 seconds and the whole time history is set as 10 seconds. The noiseless system responses are obtained by solving the system differential equations, and the noise-added system responses are generated with the ratio *Nstd* of the standard deviation of the added white noise and that of the corresponding noiseless system response set as 0.05 and the number of trials *NE* set as 15.

For the 1-DOF weakly nonlinear time-varying hard spring Duffing oscillators to be simulated, the following common information is given: the mass coefficient is assumed to be known as $m = 1.0$kg; the initial conditions are given as $y(0) = 1$m and $\dot{y}(0) = 0$m/s; An impact excitation is given at the mass by $f(t) = 1$N when $t = 0$s, $f(t) = 0$N otherwise. The differences among these oscillators are: the stiffness coefficients have different variation types; the damping ratios of these oscillators are respectively of the similar magnitudes as those of the corresponding 1-DOF linear smoothly, abruptly and periodically varying systems. For the 2-DOF weakly nonlinear time-varying chainlike Duffing systems to be simulated, the following common information is given: the mass coefficients are assumed to be constants $m_1 = m_2 = 50$kg, the system damping coefficients are given by $c_1 = 30$Ns/m, $c_2 = 0$Ns/m; the initial conditions for the two experiments are given as $y_1(0) = 0$m, $y_2(0) = 1$m, $\dot{y}_1(0) = 0$m/s, $\dot{y}_2(0) = 0$m/s as well as $y_1(0) = 1$m, $y_2(0) = 0$m, $\dot{y}_1(0) = 0$m/s, $\dot{y}_2(0) = 0$m/s; a periodic excitation is given at mass 1 by $f(t) = 50\sin(2\pi t)$N. The differences among these 2-DOF weakly nonlinear chainlike Duffing systems are: the stiffness coefficients have different variation types. For all weakly nonlinear time-varying chainlike Duffing systems to be simulated, the parameter r_d is given by $r_d = 0.1$.

The identified results of the stiffness coefficients of weakly nonlinear smoothly and abruptly varying Duffing systems are presented in the following, whereas the identified results of the damping coefficients of the former systems and all the identified results of weakly nonlinear periodically varying Duffing systems are presented in Appendices A.2.1 - A.2.3.

4.1.1 HHT-based Identification of 1-DOF weakly nonlinear time-varying hard spring Duffing oscillators

For 1-DOF weakly nonlinear time-varying hard spring Duffing oscillators to be simulated, the system stiffness coefficients and damping coefficients are given as Table 4.1:

Table 4.1: System coefficients of 1-DOF weakly nonlinear time-varying hard spring Duffing oscillators

System coefficients / Type of systems	System stiffness coefficient and damping coefficient
1-DOF weakly nonlinear smoothly varying hard spring Duffing oscillator	$k_{linear}(t) = 100\pi^2\text{N/m}, c(t) = 0.7\text{Ns/m}$ when $t < 2\text{s}$, $k_{linear}(t) = 100\pi^2 - 10\pi^2 t\text{N/m}, c(t) = 0.7 + 0.15t\text{Ns/m}$ when $2\text{s} \leq t \leq 4\text{s}$, $k_{linear}(t) = 80\pi^2\text{N/m}, c(t) = 1.0\text{Ns/m}$ when $t > 4\text{s}$, $\delta(t) = 0.1k_{linear}(t)\text{N/m}^3$ for any t.
1-DOF weakly nonlinear abruptly varying hard spring Duffing oscillator	$k_{linear}(t) = 100\pi^2\text{N/m}$ when $t < 1.5\text{s}$, $k_{linear}(t) = 60\pi^2\text{N/m}$ when $1.5\text{s} \leq t \leq 3.5\text{s}$, $k_{linear}(t) = 80\pi^2\text{N/m}$ when $t \geq 3.5\text{s}$, $\delta(t) = 0.1k_{linear}(t)\text{N/m}^3, c(t) = 0.7\text{Ns/m}$ for any t.
1-DOF weakly nonlinear periodically varying hard spring Duffing oscillator	$k_{linear}(t) = 100\pi^2 - 10\pi^2 \sin(2\pi t)\text{N/m}$, $\delta(t) = 0.1k_{linear}(t)\text{N/m}^3, c(t) = 1.26\text{Ns/m}$ for any t.

The identified results of the linear stiffness coefficient and cubic stiffness coefficient of the 1-DOF weakly nonlinear smoothly and abruptly varying hard spring Duffing oscillators as well as their relative errors are shown in Figures 4.1 - 4.2.
We can learn from the figures that: For the 1-DOF weakly nonlinear smoothly varying hard spring Duffing system, no matter using noiseless or noise-added system responses as input of the modified HHT-based identification method, the accuracies of the obtained identified results of the weakly nonlinear smoothly varying Duffing oscillator ($\delta = 0.1 * k_{linear}\,\text{N/m}^3$) are always worse than those of the linear smoothly varying oscillator ($\delta = 0\,\text{N/m}^3$) which has the same linear system coefficients, initial conditions and excitation signal as the weakly nonlinear smoothly varying Duffing oscillator due to the application of Equation (4.4); when using noise-added system responses as input, although the accuracies of the identified results are decreased, we can still obtain good identified results of linear stiffness coefficient k_{linear} and cubic stiffness coefficient δ (with maximal relative errors less than 3.0%); For the 1-DOF weakly nonlinear abruptly varying hard spring Duffing system, both the identified results for Duffing oscillator ($\delta = 0.1 * k_{linear}\,\text{N/m}^3$) and linear oscillator ($\delta = 0\,\text{N/m}^3$) have obvious abrupt changes around time instants $t = 1.5\text{s}$ and $t = 3.5\text{s}$, due to the abrupt changes of the system stiffness coefficients at these time

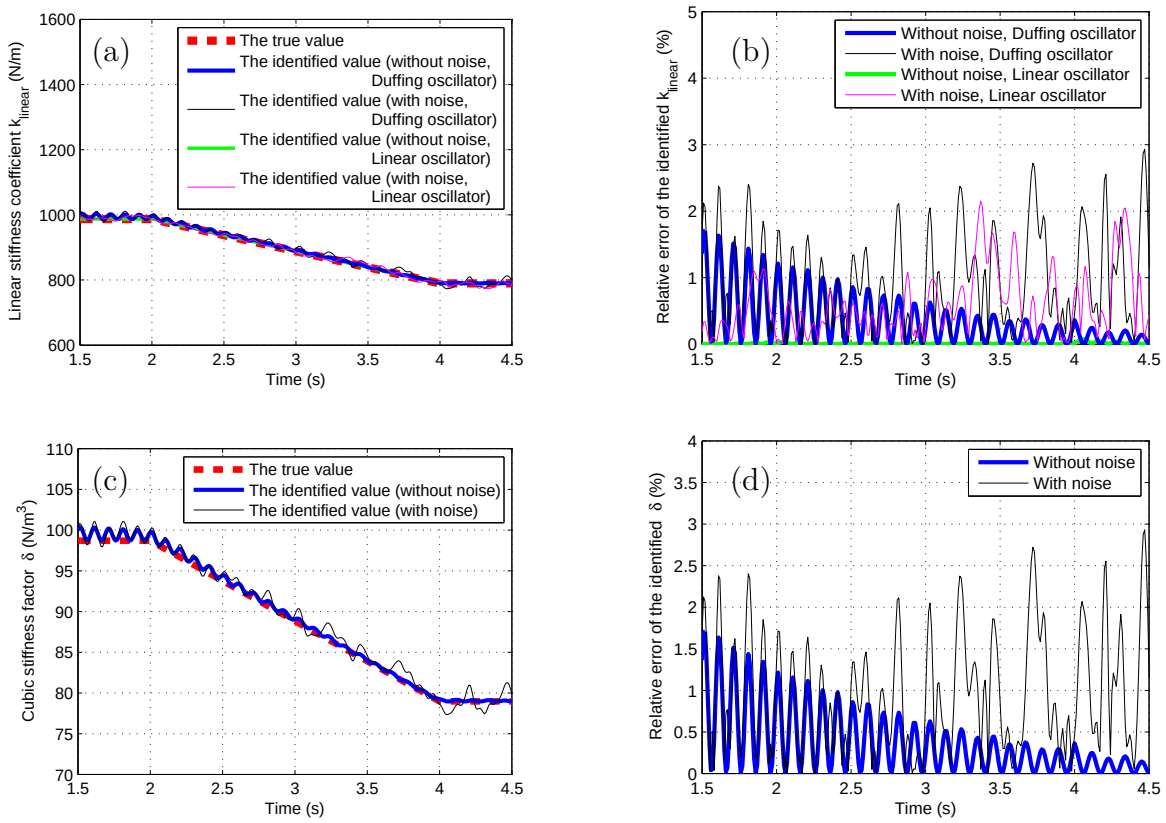

Figure 4.1: Stiffness coefficients of a 1-DOF weakly nonlinear smoothly varying hard spring Duffing system: (a) The true value and the identified values of linear stiffness coefficient k_{linear}, (b) Relative errors of the identified values of k_{linear}, (c) The true value and the identified values of cubic stiffness factor δ, (d) Relative errors of the identified values of δ.

instants. The large identification errors found around these time instants imply that the proposed method has bad ability to capture the abrupt change of the system parameters due to the limitations of Equation (2.16) and can be used to detect the abrupt changes of the original system stiffness coefficients. At other time instants, due to the application of Equation (4.4), the identified results of the weakly nonlinear abruptly varying Duffing oscillator are a little bit worse than those of the linear abruptly varying oscillator which has the same linear system coefficients, initial conditions and excitation signal as the weakly nonlinear abruptly varying Duffing oscillator, no matter using noiseless or noise-added system responses as input of the modified HHT-based identification method. When using noise-added system responses as input, although the identified results are contaminated by noise, good identified results of linear stiffness coefficient k_{linear} and cubic stiffness factor δ (with maximal relative errors less than 5.2%) can be obtained at time instants which are not around $t = 1.5$s and $t = 3.5$s.

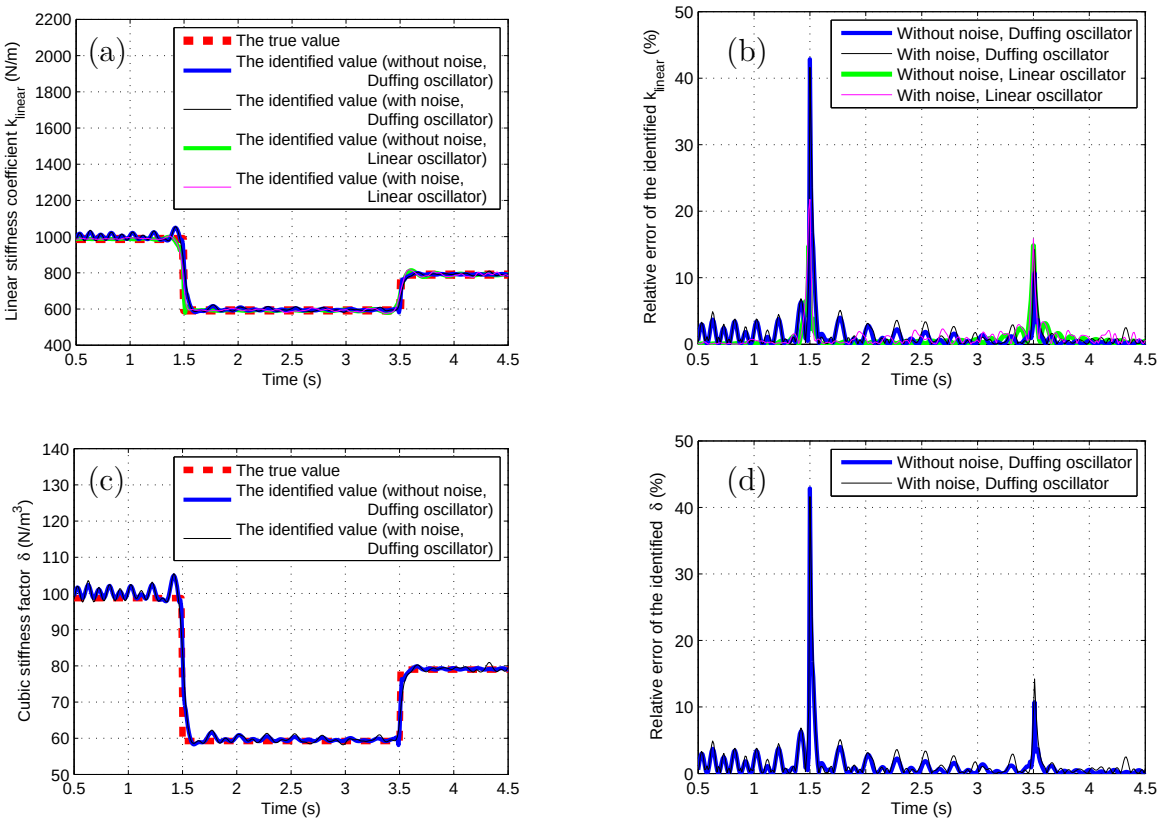

Figure 4.2: Stiffness coefficients of a 1-DOF weakly nonlinear abruptly varying hard spring Duffing system: (a) The true value and the identified values of linear stiffness coefficient k_{linear}, (b) Relative errors of the identified values of k_{linear}, (c) The true value and the identified values of cubic stiffness factor δ, (d) Relative errors of the identified values of δ.

4.1.2 HHT-based Identification of 2-DOF weakly nonlinear time-varying chainlike Duffing systems

For the 2-DOF weakly nonlinear systems which contain a weakly nonlinear time-varying hard spring Duffing oscillator and follow the chainlike model in Figure 3.1, the system stiffness coefficients are given as Table 4.2:

Table 4.2: System coefficients of 2-DOF weakly nonlinear time-varying chainlike Duffing systems

System coefficients / Type of systems	System stiffness coefficient
2-DOF weakly nonlinear smoothly varying chainlike Duffing system	$k_2(t) = 87552\text{N/m}$ when $t < 1\text{s}$, $k_2(t) = 87552 - 8755.2(t-1)\text{N/m}$ when $1\text{s} \leq t \leq 3\text{s}$, $k_2(t) = 70042\text{N/m}$ when $t > 3\text{s}$, $k_1(t) = 40053\text{N/m}$ for any t, $\delta(t) = 0.1[k_1(t) + k_2(t)]\text{N/m}^3$ for any t.
2-DOF weakly nonlinear abruptly varying chainlike Duffing system	$k_1(t) = 40053\text{N/m}, k_2(t) = 87552\text{N/m}$ when $t \leq 3\text{s}$, $k_1(t) = 36048\text{N/m}, k_2(t) = 70042\text{N/m}$ when $t > 3\text{s}$, $\delta(t) = 0.1[k_1(t) + k_2(t)]\text{N/m}^3$ for any t.
2-DOF weakly nonlinear periodically varying chainlike Duffing system	$k_1(t) = 40053\text{N/m}$ when $t < 2\text{s}$, $k_1(t) = 40053 - 4005.3\sin[\pi(t-2)]\text{N/m}$ when $t \geq 2\text{s}$, $k_2(t) = 87552\text{N/m}$ for any t, $\delta(t) = 0.1[k_1(t) + k_2(t)]\text{N/m}^3$ for any t.

The identified results of the system stiffness coefficients of the 2-DOF weakly nonlinear smoothly and abruptly varying chainlike Duffing systems and their relative errors are shown in Figures 4.3 - 4.6.
It is noted from the figures that: For the 2-DOF weakly nonlinear smoothly varying chainlike Duffing systems, no matter using noiseless or noise-added system responses as input of the modified HHT-based identification method, the identified results of cubic stiffness factor δ and stiffness coefficient k_2 are always close to their respective true values (with maximal relative error of δ less than 3.8% and that of k_2 less than 2.1%); For the 2-DOF weakly nonlinear abruptly varying chainlike Duffing system, relatively large identification errors of δ and k_2 are obtained at time instant $t = 3\text{s}$ due to the limitations of Equation (2.16), which can be used to detect the abrupt change of the system stiffness coefficient at this time instant. At other time instants, the identified results of δ and k_2 match their respective true values (the maximal relative error of δ is less than 4.0% and that of k_2 is less than 2.8%).

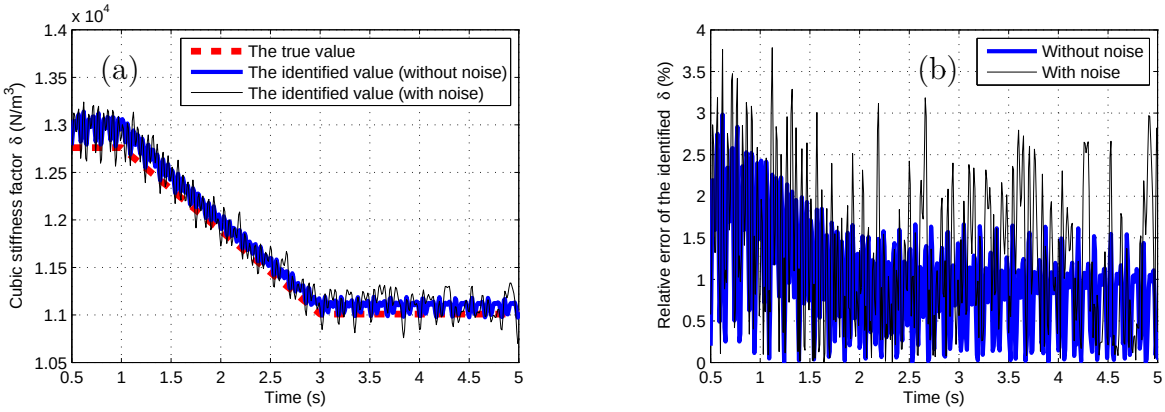

Figure 4.3: Cubic stiffness factor δ of a 2-DOF weakly nonlinear chainlike system with a weakly nonlinear smoothly varying hard spring Duffing oscillator: (a) The true value and the identified values of δ, (b) Relative errors of the identified values of δ.

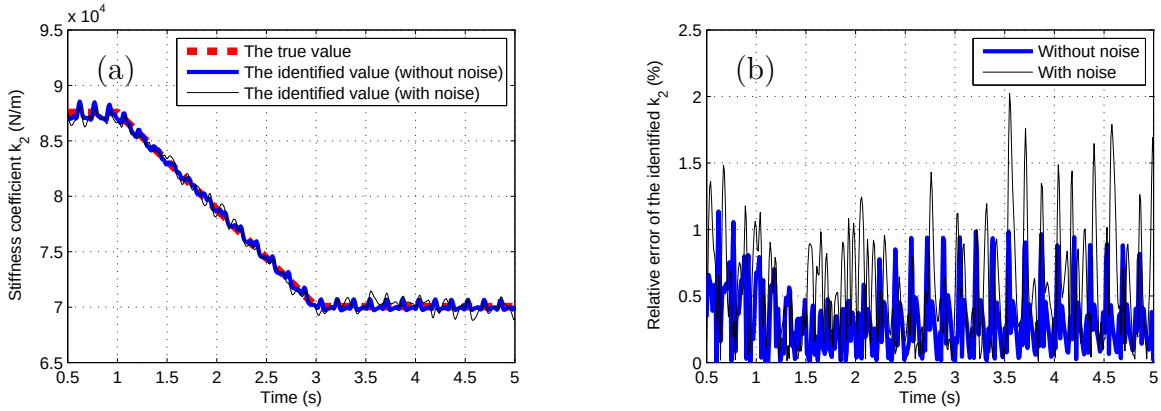

Figure 4.4: Stiffness coefficient k_2 of a 2-DOF weakly nonlinear chainlike system with a weakly nonlinear smoothly varying hard spring Duffing oscillator: (a) The true value and the identified values of k_2, (b) Relative errors of the identified values of k_2.

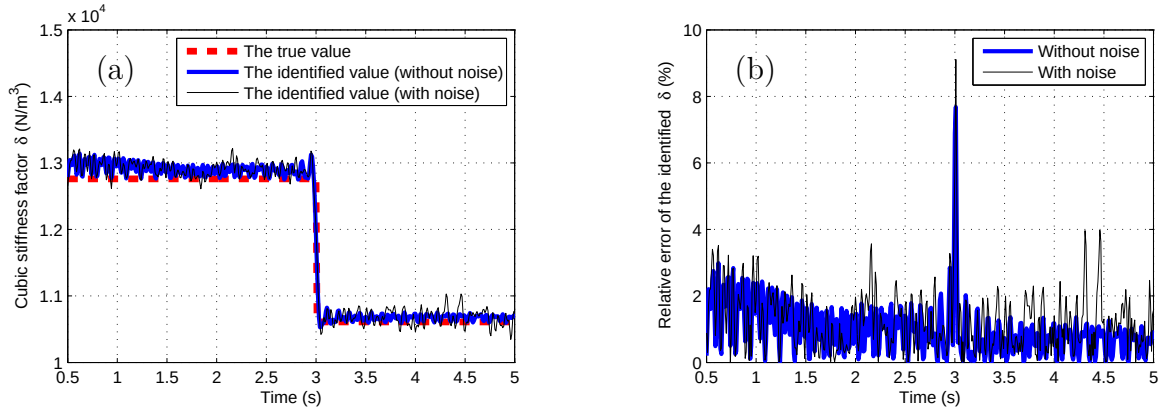

Figure 4.5: Cubic stiffness factor δ of a 2-DOF weakly nonlinear chainlike system with a weakly nonlinear abruptly varying hard spring Duffing oscillator: (a) The true value and the identified values of δ, (b) Relative errors of the identified values of δ.

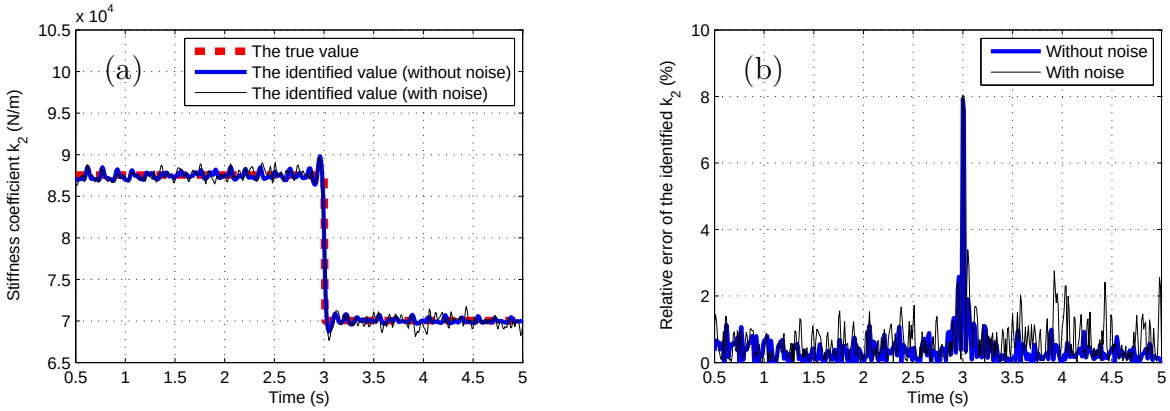

Figure 4.6: Stiffness coefficient k_2 of a 2-DOF weakly nonlinear chainlike system with a weakly nonlinear abruptly varying hard spring Duffing oscillator: (a) The true value and the identified values of k_2 , (b) Relative errors of the identified values of k_2.

4.2 HHT-based Identification of weakly nonlinear time-varying Van der Pol systems

Together with Duffing's equation, Van der Pol's equation proposed by Van der Pol [90] is one of the classical equations in nonlinear vibrations. It was originally used to model an electrical circuit with a triode valve, and then was extensively studied as the model of a rich class of dynamical behavior, such as relaxation oscillations, elementary bifurcations and chaos [91–94], etc. The differential equation of a Van der Pol oscillator is given by

$$m\ddot{y_1} + \mu(y_1^2 - 1)\dot{y_1} + ky_1 = f_1 \tag{4.7}$$

in which μ is the damping factor which controls the amount of non-linearity. Since we consider time-varying stiffness here, k is assumed to vary around 1N/m over time.
Suppose we have an n-DOF chainlike system with a weakly nonlinear time-varying Van der Pol oscillator expressed by Equation (4.7), its governing differential equations can be still expressed by Equation (3.1), but with a damping element given by $c_{11}(t) = \mu(y_1^2(t) - 1)$. As $c_{11}(t)$ contains the square of system response $y_1(t)^2$, when applying HT to process the governing differential equations of the system, Bedrosian's theorem is not valid for $H\{c_{11}(t)\dot{y}_1(t)\}$. Since the spectrum of $y_1^2(t)$ and that of $\dot{y}_1(t)$ can be approximately seen as non-overlapping and $y_1^2(t)$ can be seen as high-pass signal with respect to $\dot{y}_1(t)$, we obtain $H\left[y_1^2(t)\dot{y}_1(t)\right] \approx H\left[y_1^2(t)\right]\dot{y}_1(t)$. As the response $y_1(t)$ of the n-DOF chainlike weakly nonlinear Van der Pol system is a harmonic signal similar to $\cos\varphi$, Equation (4.3) can be also approximately applied to the square of $y_1(t)$. Then, by assuming that μ doesn't vary quickly over time and applying the formula of Hahn (see Equation (4.2)), we obtain

$$\begin{aligned}
H\{c_{11}(t)\dot{y}_1(t)\} &= H\left\{\left[\mu(y_1^2(t) - 1)\right]\dot{y}_1(t)\right\} \\
&= \mu H\left\{\left[(y_1^2(t) - 1)\right]\dot{y}_1(t)\right\} \\
&\approx \mu\left\{-H[\dot{y}_1(t)] + H\left[y_1^2(t)\right]\dot{y}_1(t)\right\} \\
&= \mu\left\{-H\left[\dot{y}_1(t)\right] + H\left[(0 + y_1(t))y_1(t)\right]\dot{y}_1(t)\right\} \\
&\approx \mu\left\{-H\left[\dot{y}_1(t)\right] + H[y_1(t)]y_1(t)\dot{y}_1(t)\right\} \\
&= \mu\left\{-\dot{\tilde{y}}_1(t) + \tilde{y}_1(t)y_1(t)\dot{y}_1(t)\right\}
\end{aligned} \tag{4.8}$$

The identification method for general linear time-varying systems can be also used for identification of the n-DOF chainlike weakly nonlinear system which contains a weakly nonlinear time-varying Van der Pol oscillator, except that Equation (3.7) and (3.9) are modified as follows:

$$\boldsymbol{\alpha}^c(t) = [\mu, c_{12}(t), \ldots, c_{1n}(t), \ldots, c_{i1}(t), \ldots, c_{in}(t), \ldots, c_{n1}(t), \ldots, c_{nn}(t),]^T \tag{4.9}$$

$$\boldsymbol{P}^c(t) = \begin{bmatrix} -\dot{Y}_1(t) + Y_1(t)y_1(t)\dot{y}_1(t) & \dot{Y}_2(t) & \cdots & \dot{Y}_n(t) & & & & & & \\ & & & & \ddots & & & & \mathbf{0} & \\ & & & & & \dot{Y}_1(t) & \cdots & \dot{Y}_n(t) & & \\ & & \mathbf{0} & & & & & & \ddots & \\ & & & & & & & & \dot{Y}_1(t) & \cdots \quad \dot{Y}_n(t) \end{bmatrix} \tag{4.10}$$

$$(n \times n^2)$$

In the following sections, by application of the modified HHT-based identification method, we process the simulations on 1-DOF and 2-DOF weakly nonlinear systems, each of which contains a weakly nonlinear time-varying Van der Pol oscillator with smooth, abrupt or periodical stiffness variations. The identification simulations are still processed by MATLAB programs. The time interval between two adjacent data points in the simulations is 0.01 seconds, and the whole time history is 10 seconds. The system differential equations are solved to obtain the noiseless system responses, the ratio of the standard deviation of the added white noise and that of the corresponding noiseless system response *Nstd* is set as 0.05 and the number of trials *NE* is set as 15 to generate the noise-added system responses.

For the 1-DOF weakly nonlinear time-varying Van der Pol oscillators to be simulated, the following common information is given: the mass coefficient is assumed to be known as $m = 1.0\text{kg}$, and the damping factor is given by $\mu = 0.1\text{Ns/m}^3$; the initial conditions are given as $y(0) = 1\text{m}$ and $\dot{y}(0) = 0\text{m/s}$. An impact excitation is given at the mass by $f(t) = 1\text{N}$ when $t = 0\text{s}$, $f(t) = 0\text{N}$ otherwise. The only differences among these oscillators are that they have stiffness coefficient with different variation types. For the 2-DOF weakly nonlinear time-varying chainlike Van der Pol systems to be simulated, the following common information is given: the mass coefficients, damping factor and damping coefficient are assumed to be constants $m_1 = m_2 = 50\text{kg}$, $\mu = 5\text{Ns/m}^3$, $c_2 = 0\text{Ns/m}$; the initial conditions for the two experiments are given as $y_1(0) = 0\text{m}$, $y_2(0) = 1\text{m}$, $\dot{y}_1(0) = 0\text{m/s}$, $\dot{y}_2(0) = 0\text{m/s}$ as well as $y_1(0) = 1\text{m}$, $y_2(0) = 0\text{m}$, $\dot{y}_1(0) = 0\text{m/s}$, $\dot{y}_2(0) = 0\text{m/s}$; a periodic excitation is given at mass 1 by $f(t) = 50\sin(2\pi t)\text{N}$. The only differences among these 2-DOF weakly nonlinear Van der Pol systems are that their stiffness coefficients have different variation types.

The identified results of the stiffness coefficients of weakly nonlinear smoothly and abruptly varying Van der Pol systems are presented in the following, whereas the identified results of the damping coefficients of the former systems and all the identified results of weakly nonlinear periodically varying Van der Pol systems are presented in Appendices A.2.4 - A.2.6.

4.2.1 HHT-based Identification of 1-DOF weakly nonlinear time-varying Van der Pol oscillators

For the 1-DOF weakly nonlinear time-varying Van der Pol oscillators to be simulated, the system stiffness coefficients are given as Table 4.3:

Table 4.3: System stiffness coefficients of 1-DOF weakly nonlinear time-varying Van der Pol oscillators

System coefficients / Type of systems	System stiffness coefficient (N/m)
1-DOF weakly nonlinear smoothly varying Van der Pol oscillator	$k(t) = 100\pi^2 \text{N/m}$ when $t < 2\text{s}$, $k(t) = 100\pi^2 - 10\pi^2 t \text{N/m}$ when $2\text{s} \leq t \leq 4\text{s}$, $k(t) = 80\pi^2 \text{N/m}$ when $t > 4\text{s}$.
1-DOF weakly nonlinear abruptly varying Van der Pol oscillator	$k(t) = 100\pi^2$ when $t < 1.5\text{s}$, $k(t) = 60\pi^2$ when $1.5\text{s} \leq t \leq 3.5\text{s}$, $k(t) = 80\pi^2$ when $t > 3.5\text{s}$.
1-DOF weakly nonlinear periodically varying Van der Pol oscillator	$k(t) = 100\pi^2 - 10\pi^2 \sin 2\pi t$ for any t.

The identified results of the stiffness coefficients of the 1-DOF weakly nonlinear smoothly and abruptly varying Van der Pol oscillators as well as their relative errors are shown in Figures 4.7 - 4.8.
It can be found that: For the 1-DOF weakly nonlinear smoothly varying Van der Pol oscillator, when using noise-added system responses as input of the modified HHT-based identification method, although the identified results are contaminated by noise, the accuracy of the obtained identified result of stiffness coefficient k is still high (with maximal relative error less than 3.6%). And no matter using noiseless system responses or noise-added ones as input, the accuracy of the obtained identified stiffness result of the weakly nonlinear smoothly varying Van der Pol oscillator is a little bit worse than the identified stiffness result of the linear smoothly varying oscillator ($\mu = 0\text{Ns/m}^3$) which has the same linear system coefficients, initial conditions and excitation signal as the weakly nonlinear smoothly varying Van der Pol oscillator, due to the approximation of Equation (4.8); For the 1-DOF weakly nonlinear abruptly varying Van der Pol oscillator, no matter using noiseless or noise-added system responses as input of the modified HHT-based identification method, the accuracies of the obtained identified results of the weakly nonlinear abruptly varying Van der Pol oscillator are similar to those of the linear abruptly varying oscillator which has the same linear system coefficients, initial conditions and excitation

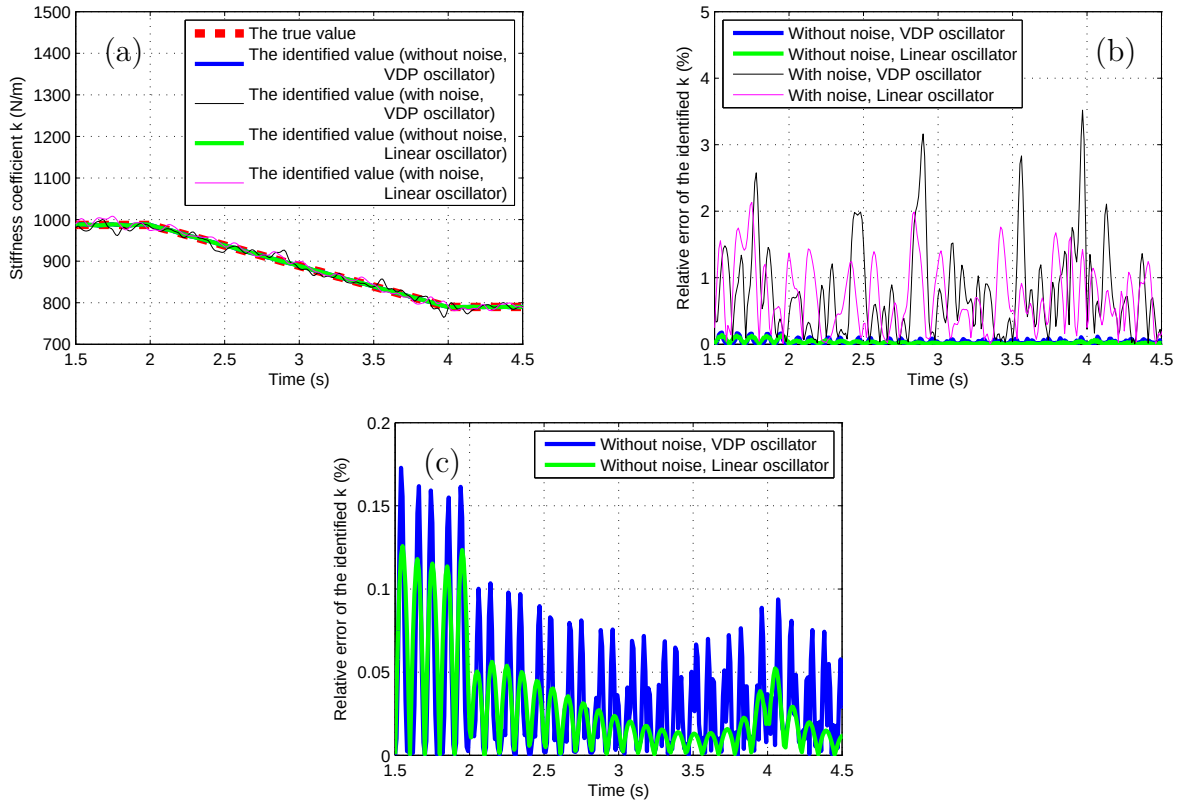

Figure 4.7: Stiffness coefficient of a weakly nonlinear smoothly varying Van der Pol oscillator: (a) The true value and the identified values of stiffness coefficient k, (b) Relative errors of the identified values of k, (c) Relative errors of the identified values of k (without noise in system responses).

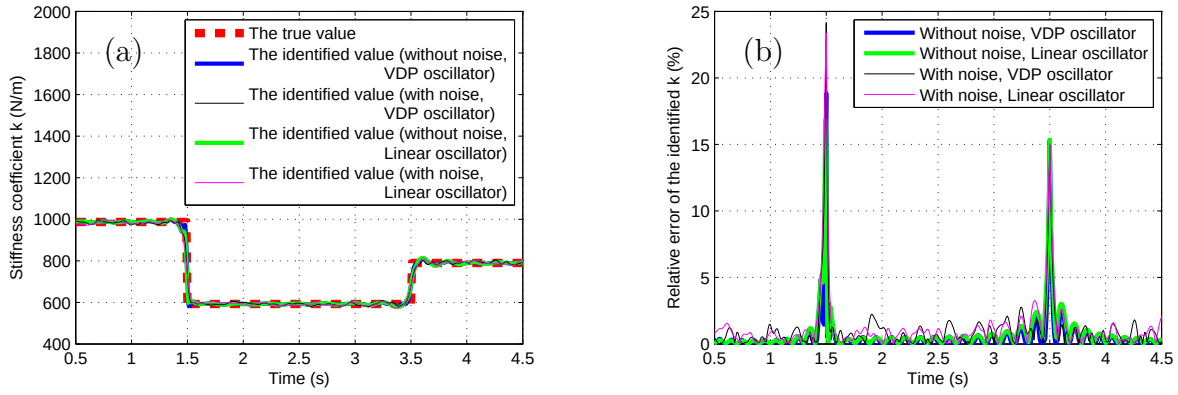

Figure 4.8: Stiffness coefficient of a weakly nonlinear abruptly varying Van der Pol oscillator: (a) The true value and the identified values of stiffness coefficient k, (b) Relative errors of the identified values of k.

signal as the weakly nonlinear abruptly varying Van der Pol oscillator. The identified result of stiffness coefficient k has relatively large identification errors around time instants

$t = 1.5$s and $t = 3.5$s, which implies that the proposed identification method has bad ability to capture the abrupt change of the system coefficient due to the limitations of Equation (2.16). At other time instants, when using noise-added system responses as input of the modified HHT-based identification method, good identified result of k (with maximal relative error less than 2.8%) can still be obtained.

4.2.2 HHT-based Identification of 2-DOF weakly nonlinear time-varying chainlike Van der Pol systems

For the 2-DOF weakly nonlinear systems which contain a weakly nonlinear time-varying Van der Pol oscillator and follow the chainlike model in Figure 3.1, the system stiffness coefficients are given as Table 3.3. The identified results of the system stiffness coefficients of the 2-DOF weakly nonlinear smoothly and abruptly varying chainlike Van der Pol systems and their relative errors are shown in Figures 4.9 - 4.12.

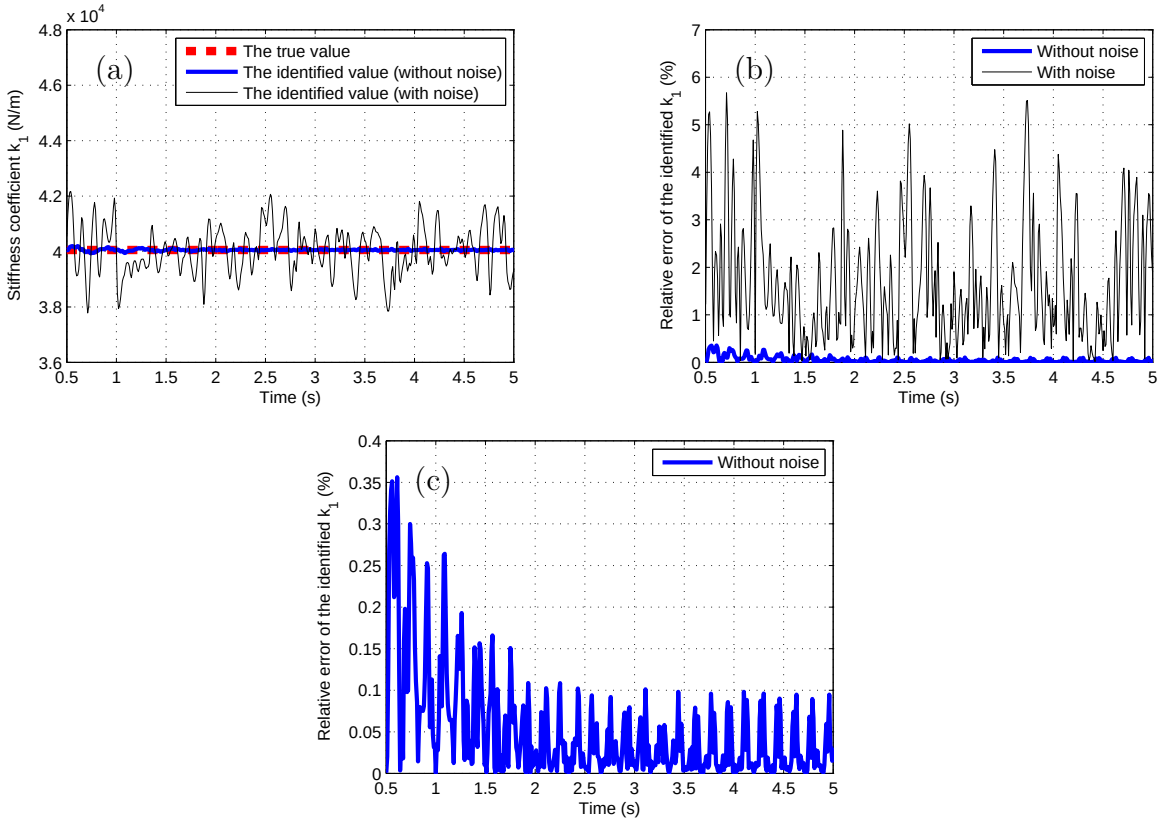

Figure 4.9: Stiffness coefficient k_1 of a 2-DOF weakly nonlinear chainlike system with a weakly nonlinear smoothly varying Van der Pol oscillator: (a) The true value and the identified values of k_1, (b) Relative errors of the identified values of k_1, (c) Relative error of the identified value of k_1 (without noise in system responses).

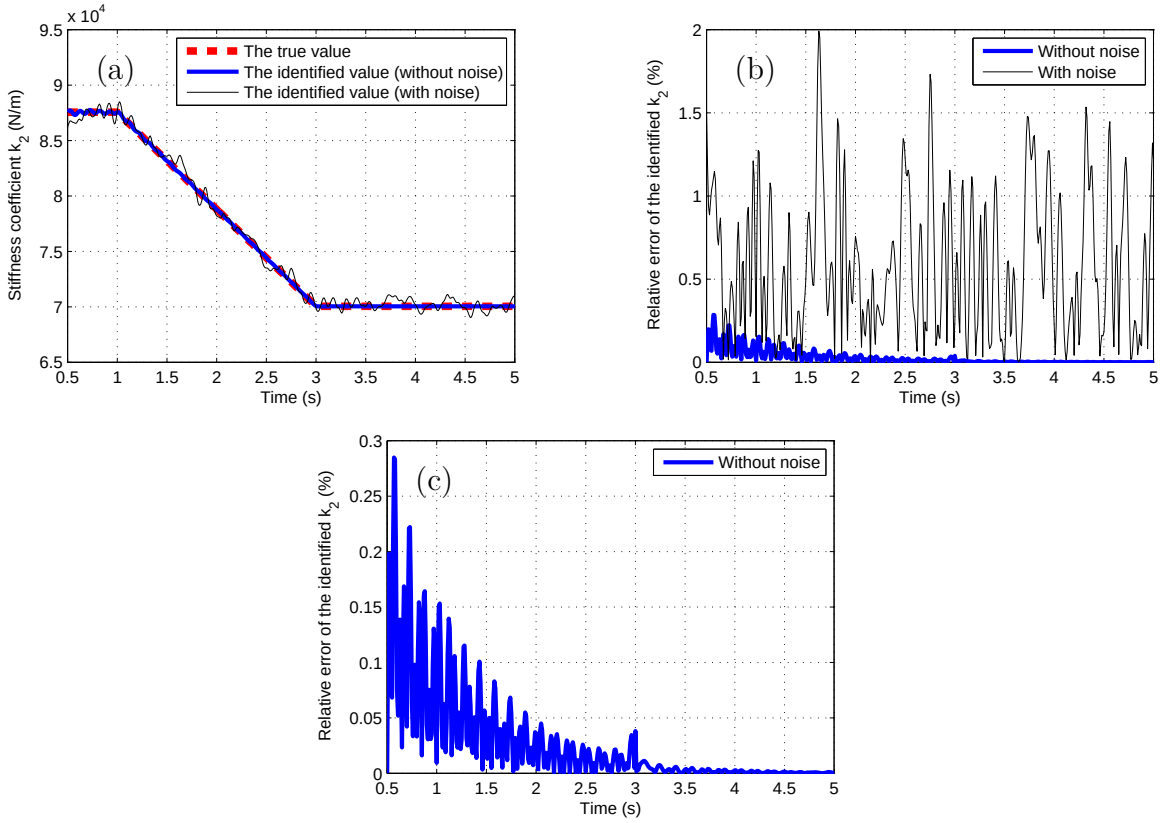

Figure 4.10: Stiffness coefficient k_2 of a 2-DOF weakly nonlinear chainlike system with a weakly nonlinear smoothly varying Van der Pol oscillator: (a) The true value and the identified values of k_2, (b) Relative errors of the identified values of k_2, (c) Relative error of the identified value of k_2 (without noise in system responses).

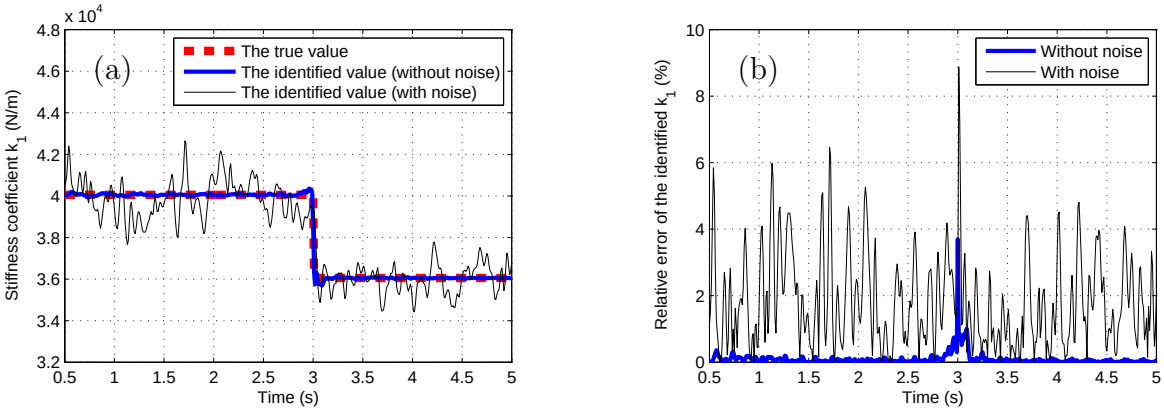

Figure 4.11: Stiffness coefficient k_1 of a 2-DOF weakly nonlinear chainlike system with a weakly nonlinear abruptly varying Van der Pol oscillator: (a) The true value and the identified values of k_1, (b) Relative errors of the identified values of k_1.

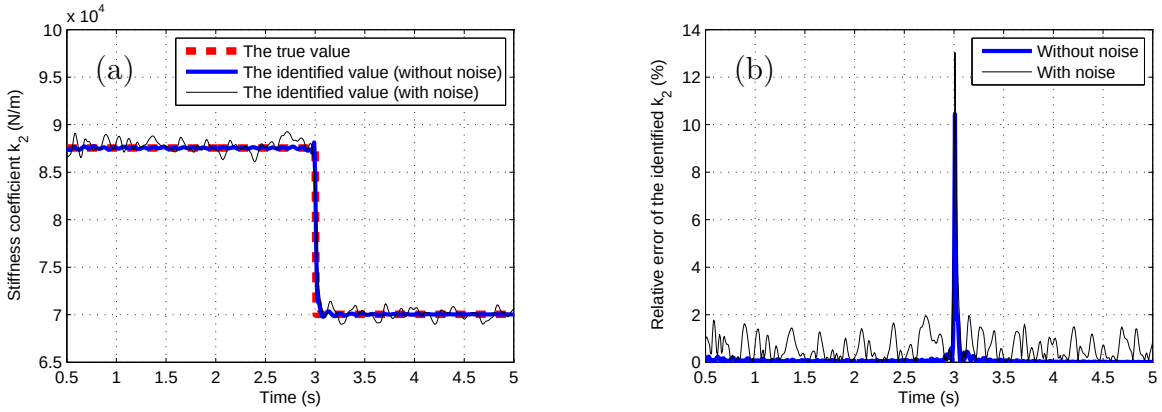

Figure 4.12: Stiffness coefficient k_2 of a 2-DOF weakly nonlinear chainlike system with a weakly nonlinear abruptly varying Van der Pol oscillator: (a) The true value and the identified values of k_2, (b) Relative errors of the identified values of k_2.

From the above figures, it can be seen that: For the 2-DOF weakly nonlinear smoothly varying chainlike Van der Pol system, no matter using noiseless or noise-added system responses as input of the modified HHT-based identification method, the resulting identified results of the stiffness coefficients always match their respective true values well (with maximal relative error of k_1 less than 5.7% and that of k_2 equal to 2.0%, respectively); For the 2-DOF weakly nonlinear abruptly varying chainlike Van der Pol system, no matter using noiseless or noise-added system responses as input of the modified HHT-based identification method, the identified results of the stiffness coefficients have relatively large identification errors around time instant $t = 3$s, which implies that the modified HHT-based identification method has bad ability to capture the abrupt change of the system parameter due to the limitations of Equation (2.16). At other time instants, the resulting identified results of the stiffness coefficients always match their respective true values well (with maximal relative error of k_1 less than 6.5% and that of k_2 less than 2.0%, respectively).

4.3 Parameter studies on weakly nonlinear time-varying systems

Forced vibration simulations are processed on a 2-DOF weakly nonlinear smoothly varying chainlike Duffing system and a 2-DOF weakly nonlinear periodically varying chainlike Van der Pol system to find the proper value range of the structural parameter in the nonlinear parameter or that of the nonlinear parameter itself, for which good identified results can be obtained by the proposed method. Like in the simulations of the above sections, noise-added system responses ($Nstd = 0.05$, $NE = 15$) are also considered here.

4.3.1 Parameter study on a 2-DOF weakly nonlinear smoothly varying chainlike Duffing system

For the parameter study on a 2-DOF weakly nonlinear smoothly varying chainlike Duffing system, the system coefficients, initial conditions as well as the external force are given the same as those of the 2-DOF weakly nonlinear smoothly varying chainlike Duffing system proposed in Section 4.1.2, except that the cubic stiffness factor δ is given as follows:
$\delta(t) = k_{up}$ when $t < 1$s,
$\delta(t) = k_{up} - (k_{up} - k_{down})/t_{duff}(t-1)$ when $1\text{s} \leq t \leq t_{duff} + 1$s,
$\delta(t) = k_{down}$ when $t > t_{duff} + 1$s,
$k_{up} = 12761$N/m, $k_{down} = 11010$N/m for any t,
where t_{duff} is the variable structural parameter. In the simulation, t_{duff} takes values in the interval $(0, 8]$s with the time interval between two adjacent t_{duff} values equal to 0.01s. Figures 4.13 - 4.16 present the mean relative errors of cubic stiffness factor δ, linear stiffness coefficient k_2, and damping coefficient c_1 as well as the mean absolute error of damping coefficient c_2.

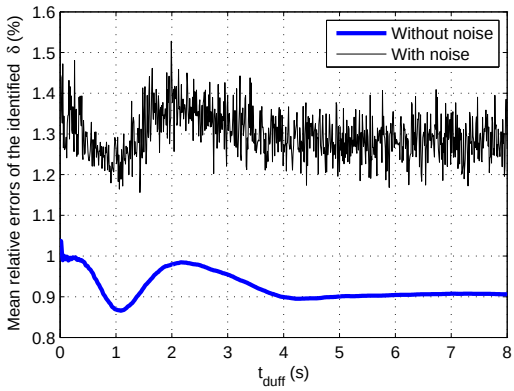

Figure 4.13: Mean relative errors of cubic stiffness factor δ of a 2-DOF weakly nonlinear smoothly varying chainlike Duffing system with respect to t_{duff}.

We can notice from these figures that: when noiseless system responses are used as input of the modified HHT-based identification method, the mean relative and absolute errors (denoted with blue lines) of the system coefficients reach their maximum values as t_{duff} takes values in the interval $(0, 0.03]$s, then they have large and rapid decrease as t_{duff} increases and reach their minimum values as t_{duff} takes values in the interval $[1, 1.33]$s. After that, they have a large increase and reach their second maximum values followed by a large decrease as t_{duff} increases to 4s. As t_{duff} increases in the interval $[4, 8]$s, they almost keep constant; when noise-added system responses are used as input, the mean relative and absolute errors (denoted with black lines) of the system coefficients also have similar large variations as their aforementioned counterparts (denoted with blue lines) when t_{duff} increases in the interval $(0, 4]$s, then they keep fluctuating around some constant values as t_{duff} increases in the interval $[4, 8]$s. Although the magnitudes of the latter (denoted with black lines) are larger than those of the former (denoted with blue

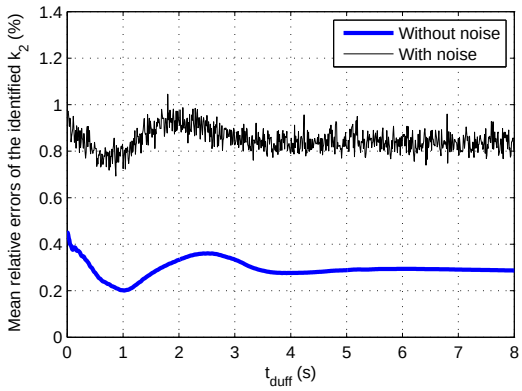

Figure 4.14: Mean relative errors of stiffness coefficient k_2 of a 2-DOF weakly nonlinear smoothly varying chainlike Duffing system with respect to t_{duff}.

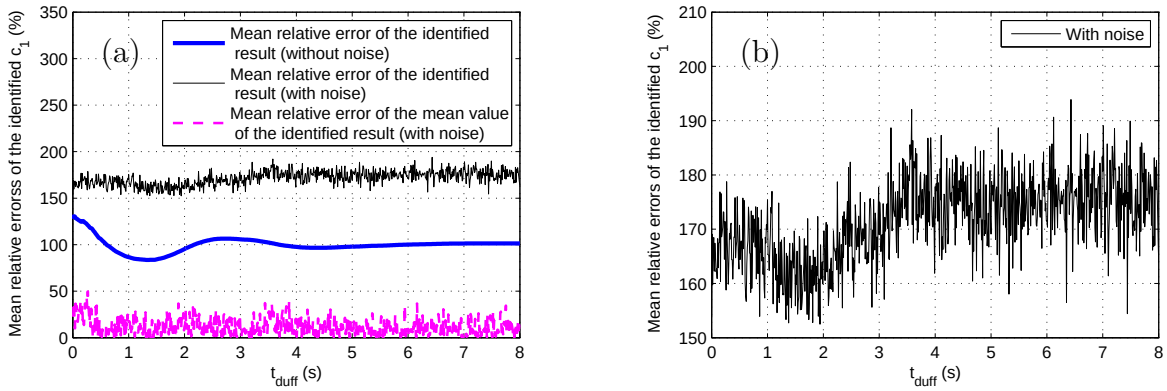

Figure 4.15: Mean relative errors of damping coefficient c_1 of a 2-DOF weakly nonlinear smoothly varying chainlike Duffing system with respect to t_{duff}: (a) Mean relative errors of the identified values of c_1, (b) Mean relative errors of the identified values of c_1 (with noise in system responses).

lines), the magnitudes of the mean relative errors of the identified cubic stiffness factor δ and linear stiffness coefficient k_2 are still sufficiently small (less than 1.6% and 1.1% respectively). The identified results of damping coefficients c_1 and c_2 have quite large mean relative and absolute errors denoted with black lines, but their mean relative and absolute errors denoted with pink dashed lines are relatively smaller than the former (The procedures to calculate the mean relative and absolute errors denoted with black lines and those denoted with pink dashed lines can be found in Section 3.3.1). At $t_{duff} = 2$s (case of the 2-DOF weakly nonlinear smoothly varying chainlike Duffing system proposed in Section 4.1.2), the mean relative and absolute errors of damping coefficients denoted with pink dashed lines are sufficiently small (less than 13% and 1.3Ns/m respectively).
Simulations that consider larger noise intensity ($(Nstd = 0.2,\ NE = 15)$) of the input system responses are also carried out, and the resulting identified system parameters are found having larger mean relative or absolute errors than their counterparts obtained

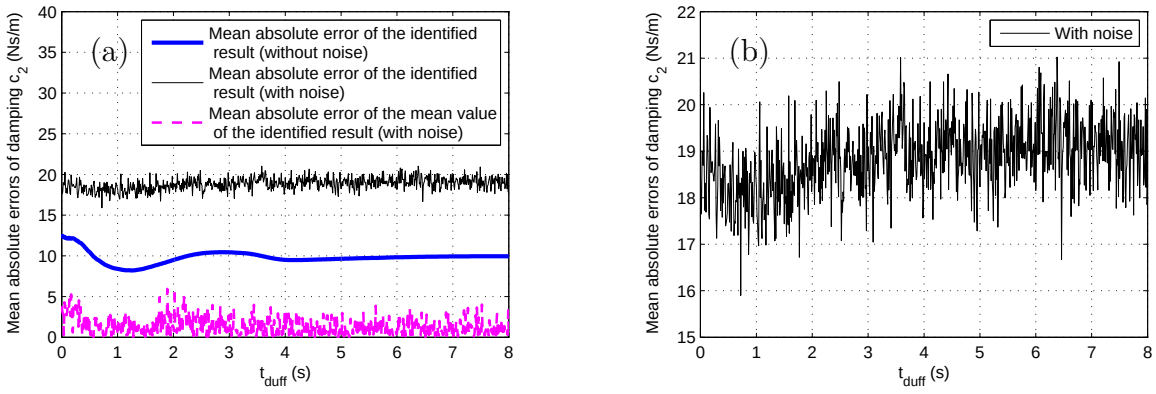

Figure 4.16: Mean absolute errors of damping coefficient c_2 of a 2-DOF weakly nonlinear smoothly varying chainlike Duffing system with respect to t_{duff}: (a) Mean absolute errors of the identified values of c_2, (b) Mean absolute errors of the identified values of c_2 (with noise in system responses).

above, which indicates that the magnitudes of the mean relative or absolute errors of the system parameters depend on the noise intensity of the input system responses.
In conclusion, good results of the mean relative and absolute errors of the identified system coefficients are obtained as t_{duff} takes values in the interval $[4, 8]$s.

4.3.2 Parameter study on a 2-DOF weakly nonlinear periodically varying chainlike Van der Pol system

For the parameter study on a 2-DOF weakly nonlinear periodically varying chainlike Van der Pol system, the system coefficients, initial conditions as well as the external force are given the same as those of the 2-DOF weakly nonlinear periodically varying chainlike Van der Pol system proposed in Section 4.2.2, except that the damping factor $\mu = 50\mu_l$ where μ_l is a variable parameter in the interval $[0.01, 1.0]\text{Ns/m}^3$ with the variation between each two adjacent μ_l values equal to 0.001Ns/m^3.
The mean relative errors of stiffness coefficients k_1 and k_2 as well as damping factor μ, and the mean absolute error of damping coefficient c_2 which are obtained at different μ_l values are shown in Figures 4.17 - 4.20.

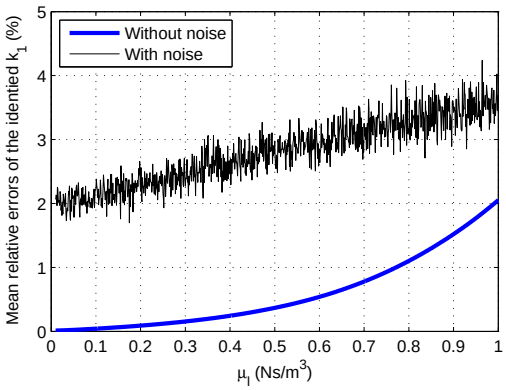

Figure 4.17: Mean relative errors of stiffness coefficient k_1 of a 2-DOF weakly nonlinear periodically varying chainlike Van der Pol system with respect to μ_l.

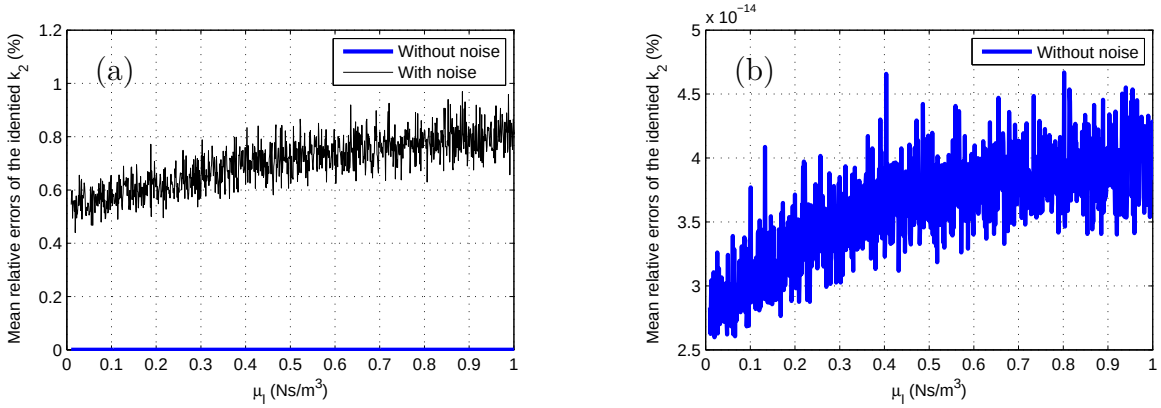

Figure 4.18: Mean relative errors of stiffness coefficient k_2 of a 2-DOF weakly nonlinear periodically varying chainlike Van der Pol system with respect to μ_l: (a) Mean relative errors of the identified values of k_2, (b) Mean relative errors of the identified values of k_2 (without noise in system responses).

From these figures, it is noticed that: no matter noiseless or noise-added system responses are used as input of the modified HHT-based identification method, the mean relative errors of the identified k_1 and k_2 as well as the mean absolute error of the identified c_2 have increasing trend as μ_l increases, and good identified results of the stiffness coefficients are always obtained (with maximal mean relative error of the identified k_1 less than 4.3% and that of k_2 less than 0.97%, respectively); the mean relative error (denoted with a blue line) of the identified μ obtained when using noiseless system responses as input is large at $\mu_l = 0.01\text{Ns/m}^3$, then it has rapidly decreasing trend as μ_l increases in the interval $[0.01, 0.065]\text{Ns/m}^3$ and reaches its minimum at $\mu_l = 0.065\text{Ns/m}^3$, after that it has almost proportionally increasing trend as μ_l increases in the interval $(0.065, 1.0]\text{Ns/m}^3$ and reaches its maximum at $\mu_l = 1.0\text{Ns/m}^3$. When noise-added system responses are used as input, the mean relative error (denoted with a black line) of the identified μ has obvious decreasing trend as μ_l increases in the interval $[0.01, 1.0]\text{Ns/m}^3$, and its magnitude as well as the

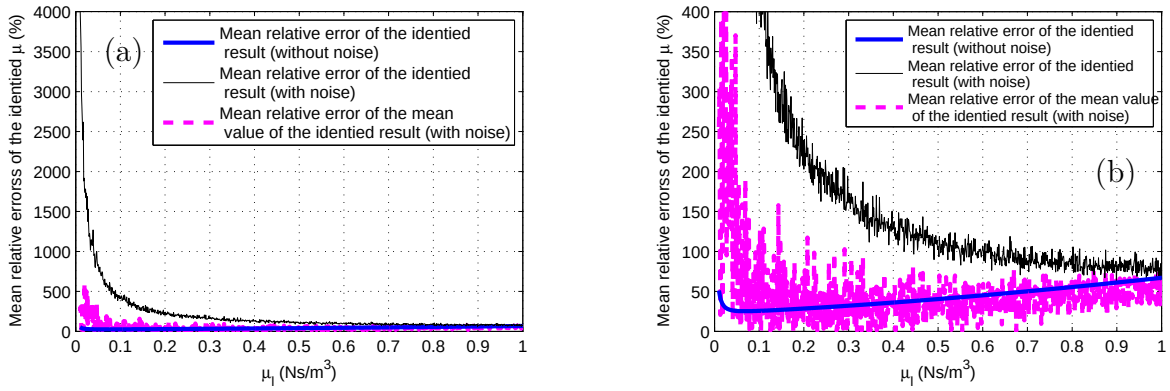

Figure 4.19: Mean relative errors of damping factor μ of a 2-DOF weakly nonlinear periodically varying chainlike Van der Pol system with respect to μ_l: (a) Mean relative errors of the identified values of μ, (b) Close-up of (a).

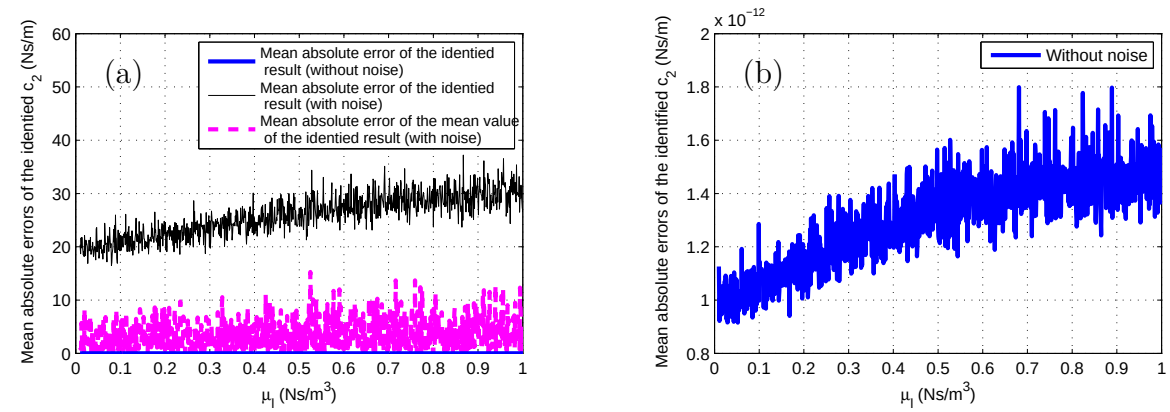

Figure 4.20: Mean absolute errors of damping coefficient c_2 of a 2-DOF weakly nonlinear periodically varying chainlike Van der Pol system with respect to μ_l: (a) Mean absolute errors of the identified values of c_2, (b) Mean absolute errors of the identified values of c_2 (without noise in system responses).

magnitude of the mean absolute error (also denoted with a black line) of the identified c_2 are quite large, but the corresponding mean relative and absolute errors denoted with pink dashed lines have relatively smaller magnitudes (The procedures to calculate the mean relative and absolute errors denoted with black lines and those denoted with pink dashed lines can be found in Section 3.3.1). The mean relative error of the identified μ denoted with a pink dashed line has variation similar as the variation of its counterpart denoted with a blue line, whereas the mean absolute error of the identified c_2 denoted with a pink dashed line keeps fluctuating around some constant value as μ_l increases. At $\mu_l = 0.1\text{Ns/m}^3$ (case of the 2-DOF weakly nonlinear periodically varying chainlike Van der Pol system proposed in Section 4.2.2), the mean relative error of the identified μ and the mean absolute error of the identified c_2 denoted with pink dashed lines are sufficiently small (less than 14% and equal to 5.0Ns/m respectively).

In conclusion, it is proper to choose small values in the interval $[0.065, 1.0]\mathrm{Ns/m}^3$ for variable parameter μ_l in order to obtain good identified results of the system coefficients.

4.4 Conclusion

In this chapter, we extend the parametric identification method for general linear time-varying systems to the identification of weakly nonlinear time-varying MDOF Duffing systems and Van der Pol systems. Due to the exist of nonlinear coefficients, when applying HT to process the governing nonlinear differential equations of the system, Bedrosian's theorem is not valid for the HT on the product of the nonlinear system coefficient and the corresponding system response. Instead, we apply the formula of Hahn and derive Equations (4.4) and (4.8) to process the HT of the product of the nonlinear system coefficient and the corresponding system response and accordingly modify the identification method for n-DOF chainlike weakly nonlinear time-varying Duffing systems and Van der Pol systems respectively. Then, in order to demonstrate the effectiveness and accuracy of the modified HHT-based identification method, three types of time variation of stiffness: smooth, abrupt and periodical variations are studied on 1-DOF and 2-DOF weakly nonlinear time-varying Duffing systems as well as Van der Pol systems.
For weakly nonlinear time-varying Duffing systems, the accuracies of the identified results of 1-DOF weakly nonlinear time-varying Duffing systems are always worse than those of the 1-DOF linear time-varying systems which have the same linear system coefficients, initial conditions and excitation signals as the corresponding 1-DOF weakly nonlinear time-varying Duffing systems due to the application of Equation (4.4) for processing the HT of the product of the nonlinear system coefficient and the corresponding system response. No matter using noiseless or noise-added system responses as input of the modified HHT-based identification method, we can always obtain good identified results of the stiffness coefficients for both 1-DOF and 2-DOF weakly nonlinear time-varying Duffing systems. Since the damping coefficients are sensitive to noise, the accuracies of their identified results are low, especially when using noise-added system responses as input of the modified HHT-based identification method, but the mean values of them are quite close to their respective true values.
For weakly nonlinear time-varying Van der Pol systems, due to the application of Equation (4.8) for processing the HT of the product of the nonlinear system coefficient and the corresponding system response, the accuracies of the identified results of 1-DOF weakly nonlinear smoothly and periodically varying Van der Pol systems are a little bit worse than those of the 1-DOF linear time-varying systems which have the same linear system coefficients, initial conditions and excitation signals as the corresponding 1-DOF weakly nonlinear time-varying Van der Pol systems. The reason for this is that we take small value of nonlinear damping factor μ. Since the identification method has bad capability to capture the abrupt change of the system coefficient for linear abruptly varying systems, the consequent identification error shadow the identification error of 1-DOF weakly nonlinear abruptly varying Van der Pol system caused by application of Equation (4.8), thus the accuracies of the identified results of 1-DOF weakly nonlinear abruptly varying Van der Pol system are similar to those of the 1-DOF linear abruptly varying system which has

the same linear system coefficients, initial conditions and excitation signal as the weakly nonlinear abruptly varying Van der Pol oscillator. For both 1-DOF and 2-DOF weakly nonlinear time-varying Van der Pol systems, no matter using noiseless or noise-added system responses as input of the modified HHT-based identification method, we can always obtain good identified results of the stiffness coefficients but quite bad identified results of the damping coefficients. By taking the mean values of them, we can still obtain good identification of the damping coefficients.
For the parameter study on a 2-DOF weakly nonlinear smoothly varying chainlike Duffing system, the simulation results demonstrate that it is proper to choose values in the interval $[4, 8]$s for structural parameter t_{duff} in order to obtain good identified results of the system coefficients. For the parameter study on a 2-DOF weakly nonlinear periodically varying chainlike Van der Pol system, the simulation results indicate that good identified results of the system coefficients can be obtained as we choose small values in the interval $[0.065, 1.0]\mathrm{Ns/m}^3$ for parameter μ_l.
In conclusion, the identified results demonstrate that the parametric identification method for general linear time-varying systems can be extended to the identification of weakly nonlinear time-varying MDOF chainlike Duffing systems and Van der Pol systems with effectiveness, accuracy and robustness.

5 HHT and Bayesian inference based identification of general time-varying systems

As we mentioned, in the application of the proposed HHT-based identification method uncertainties due to model structure errors, model parameter errors and model order errors may exist. In order to update the white noise in system responses, Bayesian inference is used, yielding the posterior distributions of the noise parameters. The referenced values of the system responses are added to the corresponding posterior distributions of the noise parameters, gaining the posterior distributions of the system responses, which are used as input of the HHT-based identification method. Then, by using the HHT-based identification method, posterior distributions of the identified results of system stiffness and damping coefficients can be obtained. The combination of Bayesian inference and the HHT-based identification method is applied in the identification of the aforementioned 1-DOF and 2-DOF linear time-varying systems and weakly nonlinear time-varying systems which have smooth, abrupt and periodical stiffness variations to demonstrate the effectiveness, accuracy and robustness of the combined method for both linear time-varying systems and weakly nonlinear time-varying systems.
Later, parameter studies on linear time-varying systems and weakly nonlinear time-varying systems are carried out with the help of Bayesian inference. With the likelihood function formulated as the product of three probability density functions, one relating to the IMFs of the acceleration responses, the other two relating to the IMFs of the corresponding velocity responses and the IMFs of the corresponding displacement responses, Bayesian model updating method is implemented by TMCMC method for a set of candidate model classes, yielding the corresponding posterior distributions of the system structural parameters for these model classes. By using Bayesian model class selection, the most probable model class and the corresponding posterior distributions of the system structural parameters for the most probable model class are selected. Numerical simulations are processed on linear time-varying systems and weakly nonlinear time-varying systems to demonstrate the effectiveness, accuracy and robustness of the proposed Bayesian inference based parameter identification method.

5.1 HHT and Bayesian inference based identification method for linear time-varying systems and weakly nonlinear time-varying systems

The main procedures of combination of Bayesian inference and the proposed HHT-based identification method are presented as follows:

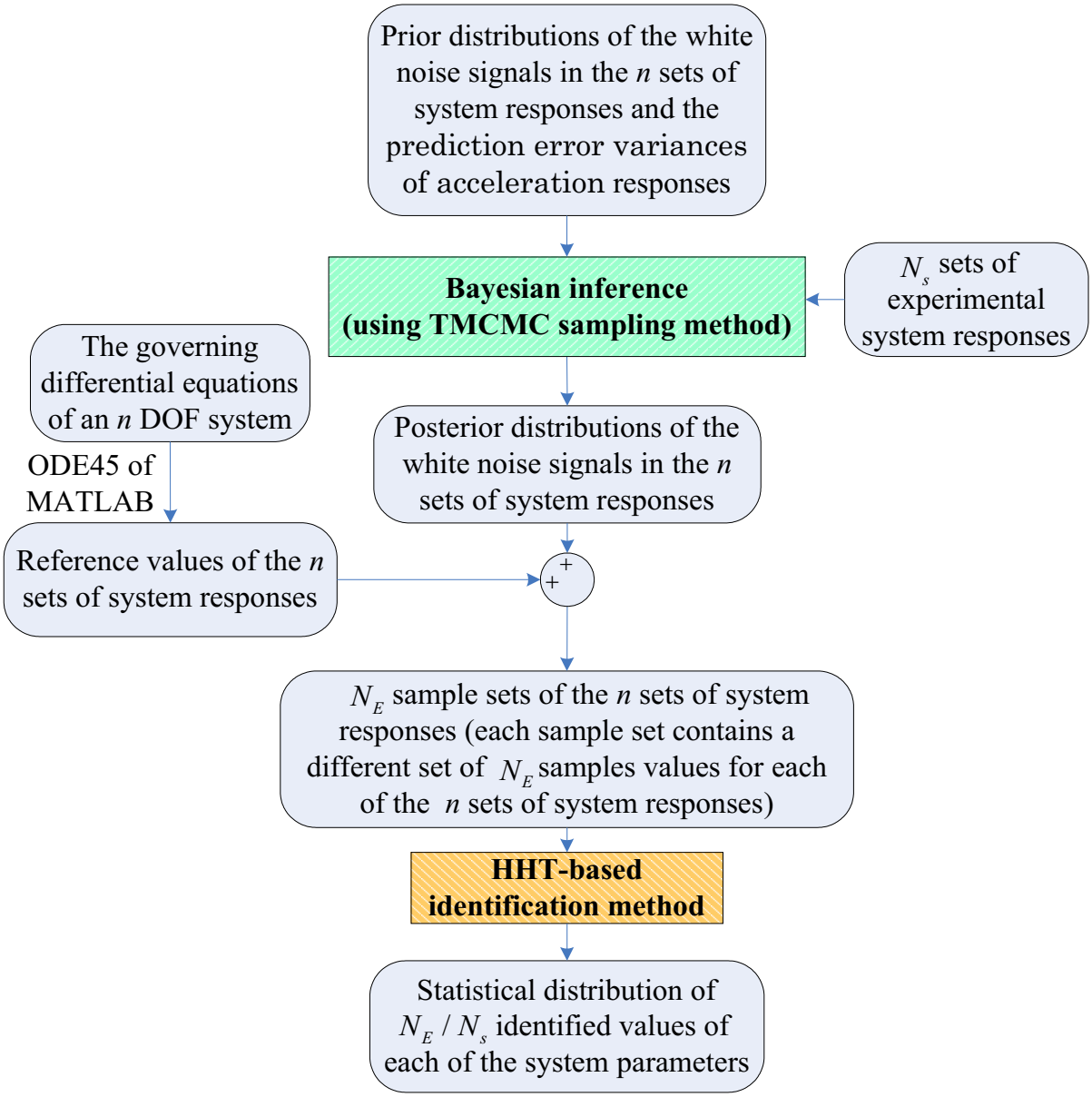

Figure 5.1: Main procedures of the HHT-based identification method applying Bayesian inference for an n-DOF linear time-varying system and an n-DOF weakly non-linear time-varying system.

1. Run n experiments (see Section 3.2) to get n sets of noiseless system responses in the required time history as the reference values of the system responses.

2. Perform Bayesian inference with the help of Equations (2.37) - (2.40) in Section 2.4 to update initial knowledge about the forced vibration system responses and the white noise in the system responses based on measured system responses.
   For a set of model classes $\boldsymbol{M} = \{M_l : l = 1, \ldots, N_{class}\}$, suppose the experimental data D consists of N_s sets of data $D = \{D^{(k)} : k = 1, \ldots, N_s\}$ at each time instant

with the kth set of data given by $D^{(k)} = \{y_{i,q}^{(k)}, \dot{y}_{i,q}^{(k)}, \ddot{y}_{i,q}^{(k)} : i,q = 1,\ldots,n\}$, where the subscript i denotes the index of DOF and the subscript q denotes the index of experiment (in each experiment, ODE of the system is solved with the same initial conditions given at a different DOF of the system). The prior distribution of the white noise in each system response is assigned to be a given uniform distribution. The prior distribution of the Prediction error variance (PEV) of each acceleration signal is a given uniform distribution. The number of samples of each distribution is given the same by N_E.
From Equations (2.37) - (2.40), for an acceleration signal $\ddot{y}_{i,q}^{(k)}$, we have

$$\ddot{y}_{i,q}^{(k)} = mo^a(\boldsymbol{\theta}_{i,q}) + e_{i,q}^a \ , \quad e_{i,q}^a \sim N\left(0, (\varepsilon_{i,q}^a)^2\right) \tag{5.1}$$

where $mo^a(\boldsymbol{\theta}_{i,q})$ is the model output of $\ddot{y}_{i,q}^{(k)}$, which is equal to the reference value of $\ddot{y}_{i,q}^{(k)}$ (supposed as noiseless) plus the white noise parameter $n_{i,q}^a$, $e_{i,q}^a$is the prediction error of $\ddot{y}_{i,q}^{(k)}$ whose PDF model is given by a Gaussian PDF with zero mean and variance $(\varepsilon_{i,q}^a)^2$. As displacement signal $y_{i,q}^{(k)}$ and velocity signal $\dot{y}_{i,q}^{(k)}$ can be obtained by integration of the corresponding acceleration signal $\ddot{y}_{i,q}^{(k)}$, we assume their PEVs are proportional to the PEV of $\ddot{y}_{i,q}^{(k)}$ with respective factors $\eta_{i,q}$ and $\rho_{i,q}$ which define the model class $M_l = \{\boldsymbol{M}\left(\eta_{i,q}(l), \rho_{i,q}(l)\right) : i,q = 1,\ldots,n\}$.
Assume the prediction errors of the system responses are modeled as statistically independent of each other, then the likelihood function which corresponds to the ith DOF and the qth experiment is given as

$$\begin{aligned} p(D_{i,q}|\boldsymbol{\theta}_{i,q}, M_l^{ik}) &= \prod_{k=1}^{N_s} p(\ddot{y}_{i,q}^{(k)}|\boldsymbol{\theta}_{i,q}, M_l^{ik}) p(\dot{y}_{i,q}^{(k)}|\boldsymbol{\theta}_{i,q}, M_l^{ik}) p(y_{i,q}^{(k)}|\boldsymbol{\theta}_{i,q}, M_l^{ik}) \\ &= \frac{1}{(2\pi)^{3N_sN_o/2}\left((\varepsilon_{i,q}^a)^2\right)^{N_s/2}\left(\eta_{i,q}(l)(\varepsilon_{i,q}^a)^2\right)^{N_s/2}\left(\rho_{i,q}(l)(\varepsilon_{i,q}^a)^2\right)^{N_s/2}} \cdot \\ &\exp\left\{-\frac{1}{2}\sum_{k=1}^{N_s}\left[\frac{\left(\ddot{y}_{i,q}^{(k)} - mo^a(\boldsymbol{\theta}_{i,q})\right)^2}{(\varepsilon_{i,q}^a)^2} + \frac{\left(\dot{y}_{i,q}^{(k)} - mo^v(\boldsymbol{\theta}_{i,q})\right)^2}{\rho_{i,q}(l)(\varepsilon_{i,q}^a)^2} + \frac{\left(y_{i,q}^{(k)} - mo^d(\boldsymbol{\theta}_{i,q})\right)^2}{\eta_{i,q}(l)(\varepsilon_{i,q}^a)^2}\right]\right\} \end{aligned} \tag{5.2}$$

where $D_{i,q} = \left\{\ddot{y}_{i,q}^{(k)}, \dot{y}_{i,q}^{(k)}, y_{i,q}^{(k)}\right\}_{k=1}^{N_s}$ is the subset of the experimental data D and $\boldsymbol{\theta}_{i,q} = \left[n_{i,q}^a, n_{i,q}^v, n_{i,q}^d, (\varepsilon_{i,q}^a)^2\right]^T$ is the parameter vector to be updated, $M_l^{ik} = \boldsymbol{M}\left(\eta_{i,q}(l), \rho_{i,q}(l)\right)$ is the subset of the model class M_l, $mo^a(\boldsymbol{\theta}_{i,q})$, $mo^v(\boldsymbol{\theta}_{i,q})$, $mo^d(\boldsymbol{\theta}_{i,q})$ are the model acceleration, velocity and displacement respectively, and $n_{i,q}^a$, $n_{i,q}^v$, $n_{i,q}^d$ are the white noise signals in the acceleration, velocity and displacement responses respectively. All these parameters correspond to the ith DOF and the qth experiment and are independent from parameters of other DOFs and other experiments.
With the help of Equation (5.2), Bayesian model updating is implemented by TMCMC method to update the initial knowledge about the white noise parameters in the system responses for each DOF in each experiment at each time instant. These

procedures are repeated for all model classes $\boldsymbol{M}$ with the posterior probability of each model class for the ith DOF and the qth experiment at each time instant calculated as follows

$$p(M_l^{ik}|D_{i,q},\boldsymbol{M}) = \frac{p(D_{i,q}|M_l^{ik})p(M_l^{ik}|\boldsymbol{M})}{p(D_{i,q}|\boldsymbol{M})} \tag{5.3}$$

where the evidence $p(D_{i,q}|M_l^{ik})$ can be calculated following the TMCMC method introduced in Section 2.4.4, the prior distribution $p(M_l^{ik}|\boldsymbol{M}) = 1/N_{class}$ since all model classes are assumed to be equally likely apriori, and the normalizing constant $p(D_{i,q}|\boldsymbol{M}) = \sum_{l=1}^{N_{class}} p(D_{i,q}|M_l^{ik})p(M_l^{ik}|\boldsymbol{M})$.

3. Perform Bayesian model class selection according to Equation (5.3) in order to choose the most probable model class which has the best values of the factors η and ρ. For each DOF in each experiment at each time instant, we choose the maximal posterior probability of the parameter vector (which means that we obtain n^2 maximal posterior probabilities for n DOF in n experiments at each time instant). The most probable model class at each time instant $M^* = \{\boldsymbol{M}\left(\eta_{i,q}^*, \rho_{i,q}^*\right) : i,q = 1,\ldots,n\}$ is the model class which has n^2 maximal posterior probabilities, where $\eta_{i,q}^*$ and $\rho_{i,q}^*$ are the best values of the factors η and ρ for the ith DOF and the qth experiment. With the help of the posterior distributions of the noise parameters for the most probable model class at each time instant, N_E sample sets of the n sets of system responses (each sample set contains a different set of sample values for the corresponding n sets of system responses) are obtained.

4. Filter the N_E sample sets of the n sets of system responses obtained in step 3 with the fourth-order zero-lag Butterworth low-pass filter, then use each N_s sample sets of the N_E sample sets of the n sets of filtered system responses as input of the proposed HHT-based identification method for general linear time-varying systems or input of the modified HHT-based identification method for weakly nonlinear time-varying systems, obtaining one set of identified values of the system parameters in the required time history. Finally, for N_E sample sets of the n sets of system responses, we obtain the statistical distribution of the N_E/N_s identified values (each sample value is a time-varying signal in the required time history) for each of the system parameters.

According to the above main procedures, numerical simulations are processed on 1-DOF and 2-DOF linear time-varying systems as well as weakly nonlinear time-varying Duffing systems and Van der Pol systems in the following sections.

5.2 HHT and Bayesian inference based identification of linear time-varying systems

In this section, HHT and Bayesian inference based identification are processed on the 1-DOF linear time-varying systems and 2-DOF linear time-varying non-chainlike systems proposed in Section 3.2 (the initial conditions and external forces for these systems are the same as in Section 3.2). The simulations are processed by MATLAB programs with the time interval between two adjacent data points given by 0.01 seconds and the whole time history given by 10 seconds. The reference values of system responses are obtained by solving the system differential equations.
For Bayesian inference, assume the experimental data consists of N_s=15 sets of system responses generated with the reference values of system responses perturbed by Gaussian noise with COV equal to 5%. The prior distribution assigned to the white noise in each system response is a uniform distribution in the range $[-1,1]*(Nstde*std(z))$, where $std(z)$ is the function of MATLAB for calculating standard deviation of signal z, and the ratio of the standard deviation of the white noise and that of the corresponding noiseless system response $Nstde$ is set to be 0.2. The PEV of the acceleration signal of each DOF in each experiment is uniformly distributed in the range $[0, eps*std(\text{acceleration})^2]$, where the ratio of the variance of the white noise and that of the corresponding noiseless acceleration eps is set to be 0.05. The factors $\eta_{i,q}$ and $\rho_{i,q}$ which define the model class M_l are assigned as $\eta_{i,q}(l) = 0.2 + 0.1(l-1), \rho_{i,q}(l) = 1, l = 1, \ldots, 29$. The number of samples of each distribution N_E is given as 450.
The statistical distributions of the identified stiffness coefficients of 1-DOF and 2-DOF linear smoothly and abruptly varying systems are presented in the following sections, whereas those of the identified damping coefficients of the same systems as well as the statistical distributions of the identified system coefficients for 1-DOF and 2-DOF linear periodically varying systems are presented in Appendix B.1.

5.2.1 HHT and Bayesian inference based identification of 1-DOF linear smoothly and abruptly varying systems

For the HHT and Bayesian inference based identification of the 1-DOF linear smoothly and abruptly varying forced vibration systems proposed in Section 3.2.1, the posterior probabilities of model classes $\boldsymbol{M}(\eta_{1,1}(l), 1), l = 1, \ldots, 29$, the statistical distributions of the identified stiffness coefficients as well as their relative errors are plotted in Figures 5.2 - 5.5.
It is noted from the figures that: For the 1-DOF linear smoothly varying forced vibration system, model classes $\boldsymbol{M}(\eta_{1,1}(l), 1), l = 1, \ldots, 29$ at the different time instants shown in Figure 5.2 have nearly 0 posterior probabilities when factor $\eta_{1,1} = 0.2$, then they have increasing posterior probabilities as $\eta_{1,1}$ increases from 0.2 to 0.7. Afterwards, they have maximal posterior probabilities as $\eta_{1,1}$ takes values in the interval $[0.7, 1.0]$, and the best values for $\eta_{1,1}$ at different time instants are obtained. Finally, their posterior probabilities decrease to nearly 0 when $\eta_{1,1}$ increases from its best values to 3 (that is the reason why $\eta_{i,q}(l) = 0.2+0.1(l-1), \rho_{i,q}(l) = 1, l = 1, \ldots, 29$ were chosen). E.g., for $t = 2.83$s, the most

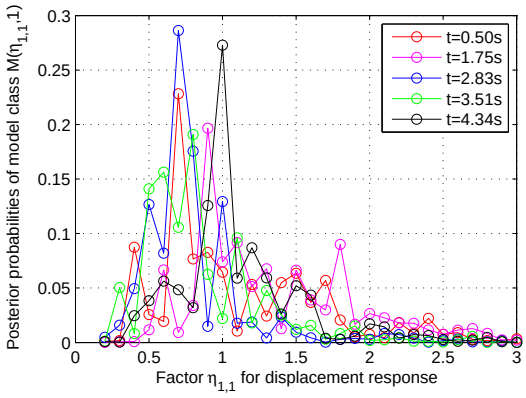

Figure 5.2: Posterior probability of model classes $\boldsymbol{M}(\eta_{1,1}, 1)$ specified by $\eta_{1,1} = [0.2, 3]$ for a 1-DOF linear smoothly varying forced vibration system.

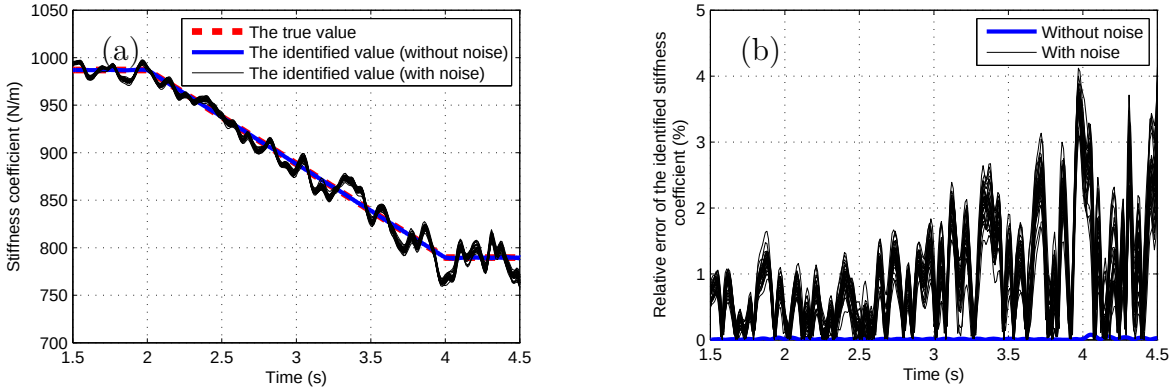

Figure 5.3: Stiffness coefficient of a 1-DOF linear smoothly varying forced vibration system: (a) The true value and the identified values of the stiffness coefficient, (b) Relative errors of the identified values of the stiffness coefficient.

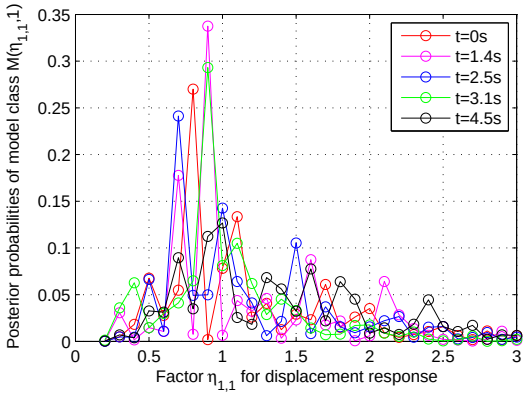

Figure 5.4: Posterior probability of model classes $\boldsymbol{M}(\eta_{1,1}, 1)$ specified by $\eta_{1,1} = [0.2, 3]$ for a 1-DOF linear abruptly varying forced vibration system.

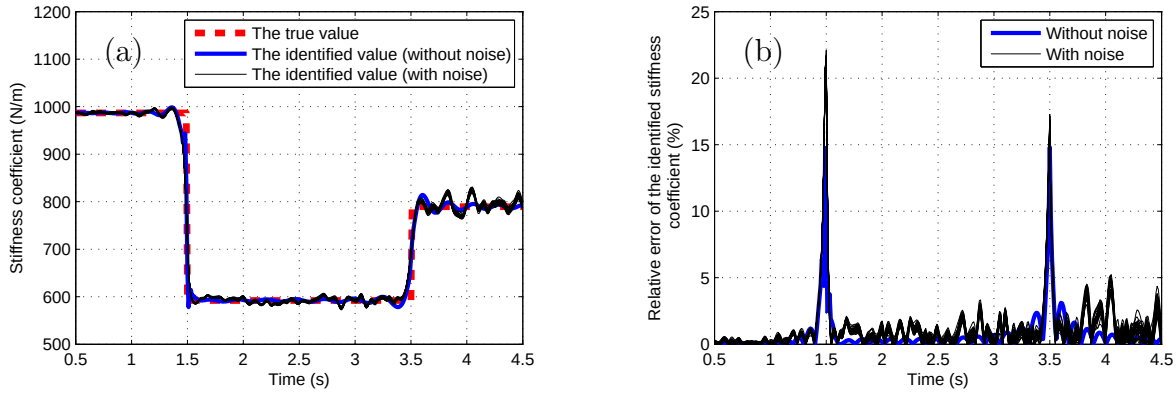

Figure 5.5: Stiffness coefficient of a 1-DOF linear abruptly varying forced vibration system: (a) The true value and the identified values of the stiffness coefficient (b) Relative errors of the identified values of the stiffness coefficient.

probable model class is $\boldsymbol{M}(\eta_{1,1}(6), 1)$ with the best value for $\eta_{1,1}$ given by $\eta_{1,1}(6) = 0.7$. Although the prior distribution assigned to the white noise in each system response has large ratio of the standard deviation of the white noise and that of the corresponding noiseless system response ($Nstde = 0.2$), by applying the combination method based on HHT and Bayesian Inference, the resulting statistical distribution of the identified values (denoted with black lines) of the stiffness coefficient shown in Figure 5.3 is concentrated and the identified values are close to its true value (with maximal relative error of its identified values less than 4.2%); For the 1-DOF linear abruptly varying forced vibration system, Figure 5.4 shows that maximal posterior probabilities of model classes $\boldsymbol{M}(\eta_{1,1}(l), 1), l = 1, \ldots, 29$ at the different time instants are found as $\eta_{1,1}$ takes values in the interval $[0.7, 1.0]$, and similar increasing as well as decreasing trends can be found for the posterior probabilities as those plotted in Figure 5.2. For $t = 3.1$s, the most probable model class is $\boldsymbol{M}(\eta_{1,1}(8), 1)$ with the best value for $\eta_{1,1}$ given by $\eta_{1,1}(8) = 0.9$. The identified values of the stiffness coefficient are concentratedly distributed and match closely its true value, except around $t = 1.5$s and $t = 3.5$s they have relatively large identification errors, since the HHT-based identification method has bad ability to capture the abrupt change of the system parameters due to the limitations of Equation (2.16). At time instants which are not around $t = 1.5$s and $t = 3.5$s, the identified values of the stiffness coefficient have small relative errors (whose maximum is less than 5.3%).

5.2.2 HHT and Bayesian inference based identification of 2-DOF linear time-varying systems

For the HHT and Bayesian inference based identification of the 2-DOF linear smoothly and abruptly varying forced vibration systems proposed in Section 3.2.2, the posterior probabilities of model classes $\boldsymbol{M}(\eta_{2,1}(l), 1), l = 1, \ldots, 29$, the statistical distributions of the identified stiffness coefficients as well as their relative errors are shown in Figures 5.6 - 5.11.

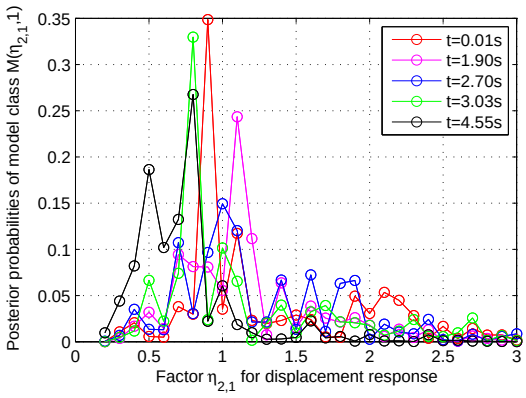

Figure 5.6: Posterior probability of model classes $\boldsymbol{M}(\eta_{2,1}, 1)$ specified by $\eta_{2,1} = [0.2, 3]$ for a 2-DOF linear smoothly varying non-chainlike forced vibration system.

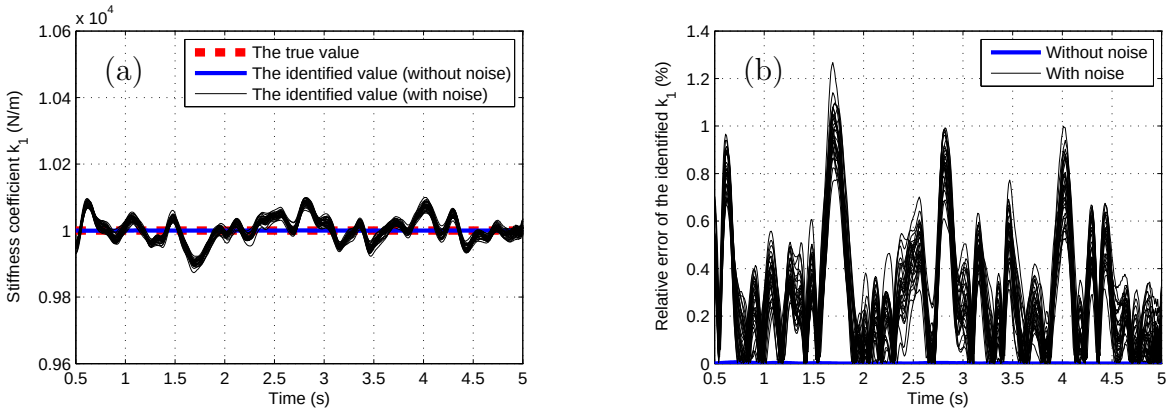

Figure 5.7: Stiffness coefficient k_1 of a 2-DOF linear smoothly varying non-chainlike forced vibration system: (a) The true value and the identified values of k_1, (b) Relative errors of the identified values of k_1.

For the 2-DOF linear smoothly varying forced vibration system, the posterior probabilities of model classes for the 2nd DOF and the 1st experiment $\boldsymbol{M}(\eta_{2,1}(l), 1), l = 1, \ldots, 29$ which are plotted in Figure 5.6 have nearly 0 posterior probabilities when factor $\eta_{2,1} = 0.2$, then they have increasing posterior probabilities as $\eta_{2,1}$ increases from 0.2 to 0.8. Afterwards, they have maximal posterior probabilities as $\eta_{2,1}$ takes values in the interval $[0.8, 1.1]$, and the best values for $\eta_{2,1}$ at different time instants are obtained. Finally, their posterior probabilities decrease to nearly 0 when $\eta_{2,1}$ increases from its best values to 3. By applying the combination method, the obtained statistical distributions of the identified values (denoted with black lines) of the stiffness coefficients shown in Figures 5.7 - 5.8 are concentrated and are close to their respective true values (with maximal relative error of the identified values of stiffness coefficient k_1 less than 1.3% and that of stiffness coefficient k_2 less than 1.4%); For the 2-DOF linear abruptly varying forced vibration system, the posterior probabilities of model classes for the 2nd DOF and the 1st experiment $\boldsymbol{M}(\eta_{2,1}(l), 1), l = 1, \ldots, 29$ which are plotted in Figure 5.9 have nearly 0 posterior probabilities when factor $\eta_{2,1} = 0.2$, then they have increasing posterior probabilities as $\eta_{2,1}$ increases from 0.2 to 0.7. Afterwards,

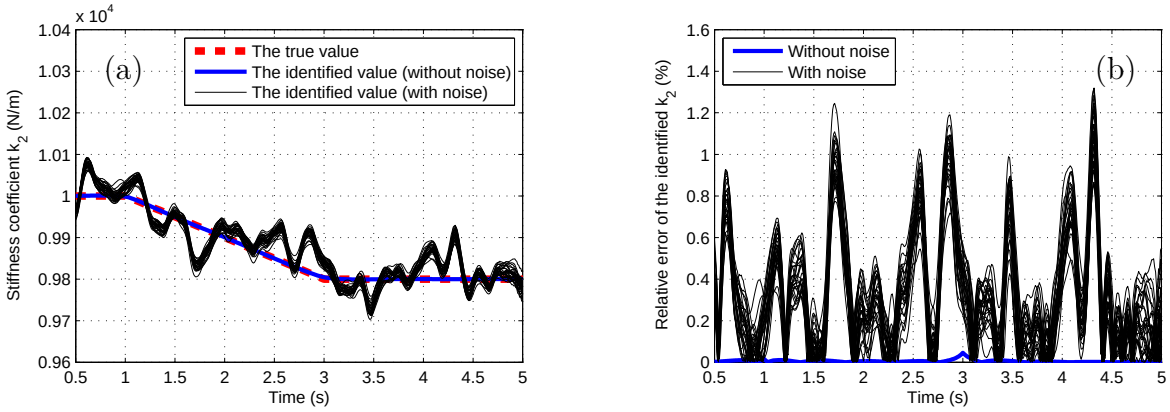

Figure 5.8: Stiffness coefficient k_2 of a 2-DOF linear smoothly varying non-chainlike forced vibration system: (a) The true value and the identified values of k_2, (b) Relative errors of the identified values of k_2.

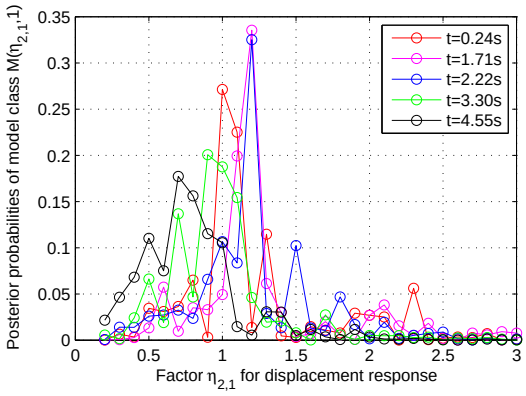

Figure 5.9: Posterior probability of model classes $\boldsymbol{M}(\eta_{2,1}, 1)$ specified by $\eta_{2,1} = [0.2, 3]$ for a 2-DOF linear abruptly varying non-chainlike forced vibration system.

they have maximal posterior probabilities as $\eta_{2,1}$ takes values in the interval $[0.7, 1.2]$, and the best values for $\eta_{2,1}$ at different time instants are obtained. Finally, their posterior probabilities decrease to nearly 0 when $\eta_{2,1}$ increases from its best values to 3. Figures 5.10 - 5.11 show that the identified values of stiffness coefficients k_1 and k_2 have relatively large identification errors around time instant $t = 3.0$s due to the limitations of Equation (2.16). At other time instants, the statistical distributions of the identified values of k_1 and k_2 are concentrated and are close to their respective true values (with maximal relative error of the identified values of k_1 less than 1.9% and that of k_2 less than 1.2%).

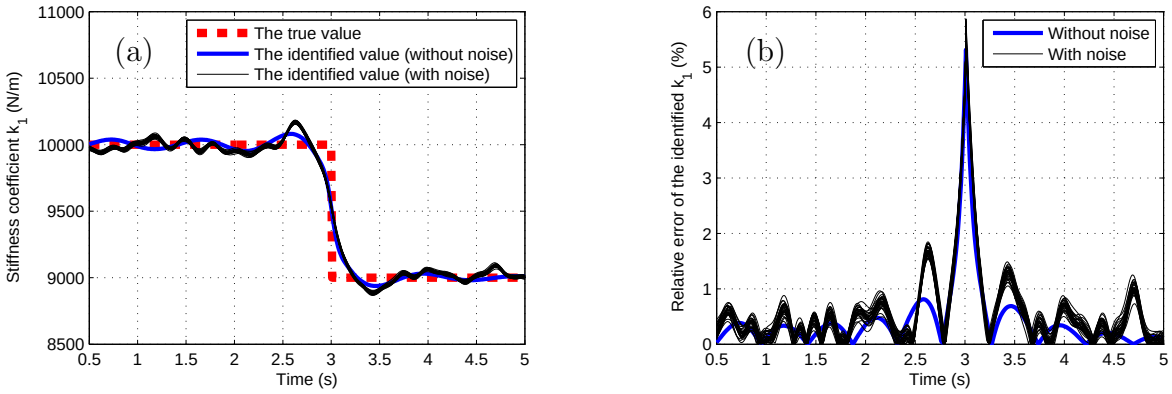

Figure 5.10: Stiffness coefficient k_1 of a 2-DOF linear abruptly varying non-chainlike forced vibration system: (a) The true value and the identified values of k_1, (b) Relative errors of the identified values of k_1.

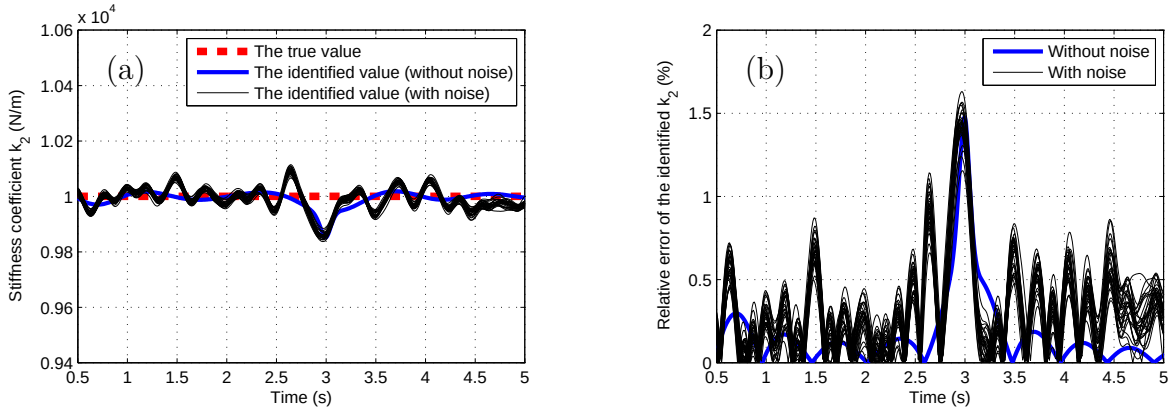

Figure 5.11: Stiffness coefficient k_2 of a 2-DOF linear abruptly varying non-chainlike forced vibration system: (a) The true value and the identified values of k_2, (b) Relative errors of the identified values of k_2.

5.3 HHT and Bayesian inference based identification of weakly nonlinear time-varying systems

In this section, by using the combination method based on the modified HHT-based identification method and Bayesian inference, numerical simulations are processed on the 1-DOF and 2-DOF weakly nonlinear time-varying Duffing as well as Van der Pol systems proposed in Sections 4.1 - 4.2 (the initial conditions and external forces for these systems are the same as in Sections 4.1 - 4.2).The simulations are processed by MATLAB programs with the time interval between two adjacent data points given by 0.01 seconds and the whole time history given by 10 seconds. The reference values of system responses are obtained by solving the system differential equations.
The important parameters and procedures of Bayesian inference are given the same as those in Section 5.2 for the linear time-varying systems.

The statistical distributions of the identified stiffness coefficients for 1-DOF and 2-DOF weakly nonlinear smoothly and abruptly varying systems are presented in the following sections, whereas those of the identified damping coefficients of the same systems as well as the statistical distributions of the identified system coefficients for 1-DOF and 2-DOF weakly nonlinear periodically varying systems are presented in Appendix B.2.

5.3.1 HHT and Bayesian inference based identification of 1-DOF weakly nonlinear smoothly and abruptly varying Duffing oscillators

For the HHT and Bayesian inference based identification of the 1-DOF weakly nonlinear smoothly and abruptly varying hard spring Duffing oscillators proposed in Section 4.1.1, the statistical distributions of the identified cubic stiffness factors as well as their relative errors are plotted in Figures 5.12 - 5.13.

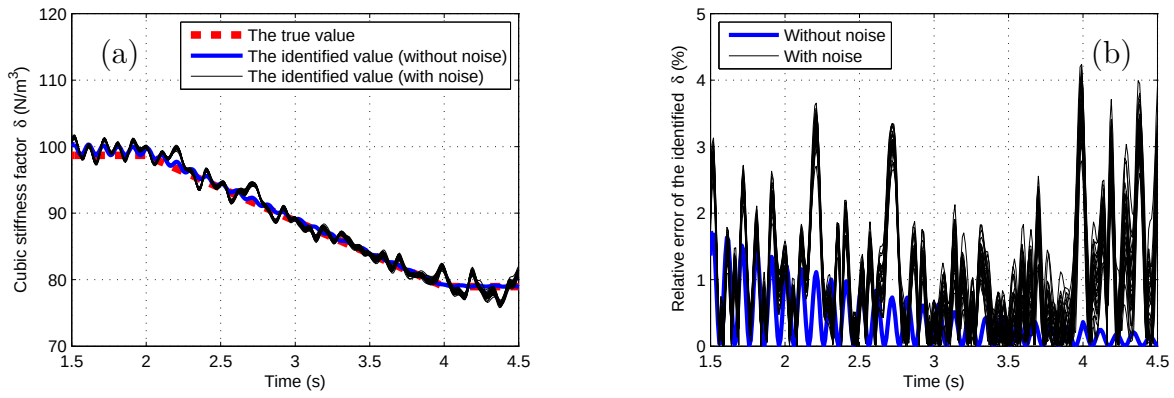

Figure 5.12: Cubic stiffness factor δ of a 1-DOF weakly nonlinear smoothly varying hard spring Duffing oscillator: (a) The true value and the identified values of δ, (b) Relative errors of the identified values of δ.

We can see from the figures that: For the 1-DOF weakly nonlinear smoothly varying hard spring Duffing oscillator, the obtained identified values (denoted with black lines) of cubic stiffness factor δ are distributed concentratedly and are close to its true value (with the maximal relative error less than 4.3%); For the 1-DOF weakly nonlinear abruptly varying hard spring Duffing oscillator, the identified values (denoted with black lines) of cubic stiffness factor δ have relatively quite large identification errors around time instants $t = 1.5$s and $t = 3.5$s due to the limitations of Equation (2.16), whereas at other time instants, the identified values of δ are concentratedly distributed and are close to its true value (with the maximal relative error less than 4.6%).

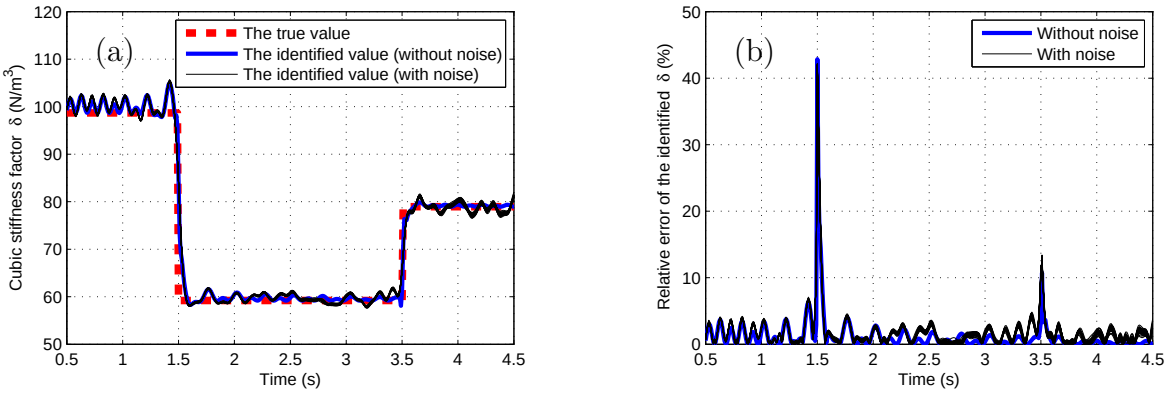

Figure 5.13: Cubic stiffness factor δ of a 1-DOF weakly nonlinear abruptly varying hard spring Duffing oscillator: (a) The true value and the identified values of δ, (b) Relative errors of the identified values of δ.

5.3.2 HHT and Bayesian inference based identification of 2-DOF weakly nonlinear smoothly and abruptly varying Duffing systems

For the HHT and Bayesian inference based identification of the 2-DOF weakly nonlinear smoothly and abruptly varying hard spring Duffing systems proposed in Section 4.1.2, the statistical distributions of the identified cubic stiffness factors and identified linear stiffness coefficients as well as their relative errors are shown in Figures 5.14 - 5.17.

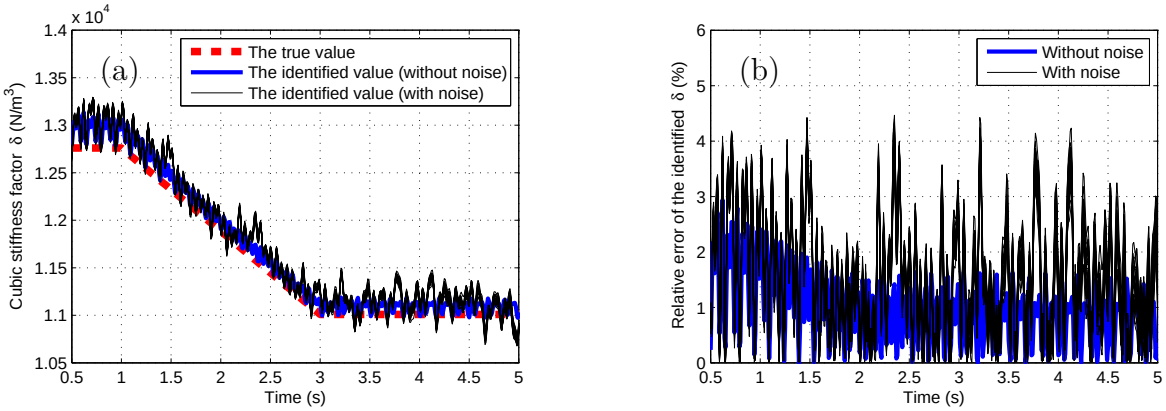

Figure 5.14: Cubic stiffness factor δ of a 2-DOF weakly nonlinear system with a weakly nonlinear smoothly varying hard spring Duffing oscillator: (a) The true value and the identified values of δ, (b) Relative errors of the identified values of δ.

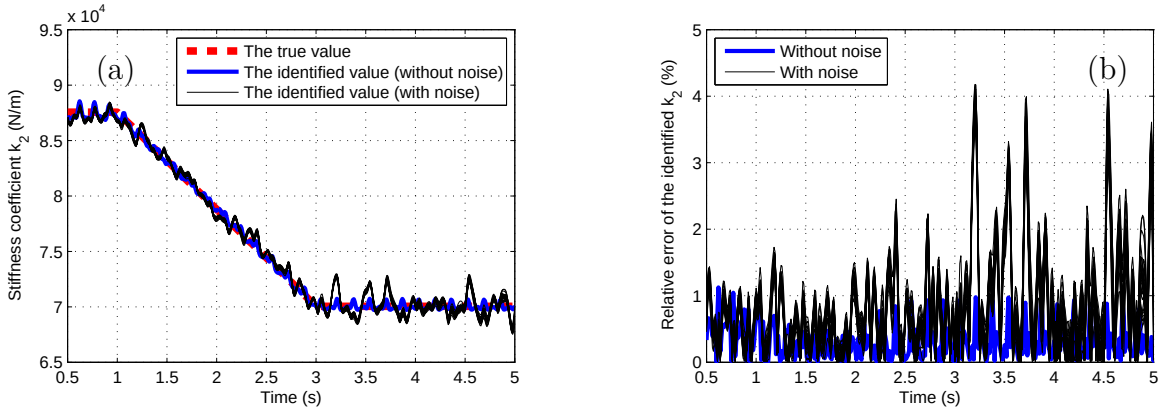

Figure 5.15: Stiffness coefficient k_2 of a 2-DOF weakly nonlinear system with a weakly nonlinear smoothly varying hard spring Duffing oscillator: (a) The true value and the identified values of k_2, (b) Relative errors of the identified values of k_2.

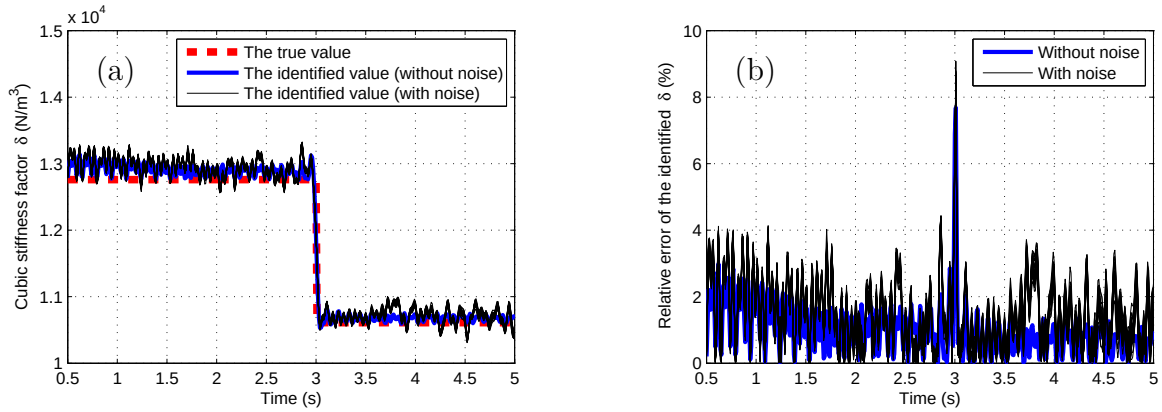

Figure 5.16: Cubic stiffness factor δ of a 2-DOF weakly nonlinear system with a weakly nonlinear abruptly varying hard spring Duffing oscillator: (a) The true value and the identified values of δ, (b) Relative errors of the identified values of δ.

It can be seen from the figures that: For the 2-DOF weakly nonlinear smoothly varying hard spring Duffing system, the identified values (denoted with black lines) of cubic stiffness factor δ and those of stiffness coefficient k_2 are concentratedly distributed and are close to their respective true values (the maximal relative error of the identified values of δ is less than 4.5% and that of k_2 is less than 4.2%); For the 2-DOF weakly nonlinear abruptly varying hard spring Duffing system, the identified values of δ and k_2 have relatively large identification errors around time instant $t = 3$s which can be used to detect the abrupt change of the system stiffness coefficient at this time instant. At other time instants, their identified values are concentratedly distributed and are close to their respective true values (with maximal relative error of the identified values of δ less than 4.2% and that of k_2 less than 3.2%).

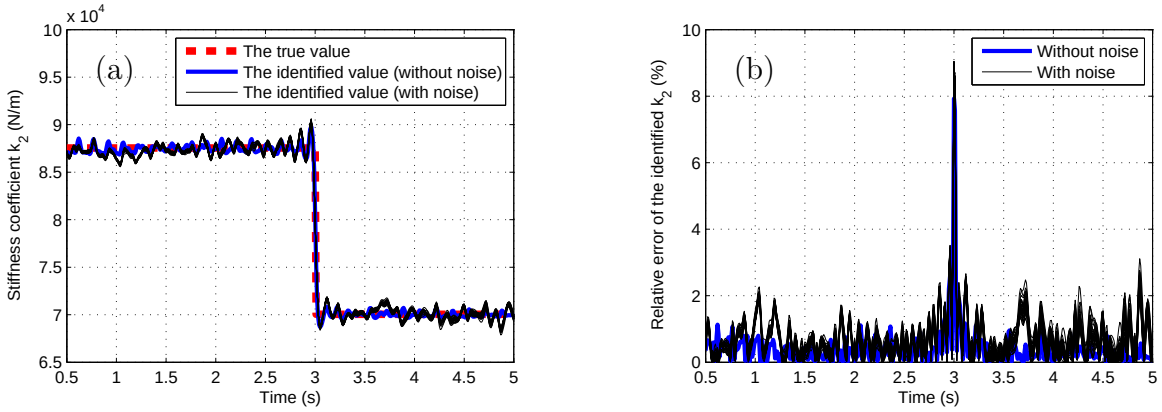

Figure 5.17: Stiffness coefficient k_2 of a 2-DOF weakly nonlinear system with a weakly nonlinear abruptly varying hard spring Duffing oscillator: (a) The true value and the identified values of k_2, (b) Relative errors of the identified values of k_2.

5.3.3 HHT and Bayesian inference based identification of 1-DOF weakly nonlinear smoothly and abruptly varying Van der Pol oscillators

For the HHT and Bayesian inference based identification of the 1-DOF weakly nonlinear smoothly and abruptly varying Van der Pol oscillators proposed in Section 4.2.1, the statistical distributions of the identified stiffness coefficients as well as their relative errors are shown in Figures 5.18 - 5.19.

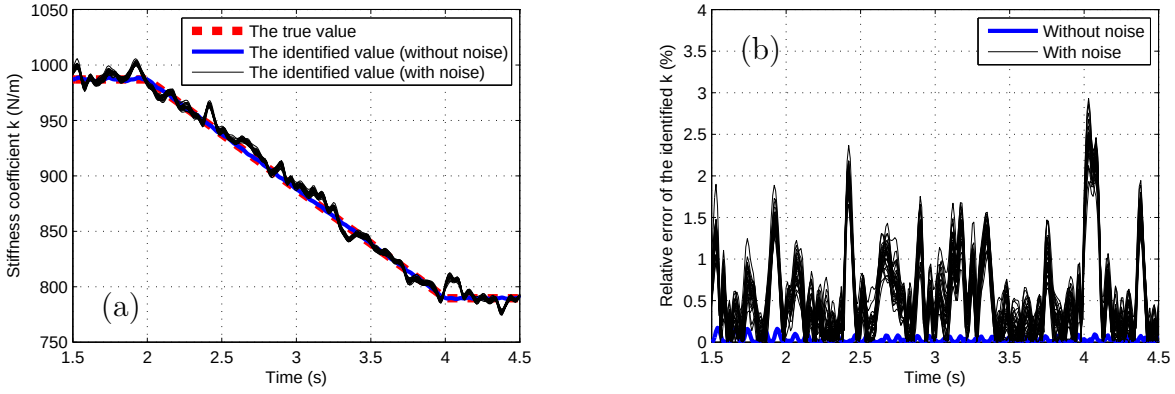

Figure 5.18: Stiffness coefficient k of a 1-DOF weakly nonlinear smoothly varying Van der Pol oscillator: (a) The true value and the identified values of k, (b) Relative errors of the identified values of k.

We can see from the figures that: For the 1-DOF weakly nonlinear smoothly varying Van der Pol oscillator, the statistical distribution of the identified values (denoted with black lines) of the stiffness coefficient k is concentrated around its true value (with the maximal relative error less than 3.0%); For the 1-DOF weakly nonlinear abruptly varying Van der

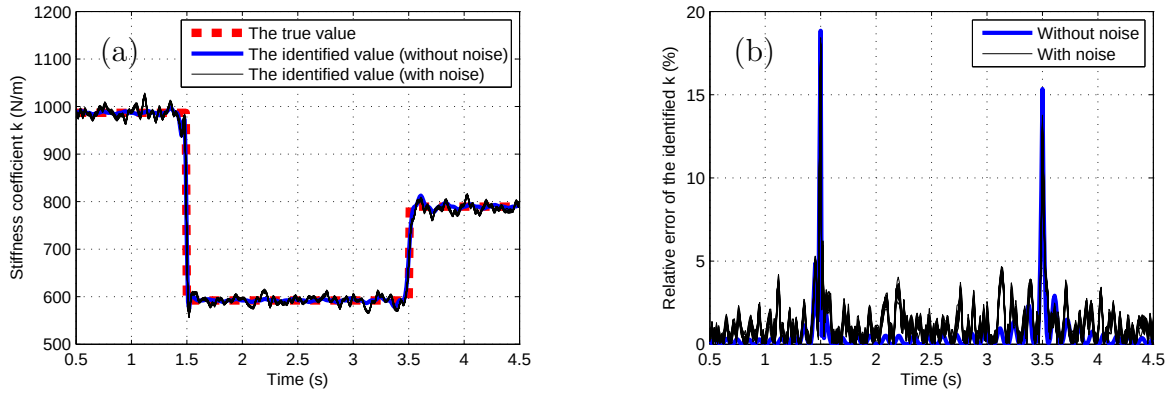

Figure 5.19: Stiffness coefficient k of a 1-DOF weakly nonlinear abruptly varying Van der Pol oscillator: (a) The true value and the identified values of k, (b) Relative errors of the identified values of k.

Pol oscillator, the identified values (denoted with black lines) of k have relatively large identification errors around time instants $t = 1.5$s and $t = 3.5$s due to the limitations of Equation (2.16). At other time instants, the identified values of k are concentratedly distributed and match its true value well (with the maximal relative error less than 4.7%).

5.3.4 HHT and Bayesian inference based identification of 2-DOF weakly nonlinear smoothly and abruptly varying chainlike Van der Pol systems

For the HHT and Bayesian inference based identification of the 2-DOF weakly nonlinear smoothly and abruptly varying chainlike Van der Pol systems proposed in Section 4.2.2, the statistical distributions of the identified stiffness coefficients as well as their relative errors are shown in Figures 5.20 - 5.23.

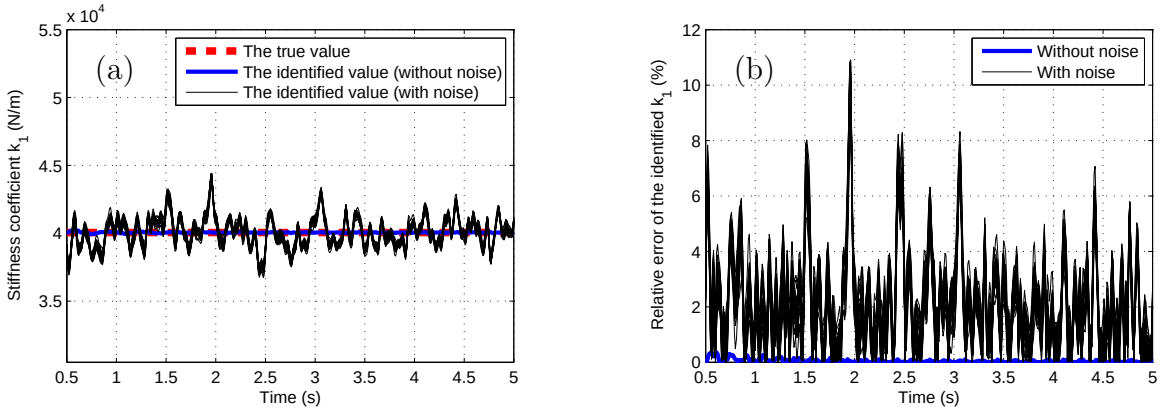

Figure 5.20: Stiffness coefficient k_1 of a 2-DOF weakly nonlinear chainlike system with a weakly nonlinear smoothly varying Van der Pol oscillator: (a) The true value and the identified values of k_1, (b) Relative errors of the identified values of k_1.

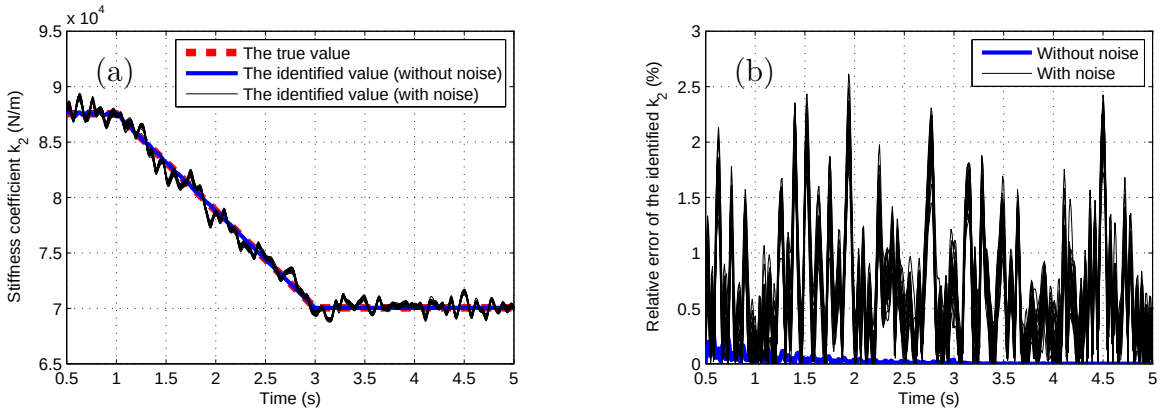

Figure 5.21: Stiffness coefficient k_2 of a 2-DOF weakly nonlinear chainlike system with a weakly nonlinear smoothly varying Van der Pol oscillator: (a) The true value and the identified values of k_2, (b) Relative errors of the identified values of k_2.

It can be seen from the figures that: For the 2-DOF weakly nonlinear smoothly varying chainlike Van der Pol system, the resulting identified values (denoted with black lines) of the stiffness coefficients are concentratedly distributed and are close to their respective true values (the maximal relative error of the identified values of k_1 is less than 11% and that of k_2 is less than 2.7%); For the 2-DOF weakly nonlinear abruptly varying chainlike Van der Pol system, the identified values of the stiffness coefficients have relatively large identification errors around time instant $t = 3$s, which implies that the modified HHT-based identification method has bad ability to capture the abrupt change of the system parameter due to the limitations of Equation (2.16) and can be used to detect the abrupt change of the system stiffness coefficient at this time instant. At other time instants, the identified values of the stiffness coefficients are concentratedly distributed and match their

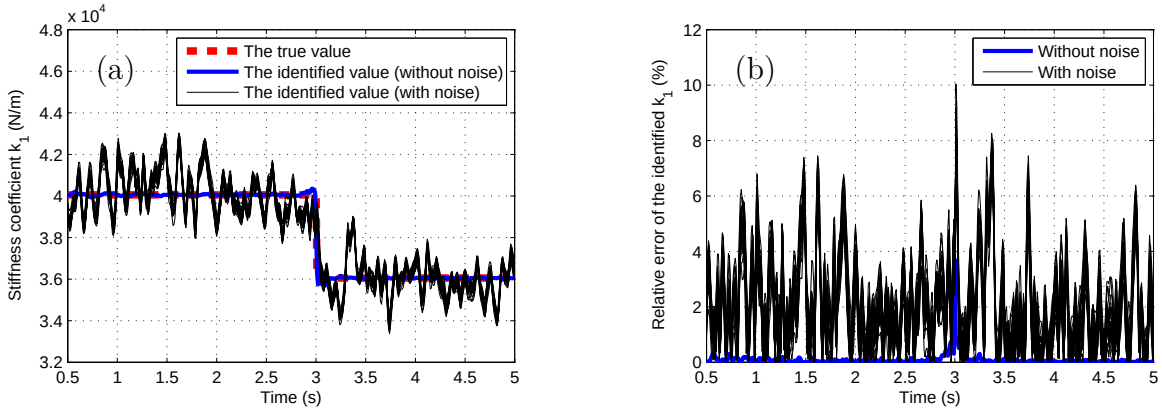

Figure 5.22: Stiffness coefficient k_1 of a 2-DOF weakly nonlinear chainlike system with a weakly nonlinear abruptly varying Van der Pol oscillator: (a) The true value and the identified values of k_1, (b) Relative errors of the identified values of k_1.

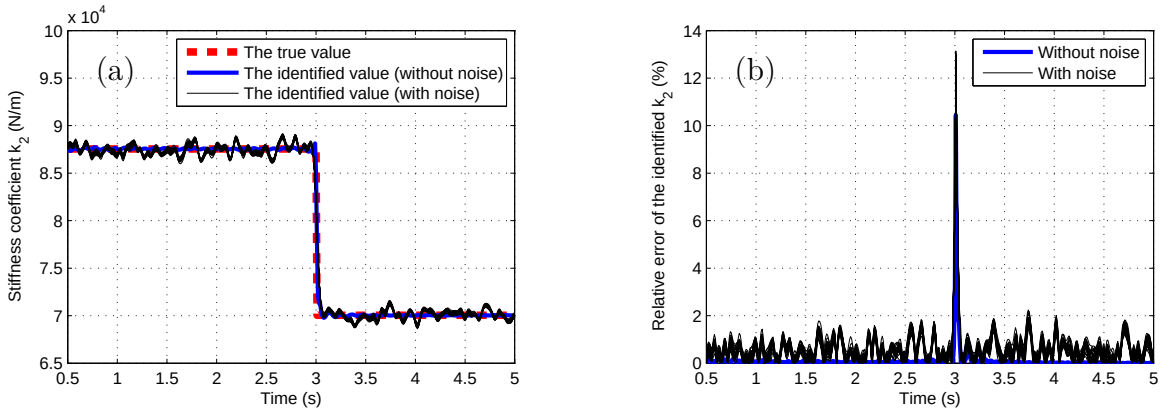

Figure 5.23: Stiffness coefficient k_2 of a 2-DOF weakly nonlinear chainlike system with a weakly nonlinear abruptly varying Van der Pol oscillator: (a) The true value and the identified values of k_2, (b) Relative errors of the identified values of k_2.

respective true values (the maximal relative error of the identified values of k_1 is less than 8.3% and that of k_2 is less than 2.3%).

5.4 Bayesian inference based parameter identification for general time-varying systems

Based on Bayesian inference, a method is proposed here in order to address the identification of system parameters. By applying TMCMC method, Bayesian model updating is implemented to update initial knowledge about the system parameters for a set of candidate model classes, with the formulation of the likelihood function as the product of three probability density functions, one relating to the IMFs of the acceleration responses and the other two relating to the IMFs of the velocity responses as well as the IMFs of the displacement responses, yielding the corresponding posterior distributions of the system parameters for these model classes. Then, the most probable model class and the corresponding posterior distributions of the system structural parameters for the most probable model class are selected. Numerical simulations on 1-DOF and 2-DOF systems are processed to demonstrate the effectiveness, accuracy and robustness of the Bayesian inference based parameter identification method for linear time-varying systems and weakly nonlinear time-varying systems.

5.4.1 Formulation of the likelihood function

As pointed out in Section 2.4.2, the value of the likelihood function is given by a probability model for the prediction error vector, and a Gaussian distribution with zero mean and covariance matrix Σ is chosen as the PDF model for the prediction error vector justified by the principle of maximum entropy. In this section, the prediction errors of the χth IMFs of the ith acceleration response, velocity response and displacement response in the kth measurement are given as

$$\begin{aligned} e^a_{i\chi k} &= \frac{1}{t_{end}} \sum_{\tau=1}^{t_{end}} \left| IMF^{Ea}_{i\chi k}(\tau) - IMF^{Ma}_{i\chi}(\boldsymbol{\theta}, \tau) \right| \sim N(0, (\bar{\varepsilon}^a_{i\chi})^2) \\ e^v_{i\chi k} &= \frac{1}{t_{end}} \sum_{\tau=1}^{t_{end}} \left| IMF^{Ev}_{i\chi k}(\tau) - IMF^{Mv}_{i\chi}(\boldsymbol{\theta}, \tau) \right| \sim N(0, (\bar{\varepsilon}^v_{i\chi})^2) \\ e^d_{i\chi k} &= \frac{1}{t_{end}} \sum_{\tau=1}^{t_{end}} \left| IMF^{Ed}_{i\chi k}(\tau) - IMF^{Md}_{i\chi}(\boldsymbol{\theta}, \tau) \right| \sim N(0, (\bar{\varepsilon}^d_{i\chi})^2) \end{aligned} \tag{5.4}$$

where subscript i denotes the index of system responses ($i = 1, \ldots, N_L$, $N_L = n^2$ is the number of DOFs of the system responses obtained in n experiments by solving ODE of the system with the same initial conditions given at a different DOF of the system for each experiment), subscript χ denotes the index of IMFs ($\chi = 1, \ldots, n$), subscript k denotes the index of the measurements ($k = 1, \ldots, N_s$), each of which leads to the same number of IMFs ($3n \times N_L$), t_{end} is the number of time instants considered in the simulation, τ is the index of time instants, $IMF^{Ea}_{i\chi k}(\tau)$, $IMF^{Ev}_{i\chi k}(\tau)$, $IMF^{Ed}_{i\chi k}(\tau)$ are the observed values at the τth time instant of the χth IMF of the ith acceleration response, velocity response as well as displacement response in the kth measurement and $IMF^{Ma}_{i\chi}(\boldsymbol{\theta}, \tau)$, $IMF^{Mv}_{i\chi}(\boldsymbol{\theta}, \tau)$, $IMF^{Md}_{i\chi}(\boldsymbol{\theta}, \tau)$ are the corresponding model responses, $(\bar{\varepsilon}^a_{i\chi})^2$, $(\bar{\varepsilon}^v_{i\chi})^2$, $(\bar{\varepsilon}^d_{i\chi})^2$ are the PEVs of

the χth IMF of the ith acceleration response, velocity response as well as displacement response, and $\boldsymbol{\theta}$ is the parameter vector which is equal to the system parameter vector together with the PEVs of the $n \times N_L$ IMFs of N_L acceleration responses:

$$\boldsymbol{\theta} = \left[(\varepsilon_{11}^a)^2, \ldots, (\varepsilon_{1n}^a)^2, \ldots, (\varepsilon_{i1}^a)^2, \ldots, (\varepsilon_{i\chi}^a)^2, \ldots, (\varepsilon_{in}^a)^2, \ldots, (\varepsilon_{N_L1}^a)^2, \ldots, (\varepsilon_{N_Ln}^a)^2, \theta_{str}\right]^T \tag{5.5}$$

where θ_{str} is the system parameter vector, and the PEV $(\varepsilon_{i\chi}^a)^2$ of the χth IMF of the ith acceleration response is given by $(\varepsilon_{i\chi}^a)^2 = (\bar{\varepsilon}_{i\chi}^a)^2/\mathrm{std}(IMF_{i\chi}^a)^2$.
Then, the PDF models for the prediction errors $e_{i\chi k}^a$, $e_{i\chi k}^v$, $e_{i\chi k}^d$ are given as

$$\begin{aligned}
p(e_{i\chi k}^a|\boldsymbol{\theta}, M) &= \frac{1}{(2\pi)^{N_o/2}\bar{\varepsilon}_{i\chi}^a} \exp\left[-\frac{\left(\frac{1}{t_{end}}\sum_{\tau=1}^{t_{end}}\left|IMF_{i\chi k}^{Ea}(\tau) - IMF_{i\chi}^{Ma}(\boldsymbol{\theta},\tau)\right|\right)^2}{2(\bar{\varepsilon}_{i\chi}^a)^2}\right] \\
p(e_{i\chi k}^v|\boldsymbol{\theta}, M) &= \frac{1}{(2\pi)^{N_o/2}\bar{\varepsilon}_{i\chi}^v} \exp\left[-\frac{\left(\frac{1}{t_{end}}\sum_{\tau=1}^{t_{end}}\left|IMF_{i\chi k}^{Ev}(\tau) - IMF_{i\chi}^{Mv}(\boldsymbol{\theta},\tau)\right|\right)^2}{2(\bar{\varepsilon}_{i\chi}^v)^2}\right] \\
p(e_{i\chi k}^d|\boldsymbol{\theta}, M) &= \frac{1}{(2\pi)^{N_o/2}\bar{\varepsilon}_{i\chi}^d} \exp\left[-\frac{\left(\frac{1}{t_{end}}\sum_{\tau=1}^{t_{end}}\left|IMF_{i\chi k}^{Ed}(\tau) - IMF_{i\chi}^{Md}(\boldsymbol{\theta},\tau)\right|\right)^2}{2(\bar{\varepsilon}_{i\chi}^d)^2}\right]
\end{aligned} \tag{5.6}$$

where the standard deviations of the prediction errors $e_{i\chi k}^a$, $e_{i\chi k}^v$, $e_{i\chi k}^d$ are given by $\bar{\varepsilon}_{i\chi}^a = \mathrm{std}(IMF_{i\chi}^a)\varepsilon_{i\chi}^a$, $\bar{\varepsilon}_{i\chi}^v = \mathrm{std}(IMF_{i\chi}^v)\varepsilon_{i\chi}^v$, $\bar{\varepsilon}_{i\chi}^d = \mathrm{std}(IMF_{i\chi}^d)\varepsilon_{i\chi}^d$ respectively.
Since IMFs are used to model time-varying systems just as their counterparts – modal parameters (e.g. modal frequencies, mode shape functions) for time-invariant systems, inspired by the model class model of Goller and Beck [95] for time-invariant systems, we define a model class $M(\alpha, \gamma)$ by ratios α and γ

$$\alpha = \frac{(\varepsilon_{i\chi}^v)^2}{(\varepsilon_{i\chi}^a)^2},\ \gamma = \frac{(\varepsilon_{i\chi}^d)^2}{(\varepsilon_{i\chi}^a)^2} \tag{5.7}$$

where α is the ratio between the PEV of each IMF of each velocity response and that of the corresponding acceleration response of the same DOF in the same experiment, γ is the ratio between the PEV of each IMF of each displacement response and that of the corresponding acceleration response of the same DOF in the same experiment.
Assume the prediction errors of the IMFs of the acceleration responses, velocity responses and displacement responses are modeled as statistically independent of each other, then

the likelihood function for model class $M(\alpha,\gamma)$ can be given as

$$
\begin{aligned}
&p(D|\boldsymbol{\theta},M(\alpha,\gamma)) \\
&= \prod_{k=1}^{N_s}\prod_{i=1}^{N_L}\prod_{\chi=1}^{n} p(e^a_{i\chi k}|\boldsymbol{\theta},M(\alpha,\gamma))p(e^v_{i\chi k}|\boldsymbol{\theta},M(\alpha,\gamma))p(e^d_{i\chi k}|\boldsymbol{\theta},M(\alpha,\gamma)) \\
&= \prod_{k=1}^{N_s}\prod_{i=1}^{N_L}\prod_{\chi=1}^{n} \left\{ \frac{1}{(2\pi)^{N_o/2}\bar{\varepsilon}^a_{i\chi}(2\pi)^{N_o/2}\bar{\varepsilon}^v_{i\chi}(2\pi)^{N_o/2}\bar{\varepsilon}^d_{i\chi}} \cdot \right. \\
&\exp\left\{ -\frac{1}{2}\left[\frac{\left(\frac{1}{t_{end}}\sum_{\tau=1}^{t_{end}}\left|IMF^{Ea}_{i\chi k}(\tau)-IMF^{Ma}_{i\chi}(\boldsymbol{\theta},\tau)\right|\right)^2}{(\bar{\varepsilon}^a_{i\chi})^2} + \right.\right. \\
&\left.\left.\left. \frac{\left(\frac{1}{t_{end}}\sum_{\tau=1}^{t_{end}}\left|IMF^{Ev}_{i\chi k}(\tau)-IMF^{Mv}_{i\chi}(\boldsymbol{\theta},\tau)\right|\right)^2}{(\bar{\varepsilon}^v_{i\chi})^2} + \frac{\left(\frac{1}{t_{end}}\sum_{\tau=1}^{t_{end}}\left|IMF^{Ed}_{i\chi k}(\tau)-IMF^{Md}_{i\chi}(\boldsymbol{\theta},\tau)\right|\right)^2}{(\bar{\varepsilon}^d_{i\chi})^2} \right] \right\} \right\} \\
&= c_4 \exp\left\{ -\frac{1}{2}\prod_{k=1}^{N_s}\prod_{i=1}^{N_L}\prod_{\chi=1}^{n}\left[J_{i\chi k}\left(\boldsymbol{\theta}|M(\alpha,\gamma)\right)\right] \right\}
\end{aligned}
\tag{5.8}
$$

where

$$
\begin{aligned}
c_4 &= \frac{1}{(2\pi)^{3N_oN_sN_Ln/2}\prod_{k=1}^{N_s}\prod_{i=1}^{N_L}\prod_{\chi=1}^{n}\left(\bar{\varepsilon}^a_{i\chi}\bar{\varepsilon}^v_{i\chi}\bar{\varepsilon}^d_{i\chi}\right)} \\
&= \frac{1}{(2\pi)^{3N_oN_sN_Ln/2}\prod_{k=1}^{N_s}\prod_{i=1}^{N_L}\prod_{\chi=1}^{n}\left[\mathrm{std}(IMF^a_{i\chi})\varepsilon^a_{i\chi}\mathrm{std}(IMF^v_{i\chi})\varepsilon^v_{i\chi}\mathrm{std}(IMF^d_{i\chi})\varepsilon^d_{i\chi}\right]} \\
&= \frac{1}{(2\pi)^{3N_oN_sN_Ln/2}\prod_{k=1}^{N_s}\prod_{i=1}^{N_L}\prod_{\chi=1}^{n}\left\{\mathrm{std}(IMF^a_{i\chi})\mathrm{std}(IMF^v_{i\chi})\mathrm{std}(IMF^d_{i\chi})\left[\alpha\gamma\left((\varepsilon^a_{i\chi})^2\right)^3\right]^{1/2}\right\}}
\end{aligned}
\tag{5.9}
$$

$$
\begin{aligned}
&J_{i\chi k}(\boldsymbol{\theta}|M(\alpha,\gamma)) \\
&= \left[\frac{\left(\frac{1}{t_{end}}\sum_{\tau=1}^{t_{end}}\left|IMF_{i\chi k}^{Ea}(\tau) - IMF_{i\chi}^{Ma}(\boldsymbol{\theta},\tau)\right|\right)^2}{(\bar{\varepsilon}_{i\chi}^{a})^2} + \frac{\left(\frac{1}{t_{end}}\sum_{\tau=1}^{t_{end}}\left|IMF_{i\chi k}^{Ev}(\tau) - IMF_{i\chi}^{Mv}(\boldsymbol{\theta},\tau)\right|\right)^2}{(\bar{\varepsilon}_{i\chi}^{v})^2} + \right. \\
&\quad \left. \frac{\left(\frac{1}{t_{end}}\sum_{\tau=1}^{t_{end}}\left|IMF_{i\chi k}^{Ed}(\tau) - IMF_{i\chi}^{Md}(\boldsymbol{\theta},\tau)\right|\right)^2}{(\bar{\varepsilon}_{i\chi}^{d})^2} \right] \\
&= \left[\frac{\left(\frac{1}{t_{end}}\sum_{\tau=1}^{t_{end}}\left|IMF_{i\chi k}^{Ea}(\tau) - IMF_{i\chi}^{Ma}(\boldsymbol{\theta},\tau)\right|\right)^2}{\mathrm{std}(IMF_{i\chi}^{a})^2(\varepsilon_{i\chi}^{a})^2} + \frac{\left(\frac{1}{t_{end}}\sum_{\tau=1}^{t_{end}}\left|IMF_{i\chi k}^{Ev}(\tau) - IMF_{i\chi}^{Mv}(\boldsymbol{\theta},\tau)\right|\right)^2}{\mathrm{std}(IMF_{i\chi}^{v})^2(\varepsilon_{i\chi}^{v})^2} + \right. \\
&\quad \left. \frac{\left(\frac{1}{t_{end}}\sum_{\tau=1}^{t_{end}}\left|IMF_{i\chi k}^{Ed}(\tau) - IMF_{i\chi}^{Md}(\boldsymbol{\theta},\tau)\right|\right)^2}{\mathrm{std}(IMF_{i\chi}^{d})^2(\varepsilon_{i\chi}^{d})^2} \right] \\
&= \left[\frac{\left(\frac{1}{t_{end}}\sum_{\tau=1}^{t_{end}}\left|IMF_{i\chi k}^{Ea}(\tau) - IMF_{i\chi}^{Ma}(\boldsymbol{\theta},\tau)\right|\right)^2}{\mathrm{std}(IMF_{i\chi}^{a})^2(\varepsilon_{i\chi}^{a})^2} + \frac{\left(\frac{1}{t_{end}}\sum_{\tau=1}^{t_{end}}\left|IMF_{i\chi k}^{Ev}(\tau) - IMF_{i\chi}^{Mv}(\boldsymbol{\theta},\tau)\right|\right)^2}{\mathrm{std}(IMF_{i\chi}^{v})^2\alpha(\varepsilon_{i\chi}^{a})^2} + \right. \\
&\quad \left. \frac{\left(\frac{1}{t_{end}}\sum_{\tau=1}^{t_{end}}\left|IMF_{i\chi k}^{Ed}(\tau) - IMF_{i\chi}^{Md}(\boldsymbol{\theta},\tau)\right|\right)^2}{\mathrm{std}(IMF_{i\chi}^{d})^2\gamma(\varepsilon_{i\chi}^{a})^2} \right]
\end{aligned}
\tag{5.10}
$$

Applying Equations (5.8) - (5.10) in the TMCMC method, Bayesian model updating is implemented for a set of model classes $\boldsymbol{M}$, gaining the posterior probability of the system parameters for each model class. Based on the resulting posterior probabilities for these model classes, Bayesian model class selection is performed according to Equation (2.49) to determine the most probable model class which has the most plausible values for ratios α and γ. Then, the posterior probabilities of the system parameters for the most probable model class is selected as the final identified result. Numerical simulations are performed on linear and weakly nonlinear time-varying systems in the following sections to demonstrate the effectiveness, accuracy and robustness of the parameter identification method.

5.4.2 Numerical simulations of Bayesian inference based parameter identification on time-varying systems

In this section, the proposed Bayesian inference based parameter identification method is applied to 1-DOF and 2-DOF smoothly varying systems.

(1) Parameter identification of a 1-DOF linear smoothly varying system
For a 1-DOF linear smoothly varying system, the system stiffness coefficient k and damping coefficient c are given by:
$k = k_{up}$, $c = c_{down}$ when $t < 2$s,

$k = k_{up} - (k_{up} - k_{down})/t_l(t-2)$, $c = c_{down} + (c_{up} - c_{down})/t_l(t-2)$ when $2\text{s} \leq t \leq t_l + 2\text{s}$,
$k = k_{down}$, $c = c_{up}$ when $t > t_l + 2\text{s}$,
$k_{up} = 100\pi^2\text{N/m}$, $k_{down} = 80\pi^2\text{N/m}$, $c_{up} = 1.0\text{Ns/m}$, $c_{down} = 0.7\text{Ns/m}$ for any t,
where t_l is the system parameter with its expectation given by $t_{lexp} = 2\text{s}$. Assume the experimental data consists of $N_s = 15$ sets of IMFs generated with the model specified by t_{lexp} and perturbed by Gaussian noise with COV equal to 5%. The prior distribution assigned to the system parameter t_l is a uniform distribution in the range $[1, 3]$. The PEV $(\varepsilon_{11}^a)^2$ of the IMF for the acceleration response is uniformly distributed in the range $[0, 0.05]$. The ratios α, γ which define the model classes $\boldsymbol{M}$ are assigned as $\alpha = 1$, $\gamma_l = 0.01 + 0.01(l-1)$, $l = 1, \ldots, 40$. The number of samples of each distribution N_E is given as 450.
Posterior probability for model classes which are characterized by parameters $\alpha = 1.0$, $\gamma = [0.01, 0.40]$ is presented in Figure 5.24. The posterior distribution of the system parameter t_l as well as the relative errors of its identified values for the most probable model class are plotted in Figure 5.25.

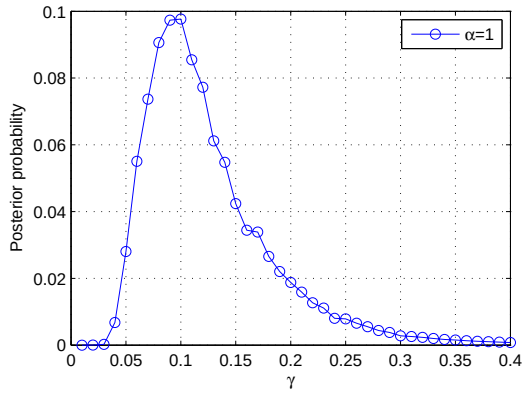

Figure 5.24: Posterior probability for model classes characterized by $\alpha = 1.0$, $\gamma = [0.01, 0.40]$ of a 1-DOF linear smoothly varying system.

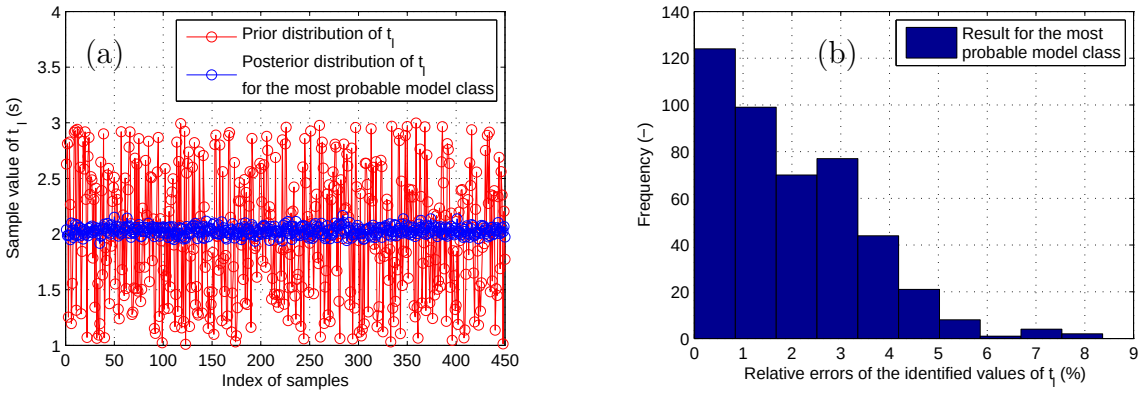

Figure 5.25: System parameter t_l of a 1-DOF linear smoothly varying system: (a) Distribution of t_l, (b) Relative errors for the identified values of t_l and for the most probable model class.

From Figure 5.24, it can be seen that the posterior probability of the model classes specified by parameters $\alpha = 1.0$, $\gamma = [0.01, 0.40]$ has increasing trend as γ increases from 0.01 to 0.10 and reaches its maximum (9.8%) at $\gamma = 0.10$, then it decreases from maximum to zero as γ increases from 0.10 to 0.40, determining the most probable model class by $\alpha^* = 1.0$, $\gamma^* = 0.10$. Based on the available experimental data and conditional on the assumption that all model classes are considered as equally likely apriori, the result in Figure 5.24 reveals that only model classes characterized by $\alpha = 1.0$ and γ in the range of $\gamma \in [0.04, 0.38]$ have significant posterior probabilities. Figure 5.25 shows that the posterior distribution of the system parameter t_l for the most probable model class $M(\alpha^* = 1.0, \gamma^* = 0.10)$ is concentrated around its expected value with small relative errors (the mean value of which is equal to 2.0%), which indicates that the relative weightings of the IMF of the acceleration response, and the IMF of the corresponding velocity response as well as the IMF of the corresponding displacement response in the likelihood function for the most probable model class $M(1.0, 0.10)$ lead to a good identification of the system parameter t_l.

(2) Parameter identification of a 2-DOF linear smoothly varying system
For a 2-DOF linear smoothly varying non-chainlike system, the system parameter to be identified is t_L which adopts the model in Figure 3.15. The expectation of t_L is given by $t_{Lexp} = 2$s. Assume the experimental data consists of $N_s = 15$ sets of IMFs generated with the model specified by t_{Lexp} and perturbed by Gaussian noise with COV equal to 5%. The prior distribution assigned to t_L is a uniform distribution in the range $[1, 3]$. The PEV $(\varepsilon_{i\chi}^a)^2$ of the IMF for the acceleration response is uniformly distributed in the range $[0, 0.05]$. The ratios α, γ which define the model classes $\boldsymbol{M}$ are assigned as $\alpha = 0.1$, $\gamma_l = 0.3 + 0.02(l-1)$, $l = 1, \ldots, 26$. The number of samples of each distribution N_E is given as 450.
Posterior probability for model classes which are characterized by parameters $\alpha = 0.1$, $\gamma = [0.3, 0.8]$ is presented in Figure 5.26. The posterior distribution of the system parameter

t_L as well as the relative errors of its identified values for the most probable model class are plotted in Figure 5.27.

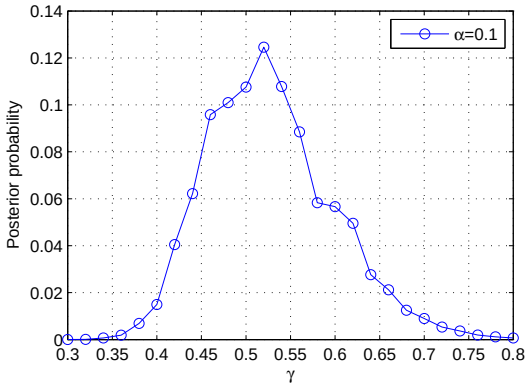

Figure 5.26: Posterior probability for model classes characterized by $\alpha = 0.1$, $\gamma = [0.3, 0.8]$ of a 2-DOF linear smoothly varying non-chainlike system.

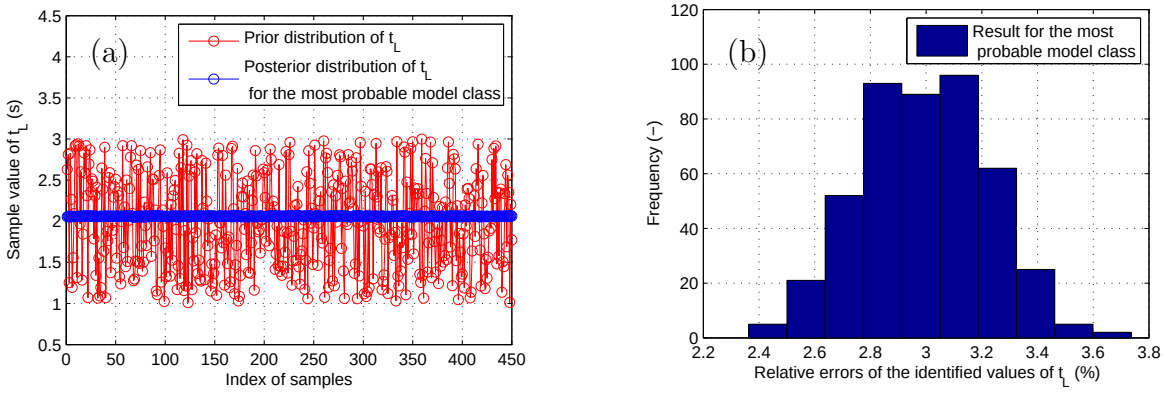

Figure 5.27: System parameter t_L of a 2-DOF linear smoothly varying non-chainlike system: (a) Distribution of t_L, (b) Relative errors for the identified values of t_L and for the most probable model class.

It can be seen from Figure 5.26 that the posterior probability of the model classes characterized by parameters $\alpha = 0.1$, $\gamma = [0.3, 0.8]$ has increasing trend as γ increases from 0.3 to 0.52 and reaches its maximum (12.5%) at $\gamma = 0.52$, then it has decreasing trend as γ increases from 0.52 to 0.8, determining the most probable model class by $\alpha^* = 0.1$, $\gamma^* = 0.52$. Since all model classes are considered as equally likely apriori, the result in Figure 5.26 reveals that only model classes characterized by $\alpha = 0.1$ and γ in the range of $\gamma \in [0.36, 0.76]$ have significant posterior probabilities. Figure 5.27 shows that the posterior distribution of the system parameter t_L for the most probable model class $M(\alpha^* = 0.1, \gamma^* = 0.52)$ is concentrated on its expected value (with the mean value of the relative errors of the identified results equal to 3.0%), implying that the relative weightings of the IMFs of the acceleration responses, the IMFs of the corresponding velocity responses

and the IMFs of the corresponding displacement responses in the likelihood function for the most probable model class $M(0.1, 0.52)$ can result in a good identification of the system parameter t_L.

(3) Parameter identification of a 2-DOF weakly nonlinear smoothly varying chainlike Duffing system
For a 2-DOF weakly nonlinear smoothly varying chainlike Duffing system, the system parameter to be identified is t_{duff} as proposed in Section 4.3.1. The expectation of t_{duff} is given by $t_{duffexp} = 2$s. Assume the experimental data consists of $N_s = 15$ sets of IMFs generated with the model specified by $t_{duffexp}$ and perturbed by Gaussian noise with COV equal to 5%. The prior distribution assigned to t_{duff} is a uniform distribution in the range $[1, 3]$. The PEV $(\varepsilon_{i\chi}^a)^2$ of the IMF for the acceleration response is uniformly distributed in the range $[0, 0.05]$. The ratios α, γ which define the model classes $\boldsymbol{M}$ are assigned as $\alpha = 1$, $\gamma = 0.3, 0.34, 0.38, 0.42, 0.45, 0.47, 0.5, 0.505, 0.51, 0.515, 0.535, 0.54, 0.545, 0.56, 0.58$. The number of samples of each distribution N_E is given as 450.
Figure 5.28 presents the posterior probability for model classes which are characterized by parameters $\alpha = 1$, $\gamma = [0.3, 0.58]$, and Figure 5.29 plots the posterior distribution of the system parameter t_{duff} as well as the relative errors of its identified values for the most probable model class.

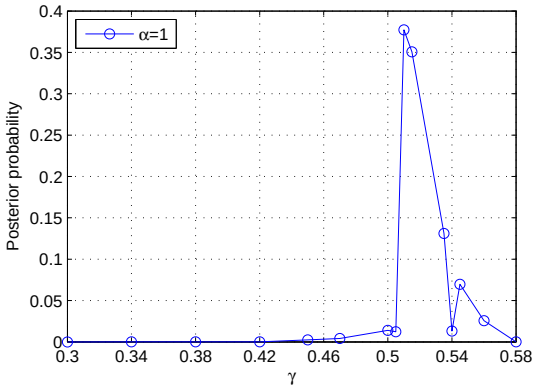

Figure 5.28: Posterior probability for model classes characterized by $\alpha = 1$, $\gamma = [0.3, 0.58]$ of a 2-DOF weakly nonlinear smoothly varying chainlike Duffing system.

It is noted from Figure 5.28 that the posterior probability of the model classes characterized by parameters $\alpha = 1$, $\gamma = [0.3, 0.58]$ has increasing trend as γ increases from 0.3 to 0.51 and reaches its maximum (37.7%) at $\gamma = 0.51$, then it has decreasing trend as γ increases from 0.51 to 0.58, determining the most probable model class by $\alpha^* = 1$, $\gamma^* = 0.51$. As all model classes are considered to be equally likely apriori, Figure 5.28 reveals that only model classes specified by $\alpha = 1$ and γ in the range of $\gamma \in [0.45, 0.56]$ have significant posterior probabilities. The posterior distribution of t_{duff} for the most probable model class $M(\alpha^* = 1, \gamma^* = 0.51)$ which is shown in Figure 5.29 is concentrated on its expected value with small relative errors (the mean value of which is equal to 2.2%). This indicates that the relative weightings of the IMFs of the acceleration responses, the IMFs of the corresponding velocity responses as well as the IMFs of

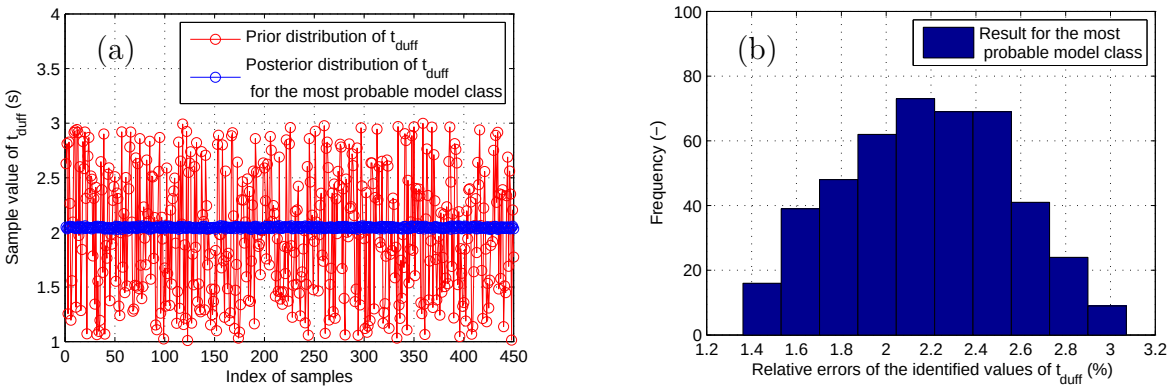

Figure 5.29: System parameter t_{duff} of a 2-DOF weakly nonlinear smoothly varying chain-like Duffing system: (a) Distribution of t_{duff}, (b) Relative errors for the identified values of t_{duff} and for the most probable model class.

the corresponding displacement responses in the likelihood function for the most probable model class $M(1, 0.51)$ can lead to a good identification of the system parameter t_{duff}.

5.5 Conclusion

In this chapter, we combine the HHT-based identification method proposed in Chapter 3 or the modified HHT-based identification methods proposed in Chapter 4 with a Bayesian model updating and model class selection method implemented by the TMCMC sampling method to obtain the statistical distributions of the system parameters for the n-DOF general linear time-varying systems or the n-DOF weakly nonlinear time-varying Duffing and Van der Pol systems. Bayesian inference is used to update the white noise in system responses at each instant of time, yielding the posterior distributions of the noise parameters. Based on these posterior distributions of the noise parameters, the posterior distributions of the system responses are obtained and then processed by the HHT-based identification method or the modified HHT-based identification methods, gaining the posterior distributions of the identified system parameters.
Results of the numerical simulations reveal possible noise levels for the system parameter: For the 1-DOF and 2-DOF general linear time-varying systems as well as weakly nonlinear time-varying Duffing systems with smooth, abrupt and periodic stiffness variations, the identified values of the stiffness coefficients and the mean values of the identified values of the damping coefficients are concentrated close to their respective true values (except for the identified stiffness coefficients of abruptly varying systems that have large identification errors at some time instants due to the limitations of Equation (2.16)), whereas the identified values of the damping coefficients are widely distributed and have large identification errors due to the sensitivity of the damping coefficients to noise (see Sections 5.2.1-5.2.2, Sections 5.3.1-5.3.2, Appendices B.1.1-B.1.3, and Appendices B.2.1-B.2.3); for the 1-DOF and 2-DOF weakly nonlinear time-varying Van der Pol systems, the statistical distribu-

tions of the identified values of the stiffness coefficients are always concentrated around their respective true values, whereas the identified values of the damping coefficients and the mean values of the identified values of the damping coefficients have large identification errors due to the sensitivity of the damping coefficients to noise and the application of the approximation Equation (4.8) (see Sections 5.3.3-5.3.4 and Appendices B.2.4-B.2.6).
Later, a Bayesian inference based parameter identification method is developed with the likelihood function formulated as the product of three probability density functions, one relating to the IMFs of the acceleration responses and the other two relating to the IMFs of the corresponding velocity responses as well as the IMFs of the corresponding displacement responses. By applying Bayesian model class selection, the most probable model class is selected from a set of candidate model classes, yielding the corresponding posterior distributions of the system parameters.
Results of the numerical simulations on linear and weakly nonlinear smoothly varying systems indicate that: By applying the proposed method, meaningful posterior probability curves for candidate model classes can be always obtained, and the resulting posterior distributions of the system parameters for the most probable model class are always found concentrated around their respective expected values with small relative errors, implying that the relative weightings of the IMFs of the acceleration responses and the IMFs of the corresponding velocity responses as well as displacement responses in the likelihood function chosen for the most probable model class can lead to good identification of the system parameters (see Section 5.4.2).
Altogether, results of the numerical simulations demonstrate the effectiveness, accuracy and robustness of the HHT and Bayesian inference based identification method as well as the Bayesian inference based parameter identification method.

6 Conclusions and Recommendations

This chapter summarizes the important results and conclusions that can be drawn from this study. This dissertation extends an identification technique based on the HHT to general time-varying systems including linear time-varying systems and nonlinear time-varying systems such as Duffing and Van der Pol systems with smooth, abrupt and periodical stiffness variations. Later, the method is combined with a Bayesian model updating and model class selection method, capable of identifying the statistical distributions of not only system stiffness and damping parameters, but also structural parameters. The key contributions of this thesis are briefly summarized as follows:

1. A HHT-based identification method has been developed for identification of general linear time-varying systems. This method extends the parametric identification technique proposed by Shi and Law to address identification of not only linear time-varying chainlike systems, but also linear time-varying non-chainlike systems. The presence of noise is always considered in this framework.
2. With the help of the formula of Hahn and the idea of Feldman, the proposed HHT-based identification method is modified and extended for identification of weakly nonlinear time-varying MDOF Duffing systems and Van der Pol systems.
3. The proposed HHT-based identification method and its modifications are combined with a Bayesian model updating and model class selection method to obtain the statistical distributions of system stiffness and damping parameters.
4. To address the identification of system parameters, a new parameter identification method based on Bayesian inference has been developed. When using Bayesian model updating techniques, the new parameter identification method is based on the formulation of the likelihood function as a product of three probability density functions, one relating to the IMFs of the acceleration responses and the other two relating to the IMFs of the corresponding velocity responses as well as the IMFs of the corresponding displacement responses.

6.1 Conclusions

Concerning the aforementioned contributions, the central conclusions in this dissertation are summarized as follows:

1. For LTV systems, priori based identification methods such as STFT and WT have difficulties to identify system parameters and mostly yield instantaneous modal parameters only; whereas adaptive based identification methods such as SVD and HHT method proposed by Shi and Law have limitations in application to parametric identification of LTV

systems. The limitations of the former method are due to the fact that the eigenfunctions are difficult to interpret, those of the latter method are due to the limited application for linear time-varying chain-like systems only. In this regard, a HHT-based identification technique, which is an extension of the HHT method proposed by Shi and Law, is proposed to identify general linear time-varying systems including not only chainlike systems, but also non-chainlike systems. It uses EMD to decompose the system responses into IMFs and residues, and then analyzes the IMFs and the residues by HT to obtain the analytical IMFs and analytical residues. After that, these analytical signals are synthesized to form new analytical response signals. Finally, the new synthesized analytical response signals are used to form the equations proposed in Section 3.1 for identification of system stiffness and damping parameters. Numerical simulations on 1-DOF and 2-DOF linear time-varying systems with smooth, abrupt and periodical stiffness variations as well as white noise perturbations considered in the system responses demonstrate the effectiveness, accuracy and robustness of the method.

2. For nonlinear time-varying systems, since the systems contain nonlinear parameters, Bedrosian's theorem is not valid for the application of HT on the product of the nonlinear system coefficient and the corresponding system response. Instead, some approximations are made based on the formula of Hahn and the idea of Feldman to modify the aforementioned HHT-based identification method for weakly nonlinear time-varying MDOF Duffing systems and Van der Pol systems respectively. In this way, the proposed HHT-based identification method is extended to address identification of nonlinear time-variant systems, which is very important since most systems in the real world exhibit non-stationary and non-linear dynamical performance.

3. Experimentally measured system responses are usually perturbed by noise, therefore a Bayesian model updating and model class selection method is proposed to address this problem. Bayesian model updating is implemented by TMCMC method to update initial knowledge about the forced vibration system responses and the white noise in these system responses based on measured system responses. In this process, the likelihood function is formulated as a product of three probability density functions, one relating to acceleration responses and the other two relating to the corresponding velocity responses and displacement responses. Then, Bayesian model class selection is performed to choose the most probable model class. With the help of the posterior distributions of the noise parameters obtained for the most probable model class as well as the reference values of the system responses, sample system responses are generated and then processed by the aforementioned HHT-based identification method, yielding the statistical distributions of system stiffness and damping parameters. The Bayesian model updating and model class selection method tries to largely reduce the noise components in the measured system responses before they are used as input of the HHT-based identification method, which is quite important for application of the HHT-based method since the existence of noise in the input system responses might result in unwanted outcomes of the EMD. Numerical simulations show that the combined method is capable to deal with relative high levels of noise (up to 20%RMS) existing in the experimentally measured system responses.

4. A new parameter identification method based on Bayesian inference has been developed to identify system parameters. Instead of using modal data such as modal frequencies and

mode-shape components, this method utilizes IMFs generated by EMD to formulate the likelihood function. Based on the IMFs decomposed from measured system responses, Bayesian inference is implemented by TMCMC method to update initial knowledge about the system parameters for a set of candidate model classes, yielding the corresponding posterior distributions of the system parameters for these model classes. In this process, the likelihood function is formulated as the product of three probability density functions, one relating to the IMFs of the acceleration responses, the other two relating to the IMFs of the corresponding velocity responses and the IMFs of the corresponding displacement responses. Then, by performing Bayesian model class selection, the most probable model class and the corresponding posterior distributions of the system parameters for the most probable model class are selected. Since IMFs can be extracted conveniently from the easily measured system responses in practice, this method enables another means to identify system parameters with avoiding the difficulties which might be confronted when measuring modal data.

6.2 Recommendations for future studies

This thesis has tried to develop new identification methods utilizing HHT and Bayesian model updating and model class selection method in the field of signal processing. In light of the current work, following work can be suggested for further research.

First, the numerical simulations in this thesis are only carried out on 1-DOF and 2-DOF systems, since the identification methods proposed in this thesis are supposed to be applied to MDOF time-varying systems, numerical simulations on systems with 3 or more DOFs should be carried out to further demonstrate the robustness of the proposed identification methods.

Second, in this thesis, only weakly nonlinear time-varying systems are considered. Further studies can be carried out to extend the proposed HHT-based identification methods for more complex strong nonlinear time-varying systems. In order to address more complex nonlinear parameters, potential algorithms have to be pursued to automatically distinguish the high-pass portion and low-pass portion of the nonlinear parameters, since application of the formula of Hahn and the idea of Feldman requires this procedure.

Besides, reasonable prescribed values for some important factors of TMCMC method such as the prescribed scaling factor s_f used to suppress the rejection rate of MCMC (see Equation (2.45)) and the COV of the plausibility weights of the samples used to generate intermediate PDFs (see Section 2.4.4), should be studied for various linear and nonlinear time-varying systems, since the suggested values of these important factors proposed by Ching and Chen might be no longer appropriate for all cases. In avoidance of unexpected program interruptions that were always confronted when improper values were chosen and in consideration of reasonable computational cost, potential algorithms for obtaining reasonable prescribed values of the important factors are utmost required.

In addition, since the proposed HHT-based identification method is able to detect the abrupt stiffness variations of the time-varying systems (see Sections 3.2, 4.1-4.2), and the Bayesian model updating and model class selection method proposed in Section 5.1 can largely reduce the noise components in the measured system responses before they are used as input of the HHT-based identification method, combination of the Bayesian model updating and model class selection method with the proposed HHT-based identification method is capable to detect the damage of time-varying structures. Application of this combined method in the field of structural health monitoring for civil and mechanical engineering structures with time-varying properties such as a train-bridge system would be very interesting and can be further studied.

Finally, the Bayesian inference based parameter identification method proposed in Section 5.4 is supposed to be applied to an n-DOF time-varying system with IMFs extracted from $3n^2$ system responses obtained in n experiments (for each experiment, ODE of the system is solved with the same initial conditions given at a different DOF of the system), which is quite time-consuming since the observed values and model values of $n \times 3n^2$ IMFs are needed in the method. For 2-DOF linear and weakly nonlinear time-varying systems, it has been proven recently that the proposed Bayesian inference based parameter identification method still works with consideration of IMFs extracted from only one set of system responses which corresponds to one DOF (see Appendix B.3). Since the original method would require much more IMFs for systems with more DOFs, application of the Bayesian inference based parameter identification method for systems with 3 or more DOFs with consideration of less IMFs could be further studied.

Appendix

A Some of the HHT-based identification results of general time-varying systems

A.1 Some of the HHT-based identification results of linear time-varying systems

A.1.1 HHT-based identification results of the damping coefficients of 1-DOF linear smoothly and abruptly varying forced vibration systems

For the 1-DOF smoothly and abruptly varying forced vibration systems proposed in Section 3.2.1, the identified results of the system damping coefficients are shown in Figures A.1 - A.2.

We can notice that: For the 1-DOF linear smoothly varying forced vibration system, when noise-added system responses are used as input of the proposed HHT-based identification method, due to the sensitivity of damping coefficient to noise, the identified result of the system damping coefficient has large identification error, but its mean value (denoted with a pink dashed line) over the required time history is close to its true value with small relative error (equal to 6.1%); For the 1-DOF linear abruptly varying forced vibration system, no matter using noiseless or noise-added system responses as input of the proposed HHT-based identification method, like the identified result of the stiffness coefficient shown in Figure 3.6, the identified result of the damping coefficient also has large identification errors around $t = 1.5$s and $t = 3.5$s, due to the abrupt changes of the system stiffness at these time instants. When noise-added system responses are used as input, the identified damping coefficient is contaminated by noise due to its sensitivity to noise, but its mean value (denoted with a pink dashed line) over the required time history matches closely its true value and has small relative error (less than 13%).For both systems, the identified values of damping coefficients gained by the proposed HHT-based identification method are equivalent to their respective counterparts which are obtained by the HHT-based method proposed by Shi and Law, since the two methods share the same equations for 1-DOF systems.

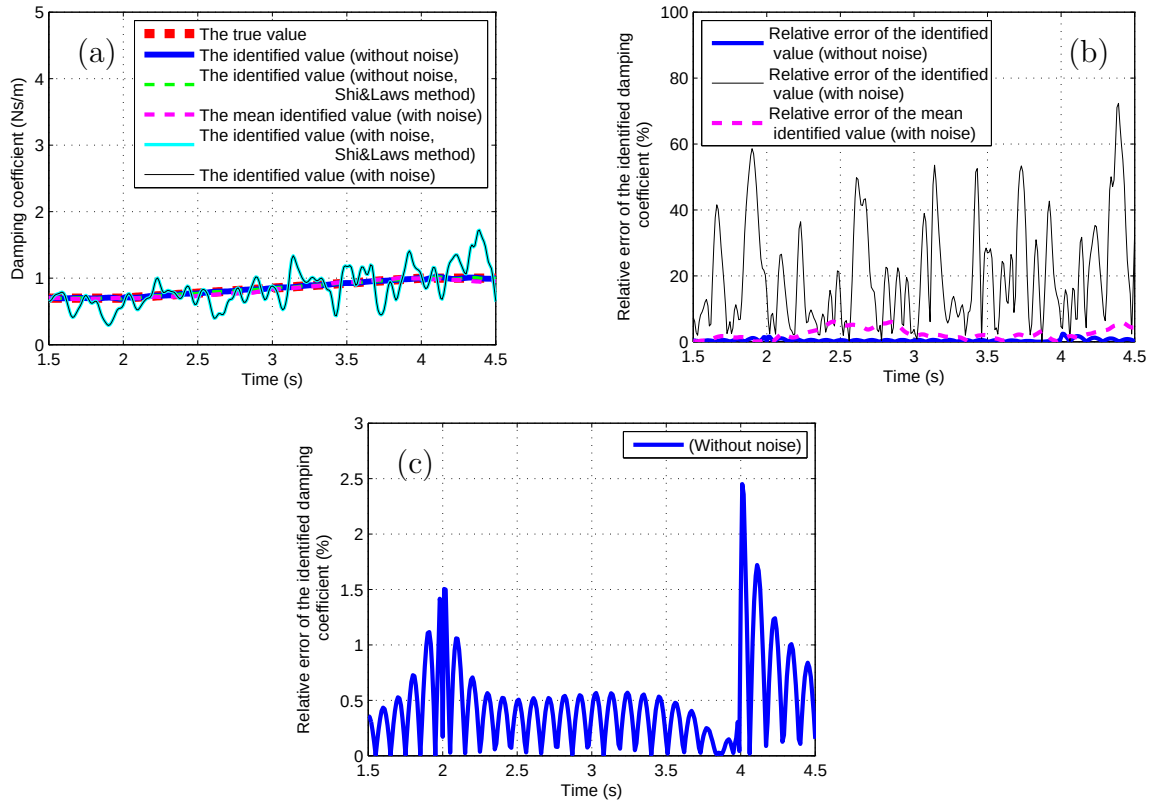

Figure A.1: Damping coefficient of a 1-DOF smoothly varying forced vibration system: (a) The true value and the identified values of the damping coefficient, (b) Relative errors of the identified values of the damping coefficient,(c) Relative error of the identified value of the damping coefficient (without noise in system responses).

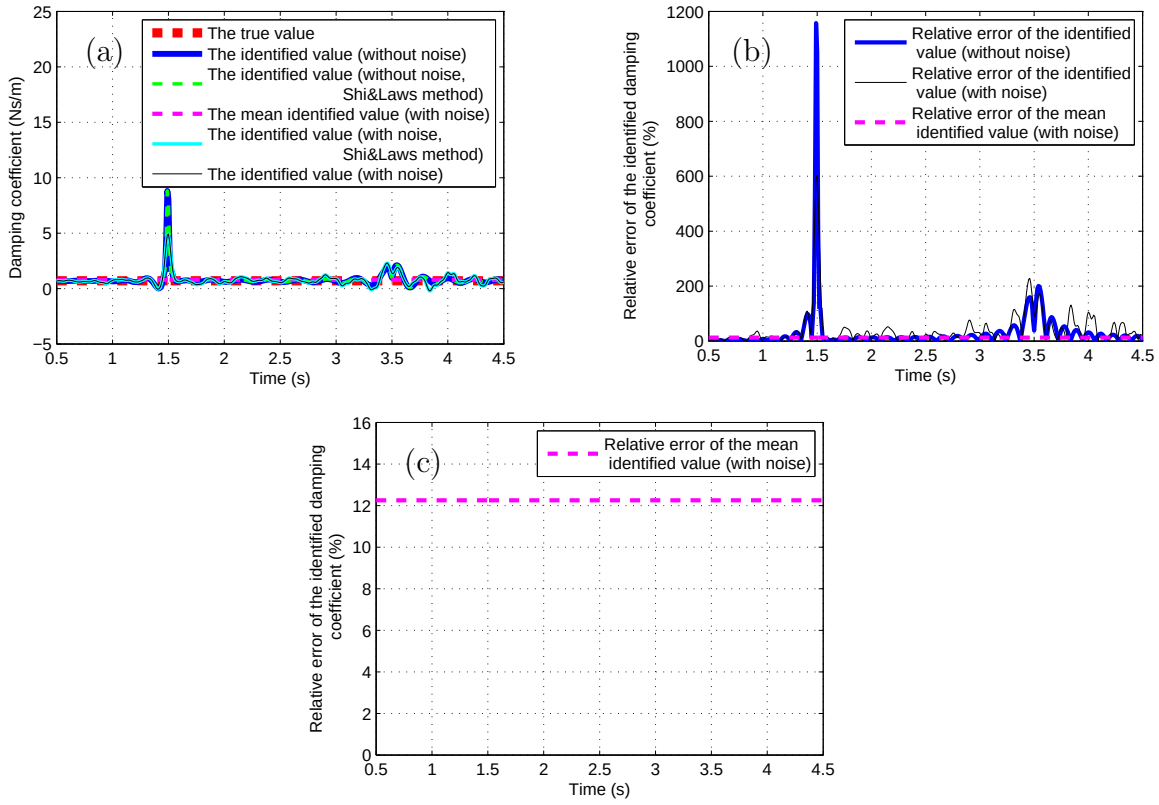

Figure A.2: Damping coefficient of a 1-DOF abruptly varying forced vibration system: (a) The true value and the identified values of the damping coefficient, (b) Relative errors of the identified values of the damping coefficient, (c) Relative error of the mean identified value of the damping coefficient.

A.1.2 HHT-based identification results of the damping coefficients of 2-DOF linear smoothly and abruptly varying non-chainlike forced vibration systems

For the 2-DOF linear smoothly and abruptly varying non-chainlike forced vibration systems proposed in Section 3.2.2, the identified results of the system damping coefficients are shown in Figures A.3 - A.6.

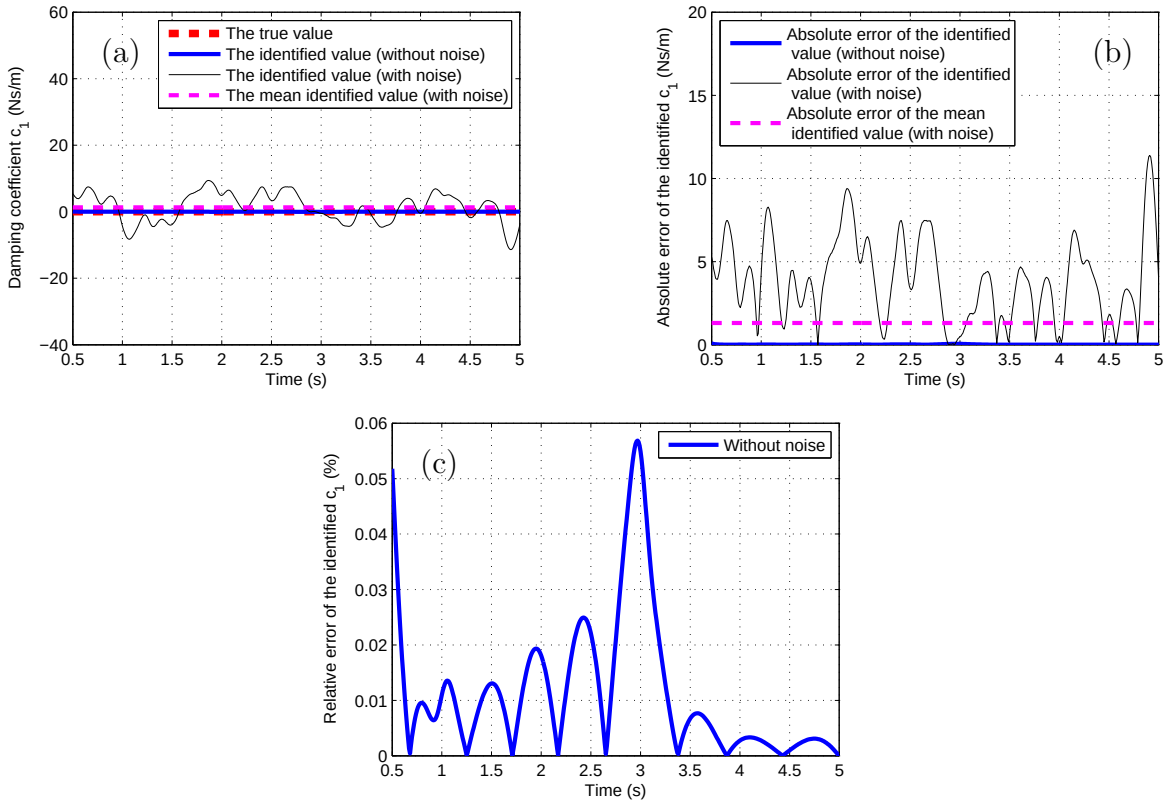

Figure A.3: Damping coefficient c_1 of a 2-DOF linear smoothly varying non-chainlike forced vibration system: (a) The true value and the identified values of c_1, (b) Absolute errors of the identified values of c_1, (c) Close-up of (b).

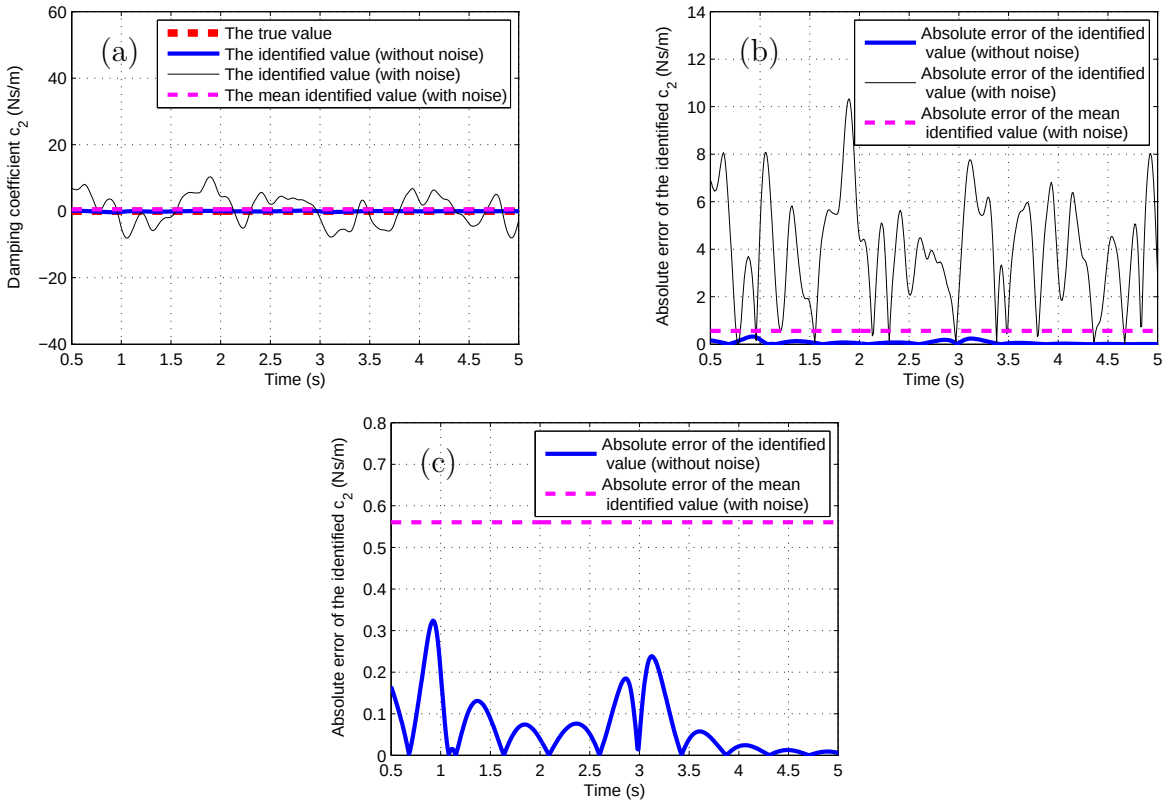

Figure A.4: Damping coefficient c_2 of a 2-DOF linear smoothly varying non-chainlike forced vibration system: (a) The true value and the identified values of c_2, (b) Absolute errors of the identified values of c_2,(c) Close-up of (b).

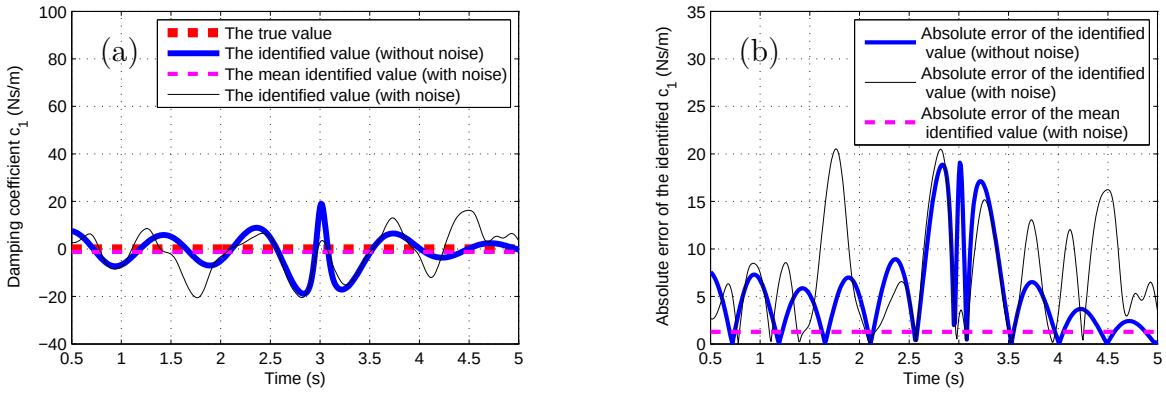

Figure A.5: Damping coefficient c_1 of a 2-DOF linear abruptly varying non-chainlike forced vibration system: (a) The true value and the identified values of c_1, (b) Absolute errors of the identified values of c_1.

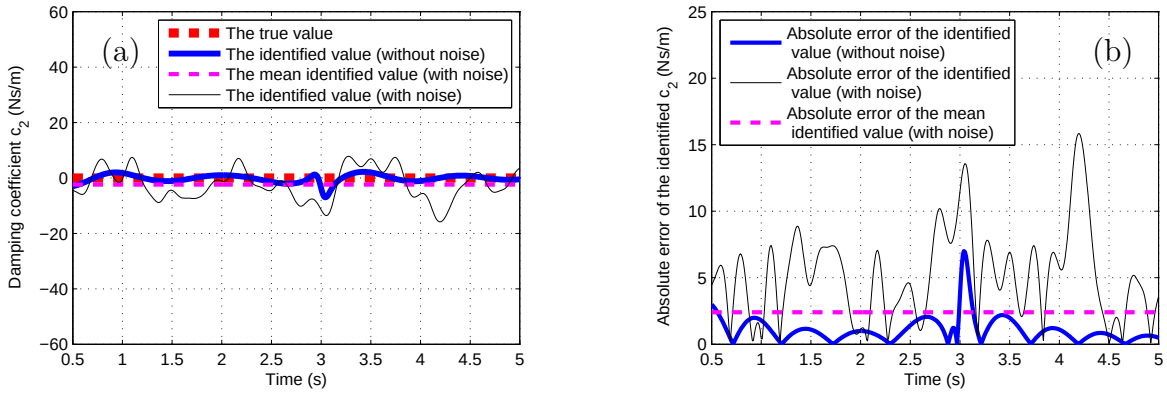

Figure A.6: Damping coefficient c_2 of a 2-DOF linear abruptly varying non-chainlike forced vibration system: (a) The true value and the identified values of c_2, (b) Absolute errors of the identified values of c_2.

It is found in the figures that: For the 2-DOF linear smoothly varying non-chainlike forced vibration system, when noise-added system responses are used as input of the proposed HHT-based identification method, the identified results of damping coefficients are contaminated by noise and have large absolute errors since they are sensitive to noise, but by taking the mean values of them over the required time history, the resulting mean identified damping coefficients (denoted with pink dashed lines) match their true values well, and their absolute errors are small (less than 1.4Ns/m and equal to 0.56Ns/m respectively); For the 2-DOF linear abruptly varying non-chainlike forced vibration system, due to the limitations of Equation (2.16), when noiseless system responses are used as input of the proposed HHT-based identification method, the identified results of damping coefficients are found having quite large identification errors around $t = 3$s; when noise-added system responses are used as input, since damping coefficients are sensitive to noise, their identified results are contaminated by noise which makes it difficult to detect abrupt stiffness variation of the system from the identified results of damping coefficients. However, the resulting mean identified damping coefficients (denoted with pink dashed lines) are obtained with small absolute errors (less than 1.3Ns/m and equal to 2.4Ns/m respectively).

A.1.3 HHT-based identification results of the damping coefficients of 2-DOF linear smoothly and abruptly varying chainlike forced vibration systems

For the 2-DOF linear smoothly and abruptly varying chainlike forced vibration systems proposed in Section 3.2.3, the identified results of the system damping coefficients are presented in Figures A.7 - A.10.

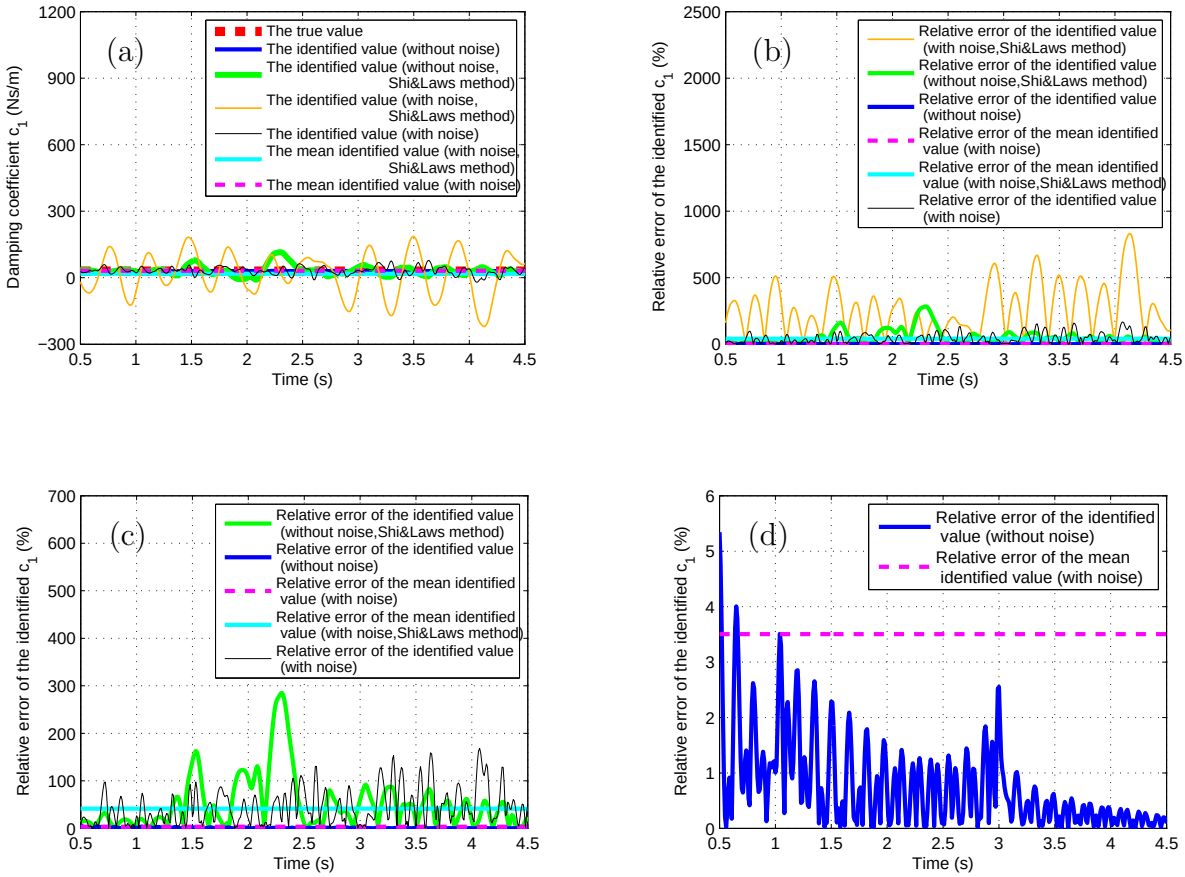

Figure A.7: Damping coefficient c_1 of a 2-DOF linear smoothly varying chainlike forced vibration system: (a) The true value and the identified values of c_1, (b) Relative errors of the identified values of c_1, (c) Close-up of (b), (d) Close-up of (c).

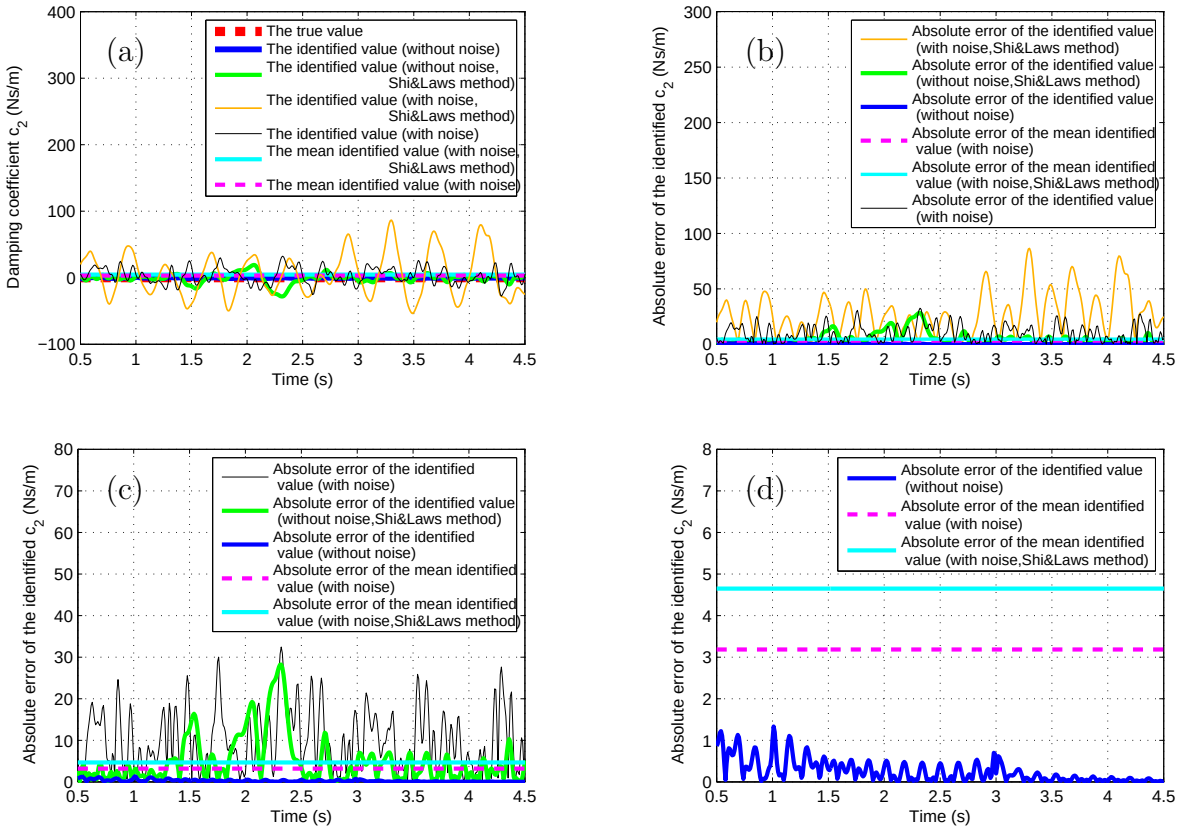

Figure A.8: Damping coefficient c_2 of a 2-DOF linear smoothly varying chainlike forced vibration system: (a) The true value and the identified values of c_2, (b) Absolute errors of the identified values of c_2, (c) Close-up of (b), (d) Close-up of (c).

From Figures A.7 - A.10, it can be seen that: For both systems, no matter using noiseless or noise-added system responses as input of the proposed HHT based identification method, the resulting identified damping coefficients are much better than their counterparts (denoted by green solid lines and orange solid lines) obtained by the identification method proposed by Shi and Law, possibly because the identification method proposed by Shi and Law adopts the assumption of orthogonality between any two IMFs and uses single IMFs as input while discarding the signal residues obtained by EMD method which might still contain some information about the system responses. When noise-added system responses are used as input, the resulting identified damping coefficients have large relative error or absolute error since they are sensitive to noise, but by taking the mean values of them over the required time history, the obtained mean identified damping coefficients (denoted by pink dashed lines) are found matching their true values well with small relative error or absolute error (the maximal relative error of the mean identified c_1 is equal to 3.5% and the maximal absolute error of the mean identified c_2 is less than 3.2Ns/m for the 2-DOF linear smoothly varying chainlike forced vibration system, their counterparts for the 2-DOF linear abruptly varying chainlike forced vibration system

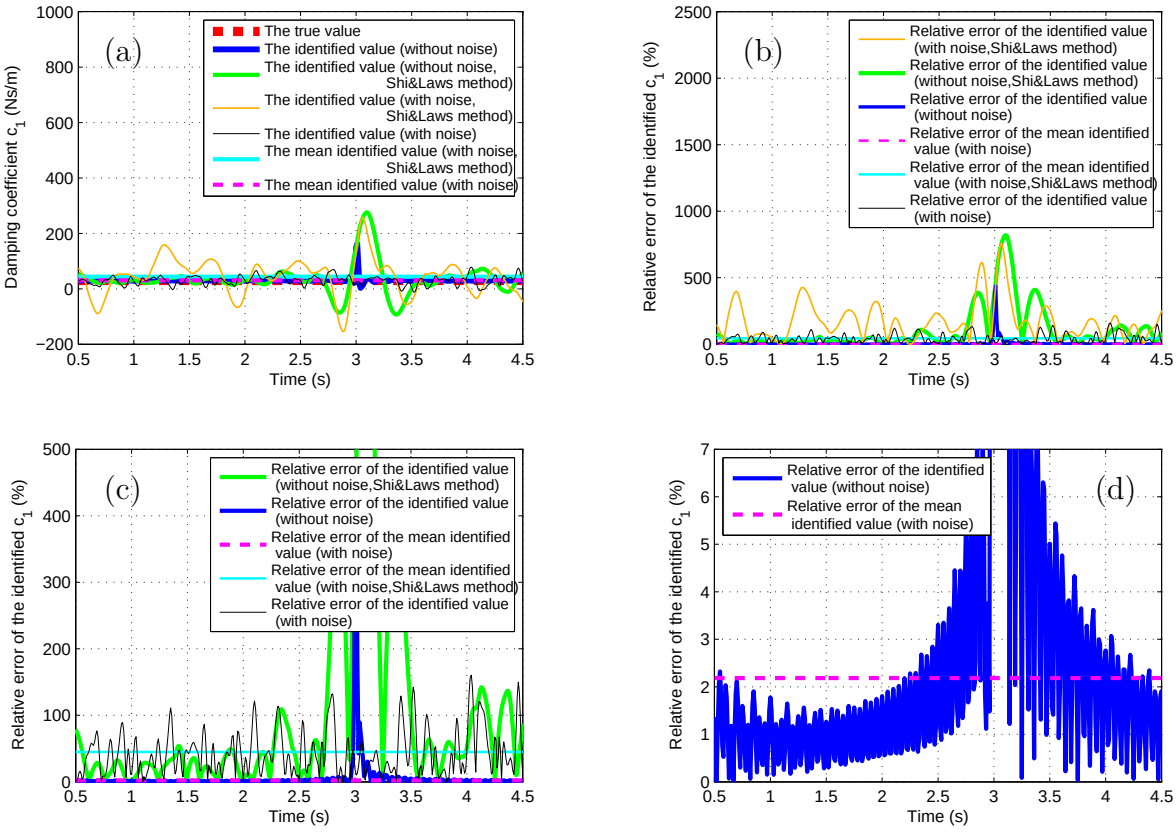

Figure A.9: Damping coefficient c_1 of a 2-DOF linear abruptly varying chainlike forced vibration system: (a) The true value and the identified values of c_1, (b) Relative errors of the identified values of c_1, (c) Close-up of (b), (d) Close-up of (c).

are less than 2.2% and 0.38Ns/m respectively). For the 2-DOF linear abruptly varying chainlike forced vibration system, when using noiseless system responses as input, the identified damping coefficients are always found having extremely large identification errors around $t = 3$s, due to the limitations of Equation (2.16); when using noise-added system responses as input, the identified damping coefficients are contaminated by noise, which makes it difficult to detect abrupt stiffness variation of system parameters from the identified damping coefficients.

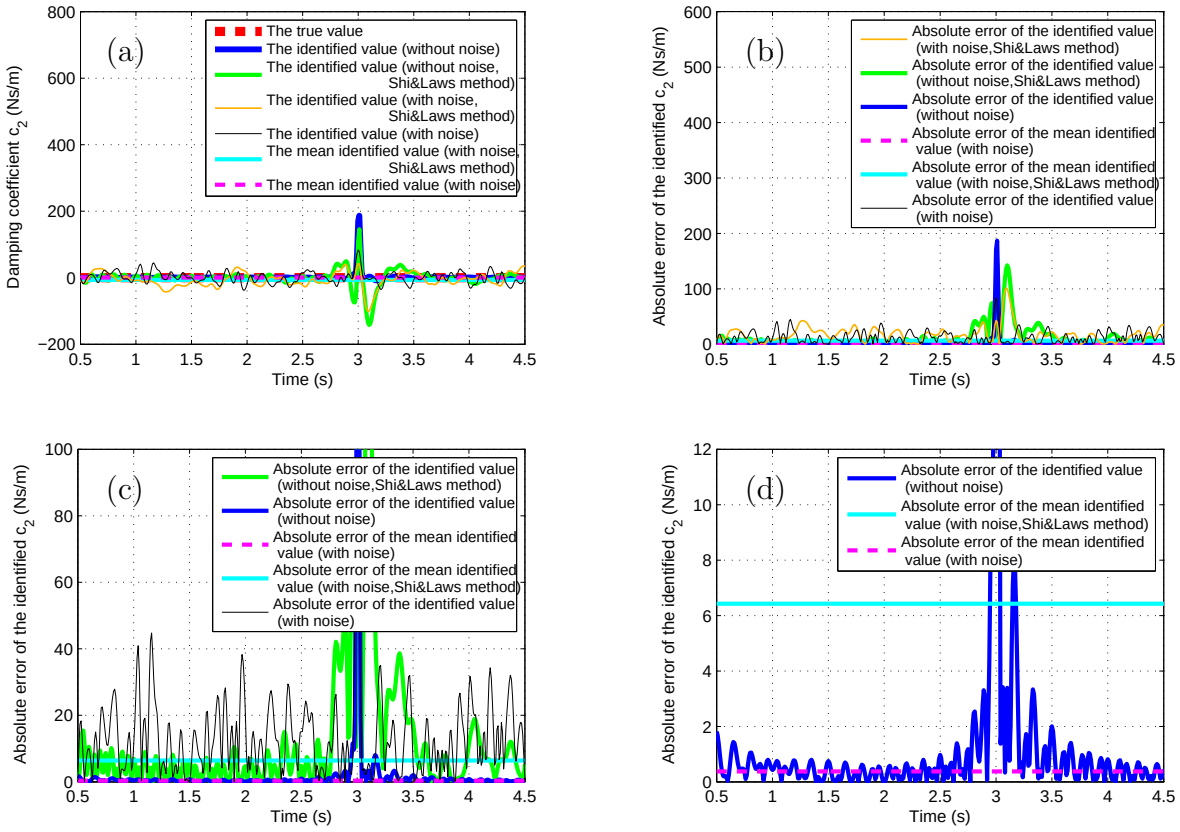

Figure A.10: Damping coefficient c_2 of a 2-DOF linear abruptly varying chainlike forced vibration system: (a) The true value and the identified values of c_2, (b) Absolute errors of the identified values of c_2, (c) Close-up of (b), (d) Close-up of (c).

A.1.4 HHT-based identification results of linear periodically varying systems

(1) 1-DOF system

For the 1-DOF linear periodically varying forced vibration system proposed in Section 3.2.1, Figure A.11 presents the identified results of the system coefficients and their relative errors. It is noted that, when using noiseless system responses as input of the proposed HHT based identification method, the identified stiffness and damping coefficients match their respective true values well; when using noise-added system responses as input, the accuracies of the corresponding identified results decrease, though good identified value of stiffness coefficient with small relative error (whose maximum is less than 4.6%) is still obtained. The identified value of damping coefficient is contaminated a lot by noise, but its mean value (denoted with a pink dashed line) over the required time history is close to its true value with small relative error (less than 2.2%). Since the HHT-based method proposed by Shi and Law and the proposed HHT-based identification method share the same equations for 1-DOF systems, the identified values of system coefficients obtained by

the former method are equivalent to their respective counterparts obtained by the latter method.

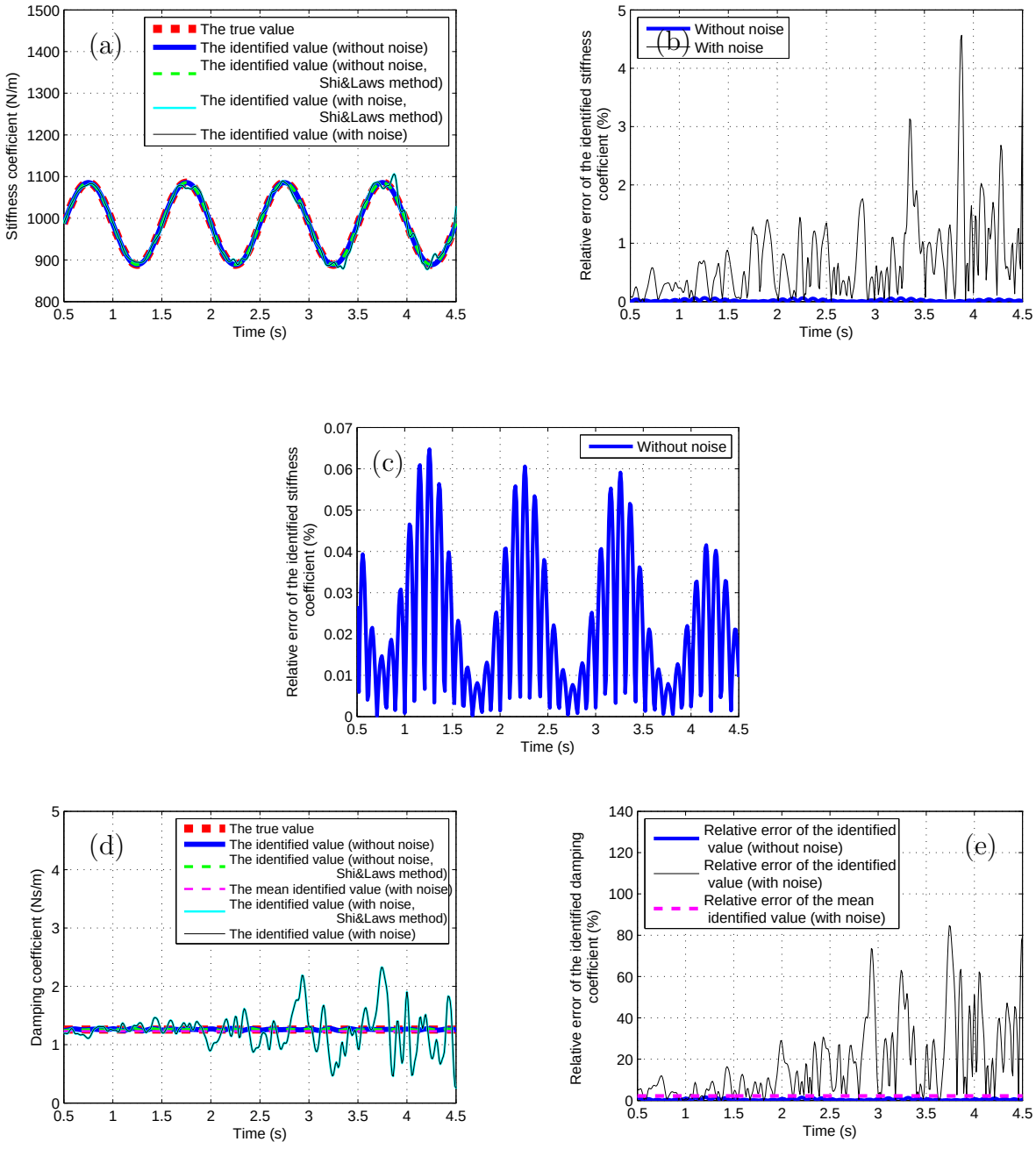

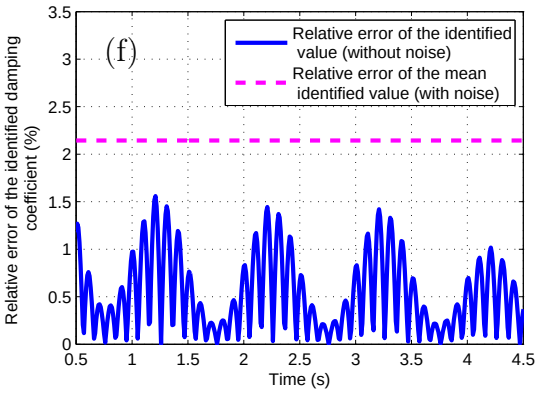

Figure A.11: System coefficients of a 1-DOF linear periodically varying forced vibration system: (a) The true value and the identified values of the stiffness coefficient, (b) Relative errors of the identified values of the stiffness coefficient, (c) Relative error of the identified value of the stiffness coefficient (without noise in system responses), (d) The true value and the identified values of the damping coefficient, (e) Relative errors of the identified values of the damping coefficient, (f) Close-up of (e).

(2) 2-DOF system

For the 2-DOF linear periodically varying non-chainlike forced vibration system proposed in Section 3.2.2, Figures A.12 - A.15 present the identified results of the system coefficients as well as their relative and absolute errors.

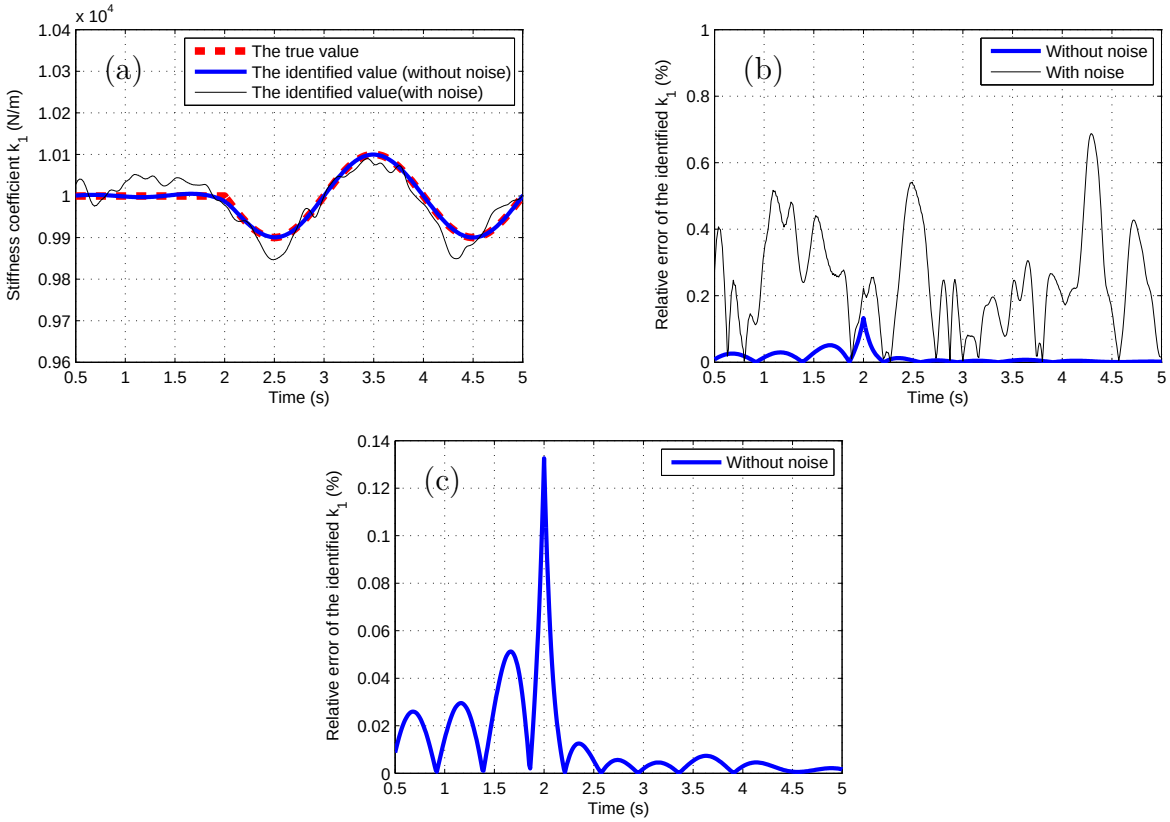

Figure A.12: Stiffness coefficient k_1 of a 2-DOF linear periodically varying non-chainlike forced vibration system: (a) The true value and the identified values of k_1, (b) Relative errors of the identified values of k_1, (c) Relative error of the identified value of k_1 (without noise in system responses).

It is noted that, when using noiseless system responses as input, the identified results nearly superpose over their respective true values, and their relative as well as absolute errors have abrupt change around time instant $t = 2$s, due to the abrupt change of the given stiffness coefficient at $t = 2$s. When using noise-added system responses as input, the identified results are contaminated by noise, their accuracies are worse, though identified stiffness coefficients with small relative errors (whose maximum is less than 0.69% for k_1 and less than 0.58% for k_2 respectively) are still obtained. The identified damping coefficients are sensitive to noise and have large absolute errors, but their mean values (denoted with pink dashed lines) are found close to their respective true values and have sufficiently small absolute errors (less than 0.24Ns/m for c_1 and less than 1.7Ns/m for c_2 respectively).

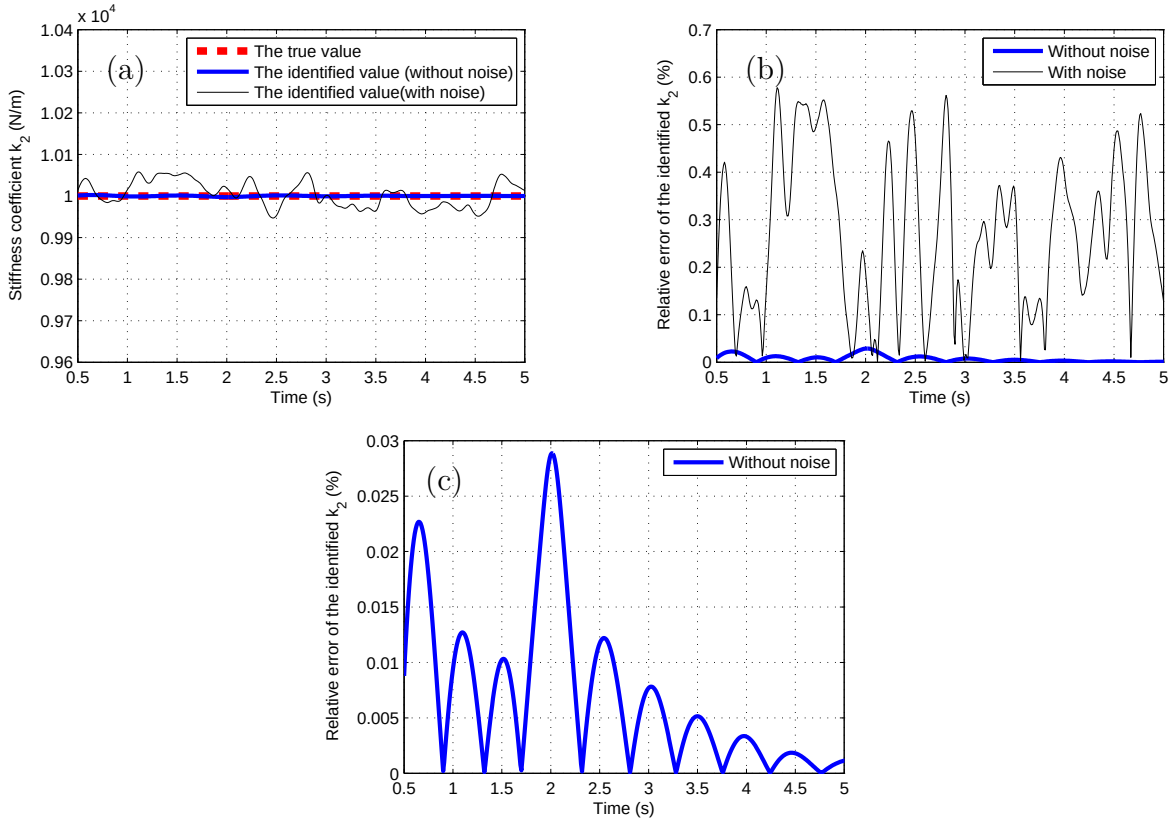

Figure A.13: Stiffness coefficient k_2 of a 2-DOF linear periodically varying non-chainlike forced vibration system: (a) The true value and the identified values of k_2, (b) Relative errors of the identified values of k_2, (c) Relative error of the identified value of k_2 (without noise in system responses).

For the 2-DOF linear periodically varying chainlike forced vibration system proposed in Section 3.2.3, the identified results of the system coefficients as well as their relative and absolute errors are presented in Figures A.16 - A.19.

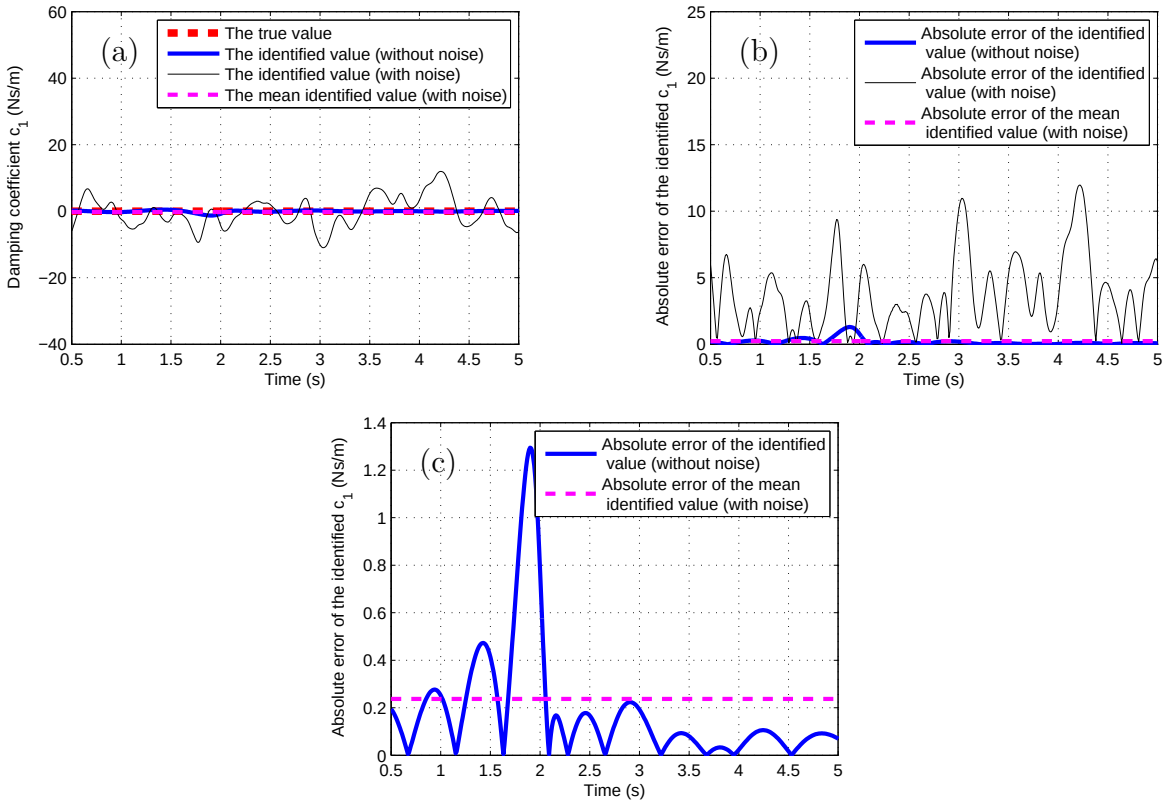

Figure A.14: Damping coefficient c_1 of a 2-DOF linear periodically varying non-chainlike forced vibration system: (a) The true value and the identified values of c_1, (b) Absolute errors of the identified values of c_1, (c) Absolute error of the identified value of c_1 (without noise in system responses).

It is found out that, when using noiseless system responses as input, the identified results nearly superpose over their corresponding true values and their relative as well as absolute errors are quite small, except that around time instant $t = 2$s abrupt changes are found in the relative errors of k_1 and c_1, which is due to the abrupt change of the given stiffness coefficient k_1 at $t = 2$s. When using noise-added system responses as input, the accuracies of the identified results are worse than their counterparts obtained without noise in system responses, but we can still obtain good identified stiffness coefficients with small relative errors (the maximal relative error of k_1 is less than 5.7% and that of k_2 is less than 1.9%). However, the identified damping coefficients are contaminated by noise. Taking the mean values of them over the required time history, the resulting mean identified damping coefficients (denoted with pink dashed lines) with small relative error or absolute error (the maximal relative error of the mean identified c_1 is less than 1.9% and the maximal absolute error of the mean identified c_2 is less than 0.18Ns/m) can be obtained. Like in the case of 2-DOF linear smoothly and abruptly varying chainlike systems, the identified results obtained by the HHT-based identification method are also better than the results obtained by the HHT-based identification method proposed by Shi and Law, possibly because the latter method adopts the assumption of orthogonality between any two IMFs,

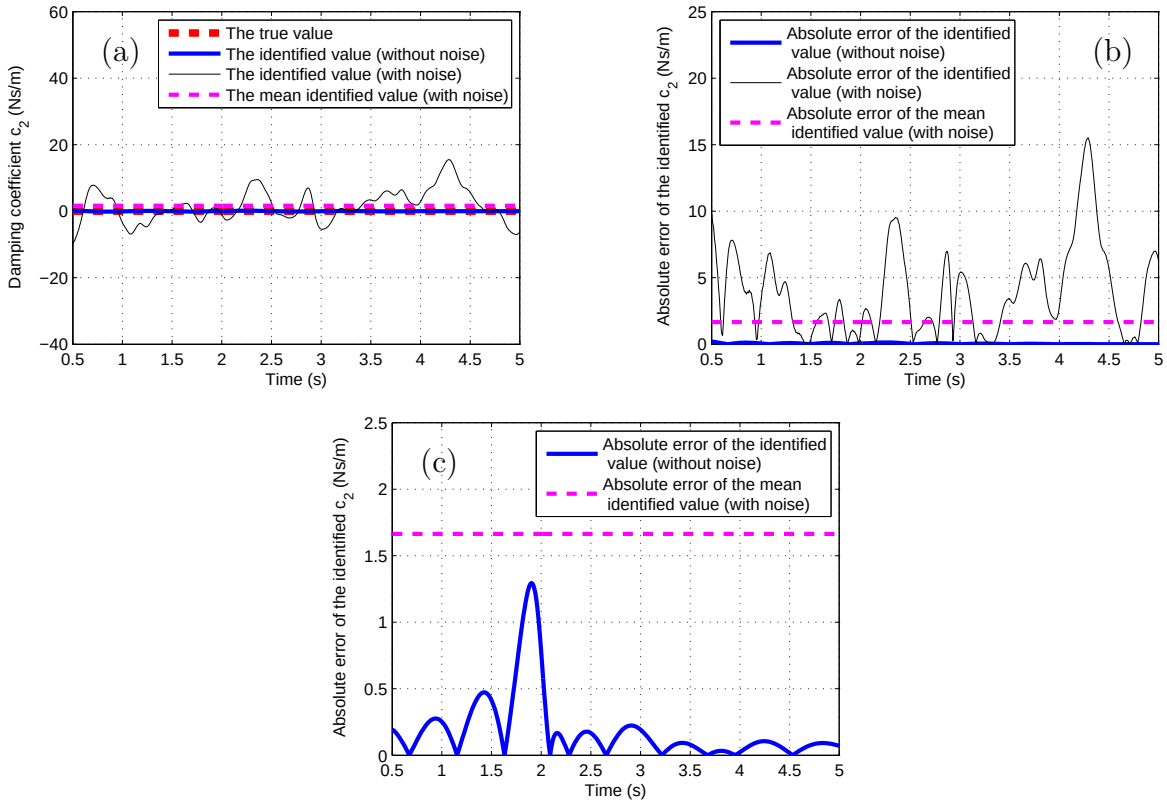

Figure A.15: Damping coefficient c_2 of a 2-DOF linear periodically varying non-chainlike forced vibration system: (a) The true value and the identified values of c_2, (b) Absolute errors of the identified values of c_2, (c) Close-up of (b).

and uses single IMFs as input while discarding the signal residues obtained by EMD method which might still contain some information about the system responses.

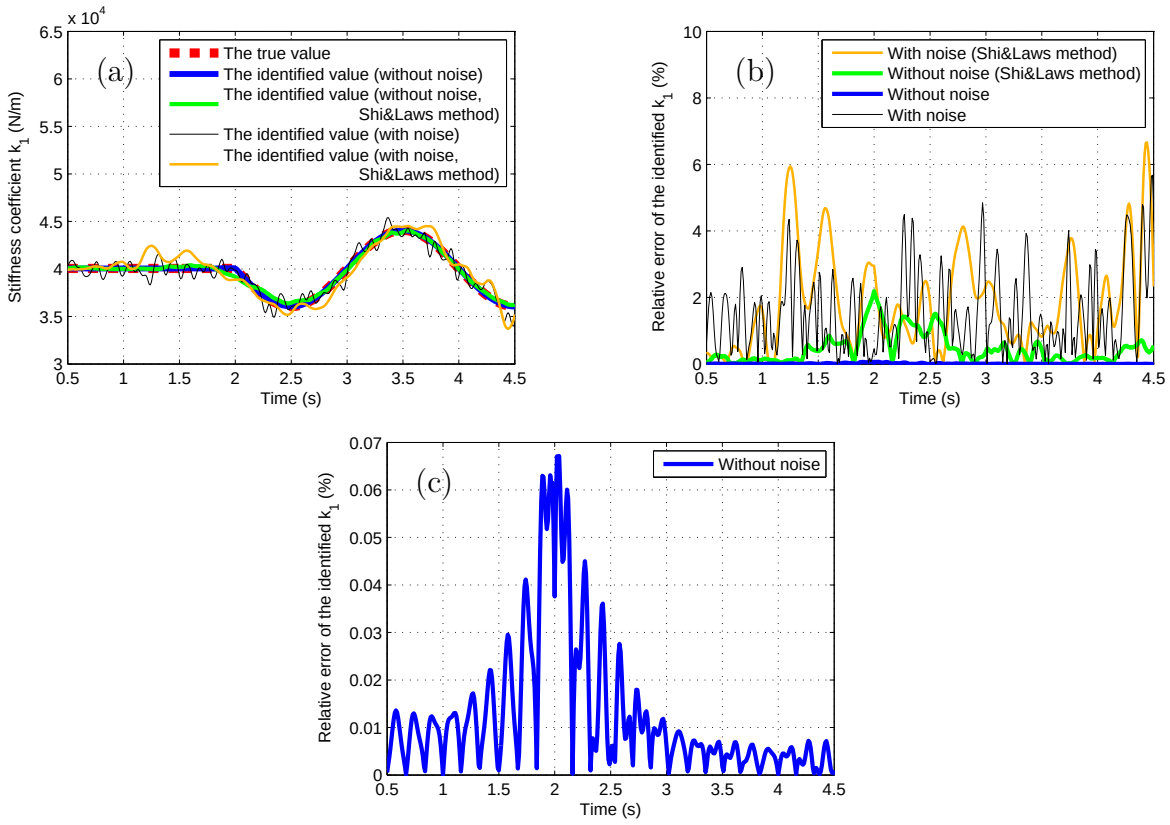

Figure A.16: Stiffness coefficient k_1 of a 2-DOF linear periodically varying chainlike forced vibration system: (a) The true value and the identified values of k_1, (b) Relative errors of the identified values of k_1, (c) Relative error of the identified value of k_1 (without noise in system responses).

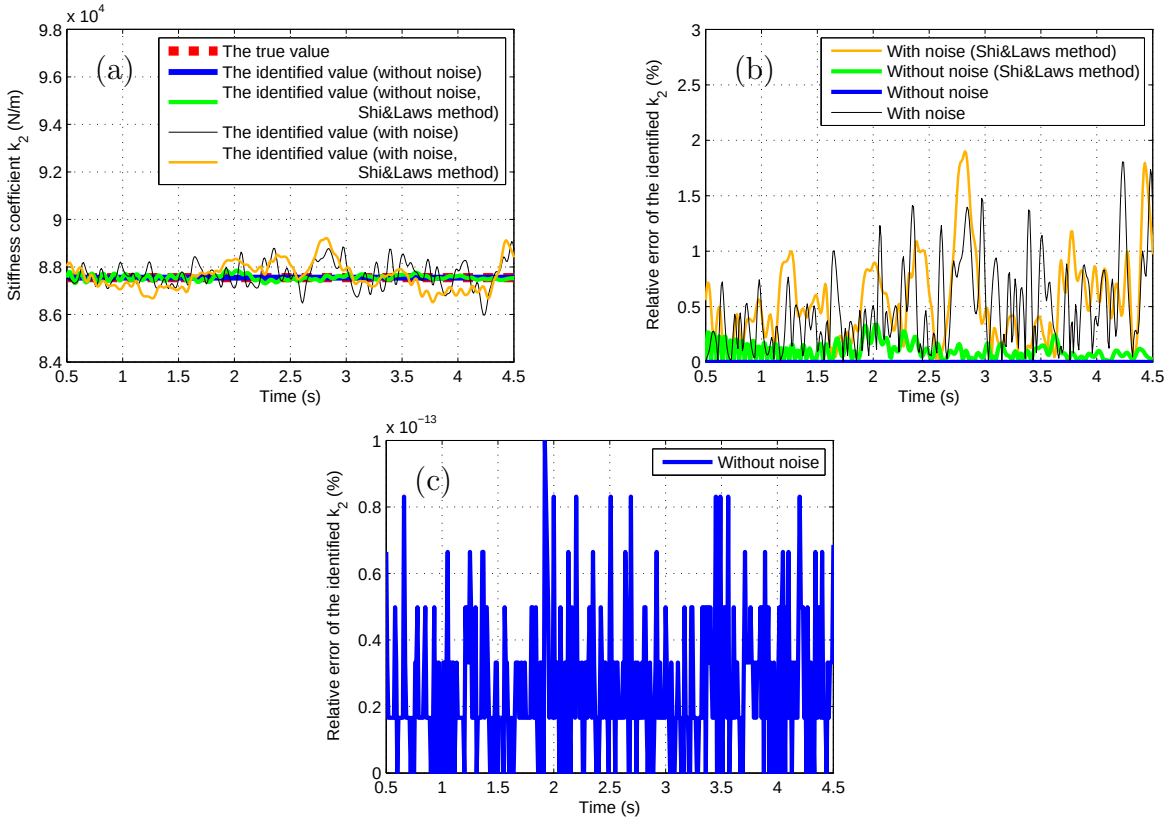

Figure A.17: Stiffness coefficient k_2 of a 2-DOF linear periodically varying chainlike forced vibration system: (a) The true value and the identified values of k_2, (b) Relative errors of the identified values of k_2, (c) Relative error of the identified value of k_2 (without noise in system responses).

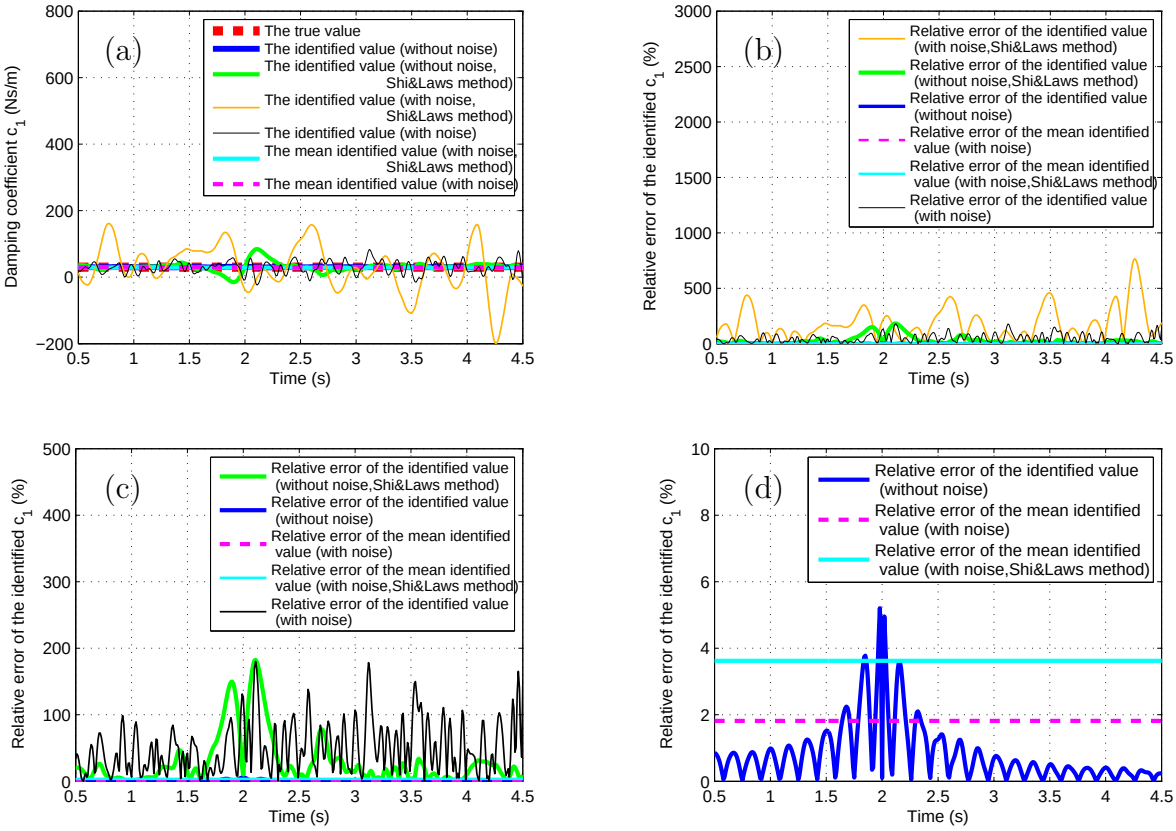

Figure A.18: Damping coefficient c_1 of a 2-DOF linear periodically varying chainlike forced vibration system: (a) The true value and the identified values of c_1, (b) Relative errors of the identified values of c_1, (c) Close-up of (b), (d) Close-up of (c).

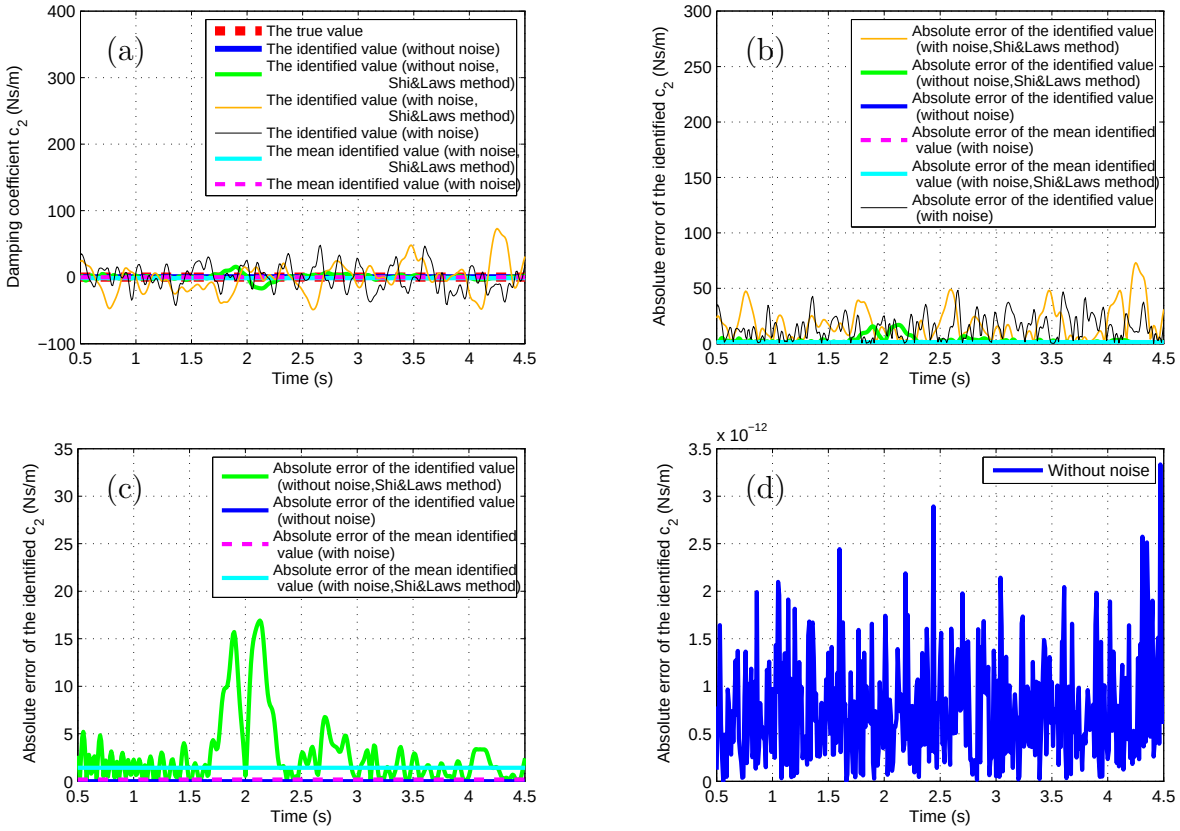

Figure A.19: Damping coefficient c_2 of a 2-DOF linear periodically varying chainlike forced vibration system: (a) The true value and the identified values of c_2, (b) Absolute errors of the identified values of c_2, (c) Close-up of (b), (d) Absolute error of the identified value of c_2 (without noise in system responses).

A.1.5 Parameter study on the forced vibration simulation of a 2-DOF linear periodically varying non-chainlike system

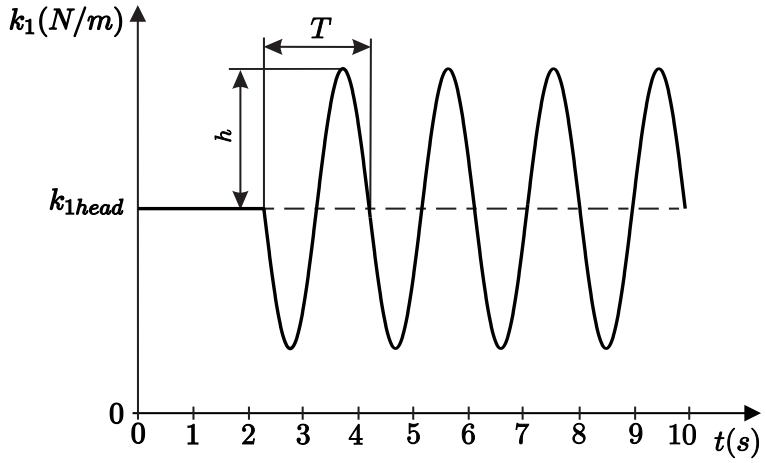

Figure A.20: Stiffness coefficient k_1 of a 2-DOF linear periodically varying non-chainlike system with structural parameters h and T.

The system coefficients, initial conditions as well as the external force are given the same as those of the 2-DOF linear periodically varying non-chainlike forced vibration system in Appendix A.1.4, except that the system stiffness k_1 adopts the model shown in Figure A.20:
$k_1 = k_{head}$ when $t < 2$s,
$k_1 = k_{head} - h\sin((2\pi/T)(t-2))$ when $t \geq 2$s,
$k_{head} = 10000$N/m for any t,
where amplitude h and period T are variable structural parameters. Two cases are considered here: Case1: Let $T = 2$s, $h = 0 \sim 5000$ N/m (the interval between two adjacent h values is 5N/m); Case2: Let $h = 100$N/m, $T = 0.01 \sim 10$s (the interval between two adjacent T values is 0.01s).
The mean relative errors of the identified stiffness coefficients k_1 and k_2,as well as the mean absolute errors of the identified damping coefficients c_1 and c_2 are presented in Figures A.21 - A.28.
Figures A.21 - A.24 show the identified results of Case1. It is noted that, when noiseless system responses are used as input of the HHT-based identification method, the mean relative errors of identified k_1 and k_2 as well as the mean absolute errors of identified c_1 and c_2 increase proportionally with h, and good identified results of these system parameters with small mean relative errors or mean absolute errors are obtained when the structural parameter h takes small values in the interval $[0, 5000]$N/m (the special case $h = 0$N/m represents that the system stiffness keeps constant); whereas when noise-added system responses are used as input of the HHT-based identification method, the mean relative error of identified k_1 as well as the mean absolute error of identified c_1 increase proportionally with h, and the mean relative error of identified k_2 as well as the mean absolute error of identified c_2 have slightly increasing trend as h increases. Although the identified results

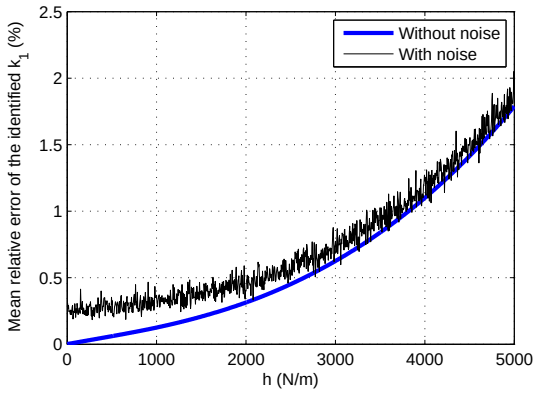

Figure A.21: Mean relative error of the identified values of stiffness coefficient k_1 of a 2-DOF linear periodically varying non-chainlike system with respect to h.

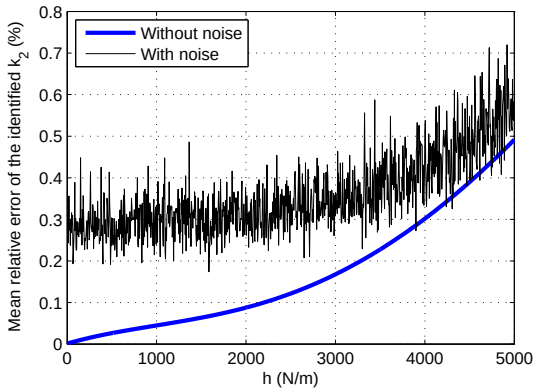

Figure A.22: Mean relative error of the identified values of stiffness coefficient k_2 of a 2-DOF linear periodically varying non-chainlike system with respect to h.

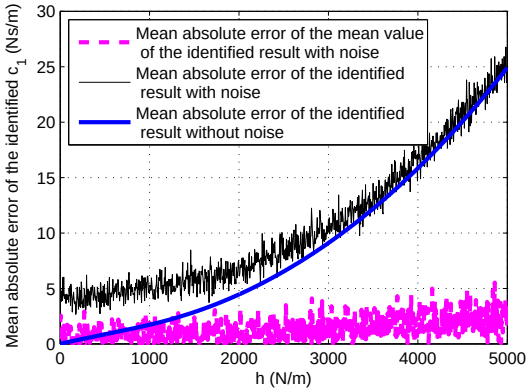

Figure A.23: Mean absolute error of the identified values of damping coefficient c_1 of a 2-DOF linear periodically varying non-chainlike system with respect to h.

are contaminated by noise, we can still obtain good identified results of stiffness coeffi-

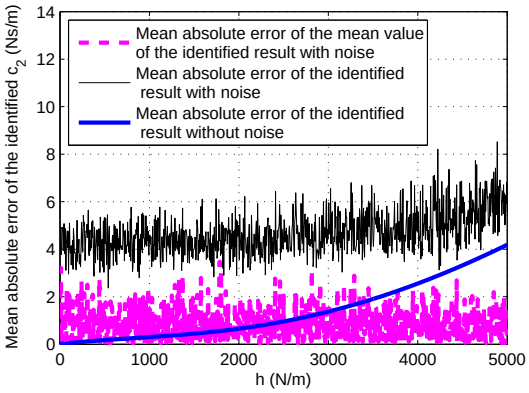

Figure A.24: Mean absolute error of the identified values of damping coefficient c_2 of a 2-DOF linear periodically varying non-chainlike system with respect to h.

cients k_1 and k_2 with small mean relative errors (whose maxima are less than 2.1% and equal to 0.72% respectively) at different h. The identified results of damping coefficients c_1 and c_2 obtained by using noise-added system responses have large mean absolute errors denoted with black lines, but their mean absolute errors denoted with pink dashed lines (whose maxima are less than 5.6Ns/m and 3.5Ns/m respectively) are relatively smaller than those denoted with black lines (The procedures to calculate the mean absolute errors denoted with black lines and those denoted with pink dashed lines can refer to the similar calculation procedures in Section 3.3.1). At $h = 100$N/m (case of the 2-DOF linear periodically varying non-chainlike forced vibration system in Appendix A.1.4), the mean absolute errors of identified c_1 and c_2 denoted with pink dashed lines are sufficiently small (less than 1.4Ns/m and 0.88Ns/m respectively).
In conclusion, no matter using noiseless or noise-added system responses as input of the proposed HHT-based identification method, good identified results of the system parameters with small mean relative errors or mean absolute errors are obtained when the structural parameter h takes small values in the interval $[0, 5000]$N/m (which represents that the system stiffness varies slowly). As a result, it is proper to choose small values in the interval $[0, 5000]$N/m for h.

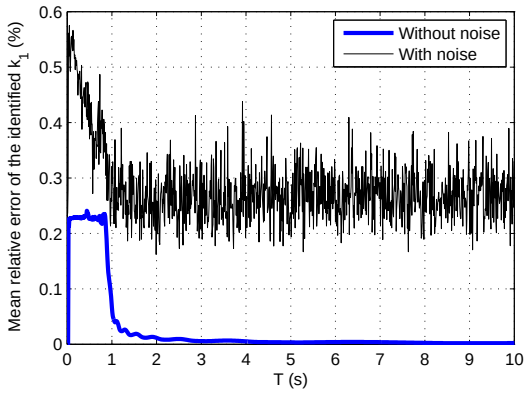

Figure A.25: Mean relative error of stiffness coefficient k_1 of a 2-DOF linear periodically varying non-chainlike system with respect to T.

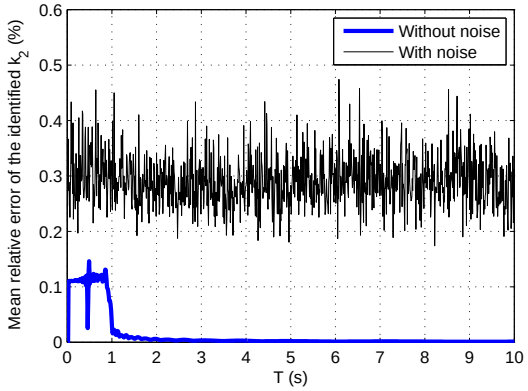

Figure A.26: Mean relative error of stiffness coefficient k_2 of a 2-DOF linear periodically varying non-chainlike system with respect to T.

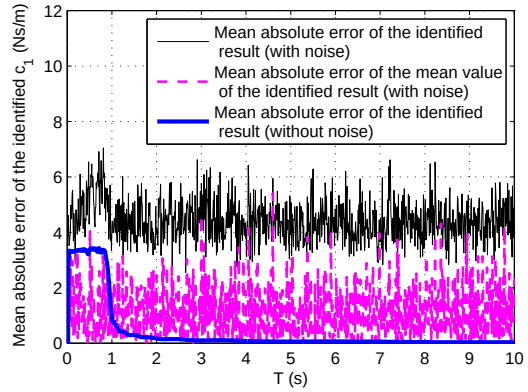

Figure A.27: Mean absolute error of damping coefficient c_1 of a 2-DOF linear periodically varying non-chainlike system with respect to T.

Figures A.25 - A.28 present the identified results of Case2. When using noiseless system responses as input of the HHT-based identification method, the resulting mean relative

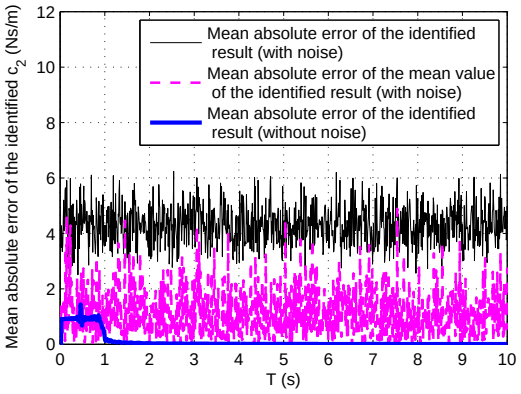

Figure A.28: Mean absolute error of damping coefficient c_2 of a 2-DOF linear periodically varying non-chainlike system with respect to T.

errors of the identified stiffness coefficients k_1 and k_2 as well as as the mean absolute errors of identified damping coefficients c_1 and c_2 have relatively large increase and decrease during $T = 0.01 \sim 1$s, then they have slightly decreasing trend as T increases in the interval $[1, 10]$s. And good identified results of the system parameters with small mean relative errors or mean absolute errors can be always obtained when T takes values in the interval $[1, 10]$s. When using noise-added system responses as input, the resulting mean relative error of k_1 has decreasing trend as T increases in the interval $[0.01, 1]$s, then it keeps fluctuating around some constant value as T increases; whereas the resulting mean relative error of k_2 as well as the mean absolute errors of c_1 and c_2 keep fluctuating around some constant values as T increases in the interval $[0.01, 10]$s. Although the identified results are contaminated by noise, good identified results of the stiffness coefficients with small mean relative errors (whose maximum is less than 0.47%) are obtained when T takes any value in the interval $[1, 10]$s. As damping coefficients are sensitive to noise, the mean absolute errors of the identified results of damping coefficients denoted with black lines are much larger than their counterparts denoted with blue lines which are obtained by using noiseless system responses as input, but their counterparts denoted with pink dashed lines (whose maximum is equal to 5.4Ns/m) are relatively smaller (The procedures to calculate the mean absolute errors denoted with black lines and those denoted with pink dashed lines can refer to the similar calculation procedures in Section 3.3.1). At $T = 2$s (case of the 2-DOF linear periodically varying non-chainlike forced vibration system in Appendix A.1.4), the mean absolute errors of identified c_1 and c_2 denoted with pink dashed lines are sufficiently small (less than 2.5Ns/m and 0.0066Ns/m respectively).
In conclusion, by using noiseless system responses as input of the proposed HHT-based identification method, good identified results of system parameters with small mean relative errors or mean absolute errors are obtained when T takes large values in the interval $[1, 10]$s (which means the system stiffness coefficient varies slowly); whereas by using noise-added system responses as input, the variation of T has almost no influence on the identified results of the system coefficients when T takes any value in the interval $[1, 10]$s, yet good identified results of the stiffness coefficients are still obtained. As a result, it is proper to choose large values in the interval $[1, 10]$s for T.

A.2 Some of the HHT-based identification results of weakly nonlinear time-varying systems

A.2.1 HHT-based identification results of the damping coefficients of 1-DOF weakly nonlinear smoothly and abruptly varying Duffing oscillators

For the 1-DOF weakly nonlinear smoothly and abruptly varying hard spring Duffing oscillators proposed in Section 4.1.1, the identified results of the system damping coefficients and their relative errors are shown in Figures A.29 - A.30.

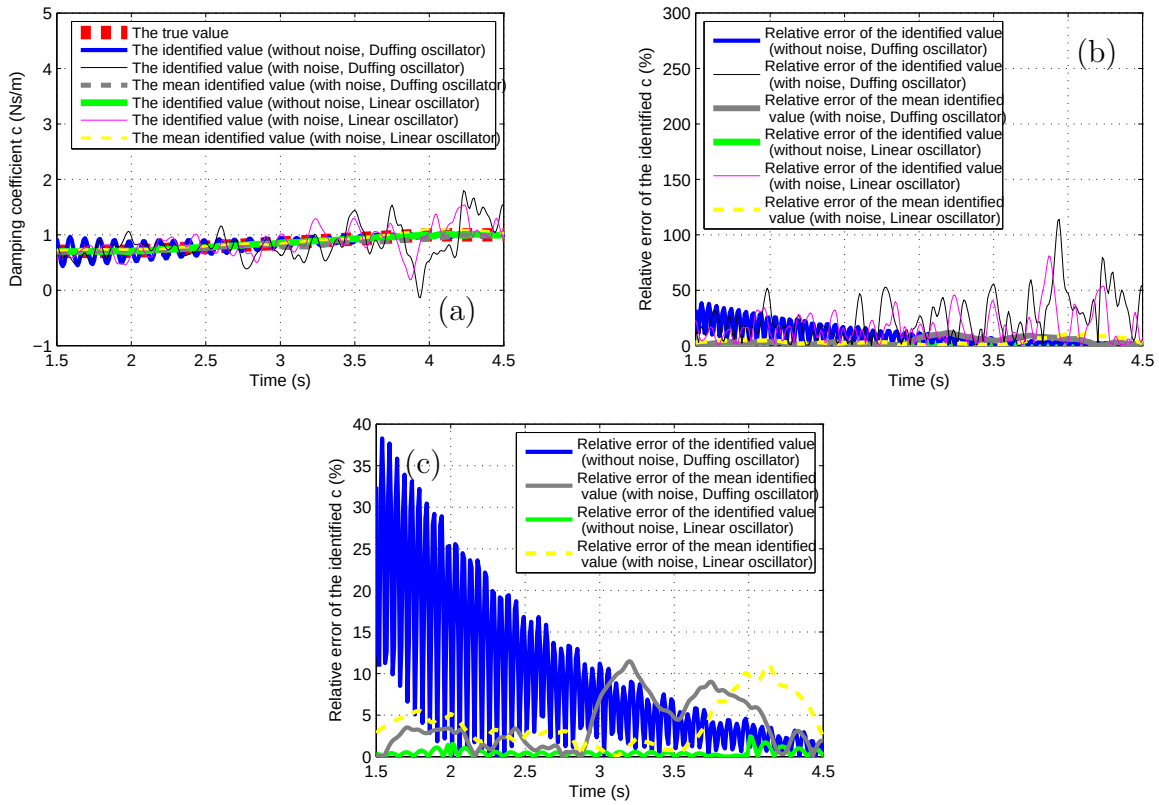

Figure A.29: Damping coefficient c of a 1-DOF weakly nonlinear smoothly varying hard spring Duffing oscillator: (a) The true value and the identified values of c, (b) Relative errors of the identified values of c, (c) Close-up of (b).

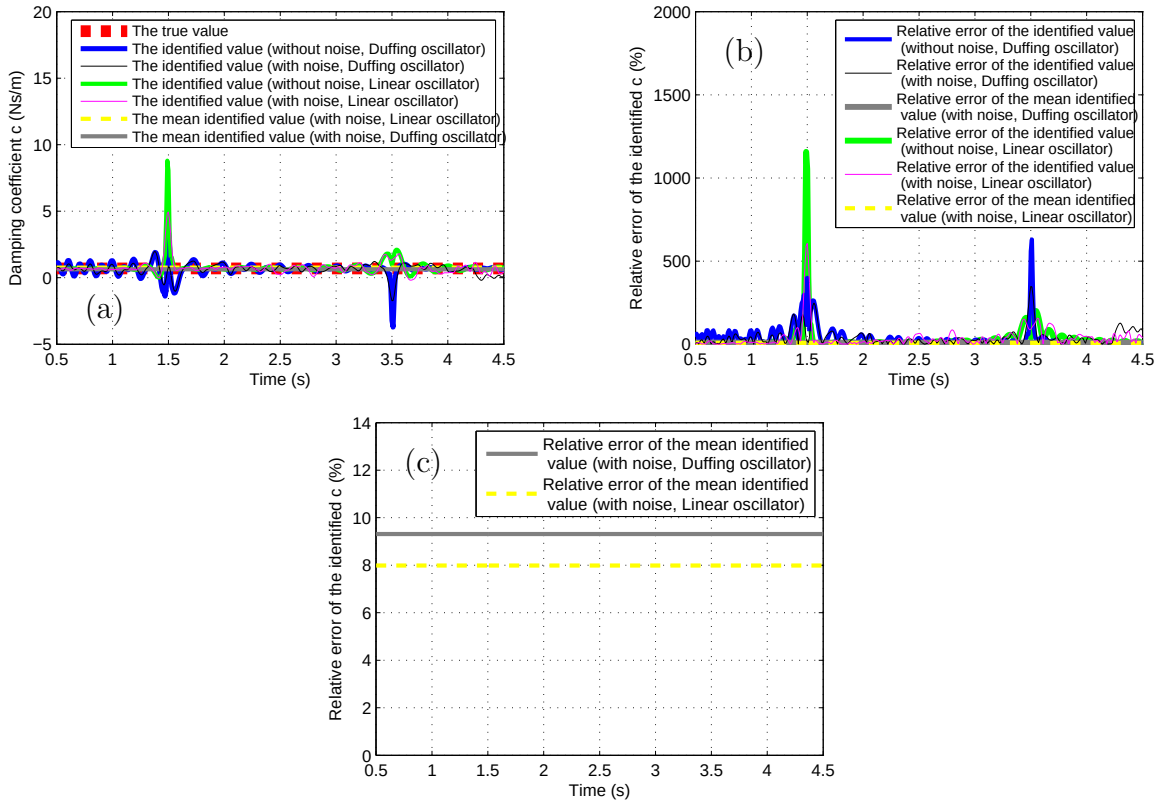

Figure A.30: Damping coefficient c of a 1-DOF weakly nonlinear abruptly varying hard spring Duffing oscillator: (a) The true value and the identified values of c, (b) Relative errors of the identified values of c, (c) Close-up of (b), (d) Relative errors of the mean identified values of c.

It can be seen from the figures that: For the 1-DOF weakly nonlinear smoothly varying hard spring Duffing oscillator, the identified result of the damping coefficient c is bad (with maximal relative error less than $1.2 \times 10^2\%$) since the sensitivity of the damping coefficient to noise and the application of Equation (4.4). However, the mean value (denoted with a gray line) of the identified result over the required time history matches its true value well and has sufficiently small relative error (less than 12%); For the 1-DOF weakly nonlinear abruptly varying hard spring Duffing oscillator, the identified result of the damping coefficient c has quite large identification errors around time instants $t = 1.5$s and $t = 3.5$s due to the limitations of Equation (2.16). Due to the sensitivity of the damping coefficient to noise and the application of Equation (4.4), large identification errors of c can be also found at other time instants, which makes it difficult to detect the exact time instants of the abrupt stiffness variations of the system from the identified result of c. The mean identified value of c (denoted with a gray line) is found close to its true value with relatively smaller relative error (less than 9.4%).

A.2.2 HHT-based identification results of the damping coefficients of 2-DOF weakly nonlinear smoothly and abruptly varying chainlike Duffing systems

For the 2-DOF weakly nonlinear smoothly and abruptly varying chainlike Duffing systems proposed in Section 4.1.2, the identified results of the system damping coefficients as well as their relative and absolute errors are shown in Figures A.31 - A.34.

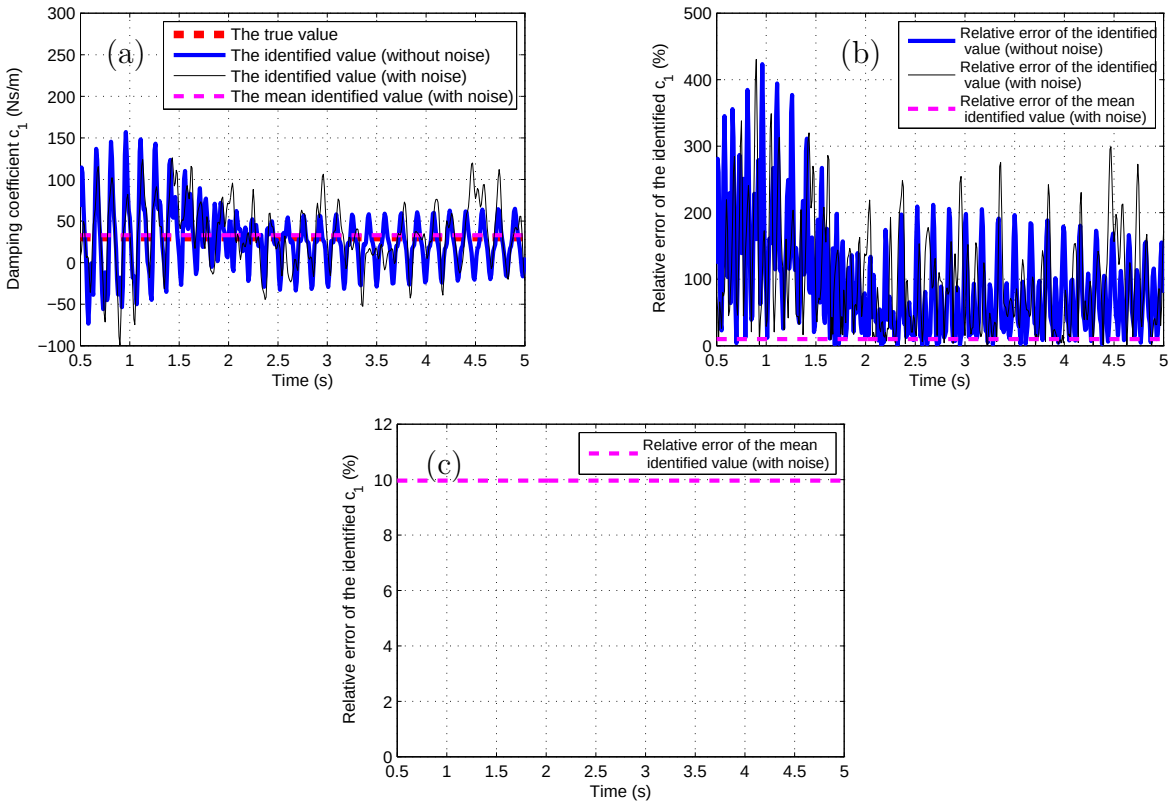

Figure A.31: Damping coefficient c_1 of a 2-DOF weakly nonlinear chainlike system with a weakly nonlinear smoothly varying hard spring Duffing oscillator: (a) The true value and the identified values of c_1, (b) Relative errors of the identified values of c_1, (c) Relative error of the mean identified value of c_1.

From these figures, it is noted that: For both the 2-DOF weakly nonlinear smoothly and abruptly varying chainlike Duffing systems, due to the sensitivity of the damping coefficients to noise and the application of Equation (4.4), the accuracies of the identified damping coefficients are quite low (with maximal relative error of c_1 equal to $4.3 \times 10^2\%$ and maximal absolute error of c_2 less than 66Ns/m for the smoothly varying system, their counterparts for the abruptly varying system are less than $7.1 \times 10^2\%$ and 74Ns/m respectively). However, the mean values (denoted with pink dashed lines) of the identified damping coefficients over the required time history are close to their respective true values (with maximal relative error of the mean value of identified c_1 less than 10% and maximal

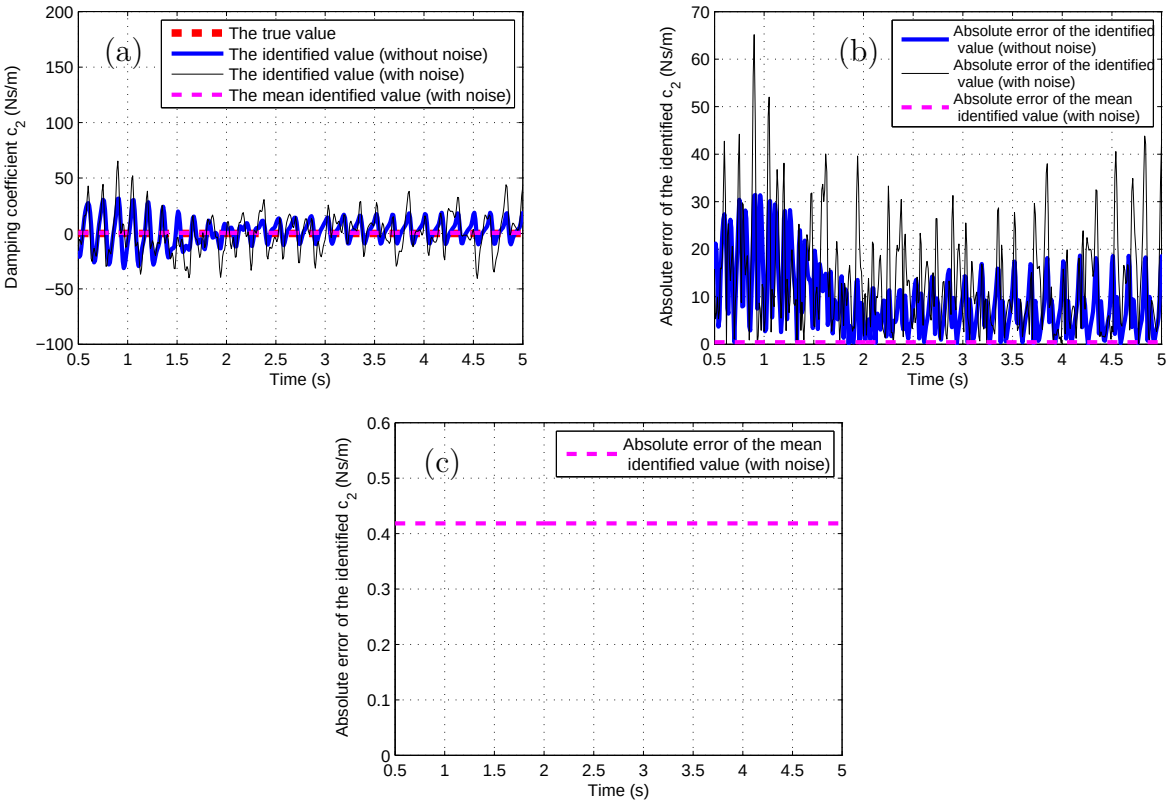

Figure A.32: Damping coefficient c_2 of a 2-DOF weakly nonlinear chainlike system with a weakly nonlinear smoothly varying hard spring Duffing oscillator: (a) The true value and the identified values of c_2, (b) Absolute errors of the identified values of c_2, (c) Absolute error of the mean identified value of c_2.

absolute error of the mean value of identified c_2 less than 0.42Ns/m for the smoothly varying system, their counterparts for the abruptly varying system are less than 1.6% and 0.037Ns/m respectively). For the 2-DOF weakly nonlinear abruptly varying chainlike Duffing system, it is difficult to find the exact time instant of the abrupt stiffness variation of the system from the identified results of damping coefficients due to the existence of large identification errors.

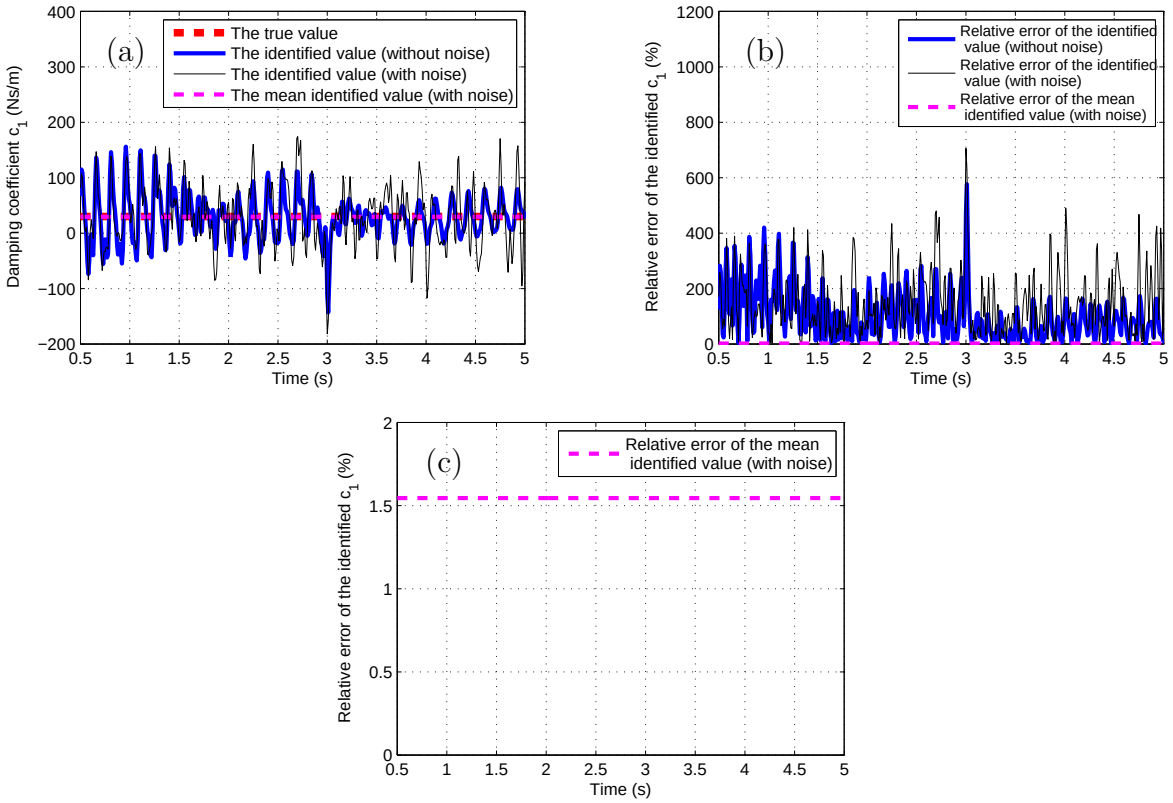

Figure A.33: Damping coefficient c_1 of a 2-DOF weakly nonlinear chainlike system with a weakly nonlinear abruptly varying hard spring Duffing oscillator: (a) The true value and the identified values of c_1, (b) Relative errors of the identified values of c_1, (c) Relative error of the mean identified value of c_1.

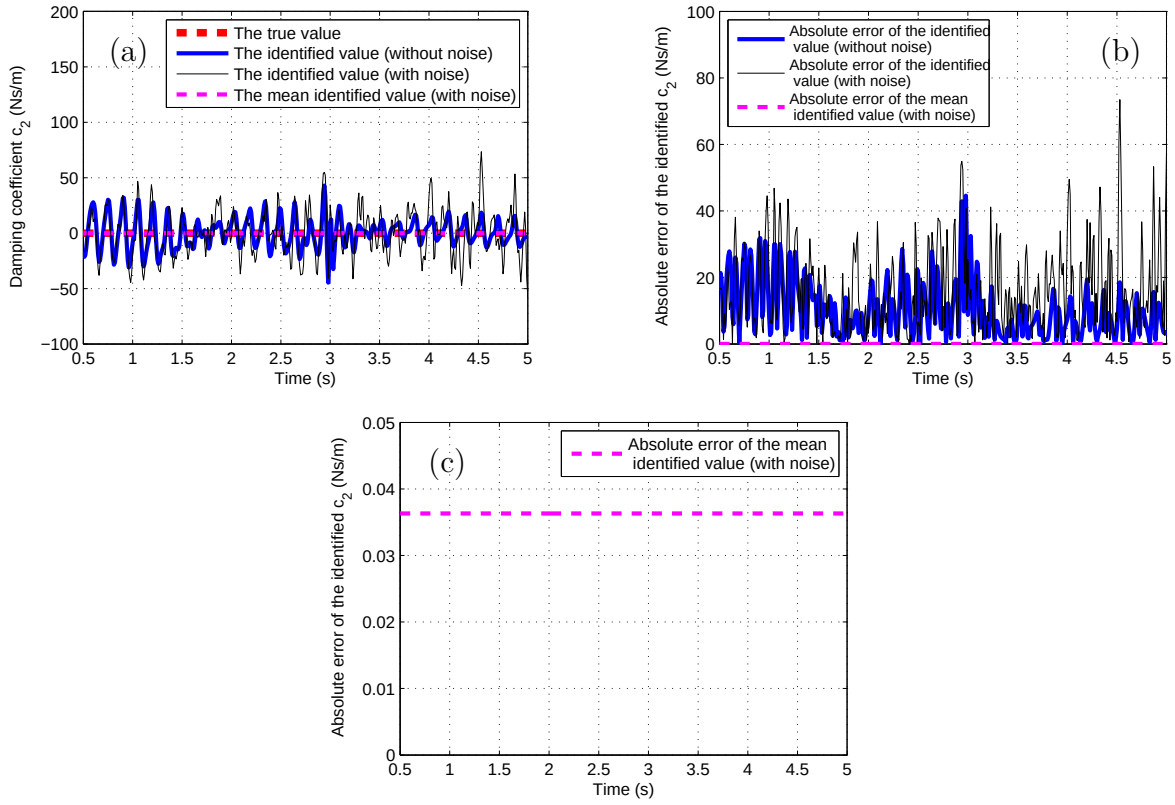

Figure A.34: Damping coefficient c_2 of a 2-DOF weakly nonlinear chainlike system with a weakly nonlinear abruptly varying hard spring Duffing oscillator: (a) The true value and the identified values of c_2, (b) Absolute errors of the identified values of c_2, (c) Absolute error of the mean identified value of c_2.

A.2.3 HHT-based identification results of weakly nonlinear periodically varying Duffing systems

(1) 1-DOF system

For the 1-DOF weakly nonlinear periodically varying hard spring Duffing oscillator proposed in Section 4.1.1, the identified results of linear stiffness coefficient k_{linear}, cubic stiffness factor δ and damping coefficient c of the oscillator as well as their relative errors are shown in Figure A.35.

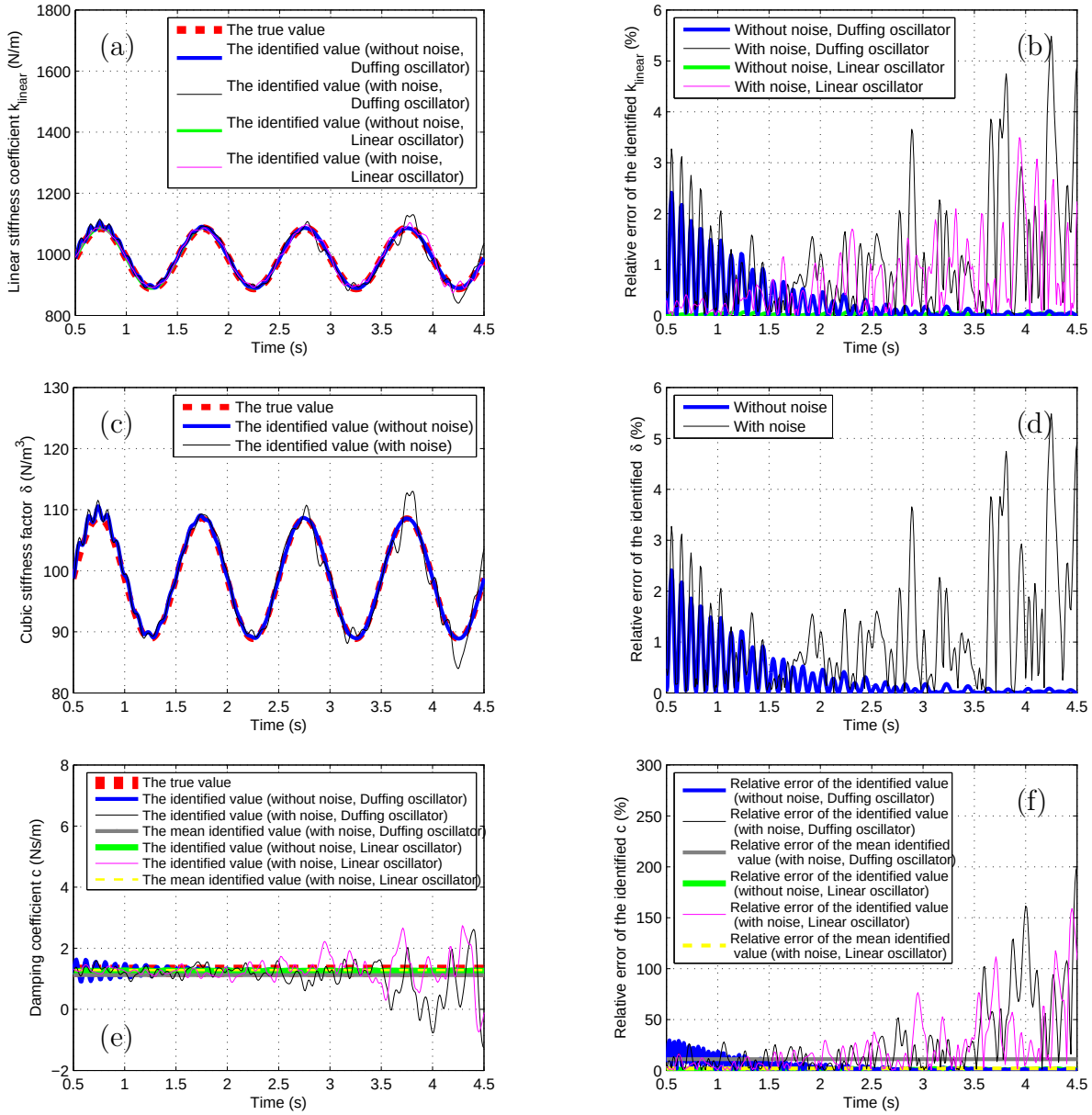

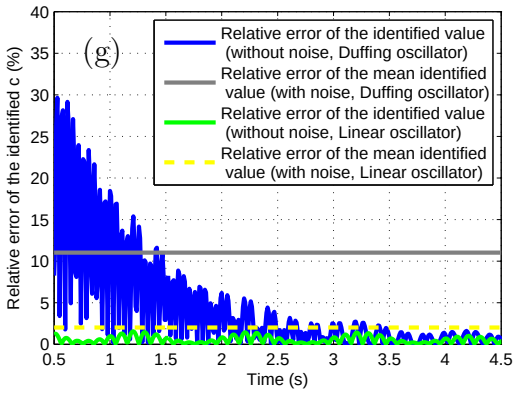

Figure A.35: System coefficients of a 1-DOF weakly nonlinear periodically varying hard spring Duffing system: (a) The true value and the identified values of linear stiffness coefficient k_{linear}, (b) Relative errors of the identified values of k_{linear}, (c) The true value and the identified values of cubic stiffness factor δ, (d) Relative errors of the identified values of δ, (e) The true value and the identified values of damping coefficient c, (f) Relative errors of the identified values of c, (g) Close-up of (f).

Like in the cases of weakly nonlinear smoothly and abruptly varying Duffing oscillators, due to the application of Equation (4.4), the obtained identified results of the weakly nonlinear periodically varying Duffing oscillator ($\delta = 0.1 * k_{linear}\,\mathrm{N/m^3}$) are also worse than those of the linear periodically varying oscillator ($\delta = 0\,\mathrm{N/m^3}$) which has the same linear system coefficients, initial conditions and excitation signal as the weakly nonlinear periodically varying Duffing oscillator, no matter using noiseless or noise-added system responses as input of the modified HHT-based identification method. When using noise-added system responses as input, good identified results of linear stiffness coefficient k_{linear} and cubic stiffness factor δ (with maximal relative errors less than 5.5%) are always obtained. The identified results of damping coefficient c (with maximal relative error equal to $2.0 \times 10^2\%$) are much worse than those of k_{linear} and δ, but its mean value (denoted with a gray line) over the required time history matches its true value well and has sufficiently small relative error (equal to 11%).

(2) 2-DOF system
For the 2-DOF weakly nonlinear periodically varying chainlike Duffing system proposed in Section 4.1.2, the identified results of the system stiffness and damping coefficients as well as their relative and absolute errors are presented in Figures A.36 - A.39.

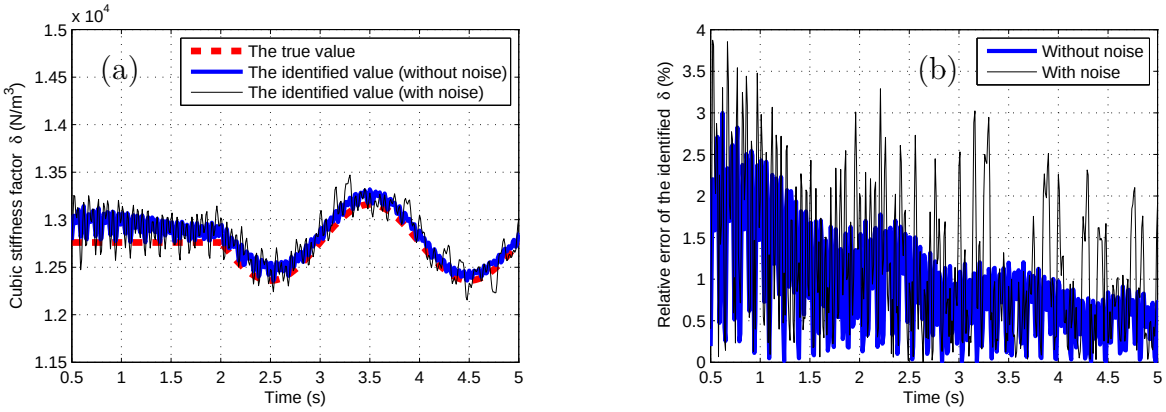

Figure A.36: Cubic stiffness factor δ of a 2-DOF weakly nonlinear chainlike system with a weakly nonlinear periodically varying hard spring Duffing oscillator: (a) The true value and the identified values of δ, (b) Relative errors of the identified values of δ.

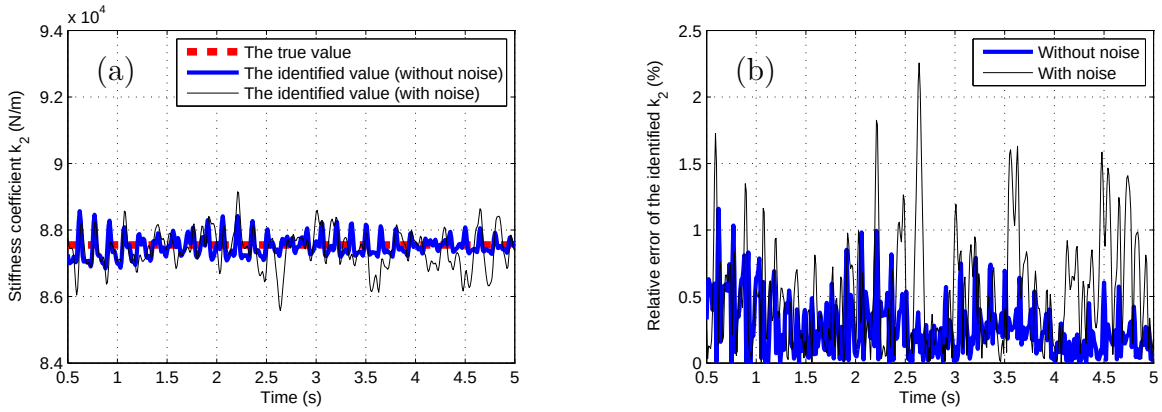

Figure A.37: Stiffness coefficient k_2 of a 2-DOF weakly nonlinear chainlike system with a weakly nonlinear periodically varying hard spring Duffing oscillator: (a) The true value and the identified values of k_2, (b) Relative errors of the identified values of k_2.

It is noted that no matter using noiseless or noise-added system responses as input of the modified HHT-based identification method, the obtained identified results of stiffness coefficients always match their corresponding true values well (with maximal relative error of δ less than 3.9% and that of k_2 less than 2.3%), whereas the accuracies of the identified results of damping coefficients are always low, especially when using noise-added system responses as input of the modified HHT-based identification method (the maximal relative error of c_1 is less than 4.8×10^2% and the maximal absolute error of c_2 is less than 67Ns/m). The mean values (denoted with pink dashed lines) of the identified values of damping coefficients are quite close to their respective true values and have sufficiently small errors (the relative error of the mean value of identified c_1 is less than 9.3% and the

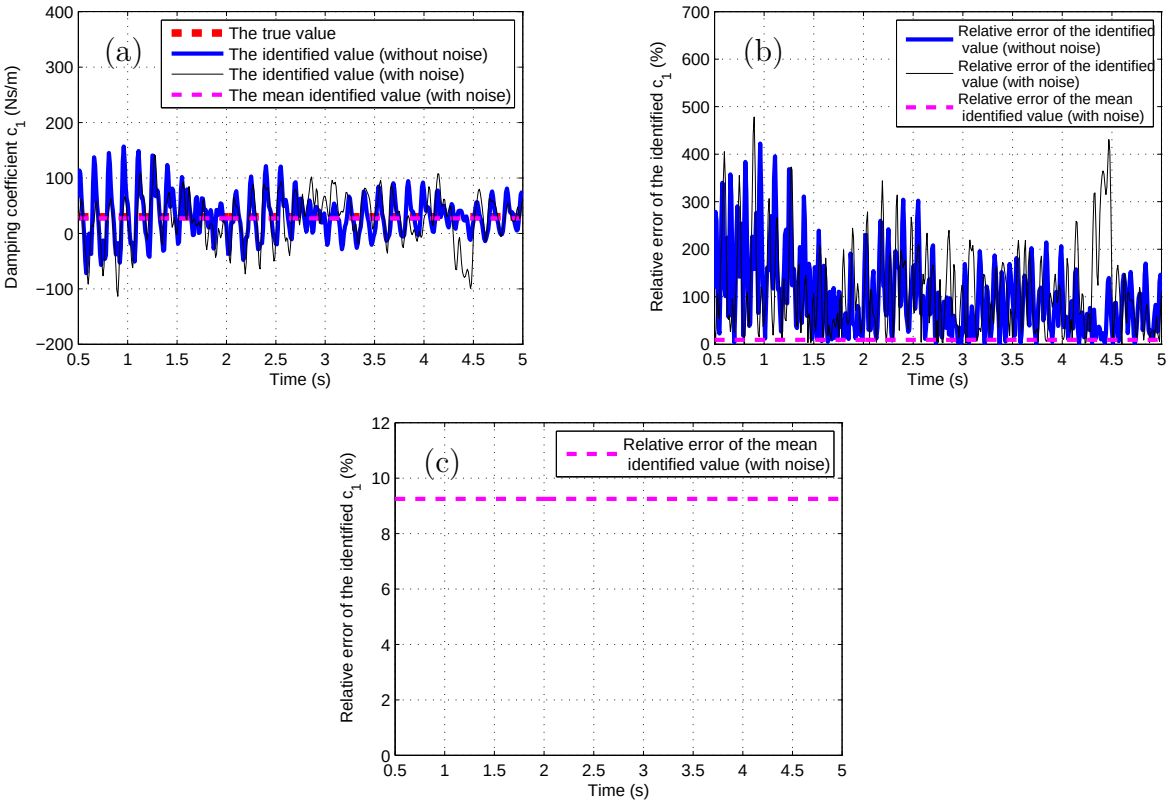

Figure A.38: Damping coefficient c_1 of a 2-DOF weakly nonlinear chainlike system with a weakly nonlinear periodically varying hard spring Duffing oscillator: (a) The true value and the identified values of c_1, (b) Relative errors of the identified values of c_1, (c) Relative error of the mean identified value of c_1.

absolute error of the mean value of identified c_2 is less than 2.0Ns/m).

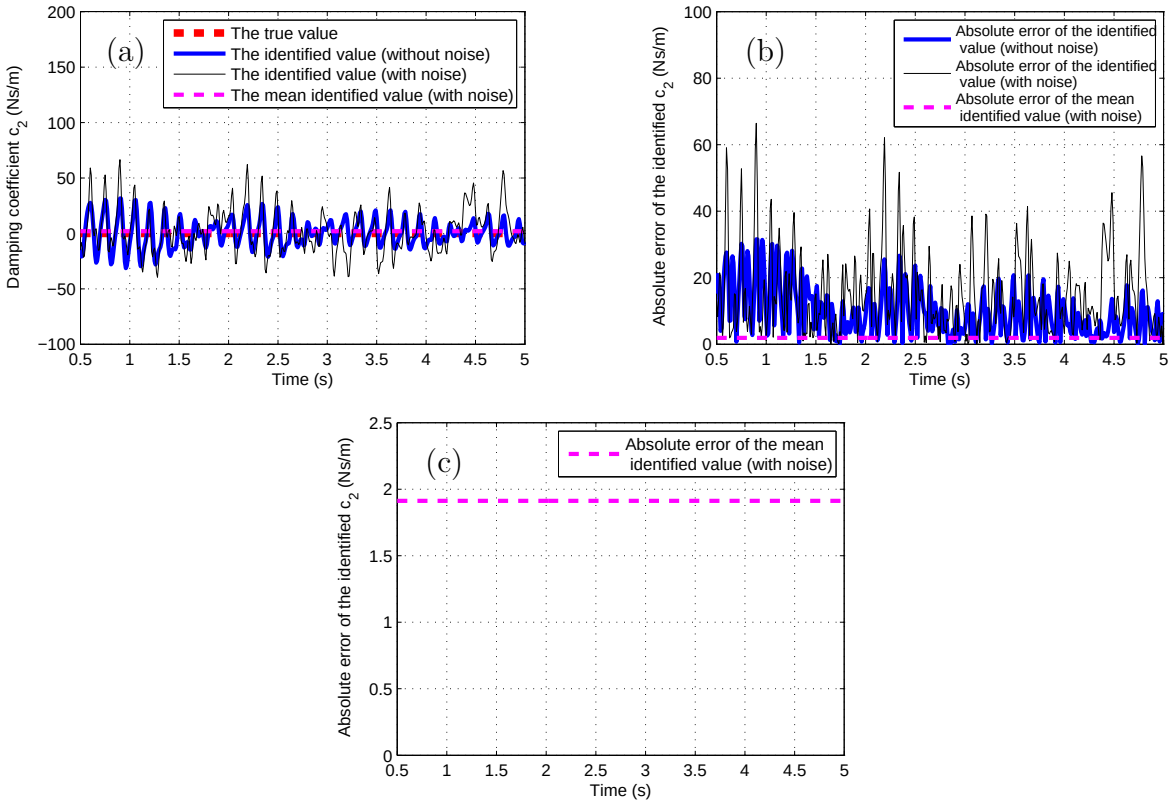

Figure A.39: Damping coefficient c_2 of a 2-DOF weakly nonlinear chainlike system with a weakly nonlinear periodically varying hard spring Duffing oscillator: (a) The true value and the identified values of c_2, (b) Absolute errors of the identified values of c_2, (c) Absolute error of the mean identified value of c_2.

A.2.4 HHT-based identification results of the damping coefficients of 1-DOF weakly nonlinear smoothly and abruptly varying Van der Pol systems

For the 1-DOF weakly nonlinear smoothly and abruptly varying Van der Pol oscillators proposed in Section 4.2.1, the identified result of the system damping coefficients and their relative error are shown in Figures A.40 - A.41.

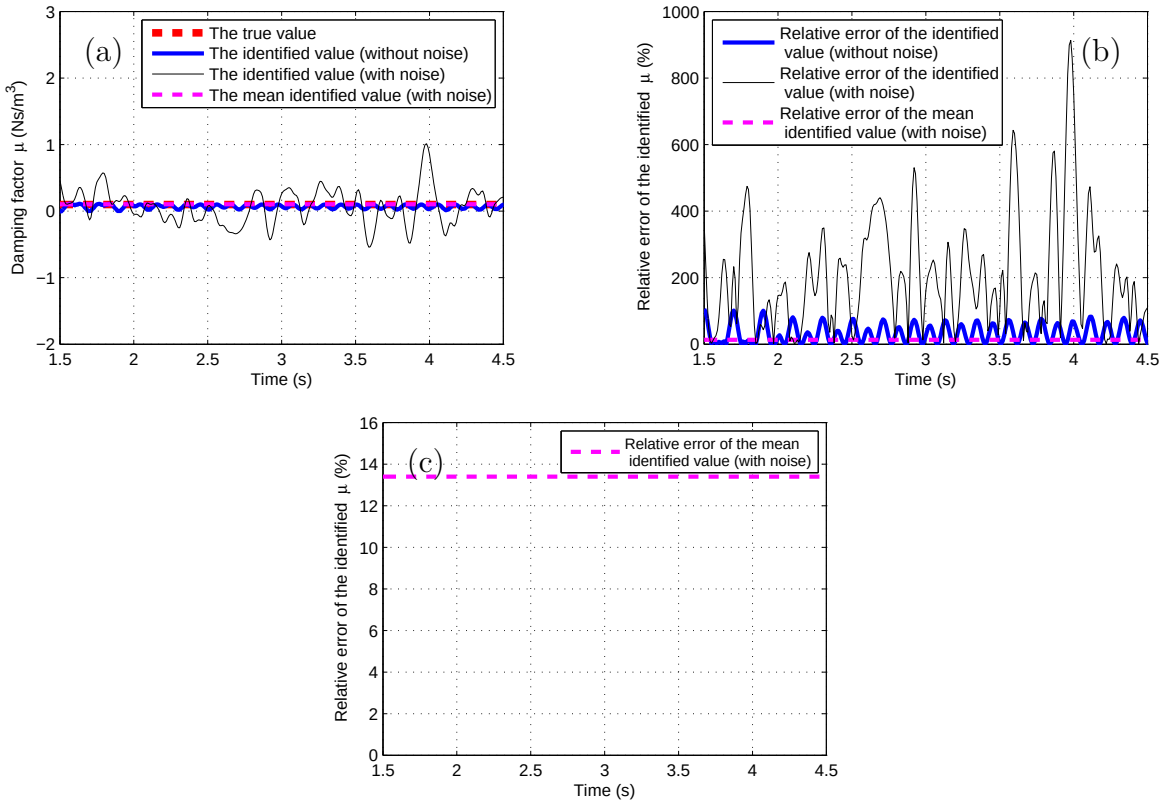

Figure A.40: Damping factor μ of a 1-DOF weakly nonlinear smoothly varying Van der Pol oscillator: (a) The true value and the identified values of μ, (b) Relative errors of the identified values of μ, (c) Relative error of the mean identified value of μ.

It is noted that: For the 1-DOF weakly nonlinear smoothly varying Van der Pol oscillator, due to the sensitivity of damping factor to noise and the application of Equation (4.8), the accuracy of the identified result of damping factor μ is quite low (with maximal relative error less than $9.2 \times 10^2\%$), but the mean value (denoted with a pink dashed line) of the identified μ over the required time history has relatively smaller relative error (less than 14%); For the 1-DOF weakly nonlinear abruptly varying Van der Pol oscillator, no matter using noiseless or noise-added system responses as input of the modified HHT-based identification method, the identified result of damping factor μ has extremely large identification errors around time instants $t = 1.5$s and $t = 3.5$s. Like those of the identified result of stiffness coefficient k, these large identification errors of μ also imply that the proposed method has bad ability to capture the abrupt change of the system coefficient. Due to the sensitivity of damping factor to noise and the application of Equation (4.8), the identified values of damping factor μ obtained at other time instants are still quite bad (with maximal relative error less than $5.7 \times 10^2\%$). The mean value (denoted with a pink dashed line) of the identified μ over the required time history also has large relative error (less than 27%).

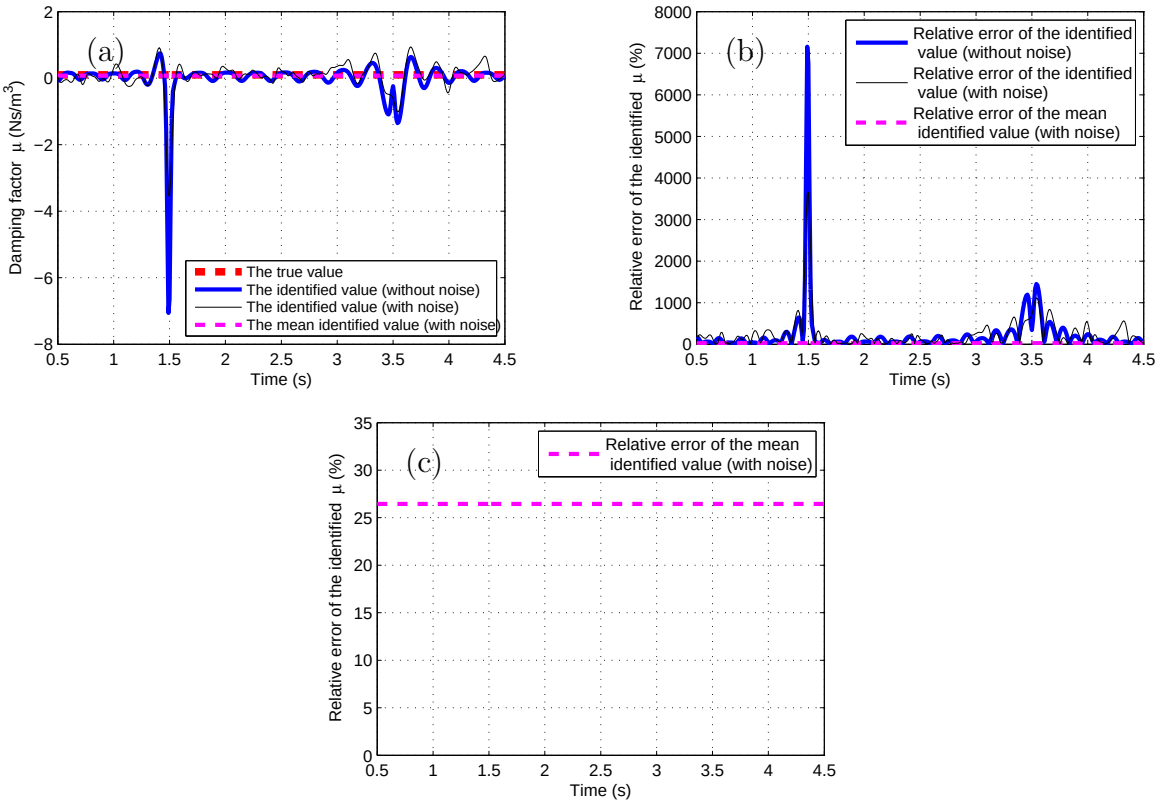

Figure A.41: Damping factor μ of a 1-DOF weakly nonlinear abruptly varying Van der Pol oscillator: (a) The true value and the identified values of μ, (b) Relative errors of the identified values of μ, (c) Relative error of the mean identified value of μ.

A.2.5 HHT-based identification results of the damping coefficients of 2-DOF weakly nonlinear smoothly and abruptly varying chainlike Van der Pol systems

For the 2-DOF weakly nonlinear smoothly and abruptly varying chainlike Van der Pol systems proposed in Section 4.2.2, the identified results of the system damping coefficients as well as their relative and absolute errors are shown in Figures A.42 - A.45.

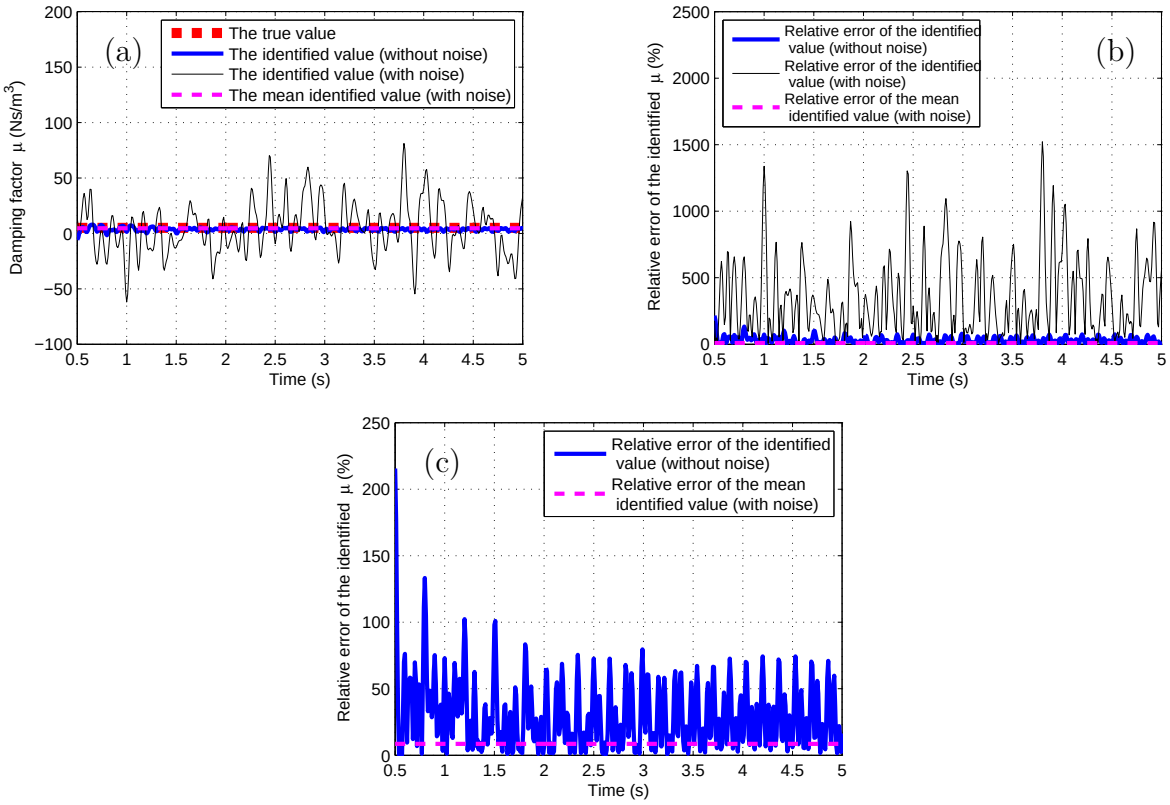

Figure A.42: Damping factor μ of a 2-DOF weakly nonlinear chainlike system with a weakly nonlinear smoothly varying Van der Pol oscillator: (a) The true value and the identified values of μ, (b) Relative errors of the identified values of μ, (c) Close-up of (b).

From the aforementioned figures, it is found out that: For both systems, the identified results of the damping factor μ and damping coefficient c_2 are quite bad, especially when using noise-added system responses as input of the modified HHT-based identification method (with maximal relative error of μ less than $1.6 \times 10^3\%$ and maximal absolute error of c_2 less than 78Ns/m for the smoothly varying system, their counterparts for the abruptly varying system are less than $1.5 \times 10^3\%$ and 1.1×10^2Ns/m respectively). However, the mean values (denoted with pink dashed lines) of the identified results of μ and c_2 of both systems are close to their respective true values (with maximal relative error of the mean identified μ less than 8.6% and maximal absolute error of the mean identified c_2 less than 8.1Ns/m for the smoothly varying system, their counterparts for the abruptly varying system are less than 14% and 5.5Ns/m respectively).

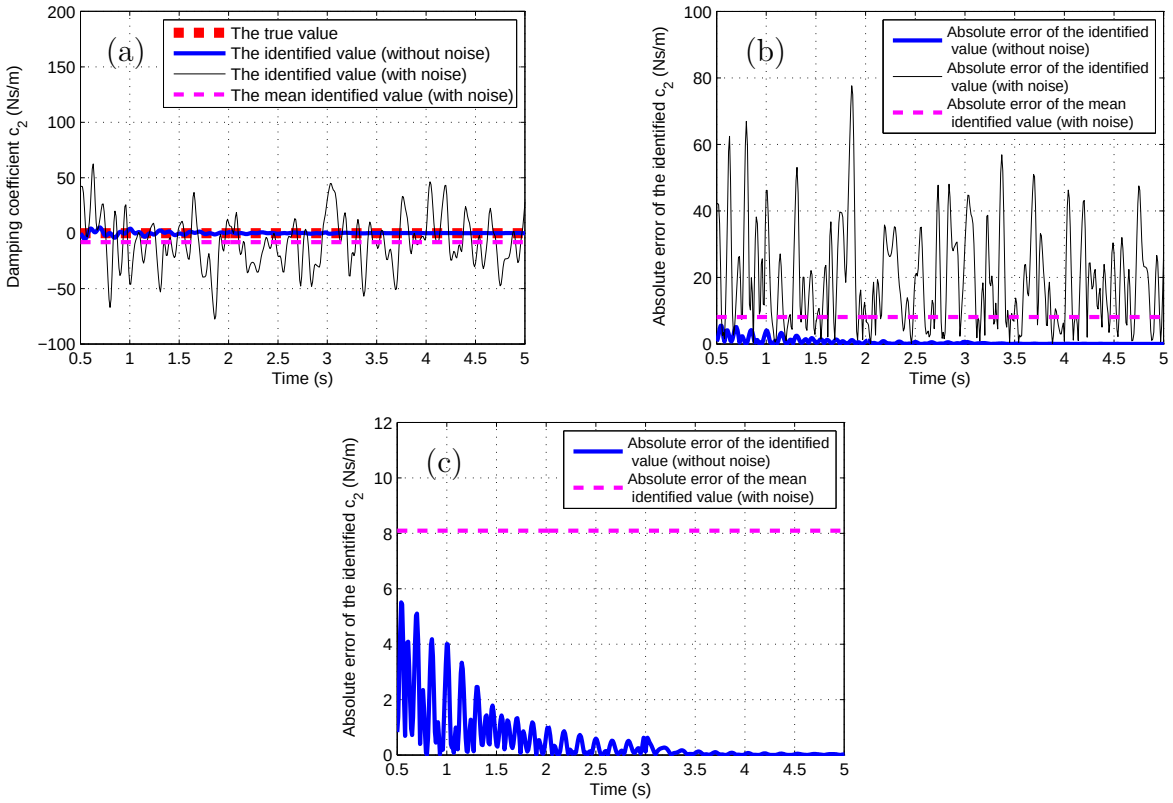

Figure A.43: Damping coefficient c_2 of a 2-DOF weakly nonlinear chainlike system with a weakly nonlinear smoothly varying Van der Pol oscillator: (a) The true value and the identified values of c_2, (b) Absolute errors of the identified values of c_2, (c) Close-up of (b).

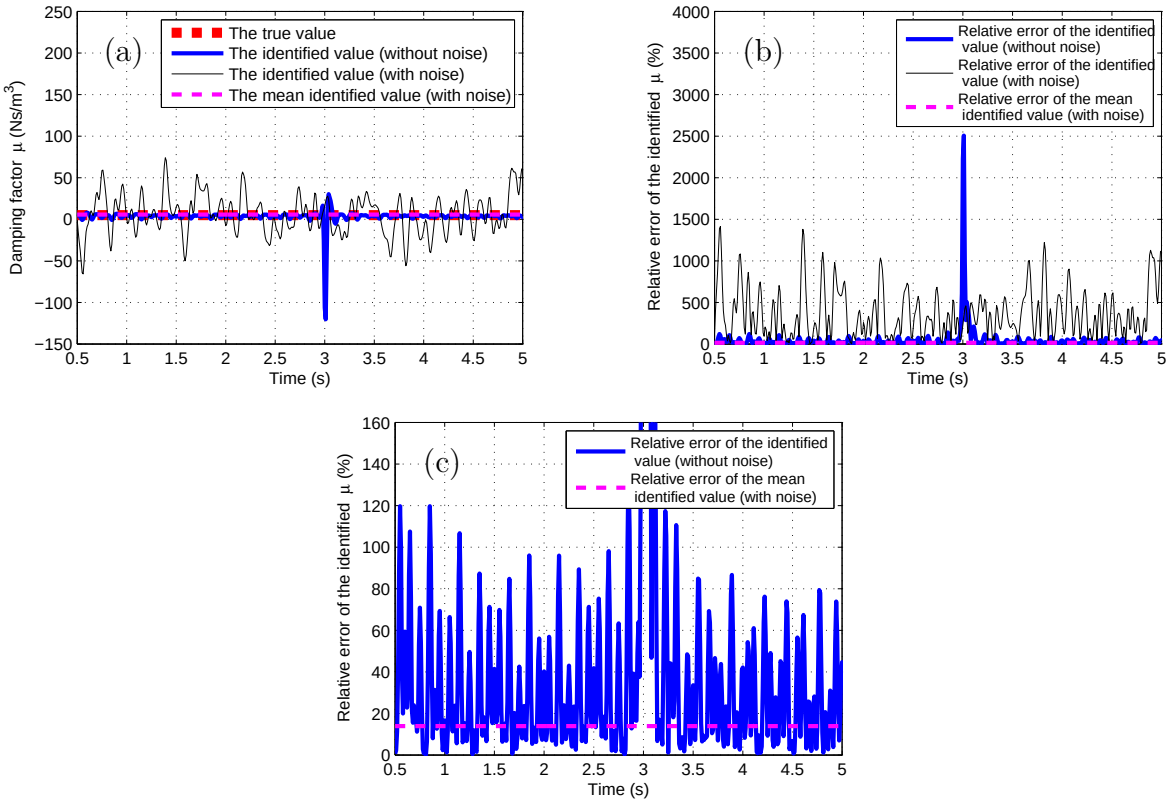

Figure A.44: Damping factor μ of a 2-DOF weakly nonlinear chainlike system with a weakly nonlinear abruptly varying Van der Pol oscillator: (a) The true value and the identified values of μ, (b) Relative errors of the identified values of μ, (c) Close-up of (b).

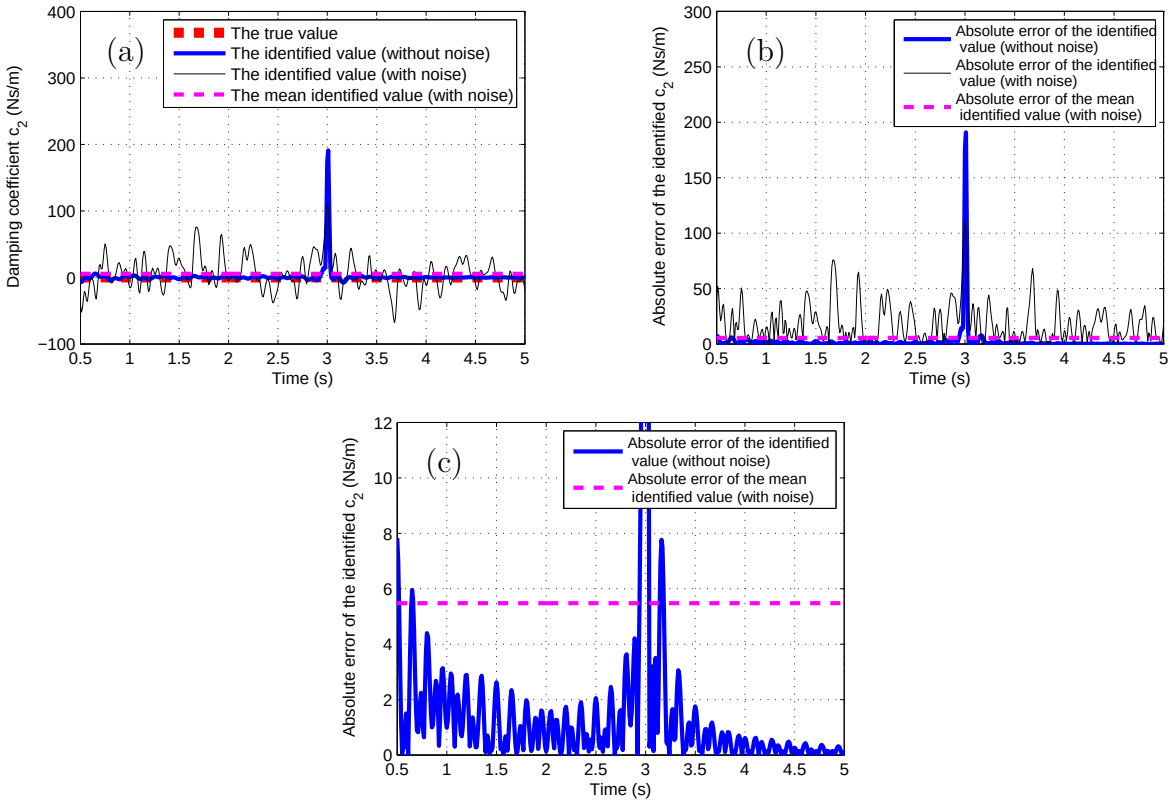

Figure A.45: Damping coefficient c_2 of a 2-DOF weakly nonlinear chainlike system with a weakly nonlinear abruptly varying Van der Pol oscillator: (a) The true value and the identified values of c_2, (b) Absolute errors of the identified values of c_2,(c) Close-up of (b).

A.2.6 HHT-based identification results of weakly nonlinear periodically varying Van der Pol systems

(1) 1-DOF system

For the 1-DOF weakly nonlinear periodically varying Van der Pol oscillator proposed in Section 4.2.1, the identified results of stiffness coefficient k and damping factor μ as well as their relative errors are presented in Figure A.46.

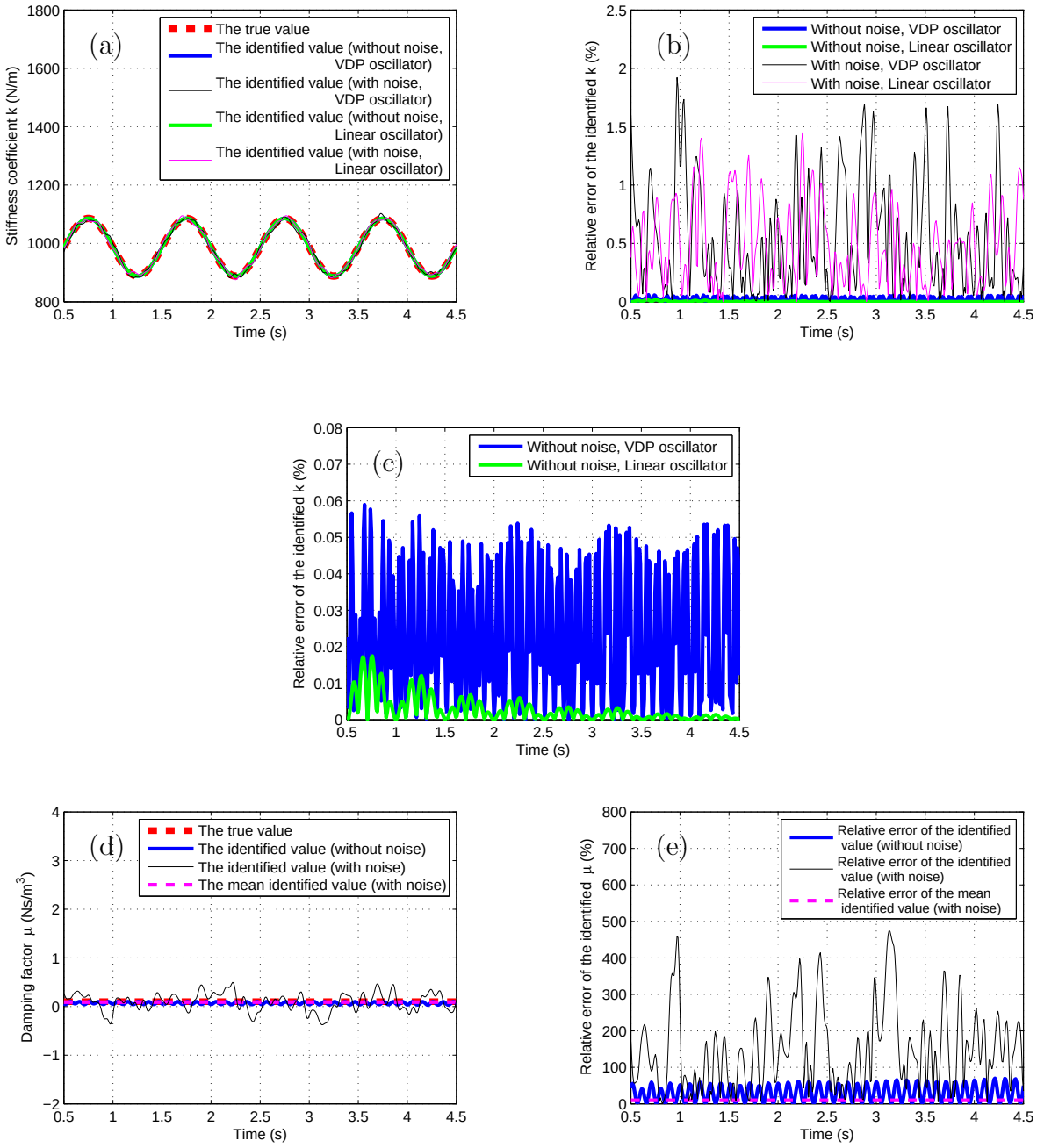

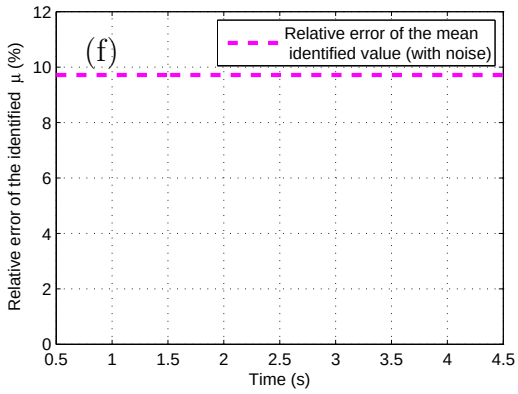

Figure A.46: System coefficients of a weakly nonlinear periodically varying Van der Pol oscillator: (a) The true value and the identified values of stiffness coefficient k, (b) Relative errors of the identified values of k, (c) Relative errors of the identified values of k (without noise in system responses), (d) The true value and the identified values of damping factor μ, (e) Relative errors of the identified values of μ, (f) Relative error of the mean identified value of μ.

We can learn from the figures that: no matter using noiseless or noise-added system responses as input of the modified HHT-based identification method, the accuracies of the obtained identified results of stiffness coefficient k of the weakly nonlinear periodically varying Van der Pol oscillator ($\mu = 0.1\text{Ns/m}^3$) are a little bit worse than those of the linear periodically varying oscillator ($\mu = 0\text{Ns/m}^3$) which has the same linear system coefficients, initial conditions and excitation signal as the weakly nonlinear periodically varying Van der Pol oscillator, due to the application of Equation (4.8). When using noise-added system responses as input, although the identified results are contaminated by noise, we can always obtain good identified result of k (with maximal relative error less than 2.0%). No matter using noiseless or noise-added system responses as input of the modified HHT-based identification method, the identified result of damping factor μ is bad (with maximal relative error less than $4.8 \times 10^2\%$), due to the sensitivity of damping factor to noise and the application of Equation (4.8). However, its mean value (denoted with a pink dashed line) is close to its true value with small relative error (less than 9.8%).

(2) 2-DOF system

For the 2-DOF weakly nonlinear periodically varying chainlike Van der Pol system proposed in Section 4.2.2, the identified results of the system stiffness and damping coefficients as well as their relative and absolute errors are shown in Figures A.47 - A.50.

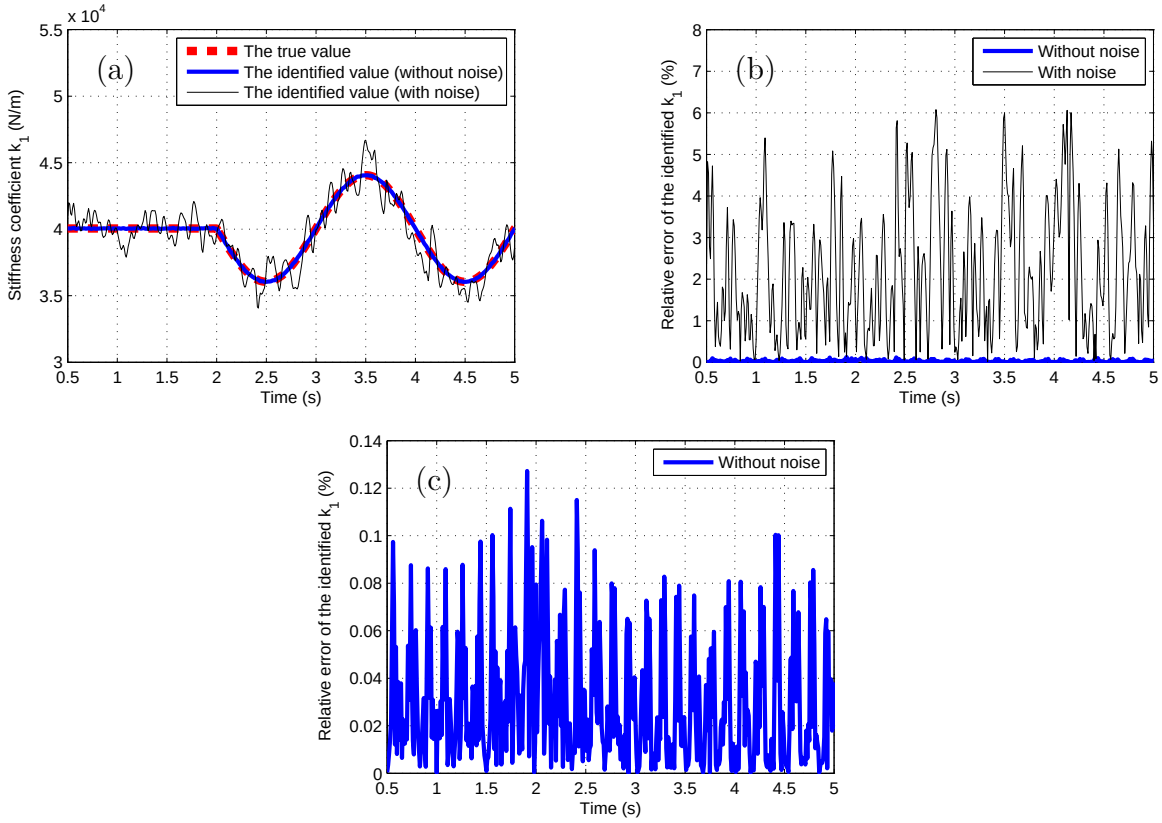

Figure A.47: Stiffness coefficient k_1 of a 2-DOF weakly nonlinear chainlike system with a weakly nonlinear periodically varying Van der Pol oscillator: (a) The true value and the identified values of k_1, (b) Relative errors of the identified values of k_1, (c) Relative error of the identified value of k_1 (without noise in system responses).

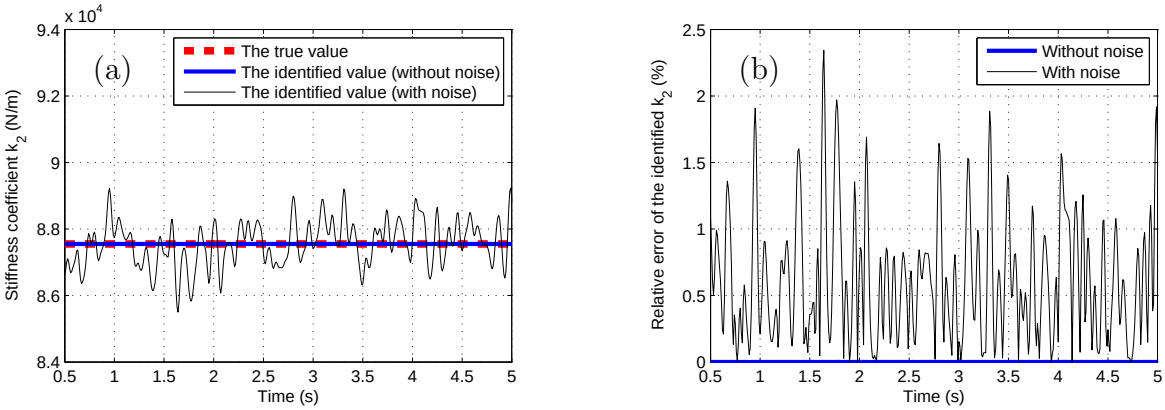

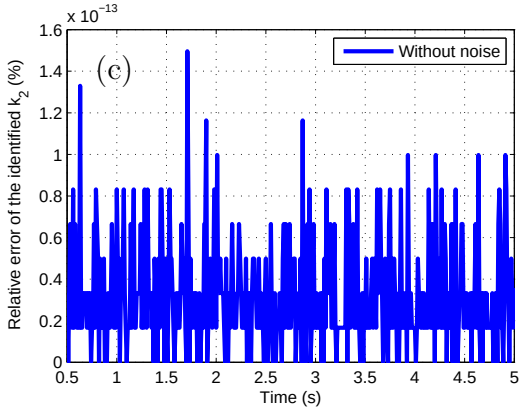

Figure A.48: Stiffness coefficient k_2 of a 2-DOF weakly nonlinear chainlike system with a weakly nonlinear periodically varying Van der Pol oscillator: (a) The true value and the identified values of k_2, (b) Relative errors of the identified values of k_2, (c) Relative error of the identified value of k_2 (without noise in system responses).

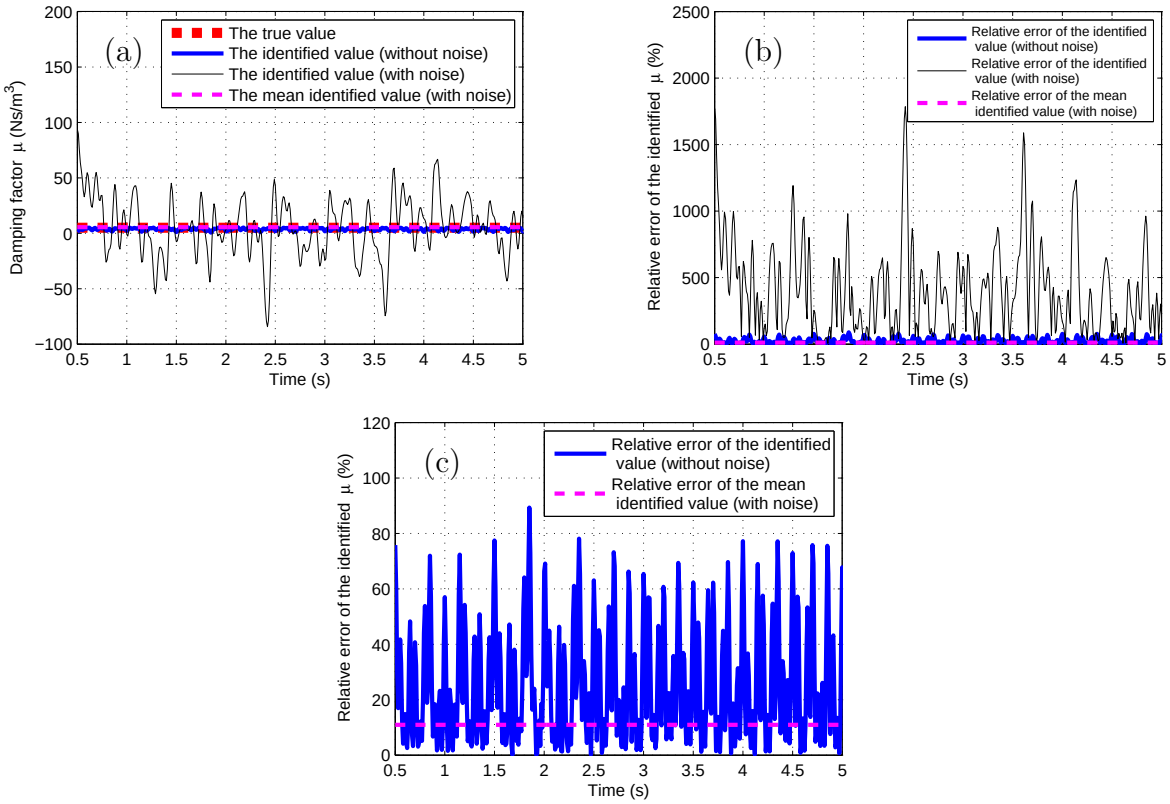

Figure A.49: Damping factor μ of a 2-DOF weakly nonlinear chainlike system with a weakly nonlinear periodically varying Van der Pol oscillator: (a) The true value and the identified values of μ, (b) Relative errors of the identified values of μ, (c) Close-up of (b).

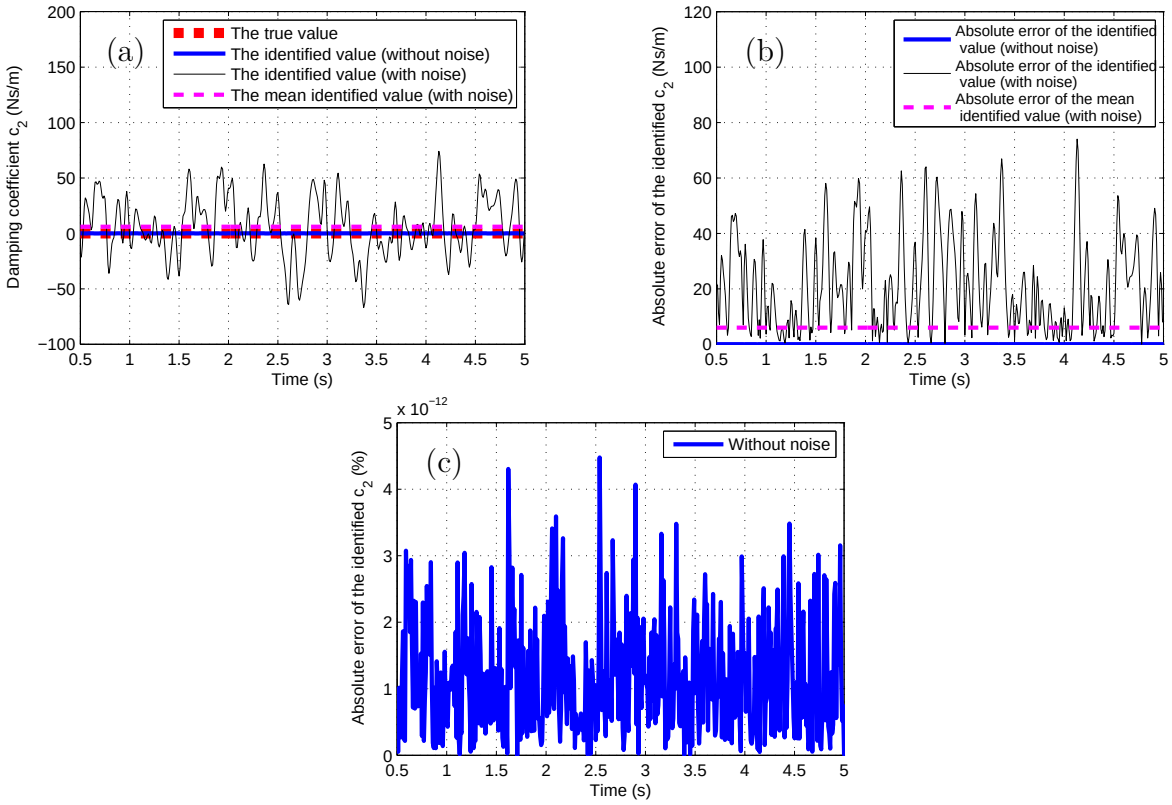

Figure A.50: Damping coefficient c_2 of a 2-DOF weakly nonlinear chainlike system with a weakly nonlinear periodically varying Van der Pol oscillator: (a) The true value and the identified values of c_2, (b) Absolute errors of the identified values of c_2, (c) Absolute error of the identified value of c_2 (without noise in system responses).

It is noted that no matter using noiseless or noise-added system responses as input of the modified HHT-based identification method, the identified results of the stiffness coefficients always match their respective true values well (with maximal relative error of k_1 less than 6.1% and that of k_2 less than 2.4%), whereas the accuracies of the identified results of the damping coefficients are quite low, especially when using noise-added system responses as input (the maximal relative error of damping factor μ is less than 1.8×10^3% and the maximal absolute error of damping coefficient c_2 is equal to 74Ns/m), due to the application of Equation (4.8) and the sensitivity of the damping coefficients to noise. The mean values (denoted with pink dashed lines) of the identified results of μ and c_2 are close to their respective true values with relatively smaller identification errors (the relative error of the mean identified μ is less than 11% and the absolute error of the mean identified c_2 is equal to 6.0Ns/m).

B Some of the HHT and Bayesian inference based identification results of general time-varying systems

B.1 Some of the HHT and Bayesian inference based identification results of linear time-varying systems

B.1.1 HHT and Bayesian inference based identification results of the damping coefficients of 1-DOF linear smoothly and abruptly varying systems

For the HHT and Bayesian inference based identification of the 1-DOF linear smoothly and abruptly varying systems, the statistical distributions of the identified damping coefficients as well as their relative errors are shown in Figures B.1 - B.2.

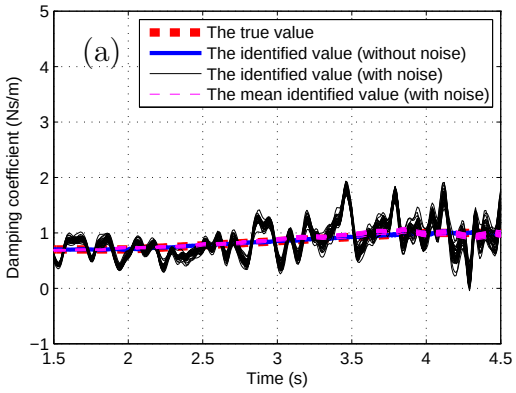

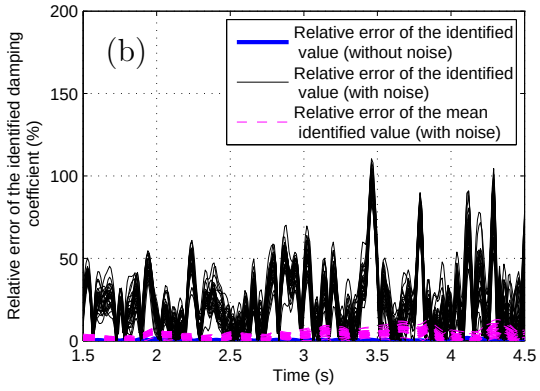

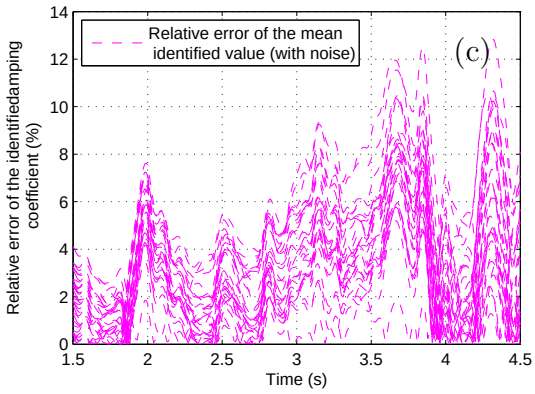

Figure B.1: Damping coefficient of a 1-DOF smoothly varying forced vibration system: (a) The true value and the identified values of the damping coefficient, (b) Relative errors of the identified values of the damping coefficient, (c) Relative errors of the mean identified values of the damping coefficient.

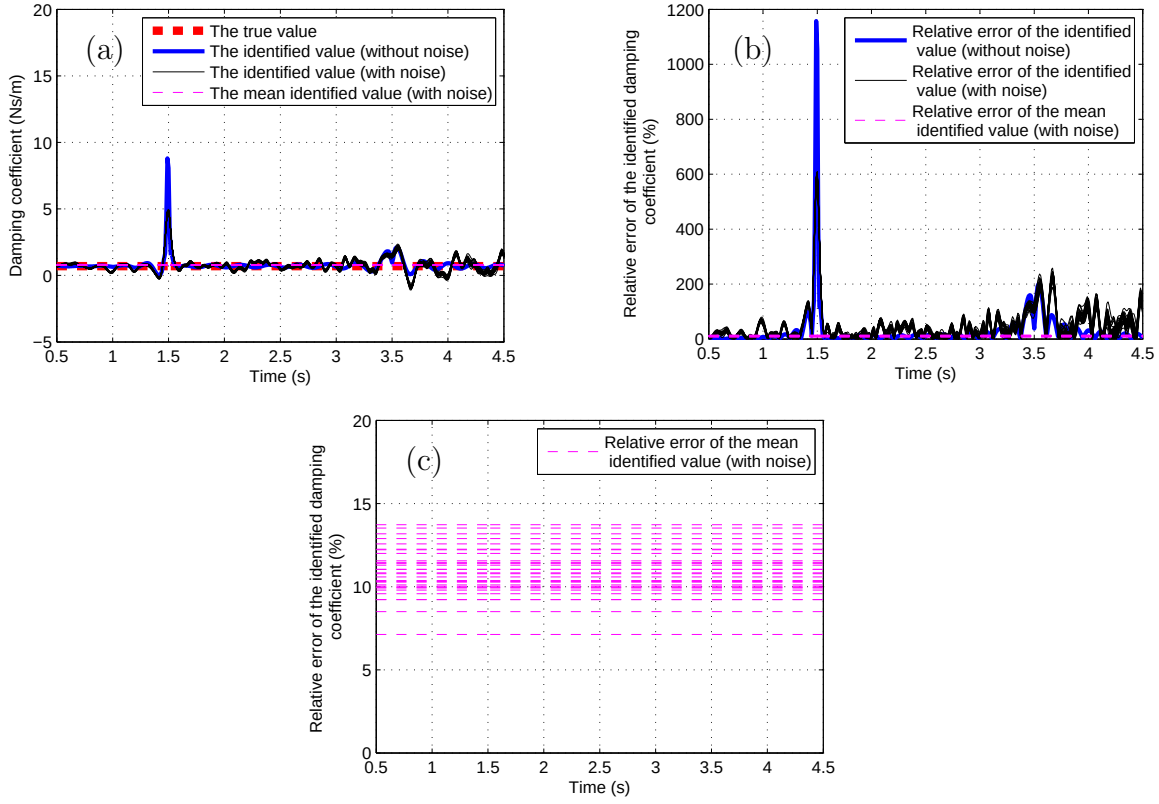

Figure B.2: Damping coefficient of a 1-DOF abruptly varying forced vibration system: (a) The true value and the identified values of the damping coefficient, (b) Relative errors of the identified values of the damping coefficient, (c) Relative errors of the mean identified values of the damping coefficient.

It is noticed that: For the 1-DOF linear smoothly and abruptly varying system, the identified values of the damping coefficient are widely distributed and have large identification errors due to the sensitivity of the damping coefficient to noise. However, the mean values (denoted with pink dashed lines) of the identified values of the damping coefficient have relatively smaller relative errors (whose maxima are less than 13% for the 1-DOF linear smoothly varying system, and less than 14% for the 1-DOF linear abruptly varying system, respectively). For the 1-DOF linear abruptly varying system, the identified values of the damping coefficient have abrupt changes with extremely large identification errors around $t = 1.5$s and $t = 3.5$s, indicating that the HHT-based identification method has bad ability to capture the abrupt change of the system parameters due to the limitations of Equation (2.16).

B.1.2 HHT and Bayesian inference based identification results of the damping coefficients of 2-DOF linear smoothly and abruptly varying systems

For the HHT and Bayesian inference based identification of the 2-DOF linear smoothly and abruptly varying non-chainlike forced vibration systems, the statistical distributions of the identified damping coefficients as well as their relative or absolute errors are presented in Figures B.3 - B.6.

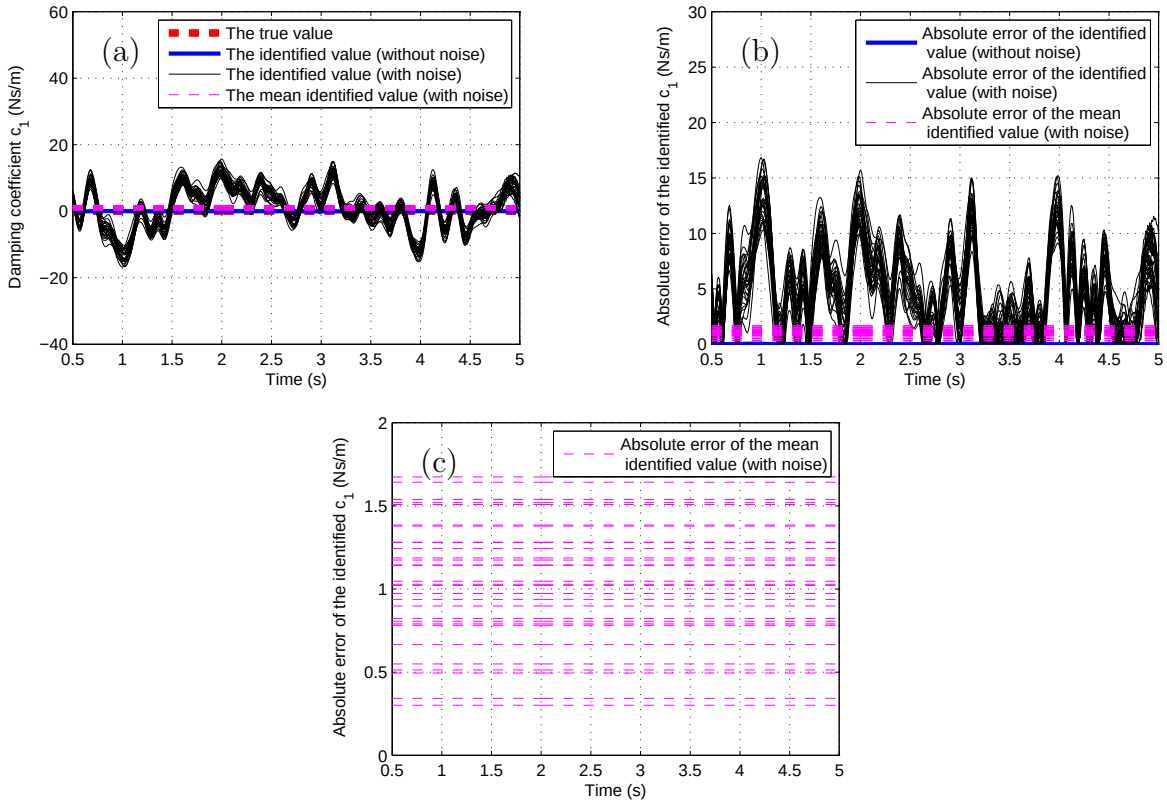

Figure B.3: Damping coefficient c_1 of a 2-DOF linear smoothly varying non-chainlike forced vibration system: (a) The true value and the identified values of c_1, (b) Absolute errors of the identified values of c_1, (c) Absolute errors of the mean identified values of c_1.

It is found from the above figures that: For the 2-DOF linear smoothly and abruptly varying non-chainlike systems, by applying the combined method, the statistical distributions of the identified damping coefficients (denoted with black lines) are quite wide (the maximal absolute error of the identified values of c_1 is less than 17Ns/m and that of c_2 is equal to 22Ns/m for the 2-DOF linear smoothly varying non-chainlike system, their counterparts for the 2-DOF linear abruptly varying non-chainlike system are less than 1.7Ns/m and 1.5Ns/m respectively). However, the mean values (denoted with pink dashed lines) of the identified values of the damping coefficients over the required time history are concentratedly distributed and are close to their respective true values (the maximal absolute error of the mean values of the identified values of c_1 is less than 1.7Ns/m and that of c_2 is less than 1.5Ns/m for the 2-DOF linear smoothly varying non-chainlike system, their counterparts for the 2-DOF linear abruptly varying non-chainlike system are less than 3.5Ns/m and 2.1Ns/m respectively).

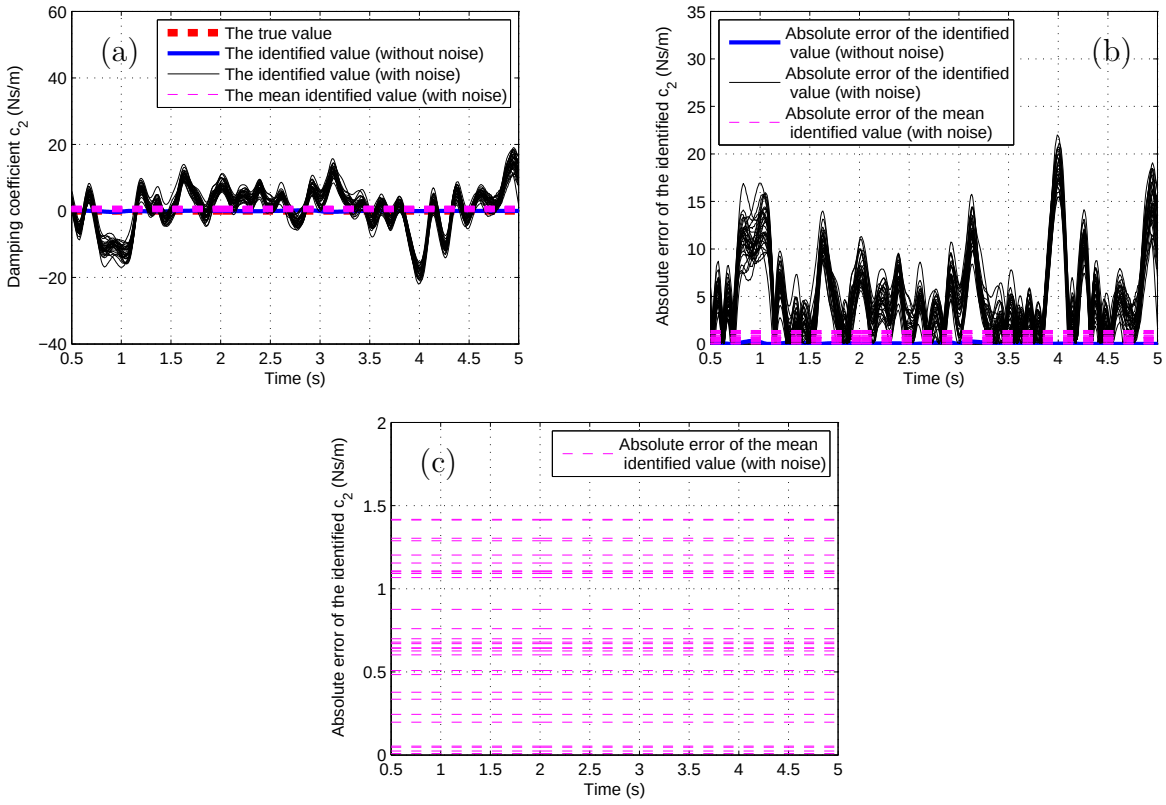

Figure B.4: Damping coefficient c_2 of a 2-DOF linear smoothly varying non-chainlike forced vibration system: (a) The true value and the identified values of c_2, (b) Absolute errors of the identified values of c_2, (c) Absolute errors of the mean identified values of c_2.

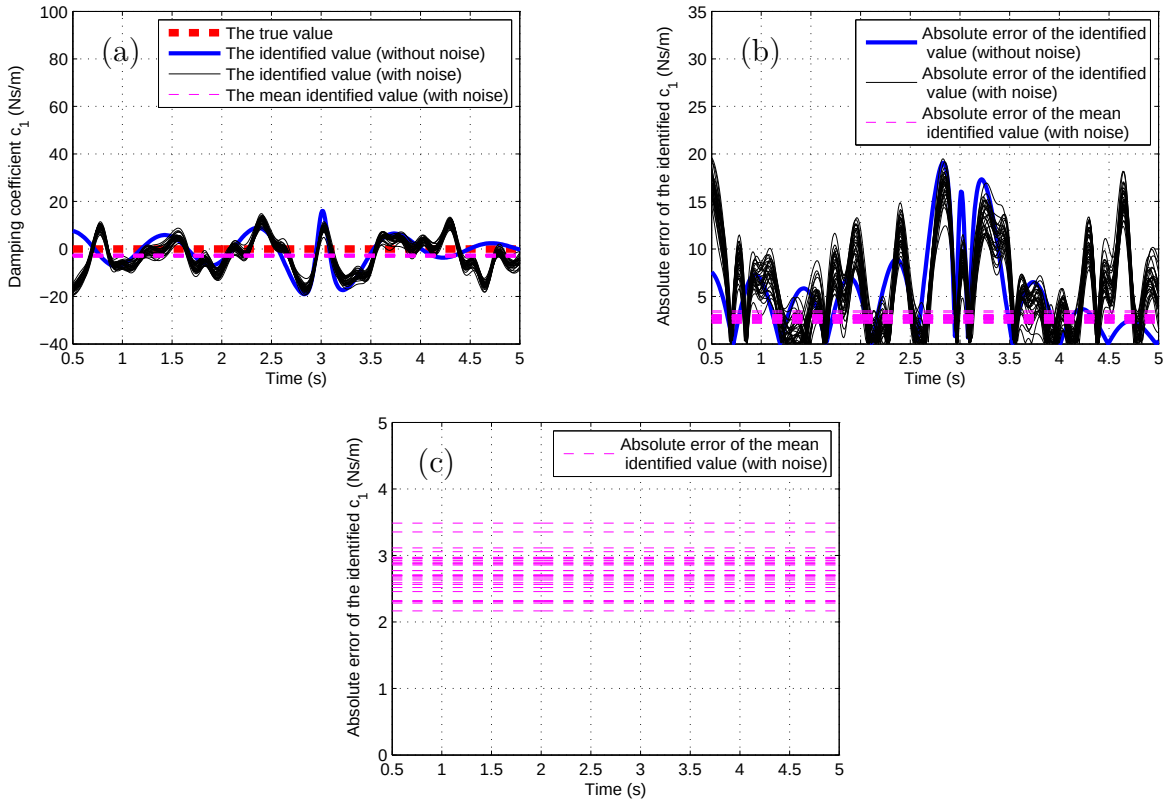

Figure B.5: Damping coefficient c_1 of a 2-DOF linear abruptly varying non-chainlike forced vibration system: (a) The true value and the identified values of c_1, (b) Relative errors of the identified values of c_1, (c) Relative errors of the mean identified values of c_1.

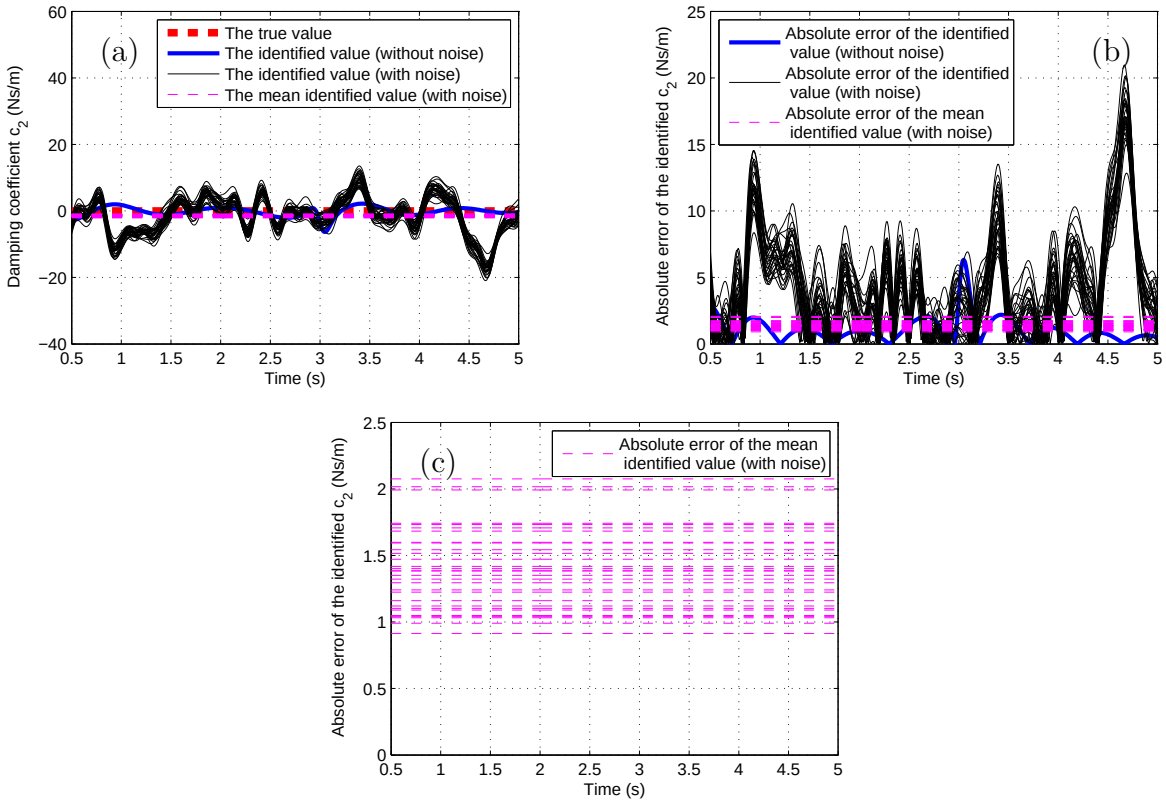

Figure B.6: Damping coefficient c_2 of a 2-DOF linear abruptly varying non-chainlike forced vibration system: (a) The true value and the identified values of c_2, (b) Absolute errors of the identified values of c_2, (c) Absolute errors of the mean identified values of c_2.

B.1.3 HHT and Bayesian inference based identification results of linear periodically varying systems

(1) 1-DOF system

For the HHT and Bayesian inference based identification of the 1-DOF linear periodically forced vibration system, the statistical distributions of the identified system coefficients as well as their relative errors are plotted in Figure B.7.

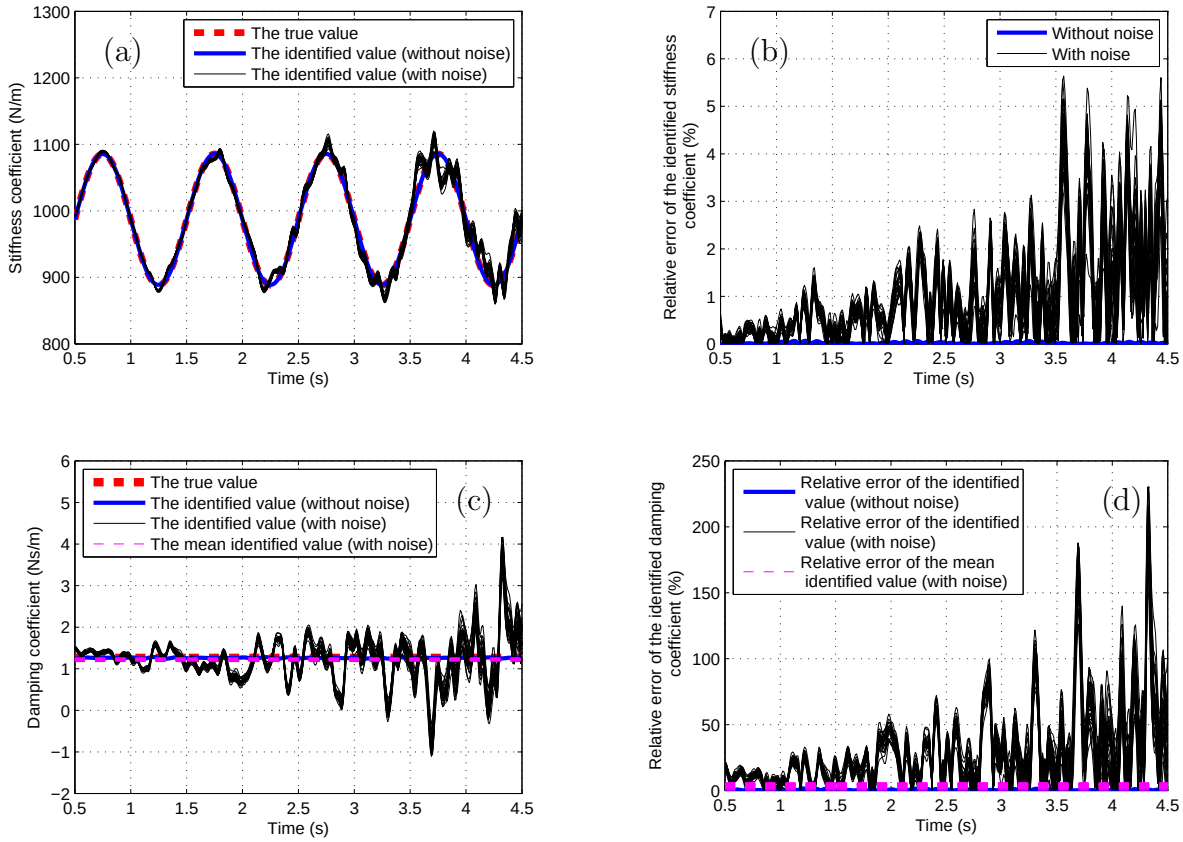

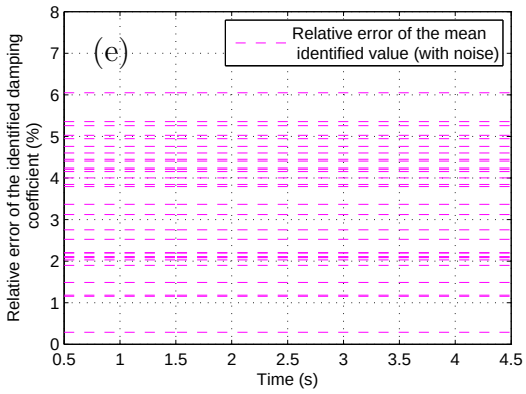

Figure B.7: System coefficients of a 1-DOF periodically varying forced vibration system: (a) The true value and the identified values of the stiffness coefficient, (b) Relative errors of the stiffness coefficient, (c) The true value and the identified values of the damping coefficient, (d) Relative errors of the identified values of the damping coefficient, (e) Relative errors of the mean identified values of the damping coefficient.

It is noted that: although the prior distribution assigned to the white noise in each system response has large ratio of the standard deviation of the white noise and that of the corresponding noiseless system response, by applying the combined method, the obtained identified values (denoted with black lines) of the stiffness coefficient are close to its true value with small relative errors (whose maximum is less than 5.7%), whereas those of the damping coefficient have large identification errors due to the sensitivity of the damping coefficient to noise (with its maximal relative error equal to $2.3 \times 10^2\%$). The mean values (denoted with pink dashed lines) of the identified values of the damping coefficient over the required time history match closely its true value with small errors (whose maximum is less than 6.1%).

(2) 2-DOF systems
For the HHT and Bayesian inference based identification of the 2-DOF linear periodically varying forced vibration system, the statistical distributions of the identified system coefficients as well as their relative or absolute errors are shown in Figures B.8 - B.11.

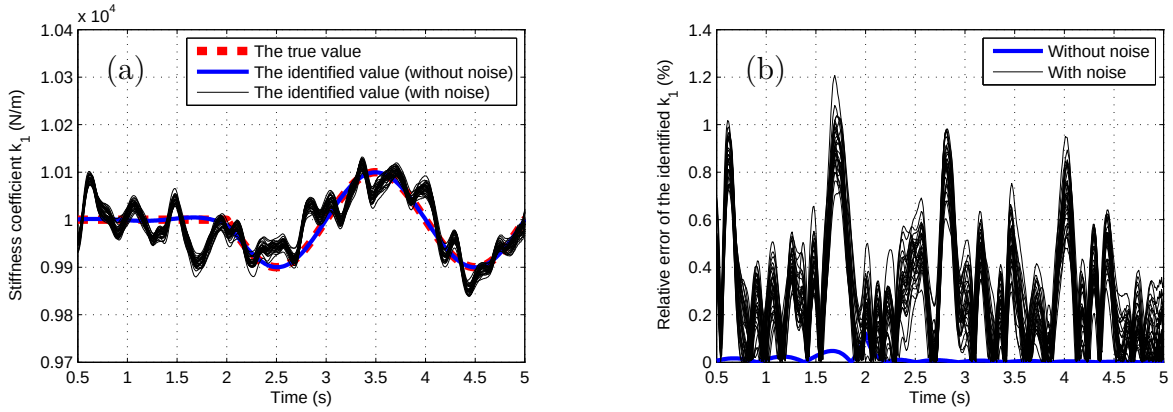

Figure B.8: Stiffness coefficient k_1 of a 2-DOF linear periodically varying non-chainlike forced vibration system: (a) The true value and the identified values of k_1, (b) Relative errors of the identified values of k_1.

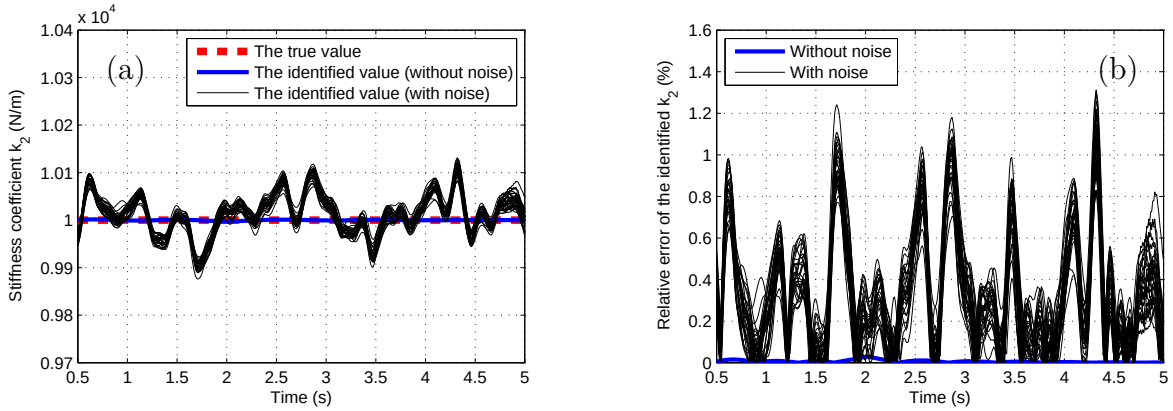

Figure B.9: Stiffness coefficient k_2 of a 2-DOF linear periodically varying non-chainlike forced vibration system: (a) The true value and the identified values of k_2, (b) Relative errors of the identified values of k_2.

It can be seen that: The resulting identified values (denoted with black lines) of the stiffness coefficients are concentratedly distributed around their respective true values (with maximal relative error of the identified values of k_1 equal to 1.2% and that of k_2 less than 1.4%), whereas those of the damping coefficients are widely distributed (with maximal absolute error of the identified values of c_1 less than 18Ns/m and that of c_2 less than 23Ns/m) due to the sensitivity of the damping coefficients to noise. The mean values (denoted with pink dashed lines) of the identified values of the damping coefficients over the required time history are concentratedly distributed and are close to their respective true values (with maximal absolute error of the mean values of the identified values of c_1 less than 1.6Ns/m and that of c_2 less than 1.4Ns/m).

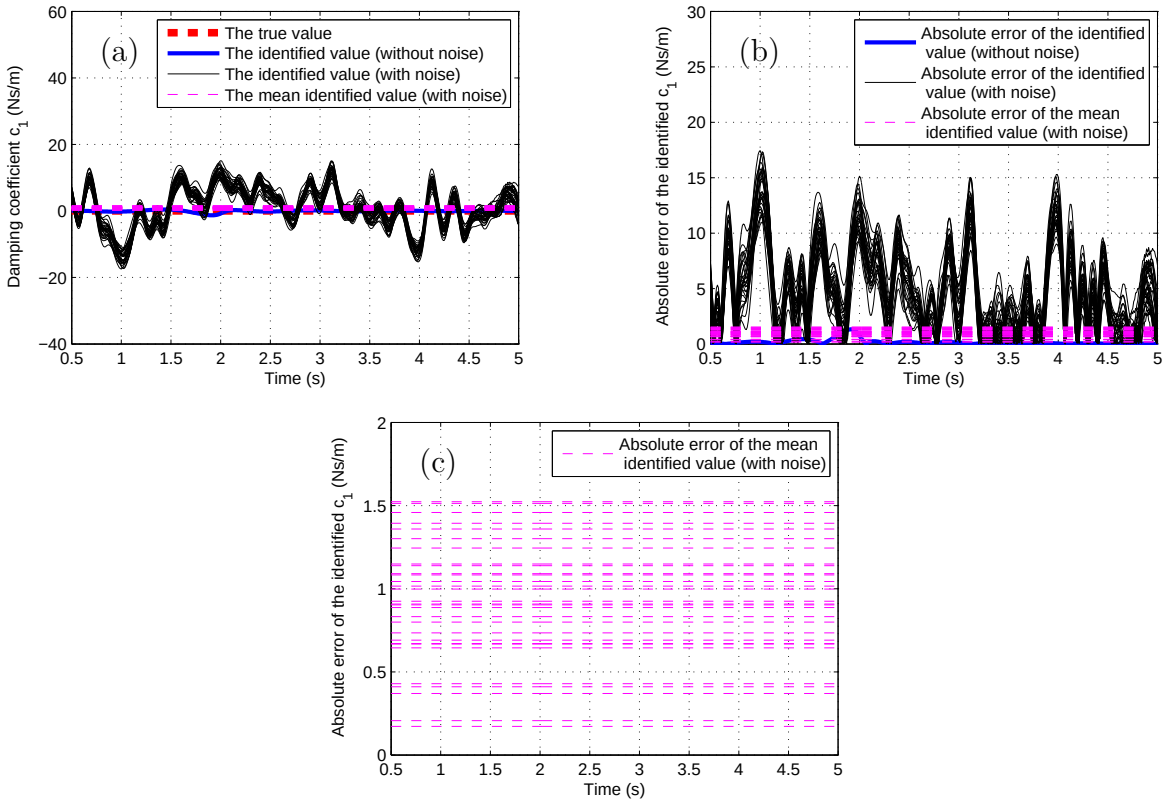

Figure B.10: Damping coefficient c_1 of a 2-DOF linear periodically varying non-chainlike forced vibration system: (a) The true value and the identified values of c_1, (b) Absolute errors of the identified values of c_1, (c) Absolute errors of the mean identified values of c_1.

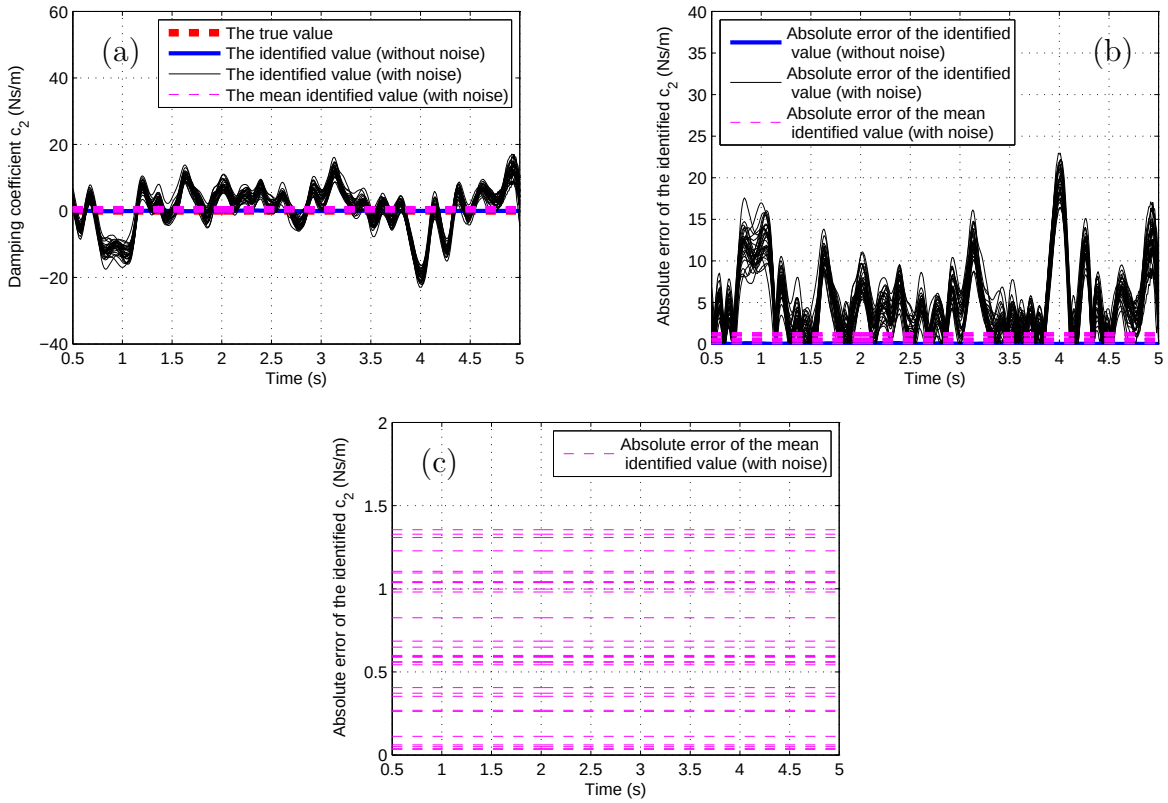

Figure B.11: Damping coefficient c_2 of a 2-DOF linear periodically varying non-chainlike forced vibration system: (a) The true value and the identified values of c_2, (b) Absolute errors of the identified values of c_2, (c) Absolute errors of the mean identified values of c_2.

B.2 Some of the HHT and Bayesian inference based identification results of weakly nonlinear time-varying systems

B.2.1 HHT and Bayesian inference based identification results of the damping coefficients of 1-DOF weakly nonlinear smoothly and abruptly varying Duffing oscillators

For the HHT and Bayesian inference based identification of the 1-DOF weakly nonlinear smoothly and abruptly varying Duffing oscillators, the statistical distributions of the identified damping coefficients as well as their relative errors are shown in Figures B.12 - B.13.

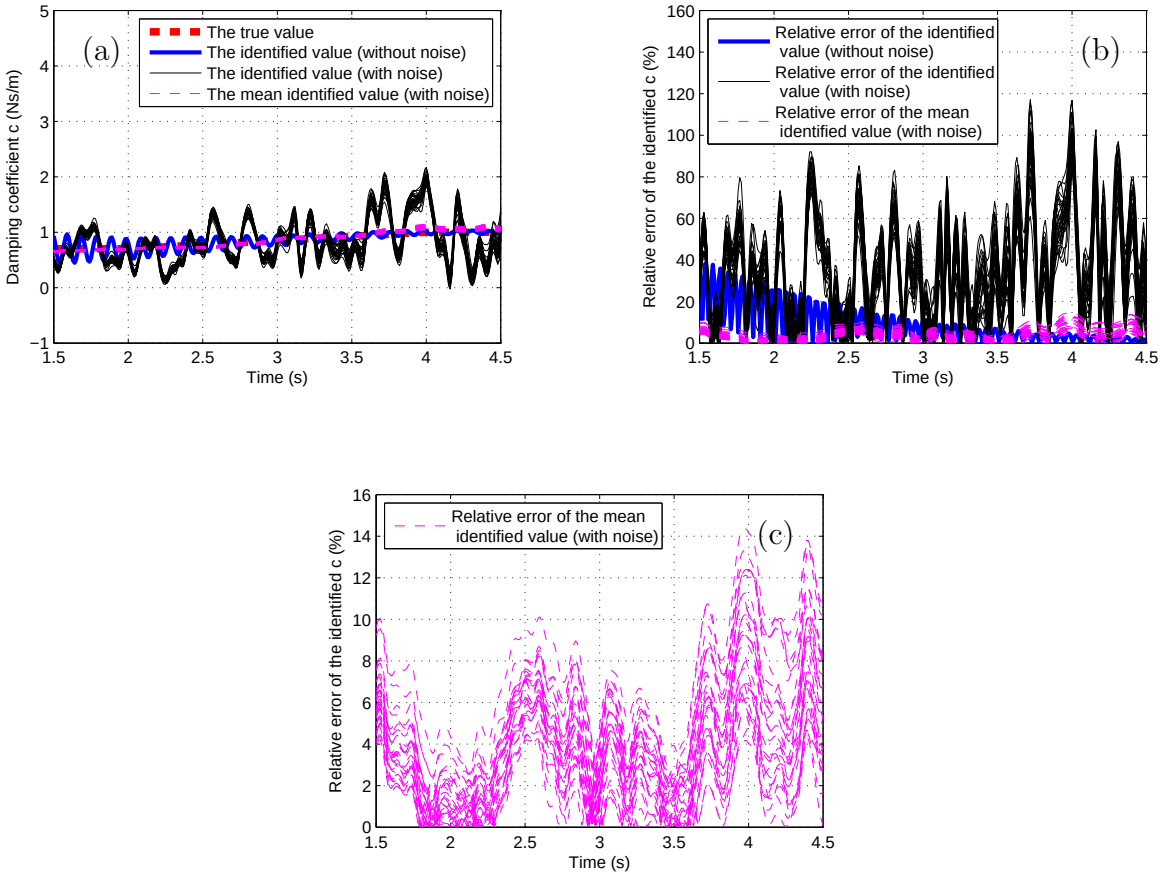

Figure B.12: Damping coefficient c of a 1-DOF weakly nonlinear smoothly varying hard spring Duffing oscillator: (a) The true value and the identified values of c, (b) Relative errors of the identified values of c, (c) Relative errors of the mean identified values of c.

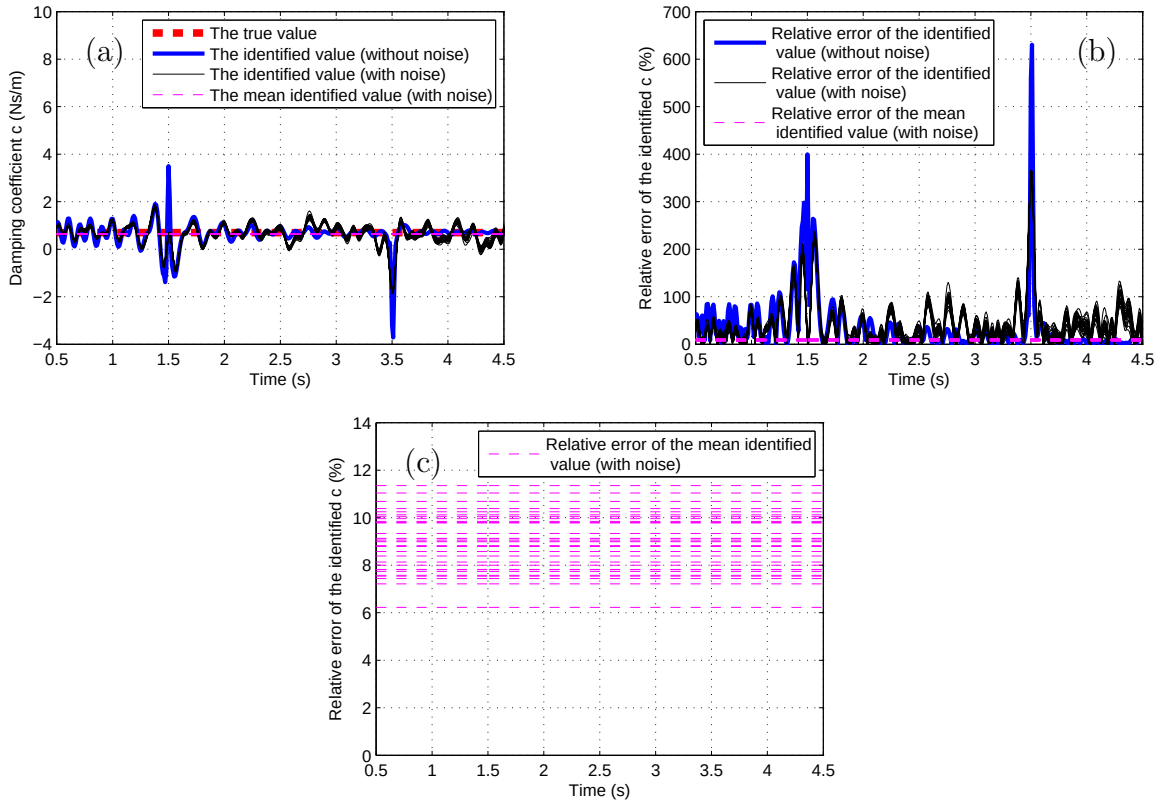

Figure B.13: Damping coefficient c of a 1-DOF weakly nonlinear abruptly varying hard spring Duffing oscillator: (a) The true value and the identified values of c, (b) Relative errors of the identified values of c, (c) Relative errors of the mean identified values of c.

It can be seen that: For both oscillators, the identified values of damping coefficient c are widely distributed and have large identification errors (the maximal relative errors of its identified values are less than 1.2×10^2 for the weakly nonlinear smoothly varying Duffing oscillator, and less than $3.7 \times 10^2\%$ for the weakly nonlinear abruptly varying Duffing oscillator, respectively), due to the sensitivity of the damping coefficient to noise and the application of the approximation Equation (4.4). However, the mean values (denoted with pink dashed lines) of the identified values of c over the required time history have relatively smaller relative errors for both oscillators (whose maxima are less than 15% for the weakly nonlinear smoothly varying Duffing oscillator, and less than 12% for the weakly nonlinear abruptly varying Duffing oscillator, respectively). For the weakly nonlinear abruptly varying Duffing oscillator, it is hard to detect the exact time instants of the abrupt changes of the system parameter from the statistical distribution of the identified damping coefficient due to the existence of large identification errors.

B.2.2 HHT and Bayesian inference based identification results of the damping coefficients of 2-DOF weakly nonlinear smoothly and abruptly varying Duffing systems

For the HHT and Bayesian inference based identification of the 2-DOF weakly nonlinear smoothly and abruptly varying Duffing systems, the statistical distributions of the identified damping coefficients as well as their relative or absolute errors are presented in Figures B.14 - B.17.

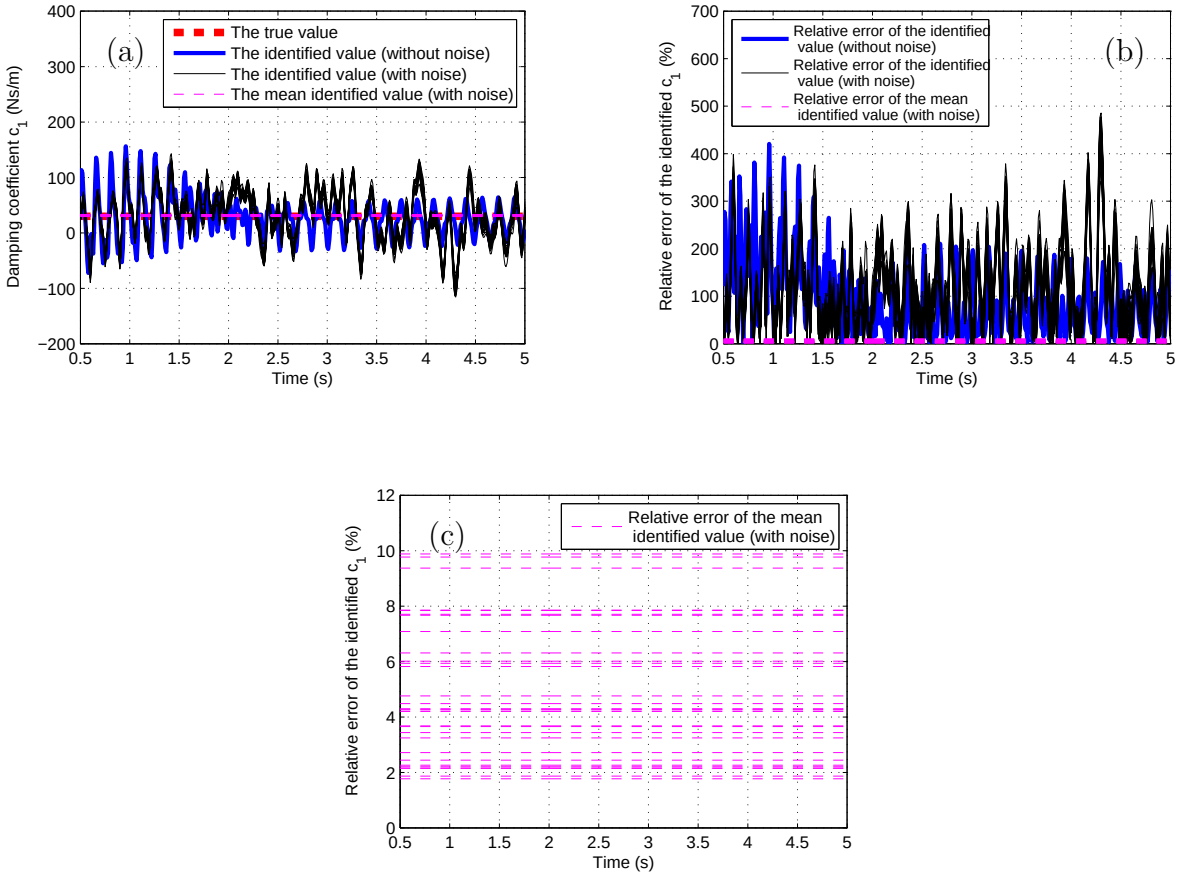

Figure B.14: Damping coefficient c_1 of a 2-DOF weakly nonlinear system with a weakly nonlinear smoothly varying hard spring Duffing oscillator: (a) The true value and the identified values of c_1, (b)Relative errors of the identified values of c_1, (c) Relative errors of the mean identified values of c_1.

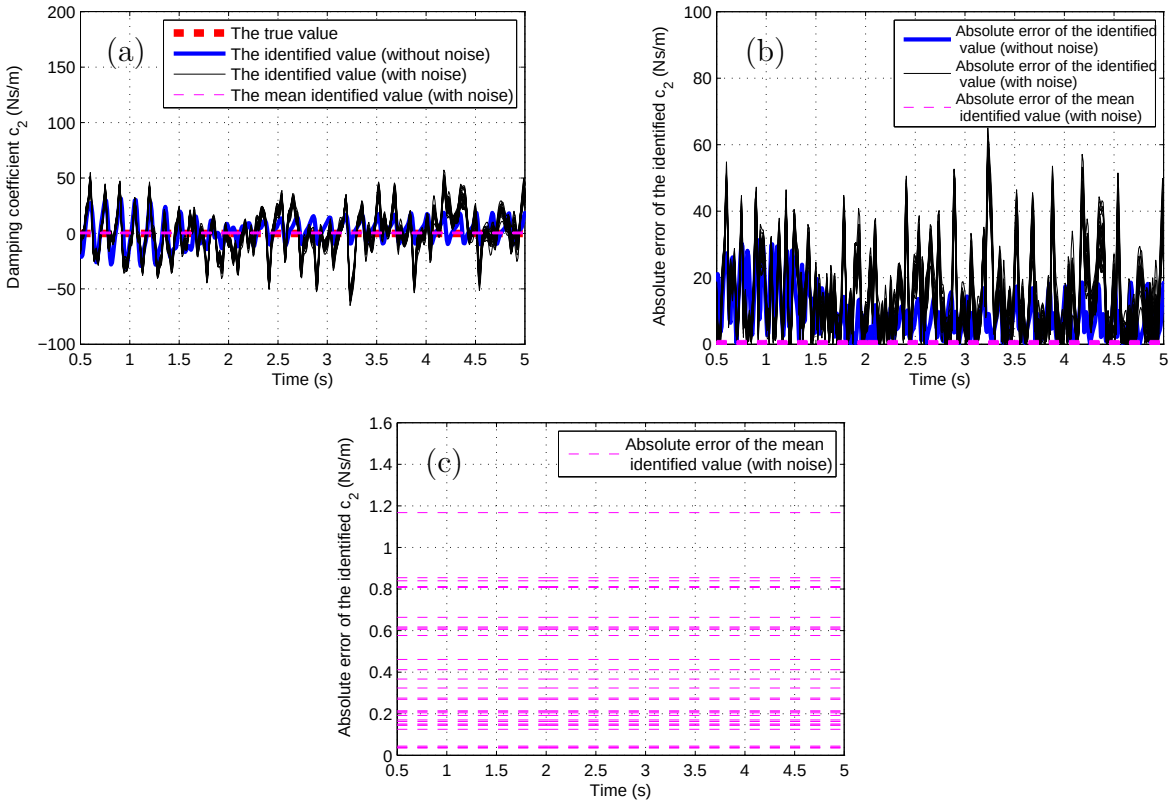

Figure B.15: Damping coefficient c_2 of a 2-DOF weakly nonlinear system with a weakly nonlinear smoothly varying hard spring Duffing oscillator: (a) The true value and the identified values of c_2, (b)Absolute errors of the identified values of c_2, (c) Absolute errors of the mean identified values of c_2.

From the figures, it is noted that: For both systems, the identified values of the damping coefficients are widely distributed with large identification errors (the maximal relative error of the identified values of c_1 is less than $4.9 \times 10^2\%$ and the maximal absolute error of the identified values of c_2 is less than 66Ns/m for the smoothly varying Duffing system, their counterparts for the abruptly varying Duffing system are less than $4.7 \times 10^2\%$ and less than 81Ns/m respectively). However, the mean values (denoted with pink dashed lines) of the identified values of the damping coefficients over the required time history are concentratedly distributed and close to their respective true values (the maximal relative error of the mean values of the identified values of c_1 is less than 9.9% and the maximal absolute error of the mean values of the identified values of c_2 is less than 1.2Ns/m for the smoothly varying Duffing system, their counterparts for the abruptly varying Duffing system are less than 11% and 2.2Ns/m respectively). For the 2-DOF weakly nonlinear abruptly varying Duffing system, due to the existence of large identification errors arising from the sensitivity of the damping coefficients to noise and the application of the approximation Equation (4.4), it is difficult to detect the exact time instant of the abrupt change of the system parameter from the identified values of the damping coefficients.

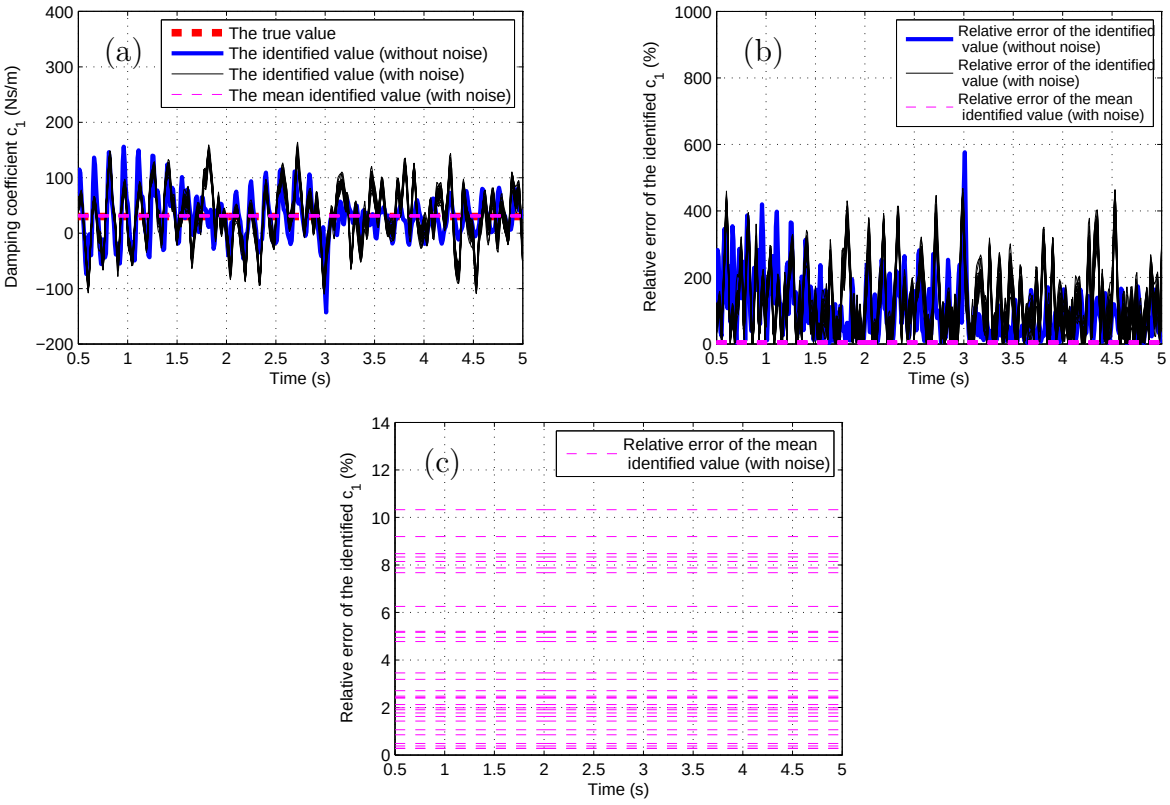

Figure B.16: Damping coefficient c_1 of a 2-DOF weakly nonlinear system with a weakly nonlinear abruptly varying hard spring Duffing oscillator: (a) The true value and the identified values of c_1, (b)Relative errors of the identified values of c_1, (c) Relative errors of the mean identified values of c_1.

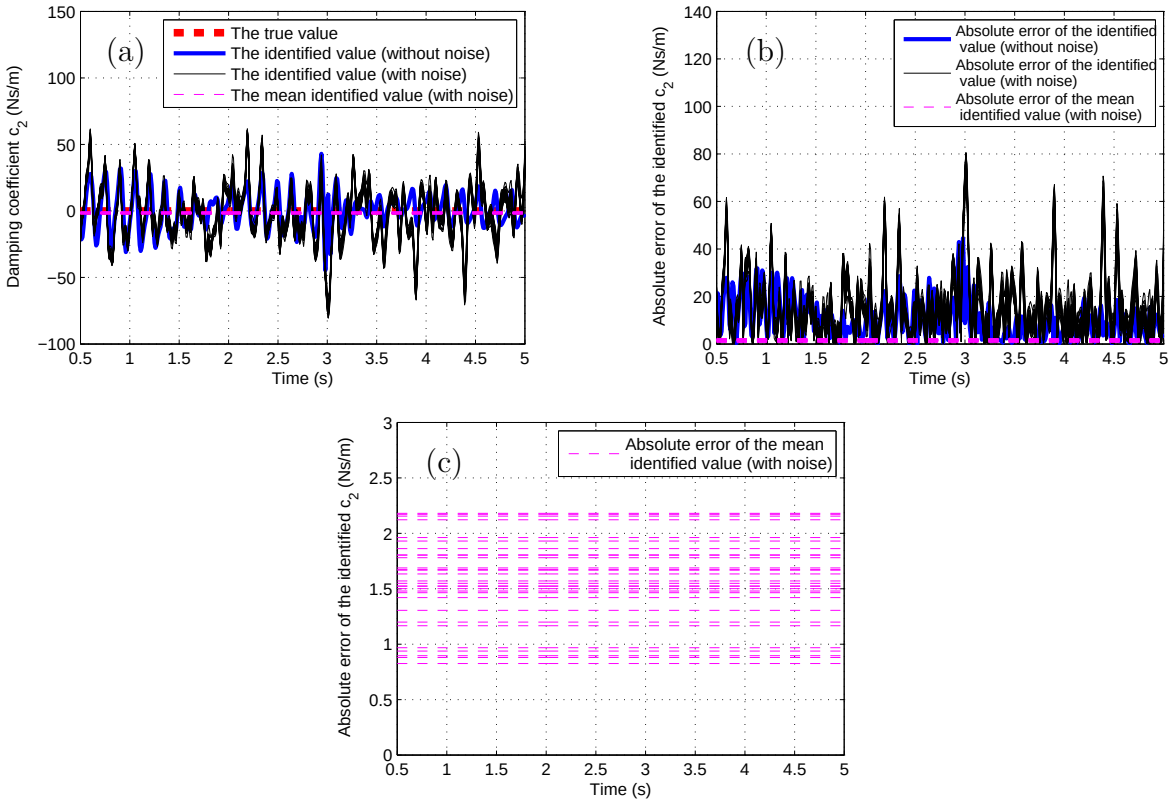

Figure B.17: Damping coefficient c_2 of a 2-DOF weakly nonlinear system with a weakly nonlinear abruptly varying hard spring Duffing oscillator: (a) The true value and the identified values of c_2, (b)Absolute errors of the identified values of c_2, (c) Absolute errors of the mean identified values of c_2.

B.2.3 HHT and Bayesian inference based identification results of weakly nonlinear periodically varying Duffing systems

(1) 1-DOF system

For the HHT and Bayesian inference based identification of the 1-DOF weakly nonlinear periodically varying hard spring Duffing oscillator, the statistical distributions of the identified values of cubic stiffness factor δ and damping coefficient c as well as the relative errors of their identified values are shown in Figure B.18. We can see from the figures that: The obtained identified values (denoted with black lines) of δ are distributed concentratedly and match its true value (with the maximal relative error less than 7.7%), whereas those of c are distributed widely and have large identification errors (with the maximal relative error less than 2.5×10^2%) due to the sensitivity of the damping coefficient to noise and the application of the approximation Equation (4.4). The mean values (denoted with pink dashed lines) of the identified values of c over the required time history are concentratedly distributed and are close to its true value with relatively smaller relative errors (whose maximum is less than 11%).

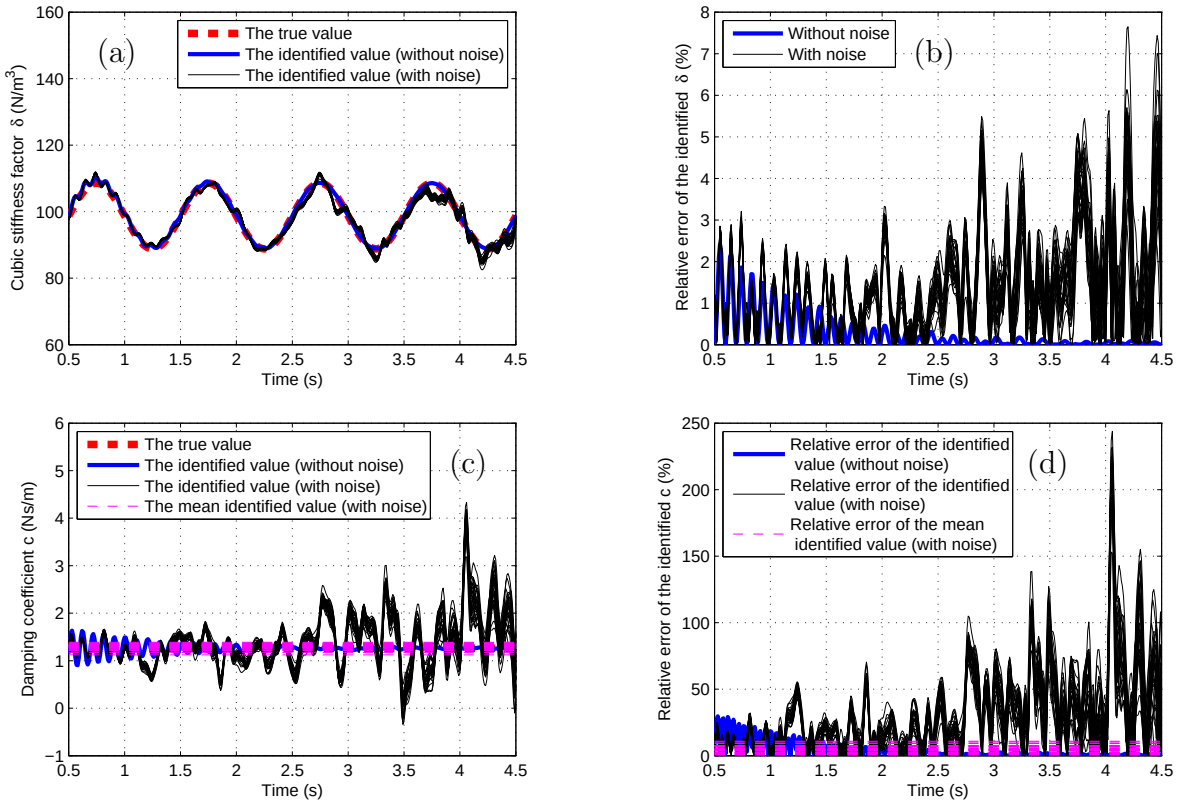

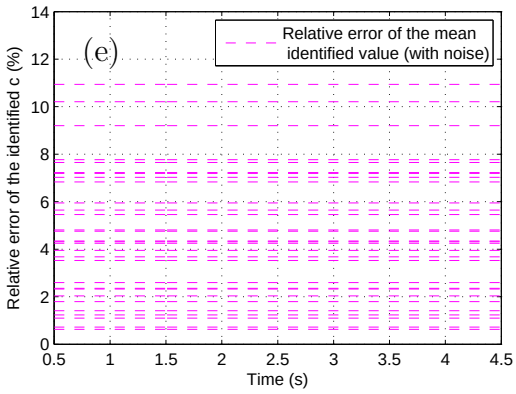

Figure B.18: System coefficients of a 1-DOF weakly nonlinear periodically varying hard spring Duffing oscillator: (a) The true value and the identified values of cubic stiffness factor δ, (b) Relative errors of the identified values of δ, (c) The true value and the identified values of damping coefficient c, (d) Relative errors of the identified values of c, (e) Relative errors of the mean identified values of c.

(2) 2-DOF system

For the HHT and Bayesian inference based identification of the 2-DOF weakly nonlinear periodically varying hard spring Duffing system, the statistical distributions of the identified system coefficients as well as their relative or absolute errors are shown in Figures B.19 - B.22.

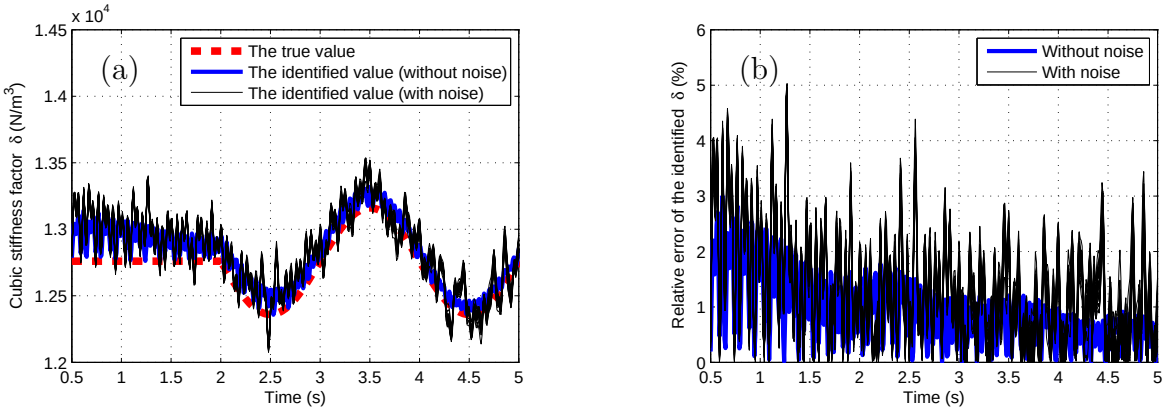

Figure B.19: Cubic stiffness factor δ of a 2-DOF weakly nonlinear chainlike system with a weakly nonlinear periodically varying hard spring Duffing oscillator: (a) The true value and the identified values of δ, (b) Relative errors of the identified values of δ.

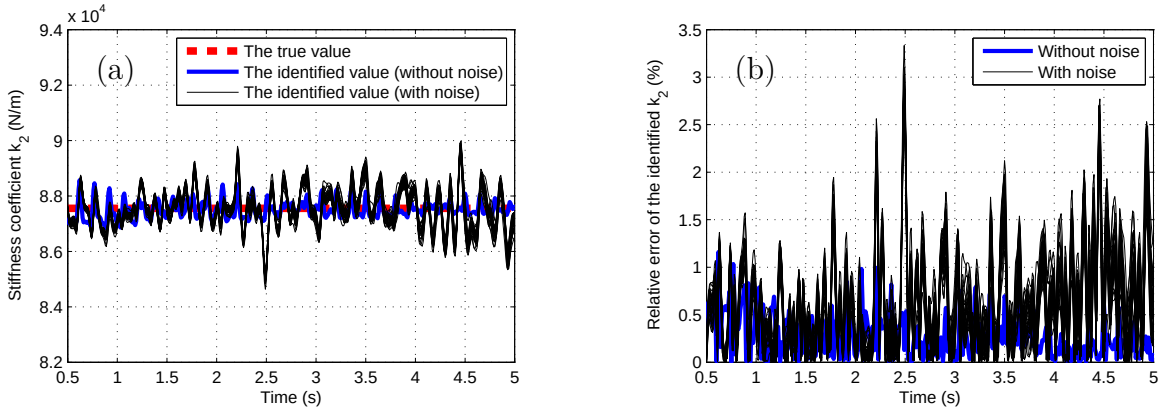

Figure B.20: Stiffness coefficient k_2 of a 2-DOF weakly nonlinear chainlike system with a weakly nonlinear periodically varying hard spring Duffing oscillator: (a) The true value and the identified values of k_2, (b) Relative errors of the identified values of k_2.

It is noted that the resulting statistical distributions of the identified values (denoted with black lines) of the stiffness coefficients are concentrated and their identified values are close to their respective true values (with maximal relative error of the identified values of δ less than 5.1% and that of k_2 less than 3.4%), whereas those of the damping coefficients are quite wide and their identified values have large identification errors (the maximal relative error of the identified values of c_1 is less than 5.1×10^2% and the maximal absolute error of the identified values of c_2 is less than 75Ns/m). The mean values (denoted with pink dashed lines) of the identified values of the damping coefficients over the required time history are concentratedly distributed and match their respective true values with relatively small relative or absolute errors (the maximal relative error of the mean values of the identified values of c_1 is less than 12%, and the maximal absolute error of the mean values of the identified values of c_2 is equal to 1.7Ns/m).

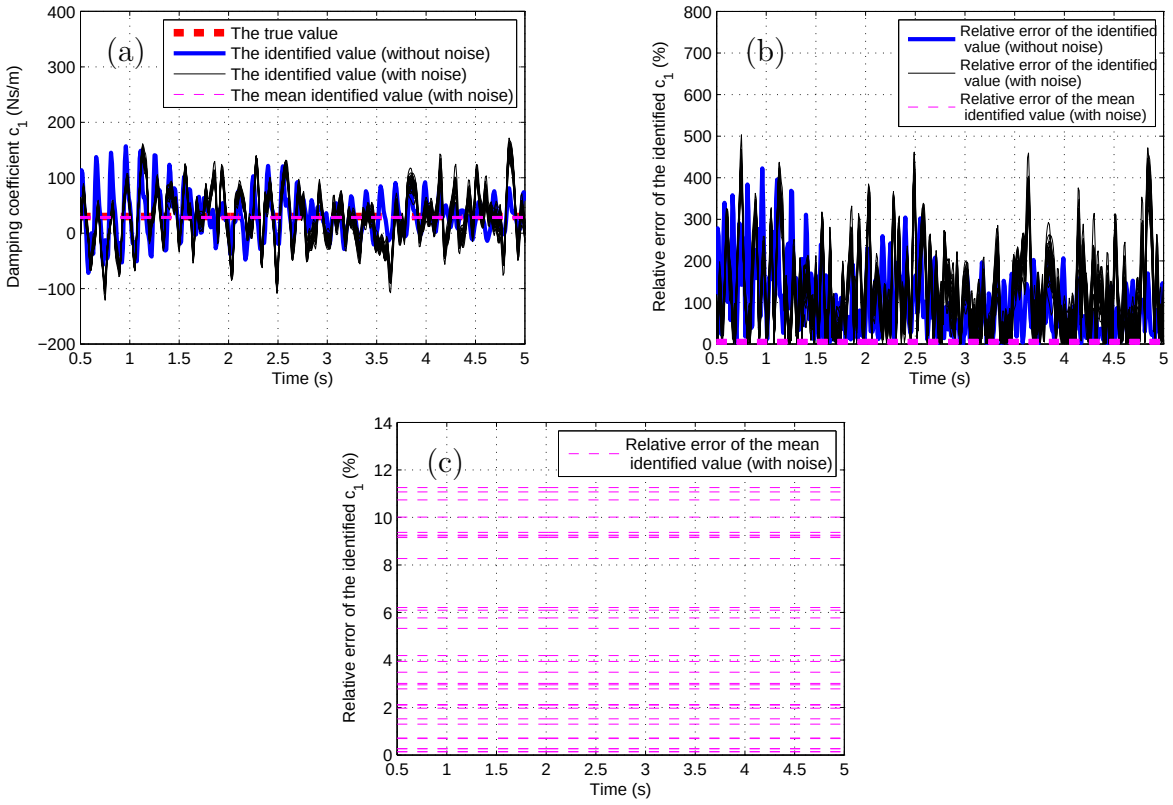

Figure B.21: Damping coefficient c_1 of a 2-DOF weakly nonlinear chainlike system with a weakly nonlinear periodically varying hard spring Duffing oscillator: (a) The true value and the identified values of c_1, (b) Relative errors of the identified values of c_1, (c) Relative errors of the mean identified values of c_1.

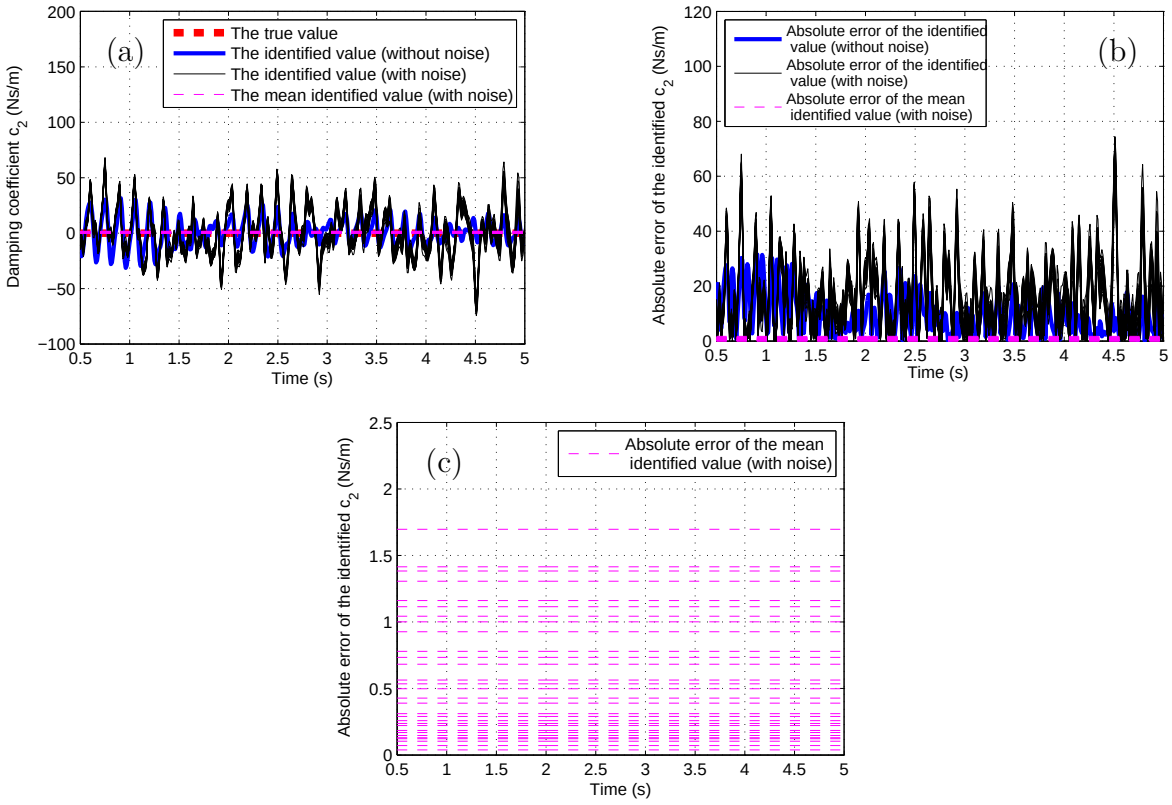

Figure B.22: Damping coefficient c_2 of a 2-DOF weakly nonlinear chainlike system with a weakly nonlinear periodically varying hard spring Duffing oscillator: (a) The true value and the identified values of c_2, (b) Absolute errors of the identified values of c_2, (c) Absolute errors of the mean identified values of c_2.

B.2.4 HHT and Bayesian inference based identification results of the damping coefficients of 1-DOF weakly nonlinear smoothly and abruptly varying Van der Pol oscillators

For the HHT and Bayesian inference based identification of the 1-DOF weakly nonlinear smoothly and abruptly varying Van der Pol oscillators, the statistical distributions of the identified damping factors as well as their relative errors are shown in Figures B.23 - B.24.

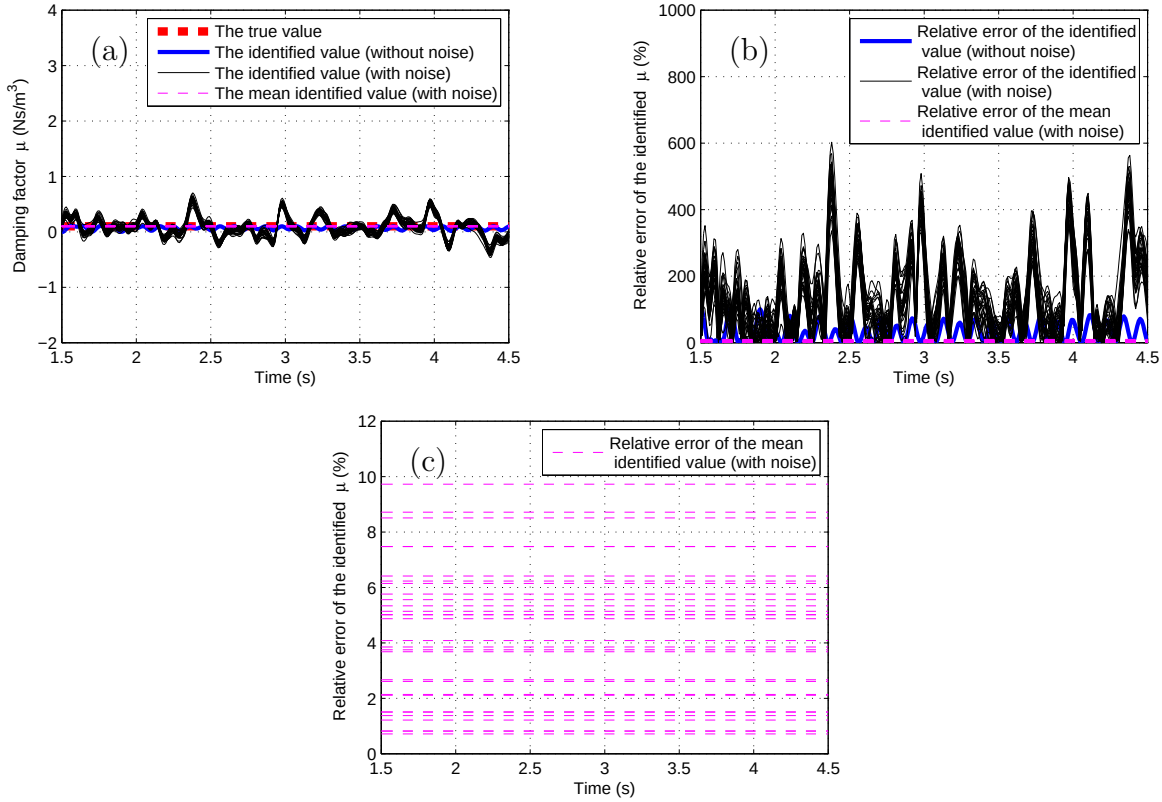

Figure B.23: Damping factor μ of a 1-DOF weakly nonlinear smoothly varying Van der Pol oscillator: (a) The true value and the identified values of μ, (b) Relative errors of the identified values of μ, (c) Relative errors of the mean identified values of μ.

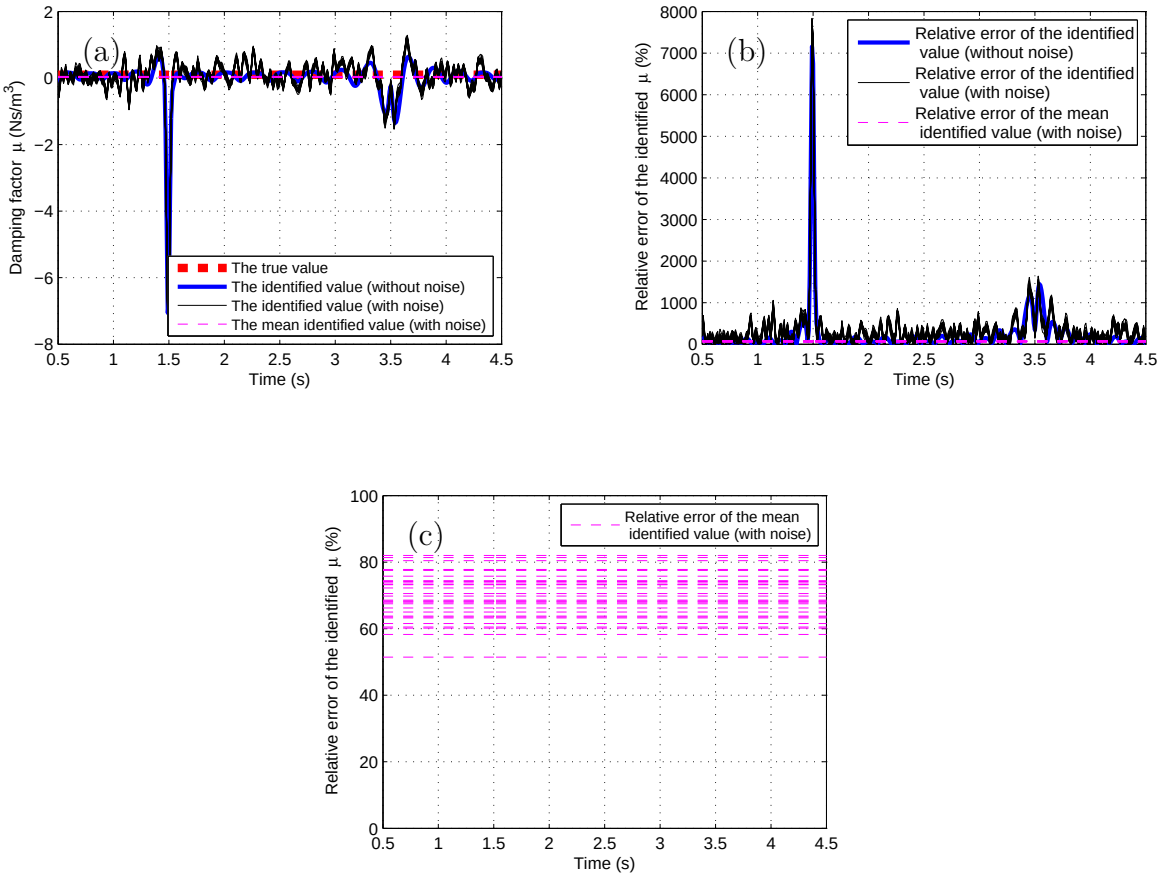

Figure B.24: Damping factor μ of a 1-DOF weakly nonlinear abruptly varying Van der Pol oscillator: (a) The true value and the identified values of μ, (b) Relative errors of the identified values of μ, (c) Relative errors of the mean identified values of μ.

We can see from the figures that: For the 1-DOF weakly nonlinear smoothly varying Van der Pol oscillator, the identified values of damping factor μ are widely distributed and have extremely large identification errors (with maximal relative error of the identified values equal to $6.0 \times 10^2\%$) due to the sensitivity of the damping coefficient to noise and the application of the approximation Equation (4.8), but the mean values (denoted with pink dashed lines) of the identified values of μ over the required time history have relatively smaller relative errors (whose maximum is less than 9.8%); For the 1-DOF weakly nonlinear abruptly varying Van der Pol oscillator, the identified values of μ have abrupt changes around time instants $t = 1.5$s and $t = 3.5$s due to the limitations of Equation (2.16). Due to the sensitivity of the damping coefficient to noise and the application of the approximation Equation (4.8), the obtained identified values of μ have extremely large identification errors. The mean values (denoted with pink dashed lines) of the identified values of μ over the required time history also have large relative errors (whose maximum is equal to 82%).

B.2.5 HHT and Bayesian inference based identification results of the damping coefficients of 2-DOF weakly nonlinear smoothly and abruptly varying Van der Pol systems

For the HHT and Bayesian inference based identification of the 2-DOF weakly nonlinear smoothly and abruptly varying Van der Pol systems, the statistical distributions of the identified damping factor μ and damping coefficient c_2 as well as their relative or absolute errors for both systems are presented in Figures B.25 - B.28.

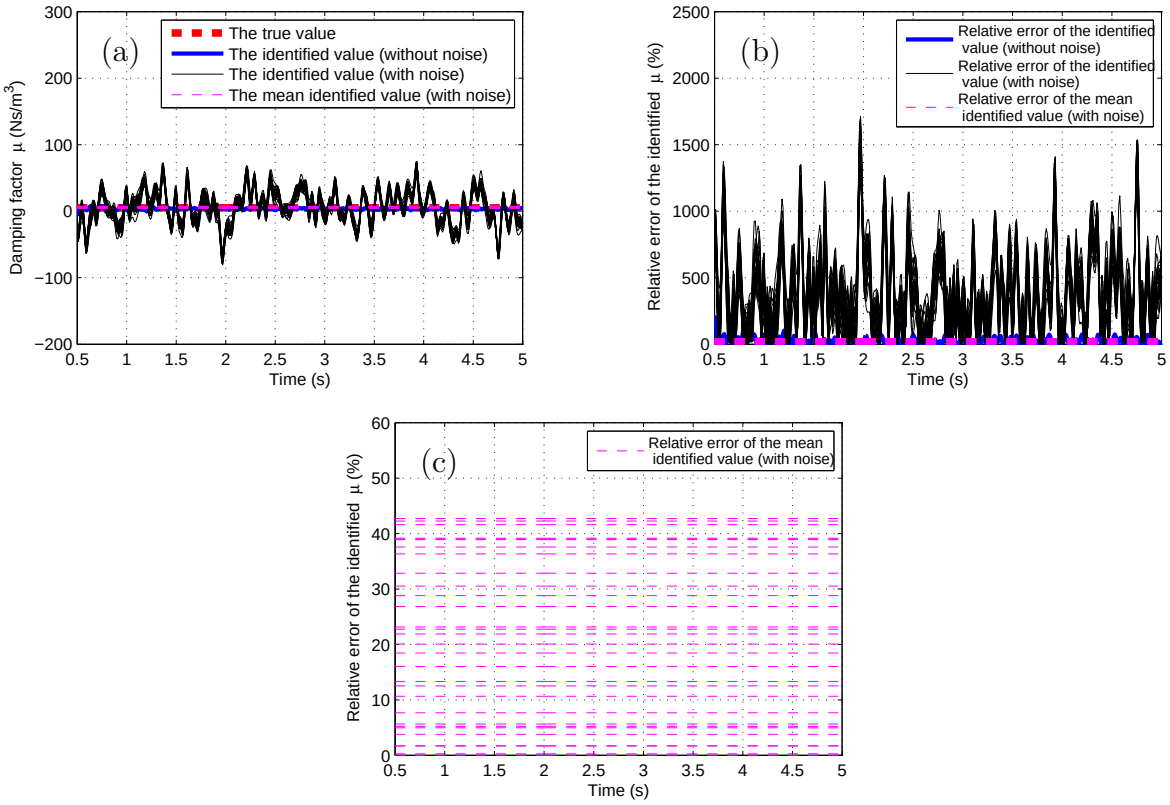

Figure B.25: Damping factor μ of a 2-DOF weakly nonlinear system with a weakly nonlinear smoothly varying Van der Pol oscillator: (a) The true value and the identified values of μ, (b) Relative errors of the identified values of μ, (c) Relative errors of the mean identified values of μ.

From the above figures, it is noted that: For both systems, due to the sensitivity of the damping coefficients to noise and the application of the approximation Equation (4.8), the statistical distributions of the identified damping factor μ and damping coefficient c_2 are quite wide with extremely large identification errors (the maximal relative error of the identified values of μ is less than $1.8 \times 10^3\%$ and the maximal absolute error of the identified values of c_2 is less than 84Ns/m for the smoothly varying Van der Pol system, their counterparts for the abruptly varying Van der Pol system are less than $2.0 \times 10^3\%$ and 91Ns/m respectively). Taking the mean values of them over the required time history, the resulting mean values (denoted with pink dashed lines) of the identified values of μ and c_2 have relatively smaller errors (the maximal relative error of the mean values of the identified values of μ is less than 43% and the maximal absolute error of the mean values of the identified values of c_2 is less than 2.0Ns/m for the smoothly varying Van der Pol system, their counterparts for the abruptly varying Van der Pol system are less than 33% and 3.9Ns/m respectively). For the 2-DOF weakly nonlinear abruptly varying chainlike Van der Pol system, due to the existence of large identification errors, it is hard to detect the exact time instant of the abrupt change of the system coefficient from the statistical

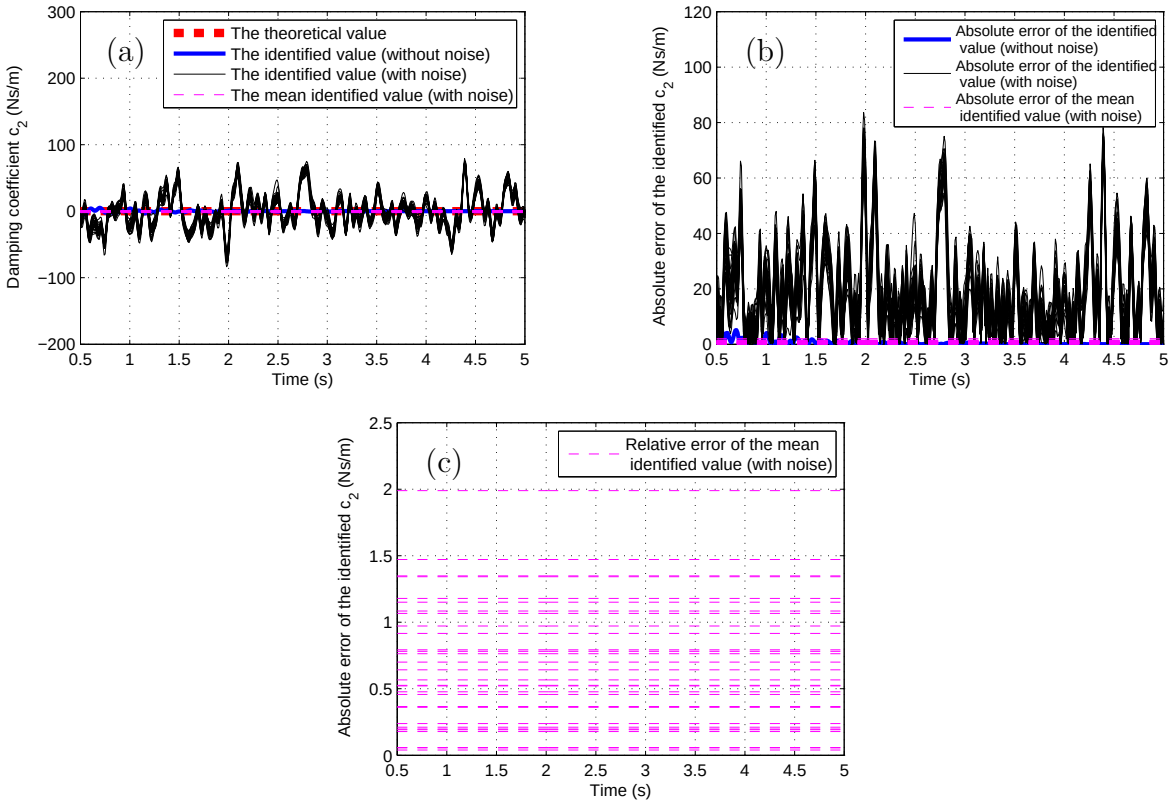

Figure B.26: Damping factor c_2 of a 2-DOF weakly nonlinear chainlike system with a weakly nonlinear smoothly varying Van der Pol oscillator: (a) The true value and the identified values of c_2, (b) Absolute errors of the identified values of c_2, (c) Absolute errors of the mean identified values of c_2.

distributions of the identified values of μ and c_2.

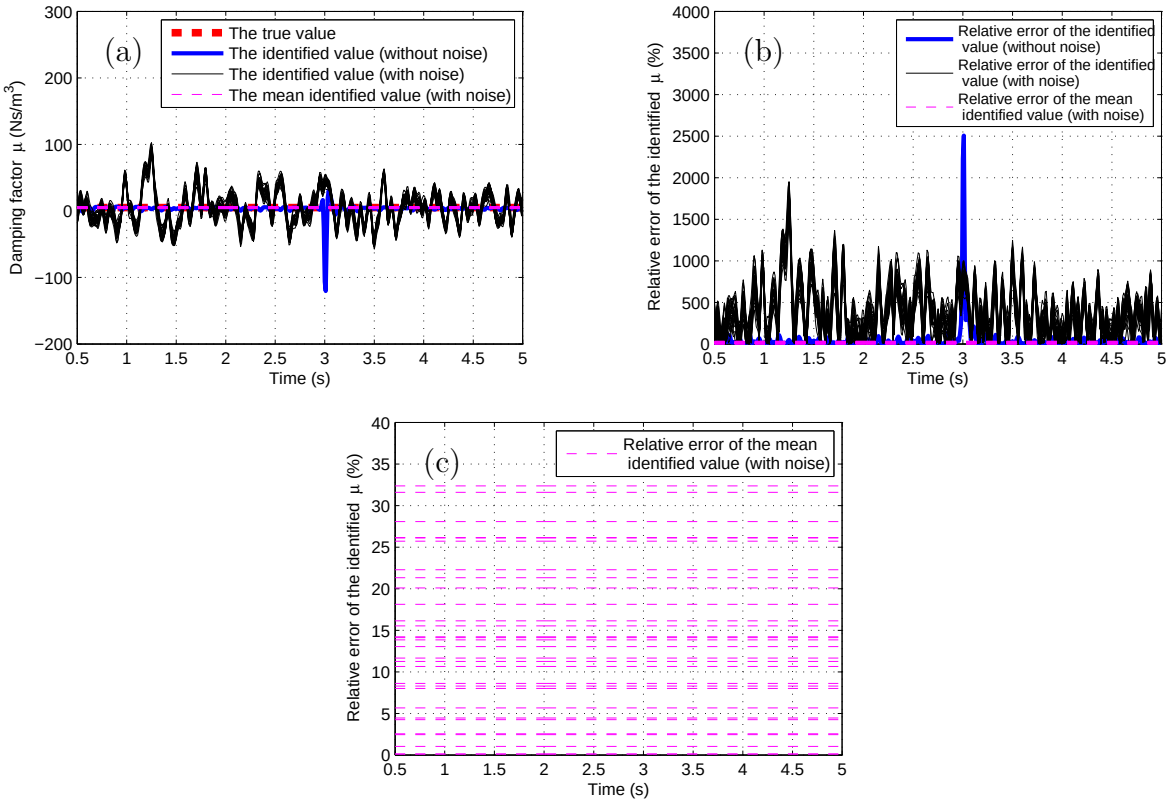

Figure B.27: Damping factor μ of a 2-DOF weakly nonlinear chainlike system with a weakly nonlinear abruptly varying Van der Pol oscillator: (a) The true value and the identified values of μ, (b) Relative errors of the identified values of μ, (c) Relative errors of the mean identified values of μ.

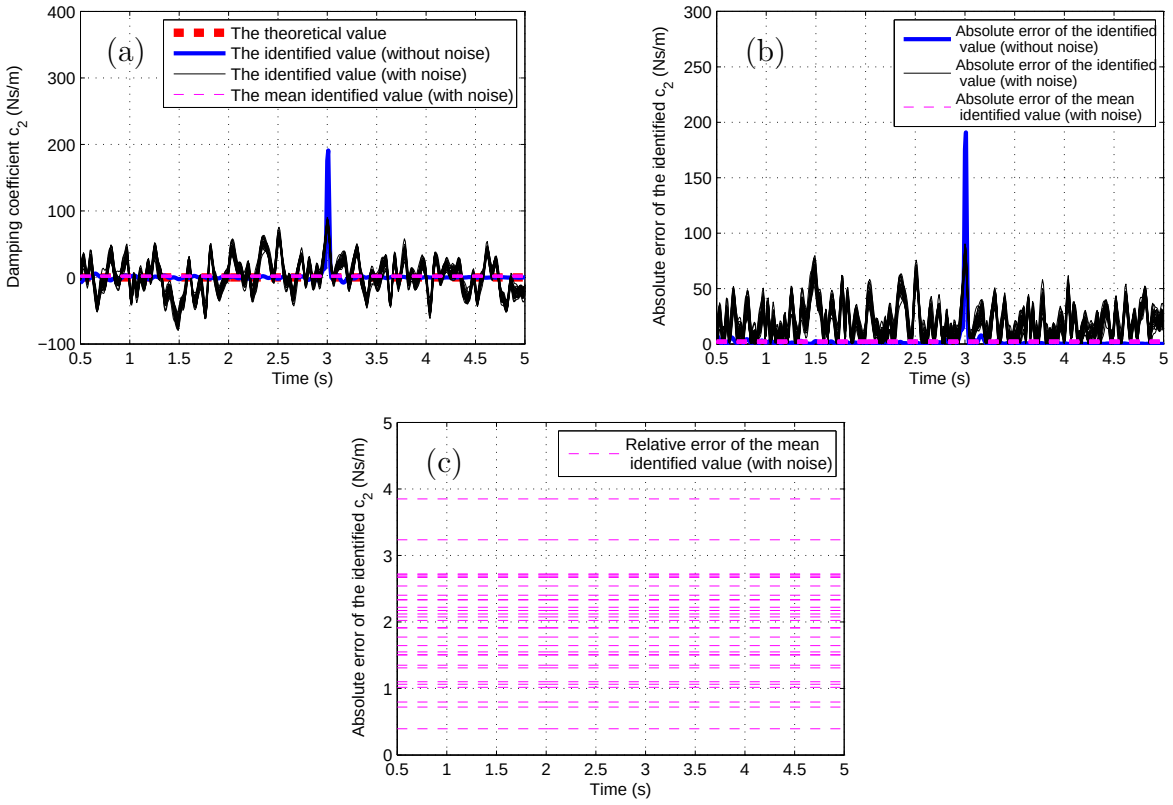

Figure B.28: Damping factor c_2 of a 2-DOF weakly nonlinear chainlike system with a weakly nonlinear abruptly varying Van der Pol oscillator: The true value and the identified values of c_2, (b) Absolute errors of the identified values of c_2, (c) Absolute errors of the mean identified values of c_2.

B.2.6 HHT and Bayesian inference based identification results of weakly nonlinear periodically varying Van der Pol systems

(1) 1-DOF system

For the HHT and Bayesian inference based identification of the 1-DOF weakly nonlinear periodically varying Van der Pol oscillator proposed in Section 4.2.1, Figure B.29 shows the statistical distributions of the identified stiffness coefficient k and damping factor μ as well as their relative errors. We can see from the figures that the obtained statistical distribution of the identified values (denoted with black lines) of k is concentrated around its true value (with maximal relative error of the identified values less than 2.4%), whereas the identified values of μ is widely distributed with extremely large identification errors (with maximal relative error of the identified values less than 6.3×10^2%). The mean values (denoted with pink dashed lines) of the identified values of μ over the required time history also have large relative errors (whose maximum is less than 22%).

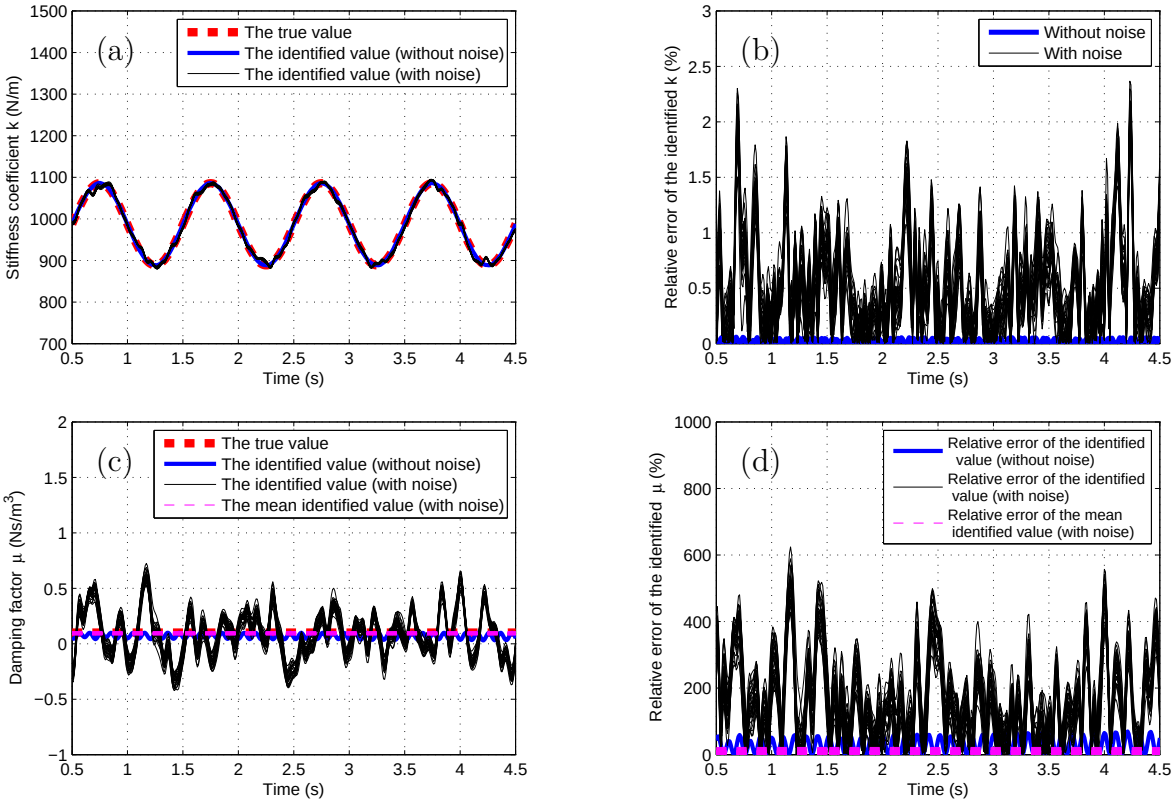

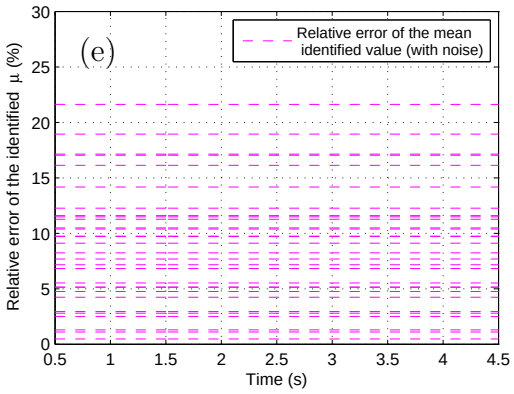

Figure B.29: System coefficients of a weakly nonlinear periodically varying Van der Pol oscillator: (a) The true value and the identified values of stiffness coefficient k, (b) Relative errors of the identified values of k, (c) The true value and the identified values of damping factor μ, (d) Relative errors of the identified values of μ, (e) Relative errors of the mean identified values of μ.

(2) 2-DOF system

For the HHT and Bayesian inference based identification of the 2-DOF weakly nonlinear periodically varying Van der Pol system proposed in Section 4.2.2, the statistical distributions of the identified system coefficients as well as their relative or absolute errors are shown in Figures B.30 - B.33.

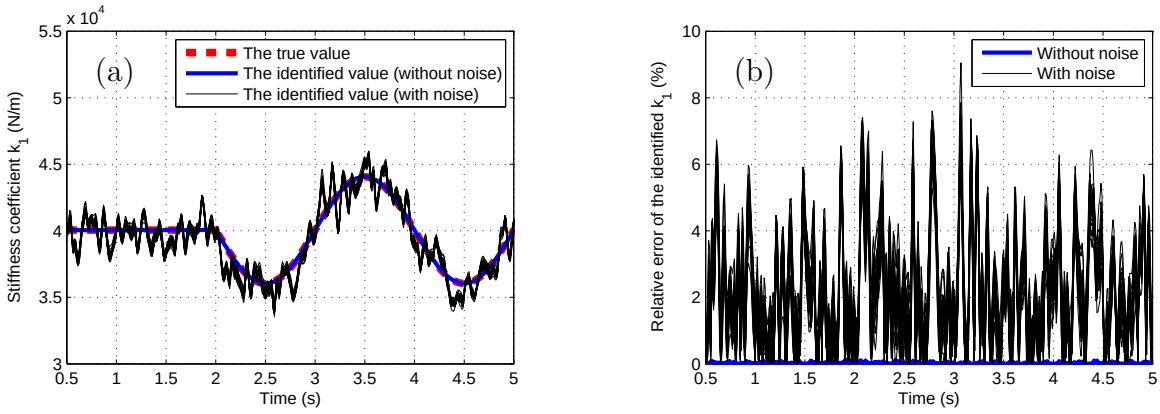

Figure B.30: Stiffness coefficient k_1 of a 2-DOF weakly nonlinear chainlike system with a weakly nonlinear periodically varying Van der Pol oscillator: (a) The true value and the identified values of k_1, (b) Relative errors of the identified values of k_1.

It is noted that the resulting identified values (denoted with black lines) of the stiffness coefficients are concentratedly distributed around their respective true values (with maximal relative error of the identified values of k_1 less than 9.1% and that of k_2 less than 2.6%), whereas those of damping factor μ and damping coefficient c_2 are widely distributed and have extremely large identification errors (the maximal relative error of the identified

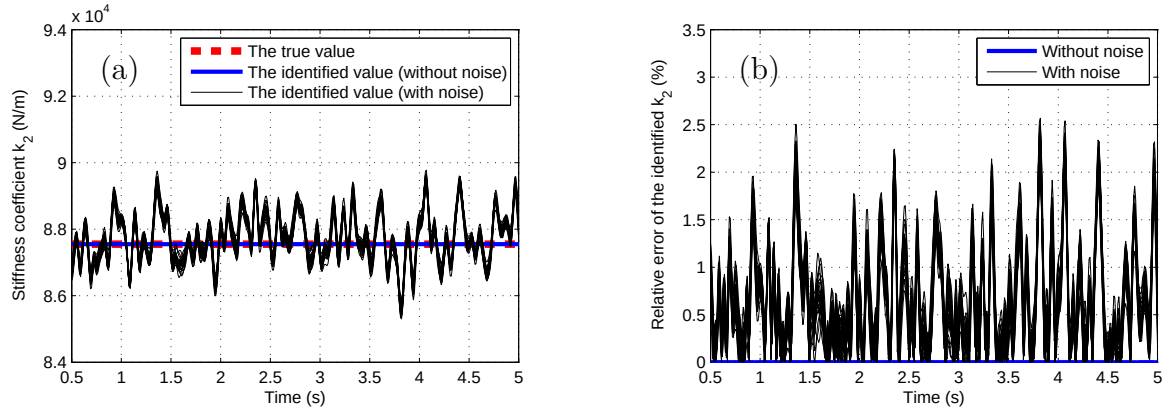

Figure B.31: Stiffness coefficient k_2 of a 2-DOF weakly nonlinear chainlike system with a weakly nonlinear periodically varying Van der Pol oscillator: (a) The true value and the identified values of k_2, (b) Relative errors of the identified values of k_2.

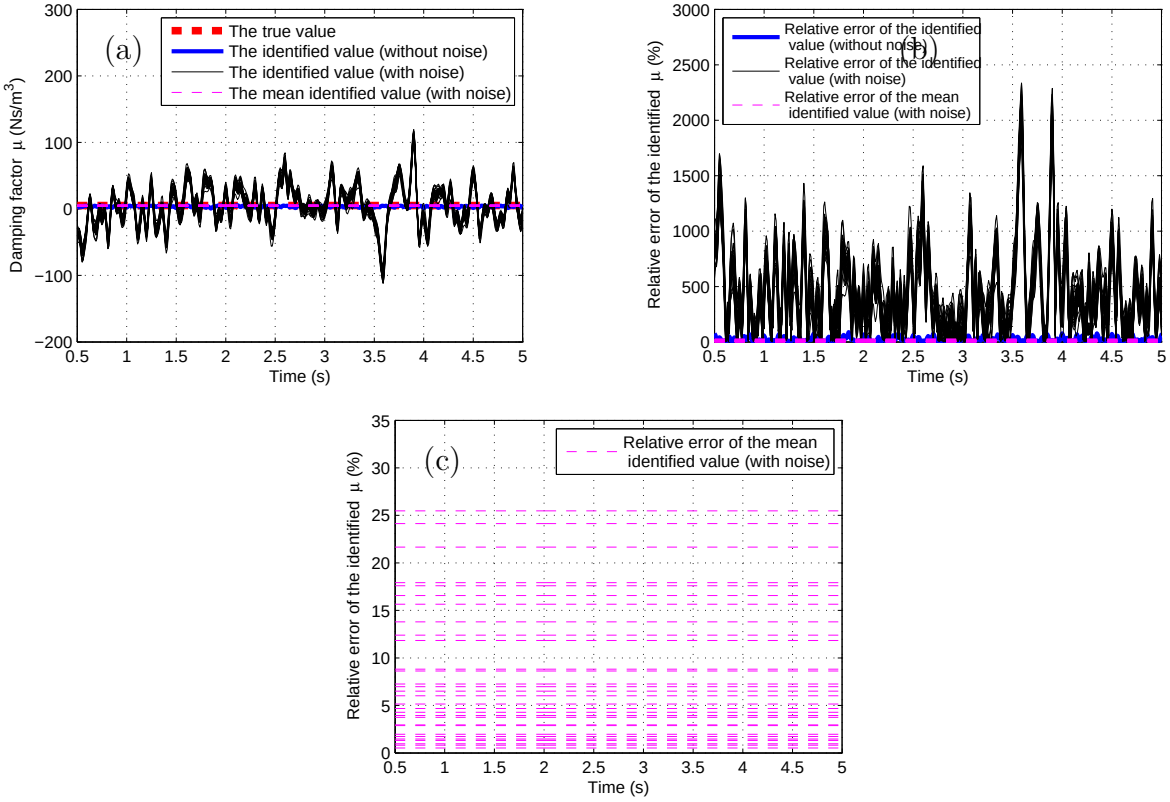

Figure B.32: Damping factor μ of a 2-DOF weakly nonlinear chainlike system with a weakly nonlinear periodically varying Van der Pol oscillator: (a) The true value and the identified values of μ, (b) Relative errors of the identified values of μ, (c) Relative errors of the mean identified values of μ.

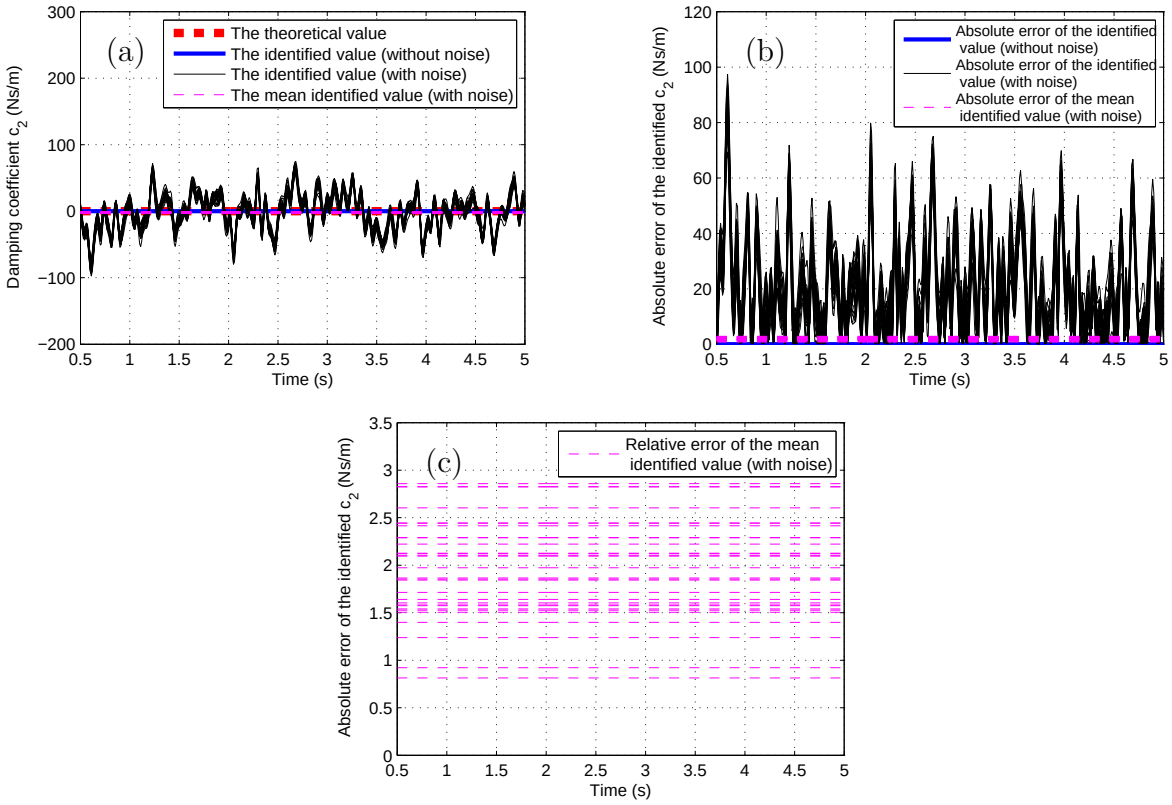

Figure B.33: Damping coefficient c_2 of a 2-DOF weakly nonlinear chainlike system with a weakly nonlinear periodically varying Van der Pol oscillator: (a) The true value and the identified values of c_2, (b) Absolute errors of the identified values of c_2, (c) Absolute errors of the mean identified values of c_2.

values of μ is less than $2.4 \times 10^3\%$ and the maximal absolute error of the identified values of c_2 is less than 98Ns/m). The mean values (denoted with pink dashed lines) of the identified values of μ and c_2 over the required time history have relatively smaller errors (with maximal relative error of the mean values of the identified values of μ less than 26% and maximal absolute error of the mean values of the identified values of c_2 less than 2.9Ns/m).

B.3 Results of numerical simulations of Bayesian inference based parameter identification on 2-DOF linear and weakly nonlinear time-varying systems with consideration of less IMFs

In this section, with the help of the Bayesian inference based parameter identification method proposed in Section 5.4.1, parameter identification is carried on the 2-DOF linear smoothly varying non-chainlike system and the 2-DOF weakly nonlinear smoothly varying

chainlike Duffing system proposed in Section 5.4.2 with consideration of IMFs extracted from only one set of system responses which corresponds to one DOF.

(1) Parameter identification of a 2-DOF linear smoothly varying system
For a 2-DOF linear smoothly varying non-chainlike system, the system parameter to be identified is t_L as in Section 5.4.2 with the expectation given by $t_{Lexp} = 2$s. Assume the experimental data consists of $N_s = 15$ sets of IMFs generated with the model specified by t_{Lexp} and perturbed by Gaussian noise with COV equal to 5%. The prior distribution assigned to t_L is a uniform distribution in the range $[1, 3]$. The PEV $(\varepsilon_{i\chi}^a)^2$ of the IMF for the acceleration response is uniformly distributed in the range $[0, 0.05]$. The ratios α, γ which define the model classes $\boldsymbol{M}$ are assigned as $\alpha = 0.1$, $\gamma_l = 0.01 + 0.01(l-1)$, $l = 1, \ldots, 50$. The number of samples of each distribution N_E is given as 450.
Posterior probability for model classes which are characterized by parameters $\alpha = 0.1$, $\gamma = [0.01, 0.5]$ is presented in Figure B.34. The posterior distribution of the system parameter t_L as well as the relative errors of its identified values for the most probable model class are plotted in Figure B.35.

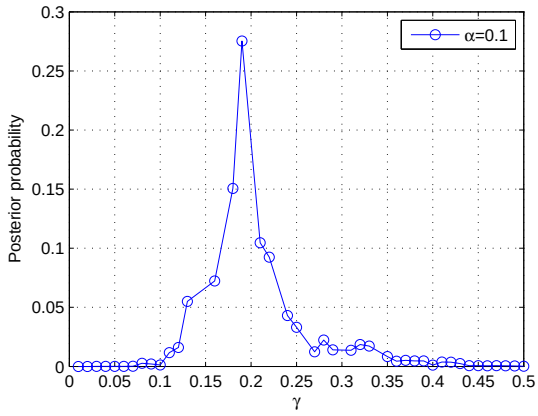

Figure B.34: Posterior probability for model classes characterized by $\alpha = 0.1$, $\gamma = [0.01, 0.5]$ of a 2-DOF linear smoothly varying non-chainlike system.

Figure B.34 shows that the posterior probability of the model classes characterized by parameters $\alpha = 0.1$, $\gamma = [0.01, 0.5]$ has increasing trend as γ increases from 0.01 to 0.19 and reaches its maximum (27.5%) at $\gamma = 0.19$, then it has decreasing trend as γ increases from 0.19 to 0.5, determining the most probable model class by $\alpha^* = 0.1$, $\gamma^* = 0.19$. As all model classes are considered as equally likely apriori, Figure B.34 reveals that only model classes characterized by $\alpha = 0.1$ and γ in the range of $\gamma \in [0.11, 0.39]$ have significant posterior probabilities. Figure B.35 shows that the posterior distribution of the system parameter t_L for the most probable model class $M(\alpha^* = 0.1, \gamma^* = 0.19)$ is concentrated on its expected value (with the mean value of the relative errors of the identified results equal to 0.32%), implying that the relative weightings of the IMFs of the acceleration responses, the IMFs of the corresponding velocity responses and the IMFs of the corresponding displacement responses in the likelihood function for the most prob-

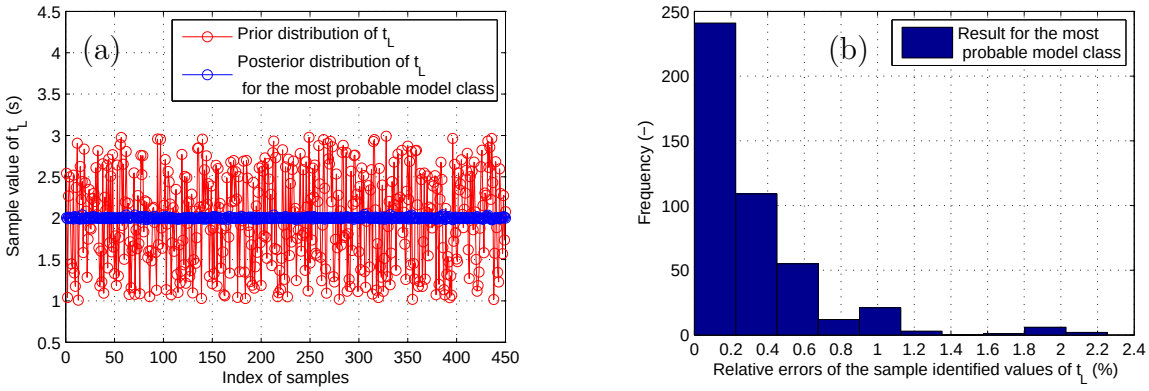

Figure B.35: System parameter t_L of a 2-DOF linear smoothly varying non-chainlike system: (a) Distribution of t_L, (b) Relative errors for the identified values of t_L and for the most probable model class.

able model class $M(0.1, 0.19)$ can result in a good identification of the system parameter t_L.

(2) Parameter identification of a 2-DOF weakly nonlinear smoothly varying chainlike Duffing system

For a 2-DOF weakly nonlinear smoothly varying chainlike Duffing system, the system parameter to be identified is t_{duff} as in Section 5.4.2 with the expectation given by $t_{duffexp} = 2$s. Assume the experimental data consists of $N_s = 15$ sets of IMFs generated with the model specified by $t_{duffexp}$ and perturbed by Gaussian noise with COV equal to 5%. The prior distribution assigned to t_{duff} is a uniform distribution in the range $[1, 3]$. The PEV $(\varepsilon^a_{i\chi})^2$ of the IMF for the acceleration response is uniformly distributed in the range $[0, 0.05]$. The ratios α, γ which define the model classes $\boldsymbol{M}$ are assigned as $\alpha = 1$, $\gamma_l = 0.1 + 0.1(l-1)$, $l = 1, \ldots, 20$. The number of samples of each distribution N_E is given as 450.

The posterior probability for model classes which are characterized by parameters $\alpha = 1$, $\gamma = [0.1, 2]$ is presented by Figure B.36, and the posterior distribution of the system parameter t_{duff} as well as the relative errors of its identified values for the most probable model class are plotted in Figure B.37.

It is noted from Figure B.36 that the posterior probability of the model classes characterized by parameters $\alpha = 1$, $\gamma = [0.1, 2]$ has increasing trend as γ increases from 0.1 to 1 and reaches its maximum (22.7%) at $\gamma = 1$, then it has decreasing trend as γ increases from 1 to 2, determining the most probable model class by $\alpha^* = 1$, $\gamma^* = 1$. Since all model classes are considered to be equally likely apriori, Figure B.36 reveals that only model classes specified by $\alpha = 1$ and γ in the range of $\gamma \in [0.5, 1.9]$ have significant posterior probabilities. The posterior distribution of t_{duff} for the most probable model class $M(\alpha^* = 1, \gamma^* = 1)$ which is shown in Figure B.37 is concentrated on its expected value with small relative errors (the mean value of which is equal to 2.9%). This indicates that the relative weightings of the IMFs of the acceleration responses, the IMFs of the corresponding velocity responses as well as the IMFs of the corresponding displacement responses in the likelihood function for the most probable model class $M(1, 1)$ can lead to

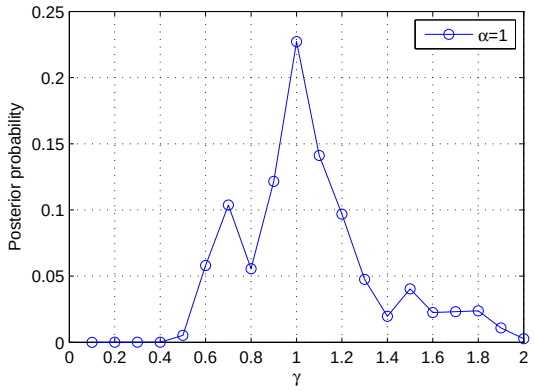

Figure B.36: Posterior probability for model classes characterized by $\alpha = 1$, $\gamma = [0.1, 2]$ of a 2-DOF weakly nonlinear smoothly varying chainlike Duffing system.

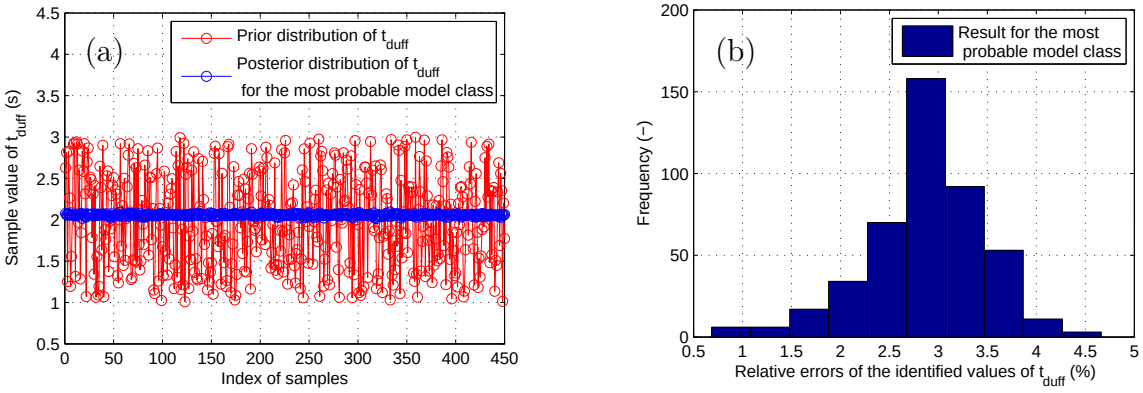

Figure B.37: System parameter t_{duff} of a 2-DOF weakly nonlinear smoothly varying chainlike Duffing system: (a) Distribution of t_{duff}, (b) Relative errors for the identified values of t_{duff} and for the most probable model class.

a good identification of the system parameter t_{duff}.

Bibliography

[1] L. Ljung. *System Identification: Theory for the User*. Prentice-Hall information and system sciences series. Prentice Hall, Englewood Cliffs, NJ, 1987.

[2] M. Gevers. System Identification without Lennart Ljung: What Would Have Been Different? In T. Glad and G. Hendeby, editors, *Forever Ljung in System Identification*. Studentlitteratur AB, Norrtalje, 2006.

[3] X.C. Xu and S.K. Agrawal. Linear Time-varying Dynamic Systems Optimization High-Order Method: A Sub-Domain Approach. *ASME J. Vib. Acoust.*, 122(1):31–35, 2000.

[4] C.C. Lin, T.T. Soong, and H.G. Natke. Real-Time System Identification of Degrading Structures. *J. Eng. Mech.*, 116(10):2258–2274, 1990.

[5] J.B. McNeil, R.E. Kearney, and I.W. Hunter. Identification of Time-varying Biological Systems from the Ensemble Data. *IEEE Trans. Biomed. Eng.*, 39(12):1213–1225, 1992.

[6] Y.S. Lee, A.F. Vakakis, D.M. McFarland, G. Kerschen, and L.A. Bergman. Empirical Mode Decomposition in the Reduced-Order Modeling of Aeroelastic Systems. In *Proc. 49th AIAA Structures, Dynamics, and Materials Conference*, pages 7–10, 2008.

[7] E.C. Titchmarsh. *Introduction to the Theory of Fourier Integrals*. Oxford University Press, New York, NY, 1948.

[8] N.E. Huang, Z. Shen, S.R. Long, M.C. Wu, H.H. Shih, Q. Zheng, N.C. Yen, C.C. Tung, and H.H. Liu. The Empirical Mode Decomposition and Hilbert Spectrum for Nonlinear and Nonstationary Time Series Analysis. In *Proc. R. Soc. London Ser. A*, volume 454, pages 903–995, 1998.

[9] D. Gabor. Theory of Communication. *J. IEE*, 93(26):429–457, 1946.

[10] M.R. Protnoff. Time-Frequency Representation of Digital Signals and Systems Based on Short-Time Fourier Analysis. In *IEEE T. Acoust., Speech, Sig. Proc.*, volume 28, pages 55–69, 1980.

[11] W. Kozek and F. Hlawatsch. Time-Frequency Representation of Linear Time-varying Systems using the Weyl Symbol. In *Proc. 6th IEEE Conf. D. Signal Process. Commun.*, pages 25–30, 1991.

[12] H. Benisty, Y. Avargel, and I. Cohen. Adaptive System Identification using Time-varying Fourier Transform. In *Proc. ICADIWT*, pages 652–657, 2009.

[13] Y. Avargel and I. Cohen. On Multiplicative Transfer Function Approximation in the Short-Time Fourier Transform Domain. *IEEE Signal Process. Lett.*, 14(5):337–340, 2007.

[14] C. K. Chui. *Wavelet Analysis and Applications: An Introduction to Wavelets*, volume 1. Academic Press, San Diego, 1992.

[15] R. Polikar. The Story of Wavelets. In *IMACS/IEEE CSCC'99 Proc.*, pages 5481–5486, 1999.

[16] I. Daubechies. Orthonormal Bases of Compactly Supported Wavelets. *Comm. Pure Appl. Math.*, 41(7):909–996, 1988.

[17] R. Ghanem and F. Romeo. A Wavelet-Based Approach for the Identification of Linear Time-varying Dynamic Systems. *J. Sound Vib.*, 234(4):555–576, 2000.

[18] S.J. Park, K.J. Kim, and S.W. Nam. Identification of A Continuous Linear Time-varying System using Haar Wavelet with Unit Energy. *WSEAS Trans. Circuits Syst.*, 7(5):382–391, 2008.

[19] X.N. Shan and J.B. Burl. Continuous Wavelet Based Linear Time-varying System Identification. *Signal Process.*, 91(6):1476–1488, 2011.

[20] S. Shokoohi and L.M. Silverman. Identification and Model Reduction of Time-varying Discrete-Time Systems. *Automatica*, 23(4):509–521, 1987.

[21] M. Verhaegen and X. Yu. A Class of Subspace Model Identification Algorithms to Identify Periodically and Arbitrarily Time-varying Systems. *Automatica*, 31(2):201–216, 1995.

[22] K. Liu. Identification of Linear Time-varying Systems. *J. Sound Vib.*, 206(4):487–505, 1997.

[23] J.N. Yang, Y. Lei, S.W. Pan, and N. Huang. System Identification of Linear Structures Based on Hilbert-Huang Spectral Analysis. Part 1: Normal Modes. *Earthquake Engng. Struct. Dyn.*, 32(9):1443–1467, 2003.

[24] J.N. Yang, Y. Lei, S. Lin, and N. Huang. Identification of Natural Frequencies and Dampings of in Situ Tall Buildings using Ambient Wind Vibration Data. *J. Eng. Mech.*, 130(5):570–577, 2004.

[25] Z.Y. Shi and S.S. Law. Identification of Linear Time-varying Dynamical Systems using Hilbert Transform and EMD Method. *J. Appl. Mech.*, 74(2):223–230, 2007.

[26] Z.Y. Shi, S.S. Law, and X. Xu. Identification of Linear Time-varying MDOF Dynamical Systems from Forced Excitation using Hilbert Transform and EMD Method. *J. Sound Vib.*, 321(3–5):572–589, 2009.

[27] H. Li and H. Ding. Progress in Model Updating for Structural Dynamics. *Adv. Mech.*, 35(2):170–180, 2005.

[28] T. Bayes. An Essay towards Solving A Problem in the Doctrine of Chances. *Phil. Trans.*, 53(1):370–418, 1763.

[29] G.A. Barnard. Thomas Bayes's Essay towards Solving A Problem in the Doctrine of Chances. *Biometrika*, 45(3-4):293–315, 1958.

[30] H. Jeffreys. *Theory of Probability (3rd Edition)*. Oxford Clarendon Press, Oxford, UK, 1961.

[31] R.T. Cox. *The Algebra of Probable Inference*. Johns Hopkins Press, Baltimore, MA, 1961.

[32] E.T. Jaynes. Prior Probabilities. *IEEE Trans. Syst. Sci. Cybern.*, 4(3):227–241, 1968.

[33] E.T. Jaynes. Bayesian Methods: General Background. In *Maximum Entropy and Bayesian Methods in Applied Statistics*, pages 1–25, Cambridge, UK, 1986.

[34] E.T. Jaynes. *Probability Theory: The Logic of Science*. Cambridge University Press, Cambridge, UK, 2003.

[35] E.T. Jaynes. *Probability Theory with Applications in Science and Engineering*. Washington University, StLouis, MO, 1974.

[36] D.J. Spiegelhalter, K.R. Abrams, and J.P. Myles. *Bayesian Approaches to Clinical Trials and Health-Care Evaluation*. John Wiley & Sons, Inc., Chichester, UK, 2004.

[37] G.G. Woodworth. *Biostatistics: A Bayesian Introduction*. John Wiley & Sons, Inc., Hoboken, NJ, 2004.

[38] S.Y. Lee. *Structural Equation Modelling: A Bayesian Approach*. John Wiley & Sons, Inc., New York, NY, 2007.

[39] T. Rivas, J.M. Matias, J. Taboada, and A. Arguelles. Application of Bayesian Networks to the Evaluation of Roofing Slate Quality. *J. Eng. Geol.*, 94(1–2):27–37, 2007.

[40] S. Mahadevan, R. Zhang, and N. Smith. Bayesian Networks for System Reliability Reassessment. *Struct. Saf.*, 23(3):231–251, 2001.

[41] R. Zhang and S. Mahadevan. Bayesian Methodology for Reliability Model Acceptance. *Reliab. Eng. Syst. Safe.*, 80(1):95–103, 2003.

[42] C.M. Vong, P.K. Wong, and Y.P. Li. Prediction of Automotive Engine Power and Torque using Least Squares Support Vector Machines and Bayesian Inference. *Eng. Appl. Artif. Intel.*, 19(3):227–297, 2006.

[43] G.C. Fraccone, M. Ruzzene, V. Volovoi, P. Cento, and C. Vining. Assessment of Uncertainty in Response Estimation for Turbine Engine Bladed Disks. *J. Sound Vib.*, 317(3–5):625–645, 2008.

[44] N.E. Huang, Z. Shen, and S.R. Long. A New View of Nonlinear Water Waves: The Hilbert Spectrum. *Annu. Rev. Fluid Mech.*, 31:417–457, 1999.

[45] G. Kerschen, A.F. Vakakis, Y.S. Lee, D.M. McFarland, and L.A. Bergman. Toward a Fundamental Understanding of the Hilbert-Huang Transform in Nonlinear Structural Dynamics. *J. of Vib. Control*, 14(1–2):77–105, 2008.

[46] N.E. Huang, M.L. Wu, W.D. Qu, S.R. Long, S.S.P. Shen, and J.E. Zhang. Applications of Hilbert-Huang transform to non-stationary financial time series analysis. *Appl. Stoch. Models Bus. Ind.*, 19(3):245–268, 2003.

[47] E.P. Souza Neto, M.A. Custaud, J.C. Cejka, P. Abry, J. Frutoso, C. Gharib, and P. Flandrin. Assessment of Cardiovascular Autonomic Control by the Empirical Mode Decomposition. *Methods Inf. Med.*, 43(1):60–65, 2004.

[48] A.M. Kakurin and I.I. Orlovsky. Hilbert-Huang Transform in MHD Plasma Diagnostics. *Plasma Phys. Rep.*, 31(12):1054–1063, 2005.

[49] I.M. Janosi and R. Mueller. Empirical Mode Decomposition and Correlation Properties of Long Daily Ozone Records. *Phys. Rev. E*, 71(5):056126, 2005.

[50] J.N. Yang, Y. Lei, S. Lin, and N. Huang. Hilbert-Huang Based Approach for Structural Damage Detection. *J. Eng. Mech.*, 130(1):85–95, 2004.

[51] M.J. Brenner and C. Prazenica. Aeroelastic Flight Data Analysis with the Hilbert-Huang Algorithm. In *2005 AIAA Atmospheric Flight Mechanics Conference and Exhibit*, pages 1–29, San Francisco, CA, 2005.

[52] B. Liu, S. Riemenschneider, and Y. Xu. Gearbox Fault Diagnosis using Empirical Mode Decomposition and Hilbert Spectrum. *Mech. Syst. Signal Pr.*, 20(3):718–734, 2006.

[53] D. Yu, J. Cheng, and Y. Yang. Application of EMD Method and Hilbert Spectrum to the Fault Diagnosis of Roller Bearings. *Mech. Syst. Signal Pr.*, 19(2):259–270, 2005.

[54] P.F. Pai and J. Hu. Nonlinear Vibration Characterization by Signal Decomposition. In *Proc. 24th IMAC*, St Louis, MO, 2006.

[55] J. S. Bendat and A. G. Piersol.

[56] M. Feldman. *Hilbert Transform Applications in Mechanical Vibrations*. John Wiley & Sons, Ltd., New York, NY, 2011.

[57] L. Cohen. What is a Multicomponent Signal? In *IEEE T. Acoust., Speech, Sig. Proc.*, volume 5, pages 113–116, 1992.

[58] T. Thayaparan, LJ. Stankovic, and M. Dakovic. Decomposition of Time-varying Multicomponent Signals using Time-Frequency Based Method. In *CCECE*, pages 60–63, 2006.

[59] M. Jabloun, N. Martin, M. Vieira, and F. Leonard. Multicomponent Signal: Local Analysis and Estimation. In *Eur. Signal Process. Conf.*, Antalya, Turkey, 2005.

[60] P. Flandrin. Empirical Mode Decomposition. `http://perso.ens-lyon.fr/patrick.flandrin/software2.html`.

[61] G. Rilling, P. Flandrin, and P. Goncalves. On Empirical Mode Decomposition and its Algorithms. In *Proc. NSIP*, 2003.

[62] E. Bedrosian. A Product Theorem for Hilbert Transforms. In *Proc. IEEE*, volume 51, pages 868–869, 1963.

[63] C.P. Robert. *The Bayesian Choice*. Springer-Verlag, New York, NY, 2 edition, 2001.

[64] J.L. Beck and S.K. Au. Important sampling in high dimensions. *Struct. Saf.*, 25(2):139–163, 2003.

[65] A.E. Gelfand, S.E. Hills, A. Racine-Poon, and A.F.M. Smith. Illustration of Bayesian inference in normal data models using Gibbs sampling. *J. Amer. Statist. Assoc.*, 85(412):972–985, 1990.

[66] W.R. Gilks, S. Richardson, and D.J. Spiegelhalter. *Markov Chain Monte Carlo in Practice*. Chapman & Hall, London, 1996.

[67] C.P. Robert and G. Casella. *Monte Carlo Statistical Methods, Springer Texts in Statistics*. Springer-Verlag, New York, NY, 2 edition, 2004.

[68] N. Metropolis, A.W. Rosenbluth, M.N. Rosenbluth, A.H. Teller, and E. Teller. Equation of State Calculations by Fast Computing Machines. *J. Chem. Phys.*, 21(6):1087–1092, 1953.

[69] W.K. Hastings. Monte Carlo Sampling Methods using Markov Chains and Their Applications. *Biometrika*, 57(1):97–109, 1970.

[70] J.L. Beck and S.K. Au. Bayesian Updating of Structural Models and Reliability using Markov Chain Monte Carlo Simulation. *J. Eng. Mech.*, 128(4):380–391, 2002.

[71] J. Ching and Y.C. Chen. Transitional Markov Chain Monte Carlo Method for Bayesian Updating, Model Class Selection, and Model Averaging. *J. Eng. Mech.*, 133(7):816–832, 2007.

[72] J. Banks. *Handbook of Simulation: Principles, Methodology, Advances, Applications, and Practice*. John Wiley & Sons, Inc., New York, NY, 1998.

[73] M. Better and F. Glover. Simulation Optimization: Applications in Risk Management. *IJITDM*, 7(4):571–587, 2008.

[74] F. Felgner and G. Frey. Multi-Phase Markov Models for Functional Safety Prediction: Efficient Simulation of Markov Models Used for Safety Engineering and the Online Integration of Individual Systems' Diagnostic and Maintenance History. In *Proc. DCDS*, pages 133–140, 2011.

[75] E.M. Bonrath, B.K. Weber, M. Fritz, S.T. Mees, H.H. Wolters, N. Senninger, and E. Rijcken. Laparoscopic simulation training: Testing for skill acquisition and retention. *Surgery*, 152(1):12–20, 2012.

[76] J.M. Rolfe and P.W. Caro. Determining the Training Effectiveness of Flight Simulators: Some Basic Issues and Practical Developments. *Appl. Ergon.*, 13(4):243–250, 1982.

[77] J.A. Sokolowski and C.M. Banks. *Principles of Modeling and Simulation: A Multidisciplinary Approach*. John Wiley & Sons, Inc., New York, NY, 2009.

[78] R. McHaney. *Understanding Computer Simulation*. Ventus Publishing ApS, 2009.

[79] D.A. Winter, H.G. Sidwall, and D.A. Hobson. Measurement and reduction of noise in kinematics of locomotion. *J. Biomech.*, 7(2):157–159, 1974.

[80] D.A. Winter. *Biomechanics and Motor Control of Human Movement*. John Wiley & Sons, Inc., New York, NY, 1990.

[81] R. Jazar. *Vehicle Dynamics: Theory And Applications*. Springer Science+Business Media, LLC., New York, NY, 2008.

[82] G. Duffing. *Erzwungene Schwingungen bei veraenderlicher Eigenfrequenz und ihre technische Bedeutung*. Vieweg & Sohn, Braunschweig, 1918.

[83] S. Timoshenko. *Vibration Problems in Engineering*. D. Van Nostrand Company, Inc., New York, 1928.

[84] T. von Kármán. The Engineer Grapples with Nonlinear Problems. *Bull. Amer. Math. Soc.*, 46:615–683, 1940.

[85] S. Fifer. Studies in Nonlinear Vibration Theory. *J. Appl. Phys.*, 22(12):1421–1428, 1951.

[86] M.L. Cartwright. Non-Linear Vibrations: A Chapter in Mathematical History. *The Mathematical Gazzette*, 36(316):81–88, 1952.

[87] W.-B. Zhang. *Differential Equations, Bifurcations, and Chaos in Economics*. World Sci. Publishing Co. Pte. Ltd., Singapore, 2005.

[88] S.L. Hahn. The Hilbert Transform of the Product $a(t)\cos(\omega_o t + \phi_o)$. *Bull. Pol. Ac.: Tech.*, 44(1):75–80, 1996.

[89] M. Feldman. Hilbert transform in vibration analysis. *Mech. Syst. Signal Pr.*, 25(3):735–802, 2011.

[90] B. van der Pol. Forced oscillations in a circuit with nonlinear resistance (receptance with reactive triode). *Edinburgh and Dublin Phil. Mag.*, 3(3):65–80, 1927.

[91] J.K. Hale. *Ordinary Differential Equations*. John Wiley & Sons, Inc., New York, NY, 1969.

[92] J. Guckenheimer and P. Holmes. *Nonlinear Oscillations, Dynamical Systems, and Bifurcations of Vector Fields*. Springer-Verlag, New York, NY, 1983.

[93] Z.M. Ge and M.Y. Hsu. Chaos in A Generalized Van der Pol System and in its Fractional Order System. *Chaos Soliton. Fract.*, 33(5):1711–1745, 2007.

[94] J.H. Chen and W.C. Chen. Chaotic Dynamics of the Fractionally Damped Van der Pol Equation. *Chaos Soliton. Fract.*, 35(1):188–198, 2008.

[95] B. Goller, J.L. Beck, and G.I. Schueller. Evidence-Based Identification of Weighting Factors in Bayesian Model Updating Using Modal Data. volume 138, pages 430–440, 2012.